

CASCaDE II Project Final Report

PROJECT TERM: OCTOBER 1, 2011 – JUNE 30, 2015

PROJECT TITLE:

CASCADE II: COMPUTATIONAL ASSESSMENTS OF SCENARIOS OF CHANGE FOR THE DELTA ECOSYSTEM

CONTRACTOR/GRANT RECIPIENT CONTACT INFORMATION

Program Administrator

NAME: Deborah Stoliker
INSTITUTION: U.S. Geological Survey
ADDRESS: 345 Middlefield Rd. MS 466, Menlo Park, CA 94025
PHONE: 650-329-4477
EMAIL: dlstoliker@usgs.gov

Principal Investigator/Lead Principal Investigator

NAME: Noah Knowles and Lisa Lucas

INSTITUTION: U.S. Geological Survey
ADDRESS: 345 Middlefield Rd. MS 496, Menlo Park, CA 94025
PHONE: 650-329-4476
EMAIL: nknowles@usgs.gov

GRANTING PROGRAM CONTACT INFORMATION

Technical Contact

NAME: Christopher Enright
TITLE: Senior Water Resources Engineer
AGENCY: Delta Stewardship Council
ADDRESS: 980 Ninth Street, Suite 1450, Sacramento, CA 95814
PHONE: 916-445-0637
EMAIL: cenright@deltacouncil.ca.gov

Project Location: U.S. Geological Survey, Menlo Park, CA

Brief Description of Project: This project constitutes a model-based approach for developing a long view of the San Francisco Bay/Delta estuary-watershed system. The long view is developed through simulations with linked models to project changes under a range of plausible scenarios of climate change

and Delta configurational changes. Elements of the estuary-watershed system addressed by this project are:

1. Climate Modeling and Downscaling
2. Sacramento-San Joaquin Watershed Modeling and Hydrologic Interactions with Sea Level Rise
3. Hydrodynamic Modeling and Ecosystem Linkages
4. Phytoplankton Dynamics
5. Turbidity and Geomorphology
6. Sediment Supply and Marsh Sustainability
 - a. Trend in Sediment supply from the Central Valley to the Delta
 - b. Projecting future sediment supply from the Sacramento River
 - c. Delta Marsh Sustainability
7. Contaminant Biodynamics
8. Food Web Effects of Invasive Bivalves
9. Native and Alien Fishes

Primary objective to be achieved: The cascading effects under scenarios of climate and Delta configurational change will be assessed as they propagate through the above elements.

TABLE OF CONTENTS

1. WHITE PAPER	1
a. Executive Summary	1
Project overview	1
Scenarios planned.....	6
Collaborative Modeling	8
Acknowledgements	9
b. Lessons Learned: How the CASCaDE 2 process has worked	11
c. Computing Resources & Data Management	17
Computing Resources	17
Scientific Data Management	18
Data Publication via the California Coastal Atlas	18
Applicability to the CASCADE 2 Project	19
d. Task-by-Task Science	21
Task 1: Project Administration & Coordination	21
Project Structure, Communication and Coordination	21
Funding	22
SFBD Modeling Strategy	24
Task 2: Climate modeling and downscaling	29
Task 3: Watershed modeling	33
Background	33
RVIC Unimpaired Streamflow Simulations and Post-Processing	35
Simulating Managed Streamflows using CalSim II	39
CRESPI.....	53
Reconciliation of CalSim II and CRESPI flow projections.....	67
Discussion.....	68
References	69
Task 4: Hydrodynamic modeling	72
Software Background and Initial Capability	72
Research and Development.....	73
Findings.....	78

Task Hurdles	101
Task Accomplishments	102
Next Steps.....	103
Task 5: Phytoplankton	104
Activity 1: Using simple models to revise entrenched paradigms	104
Activity 2: Developing a 2D/3D San Francisco Bay-Delta Phytoplankton Model	114
Next steps	126
References	127
Task 6: Turbidity and geomorphology	130
Summary of progress/status	130
Results/findings	133
Management implications.....	152
Next steps	153
References	153
Task 7a: Trend in sediment supply from the Central Valley to the Delta ..	155
Progress/status	155
Results/findings	155
Management implications.....	158
Next steps	160
References	162
Task 7b: Projecting future sediment supply from the Sacramento River .	165
Progress/status	165
Results/findings	174
Management implications.....	176
Next steps	176
References	177
Task 7c: Delta marsh sustainability.....	179
Progress/Status.....	179
Results/Findings.....	179
Management implications.....	180

Next steps	180
References	181
Task 8: Contaminant biodynamics	182
Background	182
Progress/Status.....	183
Results/Findings.....	185
Management Implications	188
Next Steps.....	188
References	189
Task 9: Food web effects of invasive bivalves Corbula, Corbicula, and Dreissena spp	190
Progress/Status.....	190
Results/Findings.....	192
Next Steps.....	197
Management Implications	198
References	216
Task 10: Native and alien fishes.....	217
Progress/Status: HABITAT.....	217
Management implications.....	231
Next Steps.....	232
References	232
2. OTHER DELIVERABLES	273
<i>a. Manuscripts.....</i>	<i>273</i>
Published	273
In preparation/review	281
<i>b. Presentations</i>	<i>283</i>
<i>c. Delta Science Program/Delta Stewardship Council Service</i>	<i>294</i>
<i>d. Other CASCaDE-Related Service and Outreach</i>	<i>297</i>

1. WHITE PAPER

a. Executive Summary

Project overview

The CASCaDE II project builds upon a prior model-based effort to develop a holistic view of the Bay-Delta-River-Watershed system. In CASCaDE I, a set of linked models to assess Delta ecosystem response to climate change was developed. In CASCaDE II, we have refined and extended those modeling capabilities to assess Delta ecosystem response to changes in climate and physical configuration. With new state-of-the-art hydrodynamic and water quality models at its core, CASCaDE II links models of climate, hydrology, hydrodynamics, sediment, phytoplankton, bivalves, contaminants, marsh accretion, and fish (see Fig. 1).

Our goals are to apply these linked models to 1) better understand Delta ecosystem function, 2) assess possible futures of the Delta under scenarios of climate and structural change, and 3) provide science-based information to support the DSC in its co-equal goals of water supply and ecosystem protection. The tools developed will provide an objective basis for anticipating and diagnosing Delta ecosystem responses to planned and unplanned changes. Experiments using the linked models are designed to address questions such as: How will climate change, together with new conveyance structures or increased flooded island habitat, alter water flow and drinking water quality? With projected changes in hydrodynamics, turbidity, temperature, and salinity, how might primary productivity, invasive bivalves, marsh processes, contaminant dynamics, and fish populations respond?

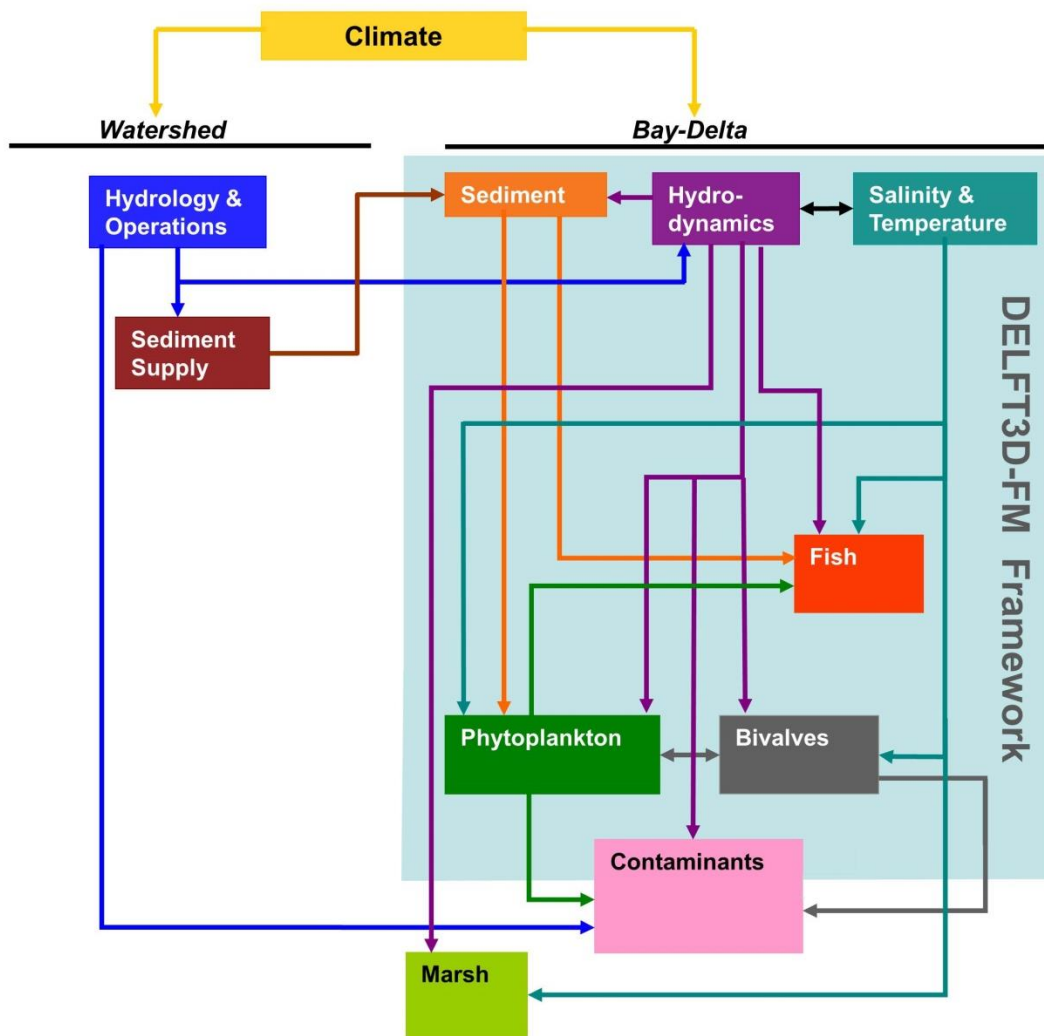


Figure 1. Schematic of CASCaDE 2 modeling tasks. Boxes represent modeling efforts. Arrows represent data flow between models. Task boxes overlaying the pale blue shaded area are either computed on the new Deltares flexible mesh “FM” grid, or coupled to it through Deltares linkage tools.

Most CASCaDE 2 modeling tasks either: 1) are entirely new initiatives in CASCaDE, (2) implement new modeling software, or (3) link to new models. A great deal of the project term has been devoted to model R&D. Not only have substantial time and effort been invested in the development of individual models and their tailoring to the San Francisco Bay-Delta (“SFBD”), but significant resources have also been devoted to the *linkages* between models. This involves data translation between one model and its dependent models, often requiring the development of specialized tools and multi-step approaches

for performing the translation. This complex web of interdependent, evolving, linked models is currently one in which individual tasks and linkages are in different stages of development and completion. We are hopeful that model development, linkages, and planned scenarios will be completed over approximately the next year.

In later sections, we provide detailed discussion of status, accomplishments, and next steps for individual modeling tasks. Here is a brief synopsis:

- *Task 1 (Project administration and coordination)*
- *Task 2 (Climate modeling and downscaling)* — A 20-member subset of CMIP5 global climate model simulations has been selected, downscaled with a new statistical downscaling method (LOCA, developed during the project term), and used to drive the VIC hydrologic model for California. Sea level projections for San Francisco have been generated for 10 of the GCM simulations. The role of atmospheric rivers in Delta flood and drought cycles has been investigated. Multiple relevant papers have been published.
- *Task 3 (Watershed modeling)* — Streamflows for all 20 GCM-based climate change scenarios produced in Task 2 were routed to produce unimpaired flow estimates at locations throughout the SFBD watershed using the RVIC routing model. These streamflows were transformed to impaired estimates and used to drive the monthly CalSim II management model and a new statistical approach to estimating downstream impaired daily flows, CRESPI. For larger basins, CRESPI output was constrained by CalSim outputs at collocated points. The end result is daily impaired streamflows at points throughout the watershed for all future scenarios. A historical gridded meteorological dataset was also used to drive the modeling chain described above, resulting in comparable estimates for the historical period.
- *Task 4 (Hydrodynamics)* — A 3D hydrodynamic model has been developed and applied for the San Francisco Bay-Delta and coastal ocean, based on the new Deltares Delft3D-FM (flexible mesh) code. Linux and parallel computing capabilities were developed and verified, and scaling on supercomputing

platforms has been optimized. Calibration and validation is nearly finished for stage, flow, and salinity. 3D temperature model refinement and calibration are underway. 3D hydrodynamic, salt transport, and temperature modeling efforts are being merged and will soon be validated together. Production runs for scenarios will begin thereafter.

- Task 5 (Phytoplankton) — Simple phytoplankton models were developed to clarify conceptual models guiding Delta restoration planning (Lucas and Thompson 2012). Progress has been made on the development of a full Bay-Delta 2D/3D phytoplankton model. The model runs in 3D, driven by Delft3D-FM hydrodynamic outputs. Multiple required pieces, datasets, and linkages have been developed, including those enabling characterization of: micro- and mesozooplankton grazing, dynamic sediment contributions to light extinction, and measurement-based benthic grazing for historical cases. Next, these pieces will be merged and fully tested, work with Task 9 on dynamic bivalve grazing will commence, and future scenarios simulations will be performed.
- Task 6 (Turbidity and geomorphology) — A detailed, multi-phase process was implemented to develop a new seamless bathymetric/topographic DEM for use in modeling hydrodynamics, sediment, and biological constituents in CASCaDE 2. A 2D model of Delta suspended sediment dynamics (driven by the Delft3D-FM hydrodynamic model) was developed, calibrated, and published (Achete et al. 2015). Influence of the Delta channel network, peak flows, and tides on sedimentation patterns has been explored in a second submitted paper. Development of a 3D sediment model is underway, and will enable characterization of dynamics in the Bay, where 3D hydrodynamic processes can be critical.
- Task 7a (Trend in sediment supply) — Multiple historic datasets have been analyzed to understand recent decadal scale decreases in sediment concentrations in and supply to the Bay-Delta. A holistic conceptual model of sediment supply step changes (associated with very large, increasingly infrequent flood events) and interactions with other factors such as submerged

aquatic vegetation has been developed and published (Schoellhamer et al. 2013, Hestir et al. 2013). Further analyses describing historical flows, sediment inputs, and changes in channel cross-sections are in various stages of publication.

- Task 7b (Projecting future sediment supply) — A detailed model of flow and sediment transport for the Sacramento River Basin has been developed, implementing diverse datasets characterizing the land surface and the stream and river channels. This model, which will provide upstream boundary conditions for the Bay-Delta sediment model (Task 6), is nearly calibrated. All 20 selected future GCM runs (Task 2) will be run through this model. Two publications describing this work are in preparation.
- Task 7c (Delta marsh sustainability) — A one-dimensional marsh surface elevation model was adapted and applied to explore Delta marsh sustainability under a broad combination of conditions (e.g. sea level rise, sediment delivery, organic matter accumulation). Marsh survival was found to depend most strongly on rate of sea level rise and sediment input, findings that represent important considerations for future restoration of the Delta. This work has been completed and published (Swanson et al. 2015).
- Task 8 (Contaminant biodynamics) — Analysis of a 17-year Selenium data set (informed by Delft3D hydrodynamic modeling) was published. That dataset was expanded upon, and an analytical method for Se in water, particulates, and biota (in prep.) was developed.
- Task 9 (Invasive bivalves) — Habitat Suitability Indices (HSI's) were developed for *C. fluminea* and *P. amurensis*, and preliminary HABITAT analyses were performed; results are consistent with current knowledge of Delta bivalve distributions. Extensive, collaborative data analysis has determined benthic biomass and grazing rates for thousands of Bay-Delta samples. This has significantly increased understanding of bivalve spatial and temporal variability and provided benthic grazing input maps for the phytoplankton model. Multiple products on the two bivalves and their ecosystem effects have been completed.

As the phytoplankton model becomes operational, development of the DEB bivalve model (or a suitable alternative) will be pursued to provide grazing rates under future scenarios.

- Task 10 (Native and alien fishes) — Newly available data were used to extend CASCaDE 1 analyses of the effects of future water temperatures on delta smelt. HSI curves were developed for 36 fish species, age classes, and environmental parameters. Multiple data-processing tools were developed by Deltares to provide a complete model-to-model workflow allowing HABITAT analyses in CASCaDE. Preliminary HABITAT analyses were performed for delta smelt, incorporating temperature, salinity, and Secchi depth preferences, and provided reasonable results. Next, HSI curves need to be finalized and batch processing capabilities within HABITAT need to be tested. When model output maps are available from other tasks for future scenarios, those will be combined with the fish HSI's to assess habitat suitability under future conditions.

Scenarios planned

As a project, we expect to evaluate 16 scenarios describing possible responses of the SFBD to climate change, alternative conveyance, and the sudden flooding of multiple Delta islands. These scenarios are described in Figures 2 and 3. Because some CASCaDE models are computationally intensive, only a limited number of scenarios can practically be completed and therefore scenarios must be chosen judiciously.

	Low-CC	Mid-CC	High-CC
CC only	A	B	C
CC+Alt Conv		D	
CC+Flood Isl		E	

Figure 2. This matrix describes the combinations of forcings examined in scenarios. "CC" refers to climate change. "Alt Conv" refers to alternative conveyance. "Flood Isl" is a multiple flooded island scenario.

Figure 2 describes the combinations of forcings to be examined in scenarios. We expect to explore three climate change scenarios approximating the “bookends” and the middle of the range of 10 GCM runs for the region. These 10 GCM runs were selected for providing reasonably faithful representations of California’s historical climate regime and for recording all GCM outputs that are required for producing all needed hydrodynamic model boundary conditions. The middle climate change scenario will then be paired with

the alternative conveyance and flooded island scenarios.

	Near-term	End of century
A. low-CC		wet, dry
B. mid-CC	wet, dry	wet, dry
C. high-CC		wet, dry
D. mid-CC+ alt conv	wet, dry	wet, dry
E. mid-CC + flooded isl	wet, dry	wet, dry

Figure 3 delves into more detail for the scenarios A-E described in Figure 2. Because computational speed limits the practical length of some (e.g. hydrodynamic, sediment, phytoplankton) model runs, we cannot perform full century-long runs. Instead, we must choose representative individual years from the century-long GCM projections for which we

will run the detailed Bay-Delta models. Runs will be paired so that near-term conditions can provide a baseline against which late-century runs can be compared. For each climate change scenario (low, middle, high), representative dry and wet years will be chosen from the GCM/hydrologic runs for both near-term and late-century. Because we do not expect the 3 near-term climate change runs to differ substantially from each other, we plan to only perform the middle climate change run for the near-term. The middle climate change scenario will also be used to force the alternative conveyance and flooded island scenarios, for both near-term and end-of-century.

Figure 3. Description of future scenario simulations.

Collaborative Modeling

Collaborative modeling approaches are needed to characterize and simulate the physical, biological, and chemical components of the Bay-Delta system.

Delta Science Program
Interim Science Action Agenda
2014

Through the course of this project, the CASCaDE team has received multiple requests to collaborate and share the modeling tools we are building. The Delta Independent Science Board and Delta Science program have stressed the importance of shared modeling capability for accelerating science and supporting science-based management of the ecosystem. We and our collaborators have taken these requests seriously, and have thus laid the foundation for broadly sharing many CASCaDE modeling tools. With the support and collaboration of the CASCaDE team and several other Bay Area scientists and organizations, Deltares has taken the initiative in establishing a “San Francisco Bay-Delta Community Model” website (see Figure 4 and <http://www.d3d-baydelta.org/>). Currently, the 2D flexible mesh hydrodynamic model for the Bay-Delta is downloadable for free from the site. Ultimately, the 3D hydrodynamic model and other Delft-based CASCaDE models will be available as well. We believe that this effort will provide an important step toward realizing the need for “collaborative modeling” identified in the Delta Science Program’s *Interim Science Action Agenda* (Action Area #16).

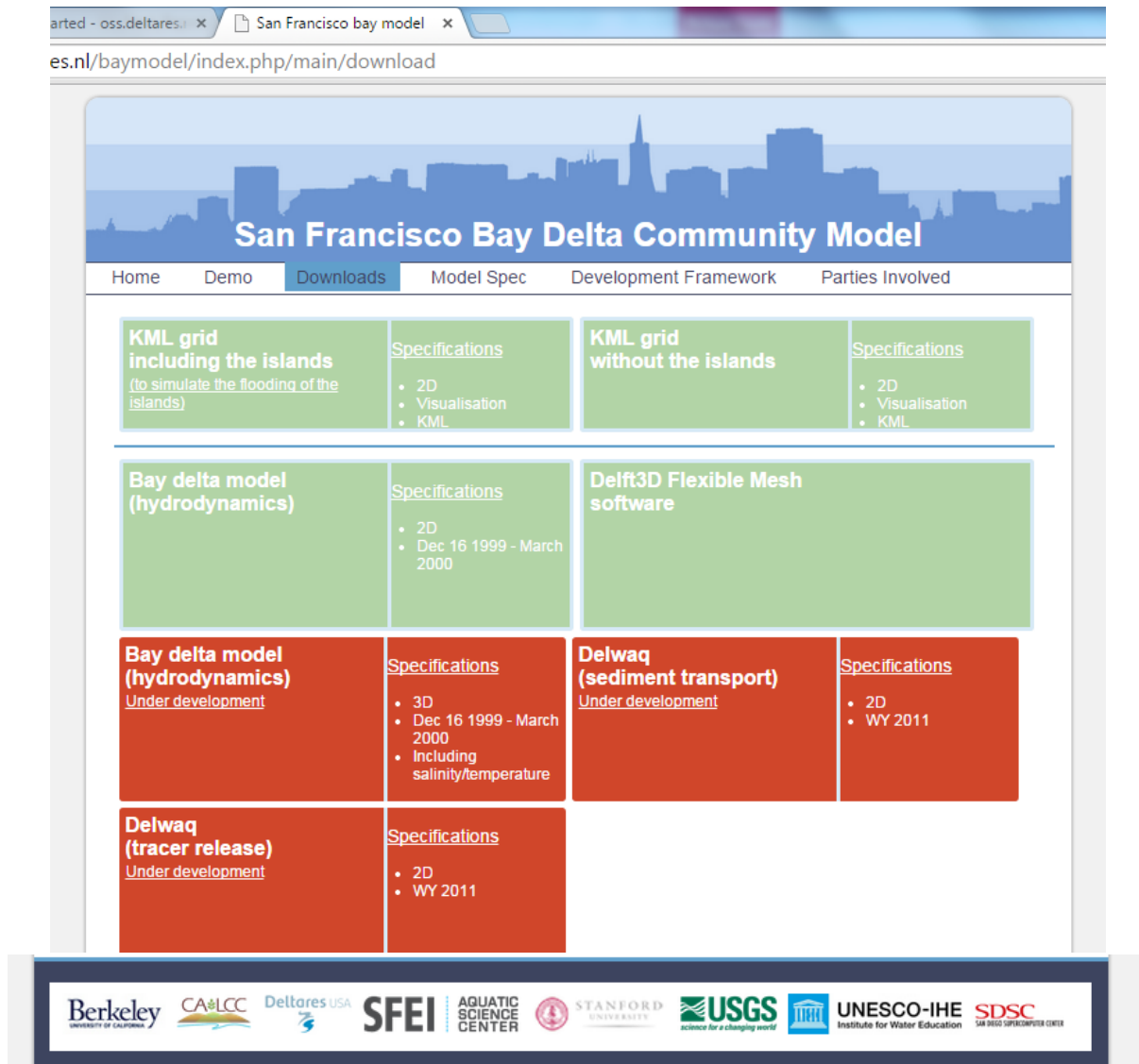


Figure 4. Deltares' San Francisco Bay-Delta "Community Model" homepage.

Acknowledgements

The CASCaDE project is grateful for major funding support we have received from the Delta Stewardship Council/Delta Science Program, USGS Priority Ecosystem Science, Hydrologic Research and Development, and National Research programs, and the San Francisco Estuary Institute. We are also grateful to our collaborators at Deltares, the USGS California Water Science Center, and University of California, and to our helpful

colleagues at the California Department of Water Resources and U.S. Bureau of Reclamation.

We thank the busy, knowledgeable, and helpful people who have taken significant time to advise us, including Jon Burau, Jim Cloern, Chris Enright, Ed Gross, Robin Grossinger, Cathy Ruhl, Deanna Sereno, Anke Muller-Solger, and Alison Whipple.

b. Lessons Learned: How the CASCaDE 2 process has worked

Numerous lessons have been learned by our team as this project has progressed. Here we summarize some of those lessons:

- **Integrated modeling software**— In CASCaDE I, our team used many models, some which they had prior experience with, some that were new to them, and some that had to be developed from scratch. Also, linkages between many of those models did not exist and needed to be developed. The hydrodynamic model implemented in CASCaDE I spanned only the Delta and Suisun Bay, and lacked connection to the coastal ocean. Although these choices were initially made with efficiency in mind, we ultimately learned that development of inter-model linkages can be resource intensive. We also realized that, with the addition of more ecological and physical process in CASCaDE II, inter-model linkages would become a larger issue. We thus opted to adopt a unified modeling framework with “built-in” linkages between many of the key models.
- **Use of new, cutting edge software**—For several reasons (see Section 1D, Task 1), the new Delft3D-FM (flexible mesh) modeling framework was selected as the core of Bay-Delta modeling in CASCaDE II. There have been several benefits as well as challenges associated with being among the first adopters of this new state-of-the-art software. Benefits include flexibility and adaptation of the software when needed, as well as attainment of the most appropriate and advanced tools for the science. However, we have learned that when using brand new software that is still under development, an interdisciplinary scientific team should expect: (1) unforeseen bugs; (2) frequent software updates containing significant code changes; (3) delays in readiness of “downstream” or dependent modeling software and inter-model linkage tools; (4) if multiple models are integrated, a major change in one model can require that all dependent models and tools be updated accordingly; (5) consequent delays in interdisciplinary modeling products. If implementing cutting edge models and data, it is recommended to double (at minimum) R&D time estimates. To decrease risk to downstream project tasks depending on upstream tasks that are strongly in R&D phase, those downstream research components may

select to not rely exclusively on the completion of work by other tasks. The responsive and collaborative relationship between software developers at Deltares and CASCaDE scientists has been essential to the significant progress made amidst the above challenges. (For a more detailed discussion of the advantages and challenges of our adopted estuarine modeling strategy, please also see Section 1D “*SFBD Modeling Strategy*”.)

- **Scientific coordination**—The time and human resources necessary for scientific coordination between tasks should not be underestimated. It is critical that the team has members that can serve as linkers, translators, and facilitators that can cross multiple disciplines and identify, bridge, and fill gaps between tasks. Time and human resources should be explicitly and generously allocated toward filling these roles.
- **Lack of synchronicity between project elements**—In part due to our adoption of a new, in-development software framework and the associated delays (see above), as well as other task-specific delays, many of our project elements were not synchronized with each other. This presented a significant challenge to several project elements. Many of the “downstream” tasks (water quality and ecology) have faced waiting an unpredictable amount of time for useable output from upstream tasks (e.g. climate, watershed, hydrodynamics). Fortunately, many of the downstream modeling elements exercised flexibility and resourcefulness that would move their science forward and provide increased data, process understanding, and model readiness for when upstream model outputs become available. Examples include:
 - The *Bivalve* task expanded its data set, allowing ultimately for (1) a more finely honed model, (2) testing of a preliminary model with calibration data, and (3) development of more robust conceptual models. This work has resulted in preliminary products that will ultimately be released to the public. Based on that data, two papers have been published and multiple presentations on conceptual models have been given.
 - The *Marsh* task charged ahead with its sensitivity analysis approach to assessing Delta marsh sustainability instead of using specific scenarios

depending on upstream model outputs. The sensitivity analysis work has been published (Swanson et al. 2015).

- The *Phytoplankton* and *Bivalve* tasks jointly conducted and published a simplified modeling analysis that was tailored to inform expectations of primary productivity in restored Bay-Delta habitats (Lucas & Thompson 2012).
- Before availability of a validated 3D hydrodynamic model, the *Sediment* task published a modeling study of 2D sediment dynamics in the Delta (Achete et al. 2015).
- *Fish* and *Bivalve* tasks have developed a suite of habitat suitability (HSI) curves for multiple species and environmental parameters in the Estuary. Bugs in the HABITAT software were identified and solved, and CASCaDE-specific software needs were identified and met by Deltares working closely with USGS partners. Habitat suitability software has been tested with preliminary model- and measurement-based datasets so the analysis tools are ready to roll when final model-based outputs are ready for habitat analysis.
- The *Contaminants* task published an analysis of a 17-year Selenium SF Bay data set (informed by preliminary Delft3D hydrodynamic model runs), expanded on that data set, and developed an analytical method for Se in water, particulates, and biota. The increased breadth of data and process understanding will inform upcoming model simulations.
- **Don't reinvent the wheel, but make sure it's the right wheel**—CASCaDE scientists developing the Bay-Delta bathymetry grid ultimately collaborated with scientists at DWR, evaluating, improving, and expanding a seamless bathymetric/topographic DEM that DWR created (based on an earlier USGS grid) and further adapting it to our project needs.
- **Keep perspective when prioritizing**—For example, are model errors that you are investing so heavily to correct going to be swamped by climate change signals? Efforts should be matched to scientific questions and to the forcings to be investigated.

- **Simpler models can fill in gaps**—In some cases, time or other resources may not allow for development of the “ultimate” model for characterizing a critical process or parameter, so a “Plan B” may be in order. Creative, simplified modeling approaches (such as the empirical point temperature model of Wagner et al. 2011, CASCaDE I) can fill critical gaps and substantially enhance overall project impact, when development of more complex models to perform a similar job is infeasible. This approach can also be useful when a more complex model already exists, but is too computationally demanding to run for desired simulation lengths. In some cases, shorter runs of the complex model may be used to develop simpler parameterizations or statistical models of important quantities. These simpler models may then be run for the full desired time period.
- **The necessity of frequent communication between tasks**—In a complex, interdisciplinary effort such as CASCaDE II, regular inter-task communication is necessary to make sure the needs of a downstream task are accounted for in the models and simulations of the other tasks. Project-wide meetings have been necessary biannually to develop rapport and workable cross-disciplinary understanding. The questions below are typical of those requiring ongoing discussion between two or more tasks:
 - *What quantities are important for the processes in each task?*
 - *What are the important time and space scales?*
 - *How long need runs be to capture critical behaviors? (E.g., what is the system memory for a particular task?)*
 - *What times of year are most important?*
 - *What levels of error and uncertainty are tolerable for specific quantities in terms of distinguishing different responses for a given downstream element?*
- **Don’t chase the momentary hot topic**—When developing the proposal, we found that it was important to be careful not to focus on issues that might be hot today but gone in two years. During the project, it is similarly important to avoid mission creep (stick to your plan; avoid chasing the big issue of the day).
- **Relevance to resource management**—Before the CASCaDE I proposal was ever written, a workshop was held by the science team to obtain feedback from the

management community and stake holders to help shape the proposed study. In early CASCaDE II discussions of future scenarios to be modeled, a team meeting was held, to which we invited several guests knowledgeable of the current Bay-Delta management and restoration scene. This was very useful. It has also been helpful to have many CASCaDE team members who are already familiar with management needs and plugged into the management community. Lastly, given the time required to develop a successful integrated ecosystem modeling system, as well as the fact that additional improvements and refinements will always be possible, it may be helpful to cast the goals of model development in terms of when the modeling tools will be “useful”, rather than when they will be “complete.”¹ What information would be useful to managers? What is the model skill required to deliver that useful information? What useful answers can be generated by the models by the end of the project?

- **Data translation**—Transformation of outputs and observations into input data for other models is not necessarily a trivial task. It is important to have project members with the necessary skills.
- **Data storage**—We have come to recognize the importance of planning ahead for data storage needs and methods of intra-project data sharing and ultimate distribution and publishing. These issues can be particularly complex when dealing with large datasets, cross-institutional collaboration, and federal/non-federal partnerships and related network security issues. This planning should include identification of funding to purchase necessary hardware.
- **Funding**—For large, multidisciplinary projects such as CASCaDE, it is important to understand that funding is being requested for the equivalent of multiple stand-alone projects, each with major R&D components, and for the additional work of linking all the efforts. This requires substantial long-term funding (5 years at a minimum). It is often the case in current funding environments that PIs of large projects such as this must severely limit the requested funding or see their proposal rejected. However, when an ambitious project starts with an overly tight budget, the PIs should expect

¹ From discussions with Prof. John Tracy (Univ. of Idaho) and Earl Green (USGS).

that the project may face difficult decisions on funding prioritization. This may result in limited personnel to perform the work and, consequently, longer timelines than initially expected.

- **History is important**—Several key ingredients were necessary to make a “CASCaDE” possible: (1) a history of extensive data collection in this estuary; (2) a rich history of built ecosystem knowledge and process understanding in this estuary; (3) a team of scientists (many of whom contributed significantly to #s 1 and 2) with a history of working together productively, supportively and generously (and liking it!); (4) funding to get those scientists working on a common problem at the same time and to sustain the effort.

c. Computing Resources & Data Management

Computing Resources

At the proposal stage, we realized that the hydrodynamic modeling component of CASCaDE would require significant computing resources. We included funding for a local computing cluster (named “Swift”), which has proven an essential tool in testing and applying Delft3D-FM. We also included a colleague at the San Diego Supercomputer Center, John Helly, as a team member, a connection which has proven very useful. In addition to having access to John’s expertise and experience in a wide range of disciplines, he has facilitated access to supercomputing resources in San Diego (Gordon supercomputer) and Texas (Stampede supercomputer), which have also proven to be essential resources in accomplishing the many testing and development runs of Delft3D-FM, as well as in performing initial scientific “production” runs. Access to this many high-performance computing platforms was not initially anticipated, but it has proven critical to achieving progress in this project component.

An unforeseen need with regard to running the Delft3D-FM model was storage. We did not anticipate the roughly 100TB storage requirement that has become evident as we understood the amount of output data that needed to be retained for use by other modeling components. USGS (NRP) provided internal funding to obtain a 100TB storage unit for this purpose.

A secondary problem arose because key collaborators needing access to these large data files were located remotely, in fact internationally. The solution we are working with IT staff to implement is to provide a dedicated computer locally with access to the 100TB storage unit that our international colleagues may access remotely. They may run their own models on this machine using the large datasets output from Delft3D-FM as input, and post-process the resulting output files remotely. They may then transfer the (relatively small) resulting data files through standard secure methods such as sftp.

With these adjustments and procurements, we believe we have achieved comprehensive solutions to our computational, storage and data-exchange needs with respect to the very large datasets produced by the Delft3D-FM model. However, there

are many other smaller datasets that must be exchanged between project components during the project (while keeping track of dataset versions and other metadata), and ultimately shared externally and published as the project is completed. For that, we have turned to our team member, John Helly, who has extensive experience in such data management issues.

Scientific Data Management

John Helly, UC San Diego-San Diego Supercomputer Center (submitted 06-04-15)

Scientific data management has important requirements that are often under-appreciated outside of the world of practicing scientists and, unfortunately, often within. The scientific method requires the ability of arbitrary, unspecified individuals to verify and validate the results of any given piece of scientific research. This is commonly called reproducibility of results. In order to ensure that this capability is protected, it is incumbent on the individuals performing the original work to (1) document their methods in written form, (2) provide the data, (3) metadata, and (4) software necessary to reproduce the results. This turns out to be more challenging than many scientists appreciate.

Ensuring that these criteria are met and that the platform (i.e., software and hardware) originally used is sufficiently described is necessary so that others have enough information to reproduce results. This has implications that reach into the depths of the cyberinfrastructure resources since modeling and analysis capabilities often have complex dependencies on file formats, operating systems and software libraries that require highly-specialized knowledge of computing systems to adequately specify all pertinent information. Fortunately, there are methods developed at the San Diego Supercomputer Center (SDSC) to help cope with these requirements and we have been able to apply them to the CASCADE 2 project and they are briefly summarized below as they pertain to this project.

Data Publication via the California Coastal Atlas

Data publication using the [California Coastal Atlas](#) (CCA) provides an end-to-end process (Figure 5) for the quality control of digital scientific data, actually any kind of data, using the same basic workflow followed for scientific manuscript publication but with some modifications to account for the wide variability in types of scientific data, software and methods. This diversity illustrates the generality of the data publication methods across a wide range of scientific domains from deep-sea ocean drilling to atmospheric science. The data publication process includes: (1) acquisition, version control, assignment of digital object identifiers (DOIs), registration with cross-referencing services and packaging, (2) automated metadata production, (3) multi-lateral metadata interfaces, and (4) distribution to end-users through the Internet. The CCA provides a convenient method of navigating the search space for whatever data is available and the data, which can be voluminous, is then delivered via the Git version control system using standard open-source tools. Git is interoperable across all major computer platforms and is a very efficient means of ensuring data synchronization across a wide-range of users.

Applicability to the CASCADE 2 Project

Within CASCADE 2, as in most scientific projects, there is a need to share data across a multi-disciplinary team as well as providing open-access to data developed with public funding. The ability to share intermediate results, as well as to publish final results, is essential to cooperation and collaboration as intra-disciplinary research evolves and integration of results develops. The integration of data provides insights and feedbacks that cannot be achieved in other ways and provides a focus for understanding.

Git-based Data Acquisition & Version Control

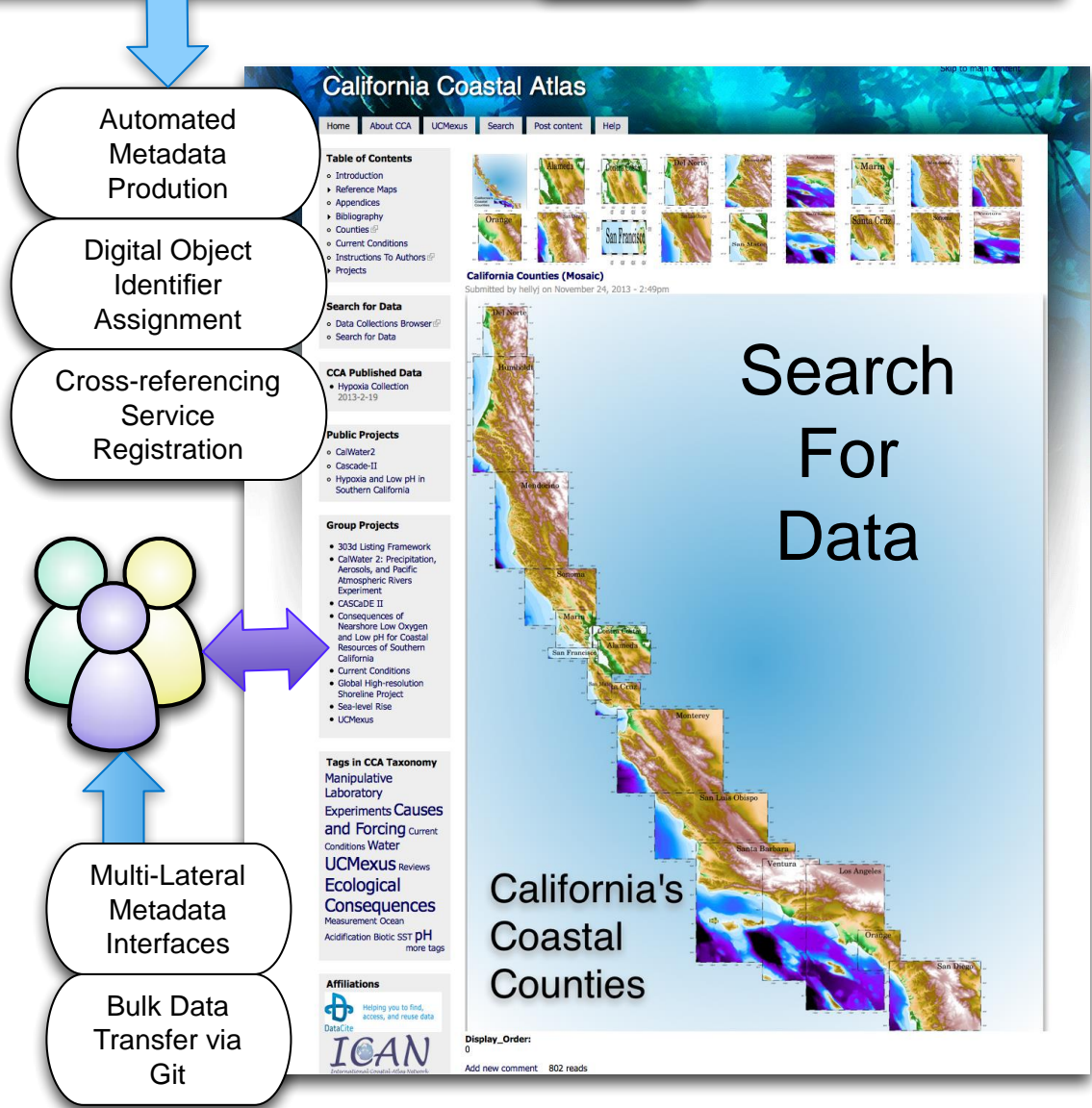
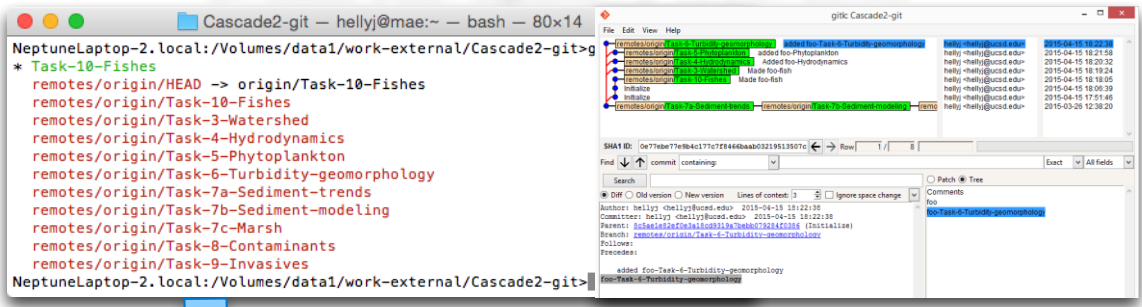


Figure 5: Data publication workflow and distribution via the California Coastal Atlas web-site. This infrastructure has been applied to a wide-range of other scientific disciplines.

d. Task-by-Task Science

Task 1: Project Administration & Coordination

Lisa Lucas and Noah Knowles

Project Structure, Communication and Coordination

The CASCaDE 2 scientific team comprises 36 members hailing from across California and the Netherlands. Institutions represented by this team include:

- Three USGS offices
 - National Research Program (Menlo Park)
 - Pacific Coastal and Marine Science Center (Santa Cruz)
 - California Water Science Center (Sacramento)
- Four academic institutions:
 - University of California, San Diego/San Diego Supercomputer Center
 - San Francisco State University
 - California State University, Sacramento
 - UNESCO-IHE (Institute for Water Education, Delft, The Netherlands)
- One non-profit research institute: Deltares

Two graduate students (Achete, Stern) and two postdoctoral researchers (Martyr, Swanson) have been supported through this project.

Given the spatial scattering, disciplinary breadth, number of team members, and the need for individual tasks to ultimately link to others, biannual whole-team meetings have been necessary throughout the project term to ensure broad coordination among tasks. These team meetings not only provide the opportunity for task teams to update the larger team, but also have been critical for identifying challenges/needs/linkages that must be addressed, proposing solutions, and producing valuable insights and ideas for task teams to take from the meeting and run with. Also, frequent smaller within-task and task-to-task meetings, conference calls, and email exchanges have ensured that technical issues are worked out and linkages between tasks are accomplished. In

addition, several US team members have visited collaborators in Delft and vice versa over the course of the project. These in-person opportunities to work together have been invaluable in helping us clear significant technical hurdles, as well as establish collegial working relationships that continue thereafter primarily over email, Skype, and phone.

Coordination of this large complex project has been shared by Knowles and Lucas. In addition to the typical budgetary, hiring, reporting, and other administrative duties, we have filled an important project need as scientific coordinators. Since the end goal of CASCaDE is not a collection of individual models but rather the application of a web of *linked* models (Fig. 1), task teams cannot operate completely independently. Rather, R&D of individual models and design of simulations must account for the needs of other tasks. In many cases, the development of additional intermediate tools has been required to accomplish task-to-task data translation. As the project progressed, we found that related tasks often needed help in coordinating their efforts and bridging gaps to ensure all data needs were met. Although this need was not foreseen at the project's outset, Knowles' and Lucas' respective and combined scientific expertise has been serendipitous in this respect. Knowles' expertise spans climate-hydrology-hydrodynamics, and Lucas' expertise spans hydrodynamics-water quality-ecology. This scientific proficiency in complementary areas has allowed Knowles and Lucas to act as translators between tasks across the project's disciplines and aided in identifying, understanding and shepherding solutions to linkage gaps between tasks. We mention this primarily as guidance (or warning) to similar future efforts that the role of cross-disciplinary coordination of tasks should be built-in to such projects at the proposal stage.

Funding

Major funding sources for CASCaDE 2 over the last 4 years (federal fiscal years 2011-2015) are summarized in Figure 1-1. The Delta Stewardship Council/Delta Science program contributed almost one-third (\$1.5M) of the funding over the past 4 years, and USGS contributed more than two-thirds (\$3.6M). USGS funding has been provided by the Priority Ecosystems Science and Hydrologic Research & Development programs.

In the last year, the San Francisco Estuary Institute also contributed key funding (\$100K) at a critical juncture, providing additional support toward temperature and ecological model development. Funds for several tasks on this project have been heavily leveraged, and this budget breakdown does not account for additional funding sources that have supported individual tasks. [Note: FY11-FY14 USGS contributions in Fig. 1-1 are based on our original proposal budgets; the FY15 USGS contribution is estimated by taking the FY14 amount from our original proposal budget and increasing by 1% for cost of living increases.]

PES funding is projected to be the same in FY16 as in prior years. We applied for and received \$70K from a USGS Bay-Delta Supplemental Funding RFP; this supports further work on the watershed sediment model (Task 7b), 3D Bay-Delta sediment model (Task 6), and hydrodynamic/temperature model (Task 4). In the coming year, SFEI and USGS-PES together will support hydrodynamic modeling (salary for hydrodynamic postdoc, Martyr).

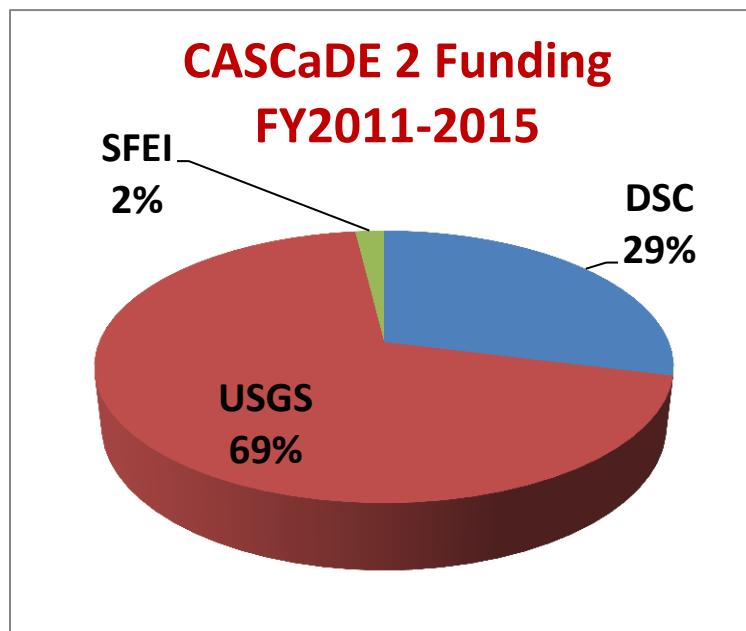


Figure 1-1. Approximate breakdown of major CASCaDE 2 funding sources for the 4-year period comprising federal fiscal years 2011-2015. See text for details.

SFBD Modeling Strategy

Climate-driven forcing of the SFBD arrives from three directions—the watershed, the ocean, and the atmosphere (Figure 1-2). All of these forcings are significant and changing. CASCaDE was designed to produce mutually consistent projections of these forcings under multiple scenarios of future change. To understand the response of the estuary to these multiple changing forcings, we needed an estuarine model or models capable of simulating all relevant quantities across an integrated river-to-coastal-ocean spatial domain. A second design objective for the project was, to the extent possible in this phase, to characterize a maximum number of estuarine physical and ecological processes within a single common modeling framework. (In other words, of the processes the CASCaDE 2 team chose to model, we aimed to maximize the number of models housed under a single modeling “roof” and across a single spatial domain.) A third objective was to implement state-of-the-art tools that were non-proprietary and relatively user-friendly, thus providing a foundational SFBD research platform well into the future. Given the plethora of critical interdisciplinary science questions facing Bay-Delta managers and requiring models, a fourth objective was to build an integrated modeling toolkit for the SFBD that could be expanded to incorporate more ecological processes in the future. Significant effort was expended before ever drafting our DSP proposal to explore various model framework options vis-à-vis these objectives.

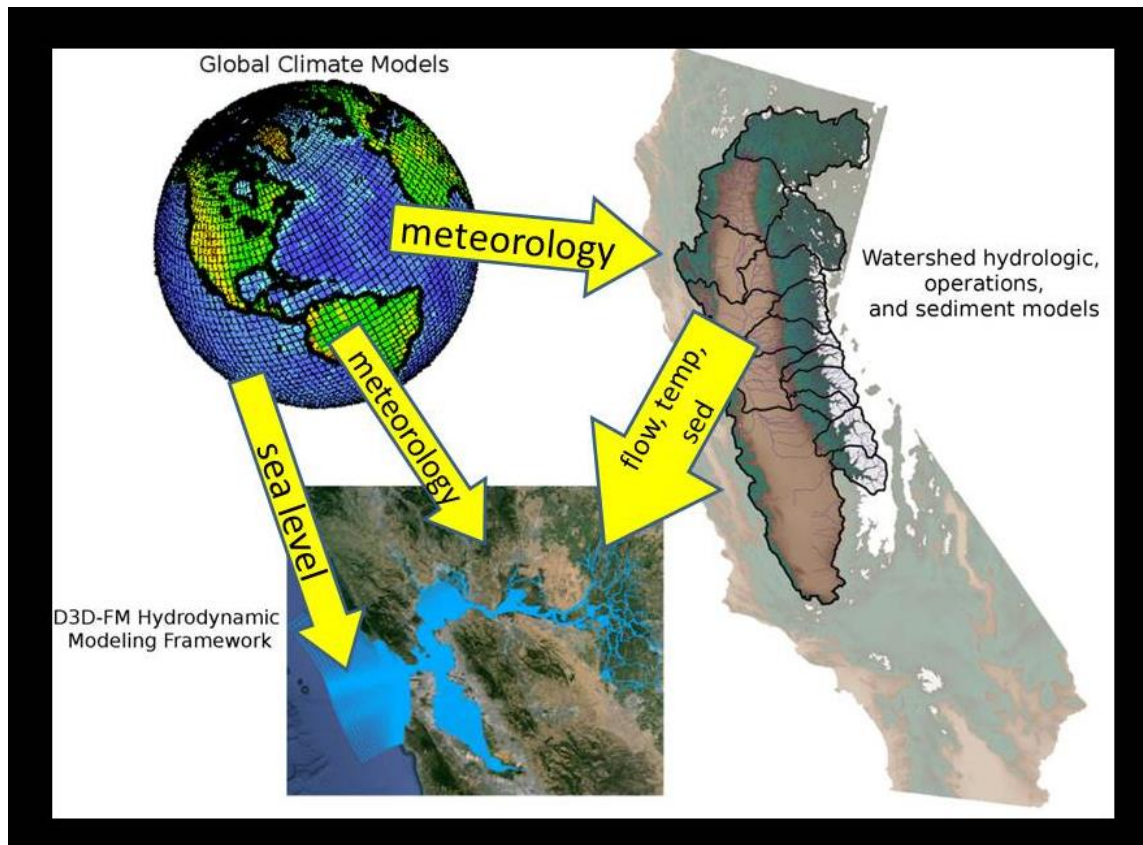


Figure 1-2. Schematic describing the paths of climate influence on the Bay-Delta and how, in simplified terms, those influences are characterized in CASCaDE.

After careful consideration of several options, Deltares’ new Delft3D-FM software was chosen as the hydrodynamic foundation for most Bay-Delta modeling in CASCaDE 2. The state-of-the-art flexible mesh (“FM”) allows for concurrent use of curvilinear and unstructured grid sections, a capability ideal for the Bay-Delta’s blend of broad open water habitats and narrow sinuous channels. The Delft3D-FM software is being released under an open-source license. Deltares’ tools are well-known for providing straightforward coupling of hydrodynamics to a variety of widely used water quality and ecological modules, including modules for suspended sediment, phytoplankton, and grazers (priorities for this project and for the Bay-Delta ecosystem). In addition, state variables and processes that are beyond the scope of the current effort (e.g. nutrients, dissolved oxygen, contaminants, macrophytes, microphytobenthos) can be incorporated in the future with existing modules. Extensive graphical interfaces, and post-processing and visualization tools are available for use with Deltares models. Moreover, scientists

and developers at Deltares were keen to collaborate on this project in this important ecosystem.

Selection of the Deltares flexible mesh model and associated tools provided a common focus for several separate project tasks. The Delft3D-FM software has provided the advantages of getting team members thinking and working towards a uniform way of modeling and dealing with similar types of data. It also provided many “automatic” linkages between models (e.g., once the FM version of the water quality/ecology engine DELWAQ was developed, it could read in and implement FM hydrodynamic model outputs for calculating transport of sediment and phytoplankton, without much fuss on the part of the user).

The Delft3D-FM software (hydrodynamic and water quality) has been under development during the CASCaDE project, which allowed for flexibility and adaptation of the software when needed. A drawback was that project progress has depended on software development and adaptation (of which timing appeared difficult to predict). For example, multiple project tasks have depended on hydrodynamic runs to carry out their work on water quality dynamics or ecological processes. Delays in the hydrodynamic software development—and thus hydrodynamic simulations—have affected progress for other tasks. Moreover, delays in development of the new hydrodynamic model translated into additional time needed for adaptation of compatible temperature and water quality/ ecology modules and the tools required to translate data between them.

The decision to implement the new Deltares FM modeling platform in CASCaDE has thus involved trade-offs:

- off-the-shelf, well tested readiness of established software *versus* the newest (though in-development and less tested) technology most appropriate to our science problem and deferment of obsolescence
- development/implementation of our own in-house code (for hydrodynamics, ecology, or both), which would:
 - require significant R&D time to start from “scratch”

- be immediately and thoroughly understandable to the scientist-developer (though not necessarily to other users)
- be easily adapted to project needs by the scientist-developer (though not necessarily by other users)
- be limited in its achievable complexity (esp. for ecological processes)
- require significant inter-model linkage effort
- require development of all necessary accoutrements (pre- and post-processing, visualization, etc.)

versus

application of software developed externally, which would:

- allow team members to focus more on *adaptation* and *application* of models than *development* of model code
- be less immediately understandable (more of a “black box”) and less readily adapted than code developed by scientist-users
- offer significant modelable process richness
- incorporate built-in model coupling designed for interdisciplinary problem solving
- be accompanied by user interfaces, pre- and post-processors, plotting and visualization capabilities
- provide an opportunity for close collaboration with Deltares’ modelers and developers
- be founded on the reputation and decades of experience behind Deltares model development

As some of the first practical users of this new software—and as users with significant and specific needs—CASCaDE team members have been at the forefront of discovering software bugs and requesting advanced model and linkage capabilities. For example, our need to maximize run length (and thus computational efficiency) has required a major joint Deltares-UCSD-USGS focus on parallel computing capability for hydrodynamics, as well as the development of new tools (by Deltares) for post-processing of parallel outputs before they can be used by other tasks. When working with brand new integrated modeling software and needing that software to satisfy a

demanding set of requirements, these are all necessary (though not all foreseen) steps, and all these steps necessarily take time. Many of these challenges have been met and solved over the project period through close, collegial, and responsive collaboration between Deltares developers, UNESCO-IHE scientists, and team members in California. The products of these efforts will be available for application to science questions and projects post-CASCaDE 2.

Task 2: Climate modeling and downscaling

Dan Cayan and Mike Dettinger (submitted 07-20-15)

Cayan (USGS and Scripps Institution of Oceanography, UCSD), Dettinger (USGS) and colleagues at Scripps Institution of Oceanography have downloaded and processed California data, and evaluated and selected a (sub)set of CMIP5 global climate model (GCM) simulations from the IPCC fifth assessment report (CMIP5 or AR5 GCMs). This effort follows previous work in which of a large set of downscaled scenarios, from both the CMIP3 (4th IPCC Assessment) and CMIP5 (5th IPCC Assessment) has been publically released, described in the Maurer et al (2014) paper that was recently accepted for publication in the Bulletin of the American Meteorological Society (BAMS). The CMIP5 models were evaluated according to their ability to represent (statistically) the observed climate variability over the region. The group implemented a procedure to eliminate models whose historical simulations depart so much from present day climate patterns that they are judged to not be trust-worthy, along with other issues. The result is a set of 10 GMCs that appear to be suitable for California climate and water resources assessment and planning.

With Scripps colleague David Pierce (lead developer), Cayan we developed a new statistical downscaling scheme. This downscaling method is localized constructed analogues ("LOCA"), which was used to translate the larger scale GCM simulations to regional scale landscapes. LOCA has improved abilities to replicate historical spatial and temporal variability, including extreme events. This new downscaling scheme is a major revision of existing analogue downscaling that improves the ability to simulate extremes and also the spatial structure of regional simulations. Pierce and colleagues also developed a newly developed, frequency dependent bias correction method which is part of the LOCA implementation. Using the new downscaling scheme and a 1/16th degree (6km) resolution gridded dataset produced by Ben Livneh, we have downscaled temperature and precipitation over Bay Delta and watershed region using LOCA (Pierce et al 2014) downscaling at 1/16° resolution for the 10 selected GCMs plus several others for two emissions scenarios (RCP 8.5 and RCP 4.5). The model runs include a 1950-2010) historical component as well as a projection over the remainder (2011-

2100) of the 21st Century. Development of LOCA statistical downscaling and frequency dependent bias correction was supported by the California Energy Commission, the U.S. Army Corps of Engineers, the USGS through the CASCaDE 2 project, as well as the Southwest Climate Science Center, and the NOAA RISA program through the California Nevada Applications Program. Collaboration with the U.S. Bureau of Reclamation in evaluating results and supporting a data archive is also an essential contribution to this effort. These downscaled data were made available to N. Knowles, and by extension, to the CASCaDE II team.

Using the LOCA downscaled precipitation and temperature data as input, we have run the VIC macroscale hydrological model over the California region (and specifically the Bay/Delta watershed for each of the 10 GCM simulations, including both RCP 4.5 and RCP 8.5 scenarios. The VIC model output includes daily values of runoff, soil water, snow water, and other hydrologic measures over the same 1/16th degree grid as the LOCA precipitation and temperature input data. The VIC simulations included both the historical (1950-2010) period for each of the 10 GCMs and projected 21st Century simulations for the 10 GCMs for both RCP 4.5 and RCP 8.5 scenarios.

We have also worked to produce hourly sea level rise projections for San Francisco using input from a GCM. These sea level model projection are derived so as to be temporally consistent with the weather and climate that is produced by that GCM, making realistic phasing of anomalous sea level variability with Bay-Delta-watershed hydrological forcing. Thus far, these sea level projections have been produced from eight members of the GCM subset that has been identified as well suited for California climate and water resources assessments. The sea level projection model includes tides, weather and short period climate input (after Cayan et al. 2008) which are superimposed upon an assumed trajectory of sea level rise, in this case the NRC (2012) “Committee” mid-range sea level rise projection.

Mike Dettinger is continuing to investigate the historical roles of atmospheric rivers (AR) in flooding, levee breaks, (Yolo Bypass and Consumnes) floodplain inundations – these have now been documented in a book chapter (Florsheim and Dettinger, 2015). This chapter also includes initial analyses of the ways that flood conditions and seasonality

at the Delta have been modified by upstream water management, and those analyses continue. More recently, Dettinger has evaluated the role of atmospheric rivers, and large storms more generally, in the making and breaking of California's recurring multiyear droughts and pluvial periods, finding that almost 90% of the year-to-year variability in annual precipitation is attributable to presence or absence of the wettest 5% of all storms in each year and 75% is attributable to the arrival or not of atmospheric-river storms (Dettinger and Cayan 2014; Dettinger, in review at WRR). Evaluation of the corresponding relations in projections of future climates shows that similar relations are broadly reproduced in current climate models, and projected changes in northern California precipitation differ from model-to-model in response to complex interplays between model-specific tendencies toward more or less increase in the contributions from largest storms versus an essentially universal (among the 10 models considered) tendency for contributions from all other (smaller) storms to decline as global warming takes hold (Dettinger, in review).

Dettinger and Cayan have also contributed papers and discussion involving climate change and regional climate and hydrology relevant to the Bay/Delta along with extreme events including flooding. Dettinger is investigating new global climate projections from some dozen GCMs used in the CMIP5 archive (each responding to two separate emissions scenarios) are being analyzed to identify the ways that future frequencies, intensities, and meteorological conditions in these kinds of AR storms (and ultimately floods) are likely to evolve under climate change. They have also investigated coastal weather namely cloudiness variability (Schwartz et al 2014) and the climate and weather associated with drought in California, with application to the current prolonged dry spell.

References

Cayan, D., Bromirski, P., Hayhoe, K., Tyree, M., Dettinger, M., and Flick, R. 2008c. Climate change projections of sea level extremes along the California coast. *Clim. Change* **87**(0): 57-73.

Dettinger, M., and D.R. Cayan, 2014: Drought and the California Delta - A Matter of Extremes. *San Francisco Estuary and Watershed Science*, **12**(2), 7 pages.

Dettinger, M.D., *in review*, On the relations between large storms and droughts in California: Water Resources Research, 29 p.

Florsheim, J.L., and M.D. Dettinger, 2015: Promoting Atmospheric-River and Snowmelt Fueled Biogeomorphic Processes by Restoring River-Floodplain Connectivity in California's Central Valley. Chapter 6 in *Geomorphic Approaches to Integrated Floodplain Management of Lowland Fluvial Systems in North America and Europe*, Hudson, P.F., and H. Middelkoop (editors), 119-141. DOI 10.1007/978-1-4939-2380-9_6.

Maurer, E.P., L. Brekke, T. Pruitt, B. Thrasher, J. Long, P. Duffy, M. Dettinger, D. Cayan and J. Arnold, 2014: An Enhanced Archive Facilitating Climate Impacts and Adaptation Analysis. *Bulletin of the American Meteorological Society*, **95**, 1011-1019. DOI:10.1175/BANS-D-13-00126.1.

National Research Council, 2012. Sea-level rise for the coasts of California, Oregon, and Washington: Past, present, and future. The National Academies Press. Washington, D.C. 201 pp.

Pierce, D.W., D.R. Cayan and B.L. Thrasher, 2014: Statistical Downscaling Using Localized Constructed Analogs (LOCA). *Journal of Hydrometeorology*, **15**, 2558-2585.\

Schwartz, R.E., A. Gershunov, S.F. Iacobellis and D.R. Cayan, 2014: North American west coast summer low cloudiness: Broad-scale variability associated with sea surface temperature. *Geophysical Research Letters*, **41**, 8 pages, online article, DOI:10.1002/2014GL059825.

Task 3: Watershed modeling

Noah Knowles and Collin Cronkite-Ratcliff (submitted 11-19-15)

Background

The primary goal of Task 3 is to translate the daily precipitation and temperature fields, produced in Task 2 using the LOCA method, into estimates of daily managed (i.e., reflecting the influences of reservoirs, diversions, groundwater pumping, etc. under a set of management goals and criteria) downstream flows at points throughout the watershed. This was done for the 20 future scenarios selected and processed in Task 2 from the CMIP5 GCM ensemble. A set of managed flow “hindcasts” will also be produced for the historical observation-based Livneh dataset using the same modeling tools, providing a historical baseline for comparison with future scenarios. These managed flow projections will then serve as inputs for the Sacramento watershed sediment model developed in Task 7b, and managed flows from a subset of the future scenarios will be used to drive the D3D-FM hydrodynamic model of the Bay-Delta estuary.

To produce the managed flow estimates, a combination of models was used to simulate managed streamflows at relevant points throughout the watershed. First, as part of Task 2, the VIC hydrological model was driven by the gridded meteorological datasets downscaled using the LOCA method (also produced in Task 2) from GCM outputs. In the present task, the resulting simulated fields of gridded unimpaired surface runoff and subsurface flow were routed to produce unimpaired streamflow estimates using the VIC routing model RVIC.

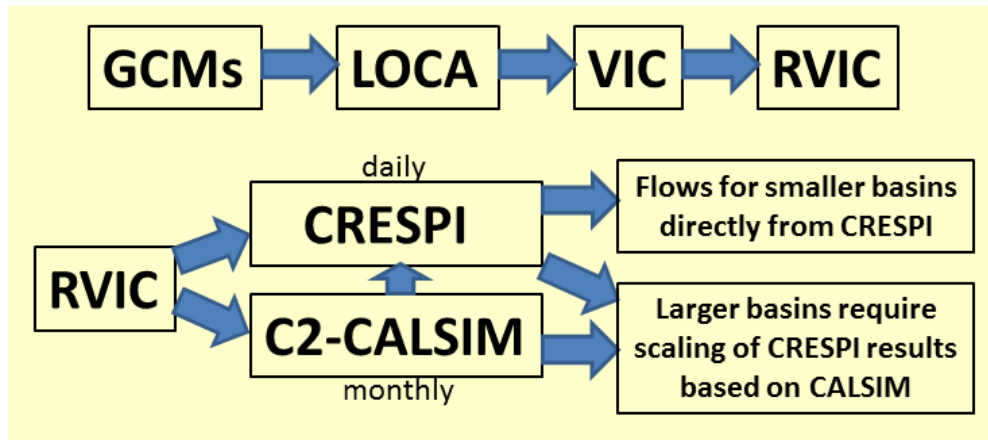


Figure 3-1. Flowchart for production of managed daily flows at points throughout the Sacramento River basin.

The unimpaired streamflow estimates were next translated into managed flows by a combination of two methods. First, the freshwater management operations model developed jointly by the California Department of Water Resources and the U.S. Bureau of Reclamation, CalSim II, was driven by inputs derived from the RVIC unimpaired flows. This produced corresponding estimates of monthly-averaged managed streamflows at outflow points of larger basins throughout the watershed. An algorithm to estimate daily managed flows, CRESPI (for Cascade RESamPling), was implemented using both RVIC and CalSim II outputs as inputs. CRESPI produces daily flow estimates by drawing from recent historical flow patterns and using the other models' outputs to drive the pattern selection process. CRESPI's strength lies in its representation of daily flows (as opposed to CalSim's monthly time scale). However, because CRESPI is limited to the historical flow regime, the resulting estimates of daily managed flows do not always faithfully represent the likely response of freshwater operations to long-term trends in flow patterns associated with long-term meteorological trends present in the GCM outputs. For smaller basins, this was not considered an important shortcoming, primarily because the contribution of those basins to the overall sediment and flow budgets of the entire Sacramento watershed (there were no smaller basins in the San Joaquin watershed studied in CASCaDE 2, just the watershed's total outflow) is relatively small. Also, smaller basins are typically not represented in CalSim II. Therefore for smaller basin outflows, the CRESPI results were used directly. However, for larger basins, it was necessary to scale the CRESPI output to more

closely represent the response of operations to long-term trends as represented in the CalSim II output. This scaling was the last step in the translation of daily meteorological quantities projected by CMIP5 GCMs into corresponding projections of managed daily flows at points throughout the Bay-Delta watersheds. Each of the steps of this procedure that were developed and conducted as part of the present task is discussed in more detail below.

RVIC Unimpaired Streamflow Simulations and Post-Processing

Applying RVIC

RVIC is a streamflow routing model designed to accept gridded VIC outputs and generate daily, unimpaired streamflow estimates at prescribed points on streams and rivers. RVIC was driven using the gridded baseflow and runoff output from the VIC hydrological model produced in Task 2. This was done for each of the 20 GCM scenarios for the period 1950-2099 (10 GCMs x 2 emissions scenarios). Additionally, a historical (1950-2013) “baseline” run of RVIC was performed using VIC output driven by the gridded, observation-based meteorological dataset produced by Livneh.

The RVIC model was set up by Knowles over the California-Nevada domain (corresponding to the domain of the Task 2 VIC runs), and configured (configuration and setup details will be documented) to produce routed daily streamflows at the numerous locations throughout the Bay-Delta watershed needed for the CASCaDE project:

- 16 locations for producing boundary conditions for the watershed sediment model (for Task 7b)
- 6 locations for producing Delft3D-FM inflow boundary conditions (for Task 4)
- 10 locations for use in generating multiple CalSim II water-year indices (present task)
- 34 locations for use in generating monthly inflows to drive CalSim II scenario runs (present task)
- 1 location (Shasta reservoir inflow) for use in computing Shasta reservoir target storages as part of the algorithm to convert CalSim II monthly outputs to daily

flows (present task)

With some overlap between locations needed for different purposes, daily unimpaired streamflow time series at a total of 57 locations were produced for the baseline (1950-2013) and for each of the 20 scenarios (1950-2099).

Bias-correcting unimpaired flows for use in producing CalSim II water-year indices

Once these unimpaired flows were produced, additional processing was needed. The historical baseline VIC model output produced in Task 2 generally compares favorably with observation-based unimpaired streamflow estimates (Figure 3-2).

However, because this implementation of the VIC model is largely uncalibrated, there are some systematic errors in its output which must be corrected if accurate unimpaired flow estimates are required. In particular, low flows are underestimated and high flows are overestimated by the VIC model (Figure 3-2, lower panel).

More accurate unimpaired flow estimates at the monthly scale were needed at 10 of the RVIC streamflow output sites to generate water-year indices used by the CalSim II model (discussed below). To achieve this, a quantile-mapping bias correction (QMBC) was applied to the RVIC streamflow outputs.

To apply QMBC, reference unimpaired flow time series for a historical period, assumed to be accurate, are needed. Reference monthly unimpaired flow data were obtained for all 10 locations used in the calculation of water-year indices needed for CalSim II. The source for these data was the California Data Exchange Center (cdec.water.ca.gov). At each flow location, the simulated historical baseline flows (based on the Livneh meteorology) for the time period covered by the reference data were extracted and paired with the reference data for use in generating maps between the two.

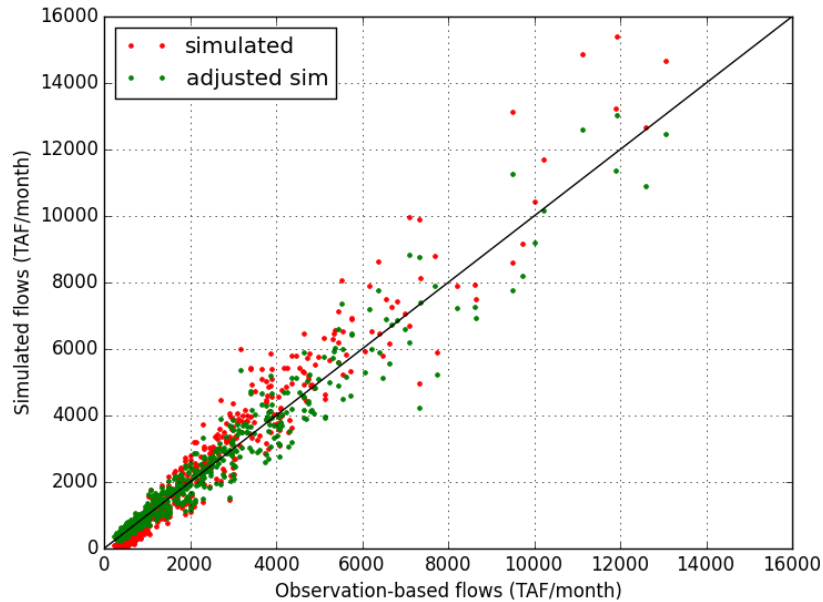
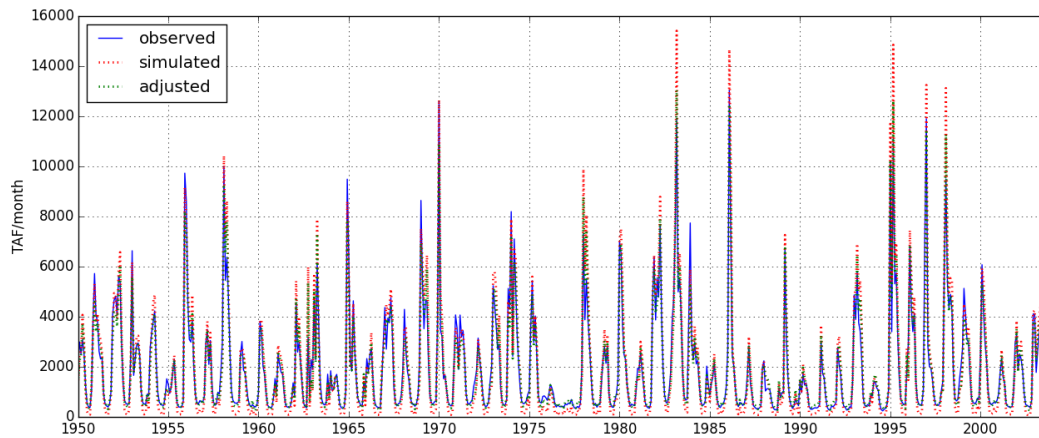


Figure 3-2. Simulated (VIC+RVIC) and estimated unimpaired Sacramento River basin total monthly flows versus time (upper), and versus each other (lower). Bias-corrected flows are shown as green dots on both panels. Unimpaired flow estimates are from CDWR (2014).

The QMBC method consists of, for each flow location, first estimating values that correspond to regularly spaced quantiles of the empirical cumulative distribution functions (CDF) for that location’s pair of historical simulated and reference time series (20 quantiles are used in this study). Then, using simulated future-scenario time series, a quantile is generated for each simulated daily flow value by interpolating of the flow values corresponding to the two nearest mapped quantiles. Finally the bias-corrected

flow value, corresponding to the same quantile in the reference data, is determined by interpolating between the two nearest quantiles in the reference data CDF. In this way, the entire simulated future-scenario time series is bias-corrected (see example of bias-corrected historical flows in Figure 3-2). [Note: for the software used—the qmap package in R—it was necessary to subtract the minimum flow of simulated and reference time series (i.e., the minimum of both time series concatenated together) from both time series to avoid spurious zeros in the results.] If this bias correction were applied to the same historical simulated flow data used to generate the mapping (instead of to the future simulated flows), the empirical CDF of the resulting corrected time series would match that of the reference data. This approach assumes that biases in the historical simulation remain the same in future simulations. Additionally, in future scenarios, any peak flows higher than the highest flow produced in the baseline simulated flows are “corrected” using the additive correction corresponding to the highest quantile in the historical mapping. This is a necessary approximation given the difficulty in implementing more sophisticated methods due to the prohibitively small length of available unimpaired monthly flow estimates (Boe et al. 2007). Future work will explore a more sophisticated approach to bias-correcting future scenarios that preserve changes in statistical moments relative to current climate (e.g., Li et al. 2010).

Application of QMBC to GCM precipitation output has been shown to have the potential to alter trends relative to the uncorrected data (Pierce and Maurer 2014). It is unclear what the effect of QMBC on trends in simulated streamflow might be. However, since the bias-corrected data are to be used here as monthly averages to calculate indices which largely portray broad annual flow categories, the importance of this shortcoming is likely minimal. Nonetheless, evaluation of the effects of QMBC on trends in the annual timing and magnitude of runoff, as well as in other parameters such extreme-flow frequency, will be undertaken in subsequent work.

Transforming unimpaired RVIC flows to managed flows for use as CalSim II flow inputs

The RVIC outputs needed to generate altered CalSim II flow inputs for historical baseline and future scenario CalSim II runs required transformation based on historical

CalSim II input data, which represent impaired flows at the model's boundary points (more on CalSim II in the next section). To generate CalSim II inputs for future scenarios, a mapping between historical baseline RVIC outputs (Julian years 1950-2013, based on the Livneh data) and CalSim II inputs representing impaired inflows from upstream basins (assuming modern infrastructure and freshwater demands in those basins for the whole time period) which were developed for CalSim II by California Department of Water Resources for the period covering water-years (WY: Oct 1-Sept 30) 1922-2003. The mapping was developed for 34 locations representing nearly all of the freshwater input to CalSim II (Table 3-1) using the water years contained in both datasets, WY1951-2003.

The mapping between the 34 RVIC output and CalSim II input time series was achieved again using QMBC as described above, except that in this case, separate mappings were developed for each location for each quarter of the calendar year. This refinement was added because unlike the previous flows mapped using QMBC, wherein fairly consistent systematic biases of the VIC and RVIC models were being corrected, the mapping here is translating from unimpaired flows to impaired flows in the rim basins. Since management goals for most reservoirs vary by season, seasonal mappings are more appropriate. Once the quantile maps were developed for each location based on the WY1951-2003 historical datasets, the maps were applied to the future scenario RVIC outputs to generate the corresponding CalSim II inputs for these scenarios.

Simulating Managed Streamflows using CalSim II

CalSim II Description

These mapped inflows, along with meteorological data (discussed in a later section) extracted from the future-scenario LOCA downscaled meteorology and historical baseline Livneh meteorology datasets, were used to drive a model of freshwater management operations—the California Department of Water Resources' CalSim II model (Draper et al. 2004). CalSim II is a management optimization model in which, given inputs of reservoir and other inflows, a set of freshwater management decisions is computationally determined on a monthly time step that optimally satisfy operational

goals and constraints. The results are estimates of monthly managed freshwater flows at points throughout the watershed. CalSim II has been applied in other climate-change studies (Brekke et al. 2004, Dracup et al. 2005, Vicuna et al. 2007, Anderson et al. 2008, Brekke et al. 2009).

Prior applications of CalSim II outside of the CASCaDE project have been based on a fixed historically based pattern of hydrologic variability. The period of these studies has generally begun with WY 1922 and, for most relatively recent studies, has ended in WY 2003. The freshwater management infrastructure and level of development (corresponding to projected population and agricultural irrigation needs) are static over the course of a CalSim II run, and the inflows over the historical period are taken to represent the range of hydrologic variability present in this watershed. Climate studies using CalSim II typically apply monthly flow “perturbation” ratios to the standard historical input time series. These ratios encapsulate climatological monthly flow changes over time based on separate, typically GCM-driven, hydrological model runs. The main limitation of this approach is that the range and types of hydrologic variability represented are limited to the recent historical hydroclimatological regime.

Modification of CalSim II for CASCaDE 2

The CASCaDE project is designed to directly use downscaled, daily GCM output to drive models of the Bay-Delta estuary and watershed to assess the response of these systems not only to long-term meteorological trends, but also to changes in multi-year variability such as droughts and wet years, and changes in the frequency and magnitude of even shorter-term events such as extreme floods. Therefore, the traditional application of CalSim II, using static historically-based hydrology, does not meet CASCaDE project needs. The chosen solution was to modify CalSim II to accept dynamic hydrology. While traditional CalSim II runs cover the period WY1922-2003, the CASCaDE implementation of CalSim II simulates WY1980-2099. The start date of WY1980 was chosen because most large modern freshwater management infrastructure in the Bay-Delta watershed was fully operational by that time, so reasonable comparisons between simulated and observed managed flows may be made from WY1980 onward.

Because CASCaDE 2 includes assessment of some version of what is now called “California WaterFix”, we chose as the starting point for our CalSim II modeling the implementation of CalSim II used in model runs for the predecessor to WaterFix, the Bay-Delta Conservation Plan (BDCP). The model files were obtained from CDWR, and of the model configurations used to evaluate alternatives for BDCP, two were chosen for use in CASCaDE 2: the “No-Action Alternative with Fall X2 management” as our scenario representing minimal in-Delta infrastructure change (see http://baydeltaconservationplan.com/Libraries/Dynamic_Document_Library/Public_Draft_BDCP_EIR-EIS_Chapter_3_-_Description_of_Alternatives.sflb.ashx, section 3.5.1), and “Alternative 4 with decision tree,” the CEQA preferred alternative, as our “alternative conveyance” scenario (ibid., section 3.5.9). Another configuration developed for the BDCP study was an “Existing Conditions” run, which used the standard historical CalSim II inputs, un-altered for climate change. Time series for 34 of the “Existing Conditions” inputs were extracted and used in developing the quarterly QMBC mapping between historical baseline RVIC outputs and historical CalSim II inputs, described earlier. All other input time series from the “Existing Conditions” CalSim II configuration were extracted for use in the resampling approach to generating future-scenario versions of these inputs (described later).

The BDCP studies evaluated these and other alternatives by modifying historical CalSim II inputs using a perturbation ratio approach. The perturbation ratios were derived from VIC runs driven by downscaled GCM outputs whose trends in precipitation and temperature over the study region fell near the medians of trends among select members of the CMIP3 GCM ensemble. The individual CalSim II inflow inputs that were modified in this manner to represent climate change are shown in section D.3.4 of http://baydeltaconservationplan.com/Libraries/Dynamic_Document_Library/Public_Draft_BDCP_EIR-EIS_Appendix_5A_-_EIR-EIS_Modeling_Technical_Appendix_-_Section_D.sflb.ashx and reproduced in part in Table 3-1. Most of the creeks and rivers referenced in this table are shown in Figure 3-3.

Table 3-1. CalSim II inflow boundary conditions that are derived from GCM-driven RVIC daily flow estimates.

Rim Basin Inflows

Trinity Lake Inflow
Lewiston Lake Inflow
Shasta Lake Inflow
Black Butte Lake Inflow
Lake Oroville Inflow
Folsom Lake Inflow
New Hogan Reservoir
New Melones Reservoir Inflow
New Don Pedro Reservoir Inflow
Lake McClure Inflow
Eastman Lake Inflow
Hensley Lake Inflow
Millerton Lake Inflow

Basin Floor Inflows

Clear Creek Inflow to Sacramento River
Cottonwood Creek Inflow to Sacramento River
Cow Creek Inflow to Sacramento River
Battle Creek Inflow to Sacramento River
Paynes Creek Inflow to Sacramento River
Red Bank Creek Inflow to Sacramento River
Antelope Creek Inflow to Sacramento River
Mill Creek Inflow to Sacramento River
Deer Creek Inflow to Sacramento River
Elder Creek Inflow to Sacramento River
Thomes Creek Inflow to Sacramento River
Big Chico Creek Inflow to Sacramento River
Butte Creek Spills to Sutter Bypass
Stony Creek Inflow to Stony Gorge Reservoir
Little Stony Creek Inflow to East Park Reservoir
Kelly Ridge Inflow to Feather River
Yuba River Inflow to Feather River
Bear River Inflow to Feather River
American River Upstream Inflow to Folsom Reservoir
Mokelumne River Inflow to Delta
Cosumnes River Inflow to Delta

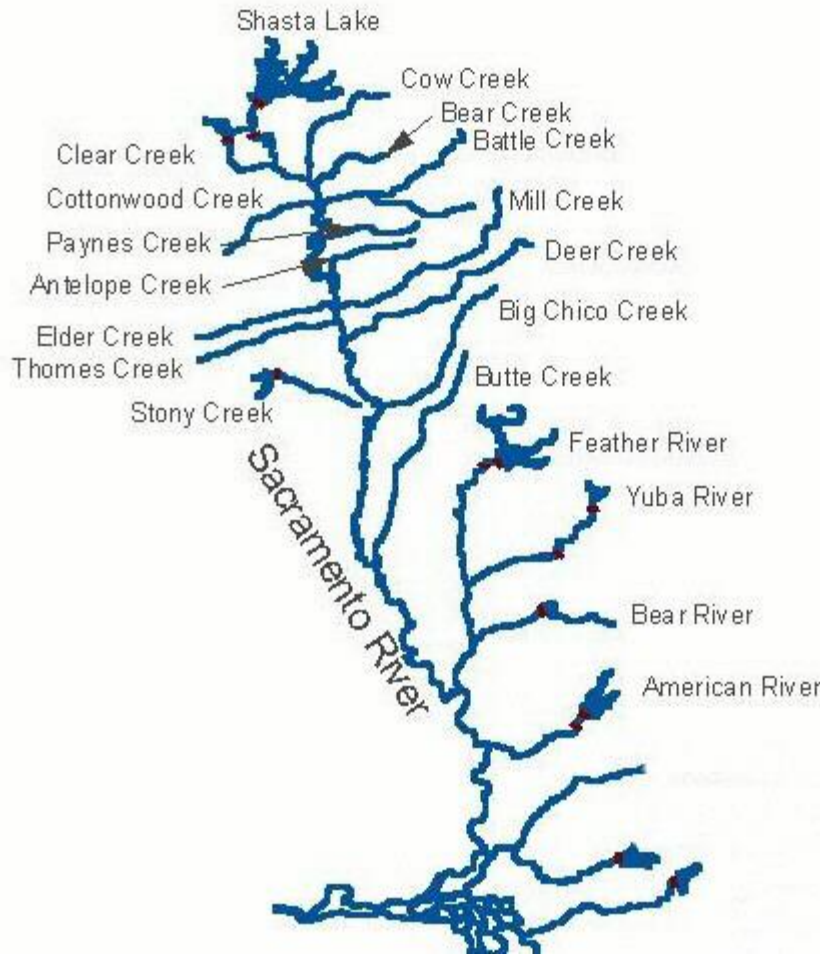


Figure 3-3. Map of major creeks and rivers in Sacramento basin (from USFWS AFRP: <http://www.fws.gov/lodi/afrp/images/allsac.jpg>).

For CASCade 2, these same inflow inputs were replaced with the values for future scenarios generated with the quarterly QMBC approach. Other inputs listed were also modified based on future-scenario VIC and RVIC outputs, as were all other time-varying CalSim II inputs (the methods used for modifying these other inputs are discussed in a later section). Running the CalSim II model with these input changes required multiple modifications to the CalSim II configuration files, which included the following steps (all steps are automated in bash or Python scripts):

1. All model files for a given alternative were extracted to a temporary folder.
2. Pathnames were corrected so CalSim II could run on the local file system.

3. Dates in the CalSim II DSS initial conditions file were modified to implement a WY1880 start date (as opposed to the usual WY 1922). Note that due to technical limitations of CalSim II, the nominal run period for future scenarios is WY1880-1999, rather than WY 1980-2099. Only the dates reflect this difference; all other data correspond to the future scenario.
4. All beginning and end dates in model configuration (“wresl”) files were changed to reflect the WY1880-1999 run time.
5. A new model input parameter, “WYORIG” was implemented in the configuration and input files. This input was needed to make the resampling approach described later work with the neural network library used to estimate salinities in the Delta.

Calculation of indices used in CalSim II

Next, some pre-processing was needed to generate time series of key annual indices needed as input to future scenario CalSim II runs. Brief descriptions of these annual indices and their derivation follow:

1. The Fish and Wildlife Service Biological Opinion “Action 3” smelt temperature threshold crossing date is the annual date on which average water temperatures at specific sites within the Delta first rises above the critical threshold of 12°C. When this occurs, specific flow restrictions are implemented in CalSim II. In this calculation, monthly mean air temperatures at the Sacramento Executive Airport are assumed to be identical to the water temperatures, as in the BDCP study. These air temperatures were extracted for future scenarios from the downscaled LOCA dataset for the grid cell containing the Airport. As in the BDCP study, monthly mean values were assumed to occur in the middle of the month, and daily data were interpolated between these values to obtain the day and month of the first ascending crossing each year. These dates typically fell in the months of Feb-Apr. However, in the warmer climates of several of the future scenarios, it frequently occurred that the resulting water temperature estimates never fell below the 12°C threshold. In those cases, the date of December 1 was used.

The remaining indices were derived using the bias-corrected unimpaired flows discussed earlier.

2. The Sacramento River WY type Index is the total unimpaired Sacramento basin flow; the following value is calculated:

$(0.4) \times \text{Current Apr-Jul runoff forecast (in MAF)} + (0.3) \times \text{Current Oct-Mar runoff (in MAF)} + (0.3) \times \text{Previous Water Year's Index (if the Previous Water Year's Index exceeds 10.0, then 10.0 is used)}$

Based on this value, the Index is assigned as per the following:

- 1 (Wet): Equal to or greater than 9.2
- 2 (Above Normal): Greater than 7.8, and less than 9.2
- 3 (Below Normal): Greater than 6.5, and equal to or less than 7.8
- 4 (Dry): Greater than 5.4, and equal to or less than 6.5
- 5 (Critical): Equal to or less than 5.4

3. The Oct-Mar Sacramento River Index is just the Oct-Mar total Sacramento basin outflow in MAF.

4. The San Joaquin River WY type Index is similar to #2, but with a calculated value of:

$(0.6) \times \text{Current Apr-Jul runoff forecast (in maf)} + (0.2) \times \text{Current Oct-Mar runoff (in maf)} + (0.2) \times \text{Previous Water Year's Index (if the Previous Water Year's Index exceeds 4.5, then 4.5 is used)}$

And index criteria:

- 1 (Wet): Equal to or greater than 3.8
- 2 (Above Normal): Greater than 3.1, and less than 3.8
- 3 (Below Normal): Greater than 2.5, and equal to or less than 3.1
- 4 (Dry): Greater than 2.1, and equal to or less than 2.5

5 (Critical): Equal to or less than 2.1

5. The “SJRAve5” Index for a given year is the average of #4 for the 5 previous years.
6. The Shasta WY Index has a more complicated logic; refer to the calc_indices.py code for details (all code will be released when scenario data are complete).
7. The “AmerD893” Index is based on the Apr-Sept total unimpaired American R. flow in TAF. The Index has value 1 if this is >600 TAF and 2 otherwise.
8. The Feather River Index has a complicated logic similar to #6. Refer to same code for details.
9. The Trinity River Index is based on unimpaired Trinity River flows. The index values are assigned as follows: if flow <650 TAF, index=5; if 650<=flow<1025, index=4; if 1025<=flow<1350, index=3 if 1350<=flow<2000, index=2; flow >=2000, index=1).
10. The Eight River Index is the total unimpaired Sacramento and San Joaquin River flows in TAF.
11. The Delta Index is the sum of the Jan-May unimpaired Sacramento and San Joaquin River flows in TAF.

Resampling of remaining standard CalSim II inputs

With the indices described above and the major CalSim II inflows (Table 3-1) derived from GCM-driven RVIC flows generated for all scenarios (and for the historical observation-based Livneh dataset), all remaining CalSim II inputs were generated for the historical baseline and future scenario runs by resampling the corresponding inputs from the standard CalSim II model configuration used in the BDCP “Existing Conditions” study.

The resampling was performed as follows:

1. Total monthly rim-basin inflows were calculated as the sum over all rim basins (see Table 3-1) of monthly flows. These were calculated using the “Existing Conditions”

study inputs and using the quarterly QMBC-mapped CalSim inflows (described above) for both the historical baseline and future scenarios.

2. For each water year in the baseline and the future scenarios, a best-match year was selected from the “Existing Conditions” rim-basin inflows, where the match metric was determined as:

$$C_{wy_c} = \sqrt{\frac{\frac{1}{12} \sum_{m=1}^{12} (Q_{m,wy_t} - T_{m,wy_c})^2}{\bar{Q} \cdot \bar{T}}}$$

$$P_{wy_c} = \frac{\frac{1}{12} \sum_{m=1}^{12} |Q_{m,wy_{t-1}} - T_{m,wy_{c-1}}|}{\frac{1}{2}(\bar{Q} + \bar{T})}$$

$$d_{wy_c} = C_{wy_c} + \frac{P_{wy_c}}{25}$$

where:

Q_{m,wy_t} is the total rim-basin flow for a given water-year month m in the “target” water year wy_t to be matched in the baseline or future scenario;

T_{m,wy_c} is total rim-basin flow for a given month m in the “candidate” matching year wy_c using historical rim-basin flows extracted from the “Existing Conditions” study;

\bar{Q} and \bar{T} are the long-term mean of the total rim-basin flows from the historical baseline or future scenario and from the “Existing Conditions” study inputs, respectively;

C_{wy_c} and P_{wy_c} are metrics for current water year flows and previous water year flows, respectively; and

d_{wy_c} is the combined metric, tuned through an iterative “leave-one-out” cross-validation to optimally represent the combined effects on the CalSim inputs being resampled of current water-year flows and previous water-year flows (important mainly for reservoir carry-over storage).

3. All CalSim II inputs, other than the 34 inflows and the 11 indices derived directly from

RVIC streamflows, for the water year being matched in the historical baseline or future scenario are filled with the corresponding inputs from the best-match year (year with minimum d_{wy}) in the standard input files of the BDCP scenario being evaluated (i.e., “No-Action Alternative” or “Alternative 4”).

Steps 1-3 are repeated until the CalSim II inputs for all 34 years of the historical baseline (WY1980-2013) and 120 years of each future scenario (WY1980-2099) have been produced.

A record of which water years were selected as best-matches for each scenario are also retained and added to the CalSim II inputs files as values for the WYORIG input variable. CalSim II calls a separate artificial neural network (ANN) algorithm to generate estimates of salinity and salinity-related quantities based on a range of inputs. One of the ANN inputs is the current water-year value. Because the ANN is a binary which is trained using WY1922-2003, the ANN calls in the CalSim configuration files were altered to use WYORIG (which still varies from 1922-2003) instead of the model run's current water-year value which, in the modified CalSim II configuration used for CASCaDE 2, varies from 1980-2099. In this way, the resampling approach described above extends to this aspect of the ANN calls.

Sequential execution of CalSim II studies

In the approach described here, there are several factors which define a given CalSim II run. The first is which study is being evaluated: Existing Conditions (EC), No Action Alternative (NAA), or Alternative 4 (A4). For CASCaDE II, the EC model configuration was used to represent the period WY1980-2029, and the NAA and A4 studies are used from WY2030-2099. This assumes the management changes represented in the NAA and A4 studies are not put into effect until WY2030. Another factor which affects a given CalSim II run is the level of development (LOD), represented as freshwater demands corresponding to future projections of population and land use. The EC configuration uses an LOD corresponding to the year 2005, while the NAA and A4 configurations use a 2030 LOD. Thus, 2030 seemed an appropriate transition date between model configurations, both due to the available LODs and to the likelihood that any major

infrastructure changes will not be completed for at least another decade. In the transition from the EC to the NAA or A4 studies at 2030, the final outputs from the EC study were transferred to the initial condition file for the 2nd study to ensure continuity across these sequential runs.

A final factor in defining a given study was the sea level rise (SLR) value used. Since salinities resulting from given inflow patterns increase with SLR, more flows are required to meet salinity standards as sea level increases. CalSim II uses an artificial neural network to estimate salinity and salinity-related quantities at points throughout the Delta (Chung and Seneviratne 2009). For the BDCP studies, This ANN was trained for conditions corresponding to sea level rise (SLR) amounts of 0 cm, 15 cm, 30.5 cm (1 ft), and 45 cm, resulting in 4 separate ANNs that could be used in a given CalSim II study. To represent the effects of SLR in the CASCade II CalSim runs, the runs were segmented according to projections of SLR (described below). Each CalSim II run sequence for a given scenario was started with the EC configuration using the ANN corresponding to 0 cm SLR. When the projected SLR for a given scenario reached one of the 4 ANN SLR values, the run was paused, the previous ANN was replaced with the new one, and the run continued. The resulting representation of SLR is a conservative one, with the SLR value implemented in CalSim II always at or below the projected SLR, but this was the best approach available given the nature of SLR implementation in CalSim II. The SLR underestimate is particularly pronounced in more extreme SLR scenarios, which reach values of 166 cm by century's end, 3.7 times the maximum value represented in the DWR ANNs. This must be considered when interpreting results.

Determining ANN transition dates

Task 2 provided 3 future SLR scenarios based on a National Research Council Report (NRC 2012) corresponding to low-end, mid-range, and high-end estimates of future SLR (Figure 3-4). Transition dates for CalSim II ANNs were determined as the WY in which each of these scenarios exceeded the amounts corresponding to the ANNs (Figure 3-4). Drawing on the correlation between SLR and global air temperature trends, and between global and regional temperature trends, the 20 GCM scenarios

were grouped into terciles based on the magnitudes of trends in Sacramento basin average air temperature over the course of the projected century. Scenarios in the top tercile were assigned ANN transition dates corresponding to the high-end SLR scenario, the middle-tercile scenarios were assigned the mid-range SLR projection transition dates, and the bottom tercile the low-end dates. These dates were then used to determine segmentation of the CalSim II runs for ANN changes for each scenario as described above.

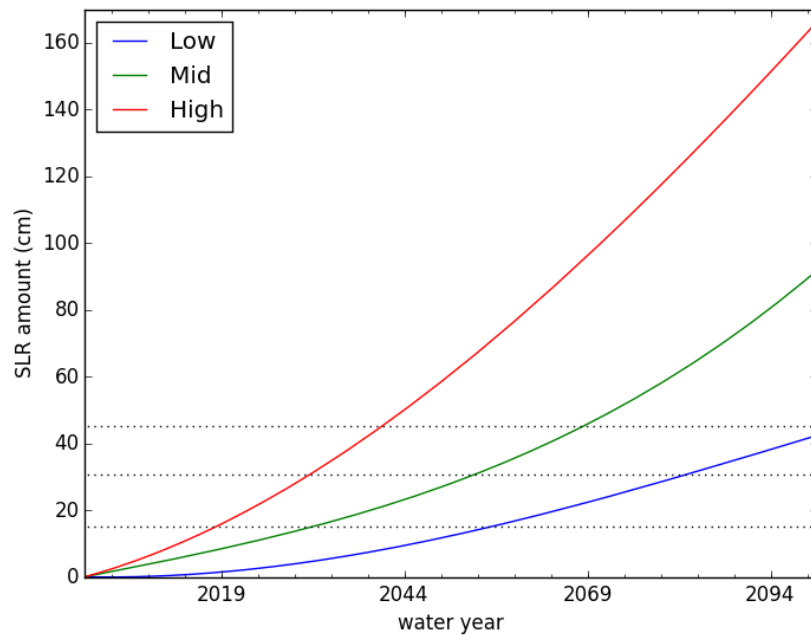


Figure 3-4. Low, middle, and high SLR projections, with crossings of SLR ANN values shown.

Automating CalSim II runs

With the BDCP study CalSim II configuration suitably modified, CalSim II inputs for the historical baseline run and for all future scenario runs generated, and run segments configured to allow for variation in management infrastructure and strategies (as represented in the different BDCP studies), LOD, and SLR, the next step was to run the modified “CASCaDE 2 version” of CalSim II. Execution of all 20 future scenarios and the historical baseline run was automated using bash, Python, and HEC-DSS Jython scripts on Linux, combined with a Windows virtual machine with Cygwin OpenSSH, Autolt, and WRIMS 1.3.0 (the underlying software on which the CalSim II model is run) installed.

Initially, it occurred that the CalSim II runs would crash when a particular combination of

inputs and state variables occurred. This most commonly occurred during very low inflows, though it occasionally occurred during very high inflows. It was prohibitively difficult to diagnose these crashes on a case-by-case basis as would have been necessary. Therefore, it was decided to increase (or decrease for high flows) all inflows listed in Table 3-1 for the month of the crash moderately, and restart the run at the beginning of the water year during which the crash occurred. This process was automated, successively increasing (or decreasing) the crash month's flows until the run was successful or a limit imposed on the multiplicative factor being applied to the flows was reached. In especially rare cases (2 months out of all scenarios), this approach still did not prevent the crash and a fallback solution of replacing the crash month's inflows with inflows from the same month in the previous water year was implemented. In this way, all CalSim II runs were completed.

Finally, all needed flows, diversions, operational time series and storages were extracted from the resulting output files. Time series extracted from the CalSim runs are as follows:

Reservoir storages: Shasta, Oroville

Reservoir outflows: Oroville, Keswick, Black Butte Dam, Nimbus, Camp Far West, Whiskeytown

Flows at these locations: Cosumnes, Vernalis, Verona, Yolo Bypass

Exports: Tracy and Banks pumping plants, North Bay Aqueduct, Rock Slough (CCWD), BDCP "isolated facility" tunnel intake (only used in the BDCP Alternative 4 scenario)

Other operations: number of days per month that CalSim II simulated the Delta Cross-Channel gates as being open.

The current status of this work is that all the steps above are complete for the Existing Conditions->No-Action Alternative sequence (which will provide flows for the CASCaDE 2 climate-change-only scenarios). The "Alternative 4" study, which will provide flows for the CASCaDE 2 alternative conveyance scenario, is not yet underway, though it is

anticipated that the largely automated framework for setting up and executing the No-Action Alternative sequence, described above, will allow this second alternative to be evaluated fairly quickly.

Application of CalSim II in CASCaDE 2: caveats and future work

In attempting to represent the behavior of a complex freshwater management network like California's in the future, several difficulties are encountered. Projecting freshwater demands is difficult, and for CalSim II, demand scenarios were only available for California's level of development (LOD) in 2005 (used in BDCP "Existing Conditions" study) and that projected for 2030 (used in "Alternative 4" and other BDCP studies). In CASCaDE 2, all CalSim II runs use the 2005 LOD until the beginning of WY2030, after which they use the 2030 LOD. This necessarily introduces errors into the results, with a key caveat that projections well past 2030 almost certainly underestimate freshwater demands, barring major changes in California water-use patterns.

Another important difficulty lies in the fact that freshwater management infrastructure is not static. Representing the numerous historical infrastructure changes is very difficult, and predicting future changes is impossible. The only infrastructure changes considered in CASCaDE 2 are those inherent in the different infrastructure scenarios—e.g., changes including new tunnels and a notch in Fremont Weir in the "Alternative 4" configuration vs. largely present-day infrastructure for the climate-change-only scenarios. For a given scenario, the only change in freshwater management infrastructure and management goals are those associated with the transition from the EC configuration to either the NAA or the A4 configurations in WY2030. The results may therefore be interpreted as potential changes which additional future adjustments to management infrastructure and goals beyond those represented here may be designed to help mitigate.

A shortcoming of CalSim II is its treatment of groundwater withdrawals, which are allowed in the model to occur at unsustainable levels if other supplies of freshwater are insufficient to meet demands. This must be considered when interpreting results. In particular, simulated unsustainable withdrawal levels are indicative of an inability to

meet freshwater demands through other means. In this situation, net depletion of aquifers to meet demand is one possible outcome; measures to increase aquifer recharge and/or reduce demand are other options.

One standard step in new applications of CalSim II is to “retrain” the Water Supply Index-Delivery Index (WSI-DI) curve for a given hydrologic regime and model configuration. The WSI-DI curve relates available water supply (represented by WSI) and deliveries and carryover storage (DI) for the State Water Project and the Central Valley Project. A procedure exists for optimizing this curve for a given set of inputs. A good description of the WSI-DI curve and the retraining is given in Section 3.3.1 of <http://baydeltaoffice.water.ca.gov/announcement/SensitivityStudyReport.pdf>. Initially, the plan for CASCaDE 2 was to use the present-day WSI-DI curve for the baseline historical run and for the period WY1980-2019 in all future scenarios, and to retrain WSI-DI separately for the periods WY2020-2059 and WY2060-2099 for each scenario. This would allow some amount of management “adaptation” to changing hydroclimatic conditions. However, the additional model runs involved in the retraining would have increased total model time by a factor of 7, resulting in about a month of total CalSim II run time. For now, this amount of additional time was considered prohibitive, and the resulting caveat is that calculated deliveries and carryover storage allocations may be suboptimal, particularly later in the future scenarios. WSI-DI retraining may be implemented in the future, as time permits.

Finally, the shortcomings of the limited SLR range available for implementation in CalSim II were already discussed above. In the implementation used here, the SLR effective in the CalSim II runs is often well below the projected amount. The effect of this is that Delta outflows required to repel saltwater in the dry season are underestimated. This is a conservative outcome in terms of evaluating the impacts of climate change on the estuary.

CRESPI

RVIC outputs to be used in deriving watershed sediment model inputs (for Task 7b), Delft3D-FM boundary conditions (For Task 4), or in disaggregation of monthly CalSim II

outputs to daily (Shasta inflows), all applications where managed flows were needed instead of unimpaired flows, were transformed from unimpaired to managed flow estimates using the CRESPI method.

Method

In this method, we work with time series of two streamflow variables, the unimpaired time series and the impaired time series. For the historical time series 1950-2013, we have observations of the impaired time series and simulations of the unimpaired time series, whereas for the projected time period, we only have the unimpaired simulation. We use a resampling-based approach to generate the time series of the impaired variable for the projected time series. This approach involves sampling contiguous sections (“blocks”) of the historical impaired time series and concatenating them together to form an impaired time series for the projected period. Our algorithm can be divided into two steps: in the first step, a daily time series of the impaired variable is generated without considering dependence or continuity between adjacent blocks; in the second step, this time series is re-generated by considering neighboring daily values, allowing artifacts from the first step to be reduced.

First step

The procedure for generating the projected impaired time series is as follows. The algorithm steps through the projected time series month by month. For each month m of length l of the projected time series, the algorithm extracts the unimpaired time series $x(\mathbf{u}_m^f)$ and searches each block of l days in the historical unimpaired time series for the most similar block $x(\mathbf{u}_m^h)$. Similarity is measured by the root mean square error between $x(\mathbf{u}_m^f)$ and $x(\mathbf{u}_m^h)$. When $x(\mathbf{u}_m^h)$ is found, the values of the simultaneous block of the impaired variable $y(\mathbf{u}_m^h)$ are copied and inserted into the projected time series to become the values of the impaired variable for the current month, $y(\mathbf{u}_m^f)$.

Second step

We approach this problem by again selecting new patterns to estimate the unimpaired time series. We achieve this task by performing a procedure similar to the one described above. However, now that the first step has generated a preliminary daily

time series of the impaired variable for the projected time period, we can now search for the best-matching block of the impaired time series directly, instead of assigning values to the impaired series based on the best match for the unimpaired series. Additionally, in this step we add neighboring values to the block in order to find patterns that are better associated with the temporal variability constructed during the first step. For example, for each month m of with length l of the projected time series, the algorithm extracts the impaired time series $y(\mathbf{u}^f_\tau)$ consisting of the k values neighboring the month m in addition to the l values of the month m . For example, these neighboring values could consist of the seven days preceding the month m and the seven days following the month m ($k=7$ is the value used in our application of this method in CASCaDE). The number of preceding or following days to consider is zero when estimating streamflow in the first or last month of the projected time series. As before, the algorithm searches each block of $k+l$ days in the historical unimpaired time series for the most similar block $y(\mathbf{u}^h_\tau)$. Again, similarity is measured by the root mean square error between $y(\mathbf{u}^h_\tau)$ and $y(\mathbf{u}^f_\tau)$. This second step is intended to reduce discrepancies between adjacent blocks that may have been generated during the first step.

Application to CASCaDE II

In the current application, the unimpaired quantity is the routed streamflow generated by VIC and the impaired quantity is impaired streamflow at the same location (though the algorithm does not require the two quantities be collocated; just that they be strongly related, as in upstream and downstream flows). The historical period is when the impaired data were observed between the beginning of calendar year 1950 and the end of calendar year 2013. The projected time period extends from the beginning of the calendar year 1950 to the end of calendar year 2099 or 2100 depending on the GCM scenario. After application of the CRESPI method, the time series are clipped to WY1980-2099, commensurate with the CalSim II results.

Training data

Training data for various points in the Sacramento River Basin (Table 3-2) come from the U.S. Geological Survey's National Water Information System (NWIS)

(<http://waterdata.usgs.gov/nwis>). We use training data starting from either 1950, the beginning of the record, or the date when major upstream impairments (e.g. construction of dams) went into service, whichever is latest. Many points are located below major impairments that went into service after 1950. If these impairments went into service after 1950, we only consider training data collected after that time. For example, for points located below major dams, we start the training data in the water year after the date that dams were fully operational. For some stations, such as station no. 11376150 (Eagle Canyon Canal Diversion), we set the cutoff date to points where the patterns of flow change significantly in the record. In most cases these stations are below the impairments. However, station number 11425310 (Lakewood) is actually located above Lakewood Dam.

For the data used for the points farthest downstream (Vernalis, Verona, Yolo, Freeport), the cutoff date is the beginning of calendar year 1970 because most of the major dams in the Sacramento-San Joaquin River Basin had been completed by then. Some dams were still completed after 1970, the largest of these being Don Pedro Dam in 1971 and New Melones Dam in 1979 (Calif. Dept of Finance, 2008).

Table 3-2. Data used as historical “library” in CRESPI method. Record beginning and end dates are shown, and the “cutoff” date prior to which data were excluded is given. See text for details.

NWIS ID	Location	Rec start	Cutoff	Rec end	Note
11388000	Black Butte	1955-07	1964-10	1990-09	Dam completed 1963 (CA DOF 2008)
11424000	Cmp Far W	1928-10	1964-10	2013-12	Dam completed 1963 (CA DOF 2008)
11423800	Cmp Far W Div	1989-10	1989-10	2013-09	
11451000	Clear Lake	1944-10	1950-01	2013-12	Dam completed 1910 (CA DOF 2008)
11376150	Eagle Cyn Div	1983-10	1995-10	2013-12	Flow behavior change in 1995

11418000	Englebright	1941-10	1970-10	2013-12	Narrows 2 Powerhouse completed 1970 (YCWA 2012)
11447650	Freeport	1948-10	1970-01	2013-12	Far-downstream point (multiple major impairments)
11451300	Indian Valley	1983-10	1983-10	2013-12	Dam completed 1976 (CA DOF 2008)
11370500	Keswick	1938-10	1950-01	2013-12	Shasta Dam completed 1945 (CA DOF 2008)
11425310	Lakewood	1980-10	1980-10	2013-09	
11376025	Macumber	1980-10	1989-10	2013-12	Dam completed 1907 (Reynolds and Scott 1980)
11375700	Misselbeck	1956-10	1956-10	1980-09	Dam completed 1920 (CA DWR 1990)
11325500	Mokelumne	1924-06	1964-10	2013-12	Dam completed 1963 (CA DOF 2008)
11458000	Napa	1929-10	1950-01	2013-12	
11446500	Nimbus	1904-10	1957-10	2013-12	Folsom Dam completed 1956 (CA DOF 2008)
11376015	N Battle Ck	1978-10	1978-10	2013-12	Dam completed 1912 (Reynolds and Scott 1980)
11407000	Oroville	1901-10	1969-10	2013-12	Dam completed 1968 (CA DOF 2008)
11459150	Petaluma	1998-11	1998-11	2013-12	
11406920	Thermalito	1967-11	1969-10	2013-09	Oroville Dam completed 1968 (CA DOF 2008)
11303500	Vernalis	1923-10	1970-01	2013-12	Far-downstream point (multiple major impairments)
11425500	Verona	1929-10	1970-01	2013-12	Far-downstream point (multiple major impairments)

11420700	Virginia Ranch	1964-08	1964-10	1980-10	Dam completed 1963 (AECOM 2011)
11372000	Whiskeytown	1940-10	1964-10	2013-12	Dam completed 1968 (CA DOF 2008)
11453000	Yolo	1939-10	1970-01	2013-12	Far-downstream point (multiple major impairments)

For the impaired point located below Oroville/Thermalito, the sum of the data from station nos. 11406920 (Thermalito) and 11407000 (Oroville) is used.

Including information on reservoir storage

The operation of Shasta Lake and Oroville Reservoir is guided in part by the “rule curve” that determines the amount of the reservoir storage capacity to be reserved for flood control (Willis et al 2011). The difference between daily storage and the top of conservation storage (“target storage”) is referred to as “storage deviation”. Releases of water from reservoir storage are governed by the release schedule. For Shasta Lake and Oroville Reservoir, the official release schedule requires releases of water in the flood control pool when storage deviation becomes positive. For Shasta and Oroville Reservoirs individually, the storage deviation can determine whether or not outflows exceed some base level.

Data show that peak flows in the lower Sacramento River Basin are associated with reservoir storage encroaching (or close to encroaching) on the flood control pool. This is because high outflows occur only when reservoir deviation is relatively high (above zero, or negative but close to zero). In our approach, we use the rule curve for two of the major reservoirs in the Sacramento River Basin, Oroville Reservoir and Shasta Lake, to help us identify periods in the historical record where reservoirs were operating under similar conditions to those projected. This approach involves restricting the search for analogous patterns to time periods where the deviation between target storage level and reservoir storage level in Oroville Reservoir and Shasta Lake are approximately similar.

In the current implementation, this restriction is asymmetric. A storage deviation threshold is established for each reservoir being considered in the model. Storage levels are interpolated from monthly values based on observations for the historical period, and on CalSim II outputs for the future scenarios. On any future day of the simulation, if the storage deviation falls below this threshold, patterns from the historical time series may not be selected if the maximum historical storage deviation reached during that pattern exceeds the threshold. However, if the storage deviation exceeds this threshold in the future period, the opposite restriction is not implemented. This method effectively prevents peaks flows from being translated downstream of major reservoirs during drought years when the reservoir storage levels are below target.

Modeling the flood control reservation

The target storage not only needs to be calculated for the future time series, but data for historical target storage values are not available for most of the historical time series. We therefore implemented a model to calculate the target storage in Shasta Lake and in Oroville Reservoir according to the guidelines provided in each reservoir's flood control operations manual.

Shasta Lake

The Shasta Lake rule curve is based on a "ground wetness index" computed as follows (USACE, 1977):

$$x_t = 0.95 x_{t-1} + q_t$$

where x_t is the ground wetness parameter and q_t is the inflow (cfs) for the current day t , and x_{t-1} is the parameter for the previous day $t-1$. x_t has the same units as inflow (cfs).

For each of the projected climate scenarios, the inflows to Shasta Lake need to be estimated from the unimpaired routed streamflow produced by VIC. The inflows are estimated by a series of linear regression models, one for each of the twelve calendar months, in which the inflow is the dependent variable and the unimpaired routed

streamflow is the dependent variable. The observed inflow and unimpaired routed streamflow from the period 1995-2013 is used to train the models.

The ground wetness index is initialized to 100,000 cfs on October 1 of each year, so that $x_t(10/01) = 100,000$ cfs. For a given x_t , the target reservoir storage $s(x_t, t)$ can take a value over the range between a time-invariant minimum storage s_{min} and a maximum storage s_{max} . The absolute minimum target storage during the flood season is $s_{min} = 3,252,100$ af while the maximum target storage during the flood season is $s_{max} = 4,552,100$ af.

Target storage can be written as a function of date t and ground wetness parameter x_t :

$$s(x_t, t) = \begin{cases} (t - 09/30)(s_{min} - s_{max})/(61 \text{ days}) + s_{max} & \text{for } 10/01 \leq t < 11/29 \\ s_{min} & \text{for } 11/30 \leq t < 12/22 \\ (a - s_{min})(t - 12/23)/(87 \text{ days}) + s_{min} & \text{for } 12/23 \leq t < 03/19 \\ ((s_{min} - s_{max})/((d_x - 03/20)(x_{max} - x_{min}))) & \text{for } 03/20 \leq t < 03/20 \text{ if } d_x > 03/20 \\ s_{max} & \text{for } d_x \leq t \leq 09/30 \end{cases}$$

where $a = (s_{min} - s_{max})/(x_{max} - x_{min}) + s_{max}$

Rule curve for Shasta Lake calculated over the range of ground wetness parameters.

Oroville Reservoir

For Oroville Reservoir, the ground wetness index is computed as follows (USACE, 1970):

$$x_t = 0.97 x_{t-1} + p_t \quad \text{under the condition } 3.5 \leq x_t \leq 11$$

where x_t is the ground wetness parameter and p_t is the “basin mean precipitation” for the current day t , and x_{t-1} is the ground wetness parameter for the previous day $t-1$. x_t has the same units as precipitation (L).

The basin mean precipitation is computed as follows (USACE, 1970):

$$p_t = ABP/NAP_i * p_t^{(i)}$$

where $ABP = 44.1$ in (average basin precipitation for the entire Feather River Basin)

where $NAP = 412.8$ in (sum of normal annual precipitation for the eight stations p_t)

where $p_t^{(i)}$ is the precipitation recorded on the current day t at the i^{th} of eight stations in the list:

Station name	Station code	Normal annual precip. (in)
Oroville Dam	ORO	33.4
Strawberry Valley	SBY	81
Brush Creek-DWR	BRS	72.1
Sierraville-DWR	SVL	26.6
Quincy-DWR	QCY	41
Camptonville-DWR	CAM	55.9
De Sabla-DWR	DES	65.3
Canyon Dam	CNY	37.5

(from M. White, Calif. Dept. of Water Resources, personal comm., 2013-04-10)

Because precipitation projections are not available for each of these eight stations for the projected climate scenarios, the basin mean precipitation is calculated directly from the gridded LOCA scenario data produced in Task 2.

The absolute minimum target storage during the flood season is $s_{min}(x_{max}) = s(11) = 2,788,000$ af while the maximum target storage during the flood season is $s(x_{min}) = s(3.5) = 3,163,000$ af.

The value of $s_{min}(x_t)$ then varies linearly between these two values as a function of x_t

$$s_{max} = 3,538,000 \text{ af}$$

$$s_{min}(x_t) = s(x_{min}) + a(x_t - x_{min})$$

where $a = (2,788,000 \text{ af} - 3,163,000 \text{ af}) / (11.0 - 3.5) = (-50,000 \text{ af} / \text{ground wetness unit})$

and $s(x_{min}) = s(3.5) = 3,163,000$ af

Target storage can be written as a function of date t and ground wetness parameter x_t :

$$s(x_t, t) = \begin{cases} (t - 09/15)(s_{min}(x_t) - s_{max}) / (30 \text{ days}) + s_{max} & \text{for } 09/15 \leq t < 10/14 \\ s_{min}(x_t) & \text{for } 10/15 \leq t < 03/30 \\ b(t - 03/31) + s_{min}(x_t) & \text{for } 03/31 \leq t < 06/14 \\ s_{max} & \text{for } 06/15 \leq t \leq 09/14 \end{cases}$$

where $b = 10,000$ af / day

Threshold selection

The task of selecting the threshold involves maximizing two quantities. The first quantity is the discrepancy between the maximum flow rate for above-threshold patterns and below-threshold patterns, which is a proxy for the effect of the threshold on restricting peak flows during years of significant water deficit. The second quantity is

the size of the training data that can be used when the projected storage deviation falls below the threshold. However, there is a tradeoff between these two quantities because increasing the maximum flow discrepancy involves reducing the storage deviation threshold, which in turn reduces the size of the training set available during below-threshold periods.

This tradeoff is visualized in Figure 3-5. In the upper panels, the red line shows the maximum flow below the threshold, and the blue line shows the maximum flow above the threshold. The percent of patterns where the maximum falls below the threshold are labeled on the red line. Based on these plots, we recommend a threshold deviation of approximately -500,000 af for Shasta and -100,000 af for Oroville. In the lower panels, the percent below threshold is plotted against the tradeoff between the discrepancy between max flow above and below the threshold. The points are labeled with the maximum deviation threshold for that point in the 2D space.

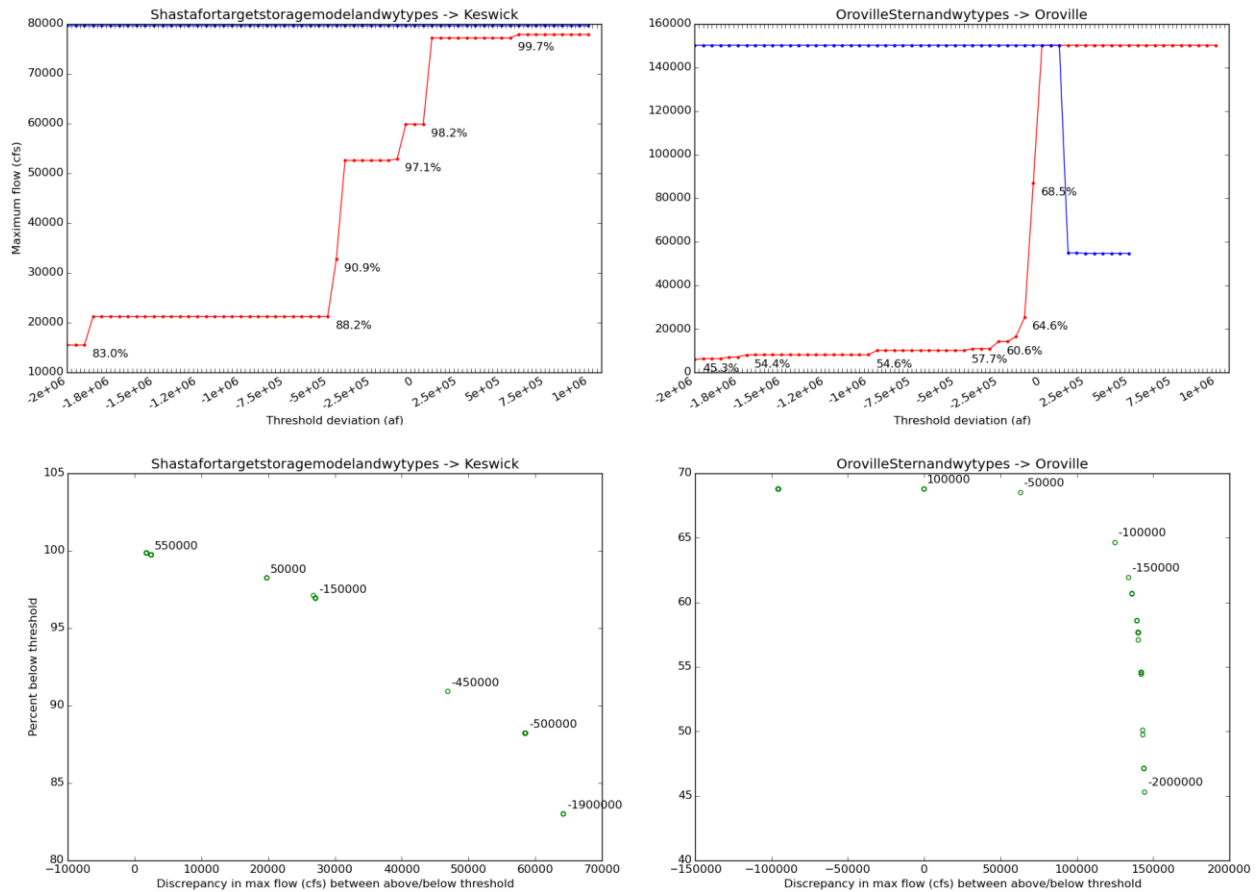


Figure 3-5. Tradeoffs in selection of storage deviation thresholds for Shasta (left) and Oroville (right). See text for details.

Constraining pattern selection using CalSim II outputs

In addition to reservoir storage, other CalSim II outputs are used to constrain pattern selection. Where CRESPI is being applied at outflow points from larger basins, monthly-averaged flows for the baseline and scenarios are usually available from the CalSim II runs. The need for daily flow data in the CASCaDE project was the major impetus for developing CRESPI. However, CRESPI-generated flow projections are limited to historical patterns, while CalSim II provides a more dynamic response of the integrated freshwater management system to long-term changes in climate forcings, albeit at the monthly scale. Fortunately, CRESPI allows for pattern selection to be further constrained using external monthly values for the time series being projected. In our case, the impaired monthly flow pattern that most closely matches the corresponding

CalSim II (impaired) monthly flow was selected from the top 30 matches using the unimpaired flow metric described previously. This allowed generation of daily flow projections whose monthly averaged were more closely aligned with the monthly CalSim II projections.

Modeling separation of flow by Fremont Weir

The Sacramento River at Verona is located immediately downstream from the junction of the Feather River and the Sacramento River. Immediately upstream of its discharge into the Sacramento River, the Feather River also receives flow from the Sutter Bypass, some of which had previously been diverted from the Sacramento River further upstream.

The Fremont Weir is the primary source of flow into the Yolo Bypass (design capacity 343,000 cfs). Of the remaining sources to the Yolo Bypass, the largest is the Sacramento Weir, located downstream of Verona. The Sacramento Weir is manually operated and has a design capacity of 112,000 cfs. Most of the remaining flow into the bypass comes from Cache Creek (design capacity 30,000 cfs), Putah Creek (design capacity 42,000 cfs), and Willow Slough (design capacity 6,000 cfs), all of which drain into the Yolo Bypass from the west. The only remaining source of flow into the Yolo Bypass from the Sacramento River that is unaccounted for is flow from the Knights Landing Ridge Cut, which is a relatively very small source (design capacity 20,000 cfs).

Water flows over the Fremont Weir into Yolo Bypass when the Sacramento River exceeds a stage of 33.5 feet, which corresponds to a flow rate of approximately 62,000 cfs at Verona (USACE, 1999). The flow rate cutoff at a given time depends on the relative contribution of flow from the Sacramento River, Feather River, and Sutter Bypass.

Data for daily discharge over Fremont Weir are not available between July 1976 and January 1984. However, a record of daily discharge in Yolo Bypass near Woodland is available for the full time series from 1970-2010. An analysis of the relationship between flow over Fremont Weir and flow over Yolo Bypass for the period 1984-2010 suggests that flows over the Fremont Weir can be well approximated by the data from

Yolo Bypass at Woodland (fig. below). To improve this approximation, we could subtract flow into Yolo Bypass from Sacramento Weir, Cache Creek, and Putah Creek. Although we would still be missing data from Willow Slough and Knights Landing Ridge Cut, these sources have a relatively small design capacity compared to Fremont Weir. If we attempt to approximate flows over Fremont Weir by subtracting flow from the other sources in Yolo Bypass, we may need to account for the lag between the gauge at the inputs and the gauge in Yolo Bypass itself.

Figure 3-6 shows the relationship between flow over Fremont Weir and flow in Yolo Bypass. Flow from the Fremont Weir may have attenuated somewhat by the time it is measured at the Yolo Bypass gauge. Another question is whether (and to what extent) the additional flow from the other inputs compensates for the attenuation of Fremont Weir flows when measured at the Yolo Bypass gauge.

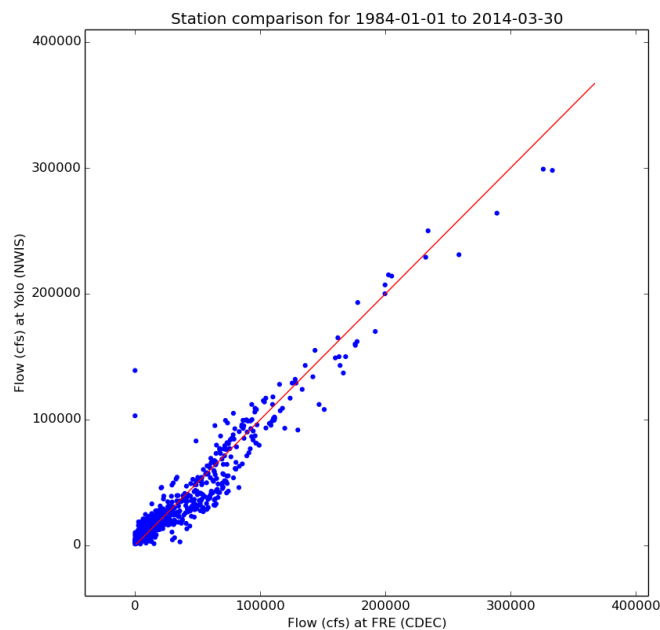


Figure 3-6. Relationship between flow over Fremont Weir and flow in Yolo Bypass.

Fremont Weir accommodates the majority of the “peak” flow from the Sacramento River near Verona. When the stage is above 33.5 feet the majority of the additional flow is diverted into Yolo Bypass.

There is a clear (positive nonlinear) relationship between flow in Sacramento River at Verona and flow in Yolo Bypass (Fremont Weir) resulting from the stage-discharge relationship as governed by the rating curve of the weir. One possible approach to estimating flow at the boundary condition is to first estimate stage or discharge at Verona and then estimate the spill over the Fremont Weir based on an estimate of this relationship.

However, the relationship between stage and discharge at Fremont Weir has changed several times in the historical record, at least in part as a result of the deposition and removal of sediment from Yolo Bypass downstream of the weir (Singer and others, 2008). The currently available rating curve (from CDEC) appears to be accurate only since 2006. The difference between stage-discharge relationships for flow through Fremont Weir is particularly important for high flow rates, as flow through Fremont Weir approaches the design capacity of the weir. Unfortunately, our information on the relationship between flow at Verona and flow through the Fremont Weir is least complete for flow rates in this range.

The hydrodynamic model of the Bay-Delta (Task 4) system requires two separate boundaries, Sacramento River at Verona and flow over the Fremont Weir into the Yolo Bypass. In order to separate flow at Verona from flow in the Yolo Bypass, we use a linear regression. This regression is estimated from data where combined Verona and Yolo flow exceeds 62,000 cfs. The dependent variable is flow in Yolo and the independent variable is the combined flow. Note that we are training this model using data from the NWIS gauge at Yolo and that this is a biased representation of flow over Fremont Weir as described earlier.

Reconciliation of CalSim II and CRESPI flow projections

With monthly flows from CalSim II and daily flows from CRESPI produced for all scenarios, the final step was to reconcile these two sets of projections to produce a single set of projected impaired flows. The goal in this process was not to modify CRESPI output to exactly match each month's CalSim projection, but instead to ensure

that long-term flow timing and magnitude trends simulated by CalSim were accurately reflected in the final daily projections. This was accomplished by using trends in CalSim outputs to produce multiplicative adjustment factors that could be applied to the CRESPI data such that the result satisfied the goal of flow trend preservation. This approach entailed the following steps for flows at each location and in each scenario:

1. For each WY month, calculate 31-year moving average of both monthly-averaged CRESPI and CalSim flow values.
2. Calculate multiplicative trend factors for trends in both CalSim and CRESPI outputs by dividing the time series from Step 1 by their WY1995 (center of WY1980-2010 period) value.
3. Divide the CalSim trend factor time series from Step 2 by the CRESPI trend factor time series from Step 2 to obtain the trend "adjustment factor" (AF) annual time series. This results in 12 AF time series, one for each WY month.
4. Combine the 12 AF time series into a single monthly AF time series.
5. Interpolate monthly AF to daily using interpolation method that preserves monthly means (Rymes and Myers 2001).
6. Apply interpolated AF to original CRESPI output.

The final result preserves the CalSim-generated flow trends, but retains the daily flow information produced with the CRESPI method. Since the CRESPI outputs were already constrained by CalSim outputs, the resulting AF values are generally moderate, such that the final time series remain physically realistic.

Discussion

The new approach to applying CalSim II, the State of California Department of Water Resources freshwater operations model, and the joint application of the new CRESPI method that has been presented here provide a robust and flexible capability for evaluating the response of the freshwater management infrastructure to scenarios of future change. While many caveats and opportunities for improvement remain, the basic approach outlined here allows for the direct evaluation of new hydroclimatic scenarios, such as those derived from GCM outputs. This approach was developed to provide

estimates of managed downstream flows for inputs to watershed sediment and estuarine hydrodynamic and ecological models as part of the CASCaDE 2 project, but could ultimately prove useful for similar projects whose goal is to translate GCM scenarios into downstream boundary conditions for studies of regional and local impacts for climate change. Some of the methods and code presented here should also be transferable to similar studies in other highly impaired watersheds.

References

- Acharya, A, Ryu, J.H. (2014) "Simple method for streamflow disaggregation", *Journal of Hydrologic Engineering*, 19, 509-519.
- AECOM (2011) "Yuba County 2030 General Plan Environmental Impact Report", prepared for Yuba County Planning Dept., <http://www.yubavision2030.org>.
- Anderson J, Chung F, Anderson M, Brekke L, Easton D, et al. (2008) Progress on incorporating climate change into management of California's water resources. *Climatic Change* 87: S91-S108.
- Boe, J.; Terray, L.; Habets, F. & Martin, E. Statistical and dynamical downscaling of the Seine basin climate for hydro-meteorological studies. *International Journal of Climatology*, 2007, 27,1643-1655, doi: 10.1002/joc.1602.
- Brekke LD, Miller NL, Bashford KE, Quinn NWT, Dracup JA (2004) Climate change impacts uncertainty for water resources in the San Joaquin River Basin, California. *Journal of the American Water Resources Association* 40: 149-164
- Brekke LD, Maurer EP, Anderson JD, Dettinger MD, Townsley ES, et al. (2009) Assessing reservoir operations risk under climate change. *Water Resources Research* 45.
- California Department of Water Resources (1990) "Final environmental impact report on the revocation of the certificate of approval for Misselbeck Dam and Reservoir".

California Department of Finance (2008) "Major dams and reservoirs of California", Table G-3 of California Statistical Abstract, <http://www.dof.ca.gov/html/FS\ DATA/STAT-ABS/documents/G3.pdf>.

CDWR (California Department of Water Resources) 2014. California Central Valley Unimpaired Flow Data, Fourth Edition. http://www.waterboards.ca.gov/waterrights/water_issues/programs/bay_delta/bay_delta_plan/water_quality_control_planning/docs/sjrf_spprtinfo/dwr_2007a.pdf

Chung, F. and Seneviratne, S. (2009) Developing Artificial Neural Networks to Represent Salinity Intrusions in the Delta. World Environmental and Water Resources Congress 2009: pp. 1-10.

Draper AJ, Munevar A, Arora SK, Reyes E, Parker NL, et al. (2004) CalSim: Generalized Model for Reservoir System Analysis. Journal of Water Resources Planning and Management 130: 480-489.

Dracup JA, Vicuna S, Leonardson R, Dale L, Hanneman M (2005) Climate Change and water Supply Reliability. . California Energy Commission, PIER Energy-Related Environmental Research CEC-500-2005-053.

Li, H.; Sheffield, J. & Wood, E. F. Bias correction of monthly precipitation and temperature fields from Intergovernmental Panel on Climate Change AR4 models using equidistant quantile matching. J. Geophys. Res., 2010, 115, D10101, doi:10.1029/2009JD012882.

Maurer, E.P. and D.W. Pierce, 2007. Bias correction can modify climate model-simulated precipitation changes without adverse affect on the ensemble mean, Hydrol. Earth Syst. Sci., 18, 915-925, doi:10.5194/hess-18-915-2014.

NRC: National Research Council, 2012. Sea-Level Rise for the Coasts of California, Oregon, and Washington: Past, Present, and Future. National Academies Press. 201 pp.

- Reynolds, T.S., Scott, C. (1980) "The Battle Creek Hydroelectric System and the Northern California Power Company 1900-1919 with a 1919-1980 Postscript", *Historic American Engineering Record CA-2*.
- Rymes, M. D. and Myers, D. R. 2001. Mean-Preserving Algorithm for Smoothly Interpolating Averaged Data. *Solar Energy*. Vol. 71(4), 2001; pp. 225-231
- Singer, M.B., Aalto, R., and L.A. James (2008), Status of the lower Sacramento Valley Flood-Control System within the context of its natural geomorphic setting, *Natural Hazards Review*, 99 (3), 104-115.
- U.S. Army Corps of Engineers (1970) "Oroville Dam and Reservoir -- Report on reservoir regulation for flood control. Appendix IV to Master Manual of Reservoir Regulation, Sacramento River Basin, California"
- U.S. Army Corps of Engineers (1962, rev. 1977), "Shasta Dam and Lake -- Report on reservoir regulation for flood control. Appendix IV to Master Manual of Reservoir Regulation, Sacramento River Basin, California"
- U.S. Army Corps of Engineers (1999), Central Valley flood management systems, Chapter 3 of Post-Flood Assessment for 1983, 1986, 1995, and 1997, Central Valley, Calif., published March 1999.
- Vicuna S, Maurer EP, Joyce B, Dracup JA, Purkey D (2007) The Sensitivity of California Water Resources to Climate Change Scenarios¹. *JAWRA Journal of the American Water Resources Association* 43: 482-498.
- Willis, A.D., Lund, J.R., Townsley, E.S., Faber, B.A. (2011) "Climate change and flood operations in the Sacramento Basin, California", *San Francisco Estuary & Watershed Science*, 9 (2).
- Yuba County Water Agency (2012) "Technical Memorandum 2-2 -- Water Balance/Operations Model", Yuba River Development Project, FERC Project No. 2246.

Task 4: Hydrodynamic modeling

Rosanne Martyr, John Helly, Lisa Lucas, Noah Knowles, Mick van der Wegen and Dano Roelvink, in collaboration with Arthur van Dam, Sander van der Pijl, Herman Kernkamp, and Julia Vroom, Deltares (submitted 06-29-15)

Software Background and Initial Capability

Delft3D-FM is an unstructured version of Delft3D, a widely used hydrodynamic modeling software suite developed by Deltares of the Netherlands (<http://oss.deltares.nl/web/delft3d/d-flow-flexible-mesh>, also www.d3d-baydelta.org). Deltares, in conjunction with the University of Delft, has a wealth of experience in hydrodynamic modeling of complex bathymetric and topographic regions through the development and application of the Delft3D model. Delft3D is a structured, finite difference model that solves the shallow water equations in 2 and 3 dimensions, and includes sediment transport, waves, water quality and ecology sub-models. Like Delft3D, Delft3D-FM also includes formulations for sediment transport and morphodynamic development. Delft3D-FM, in contrast to Delft3D, utilizes a finite volume, unstructured grid framework, allowing for variable resolution in regions of complex topography and bathymetry, and in regions where forcing functions and responses change rapidly. The unstructured grid framework allows for polygon-shaped grid cells of arbitrary degree in 2-D (latitude and longitude) space, and includes 1D channel networks, and 3-D finite difference grids. The new software was thus well-suited for riverine flows, shallow seas, estuaries and shelf breaks, all present in the Bay-Delta system.

At the onset of the project, Delft3D-FM was available in serial, Windows format, and capable of 2D computations of water levels, velocity, and discharge. This initial capability was insufficient to meet the CASCaDE II project needs. The modeling needs of the project can be categorized into two main groups:

1. Need for parallel, scalable software
2. Need for 3D hydrodynamics, salinity, and temperature capability

Parallel, scalable computing software would satisfy the project's need for software that could perform multiple simulations simultaneously and quickly, thus accommodating the types of simulations envisioned in the project. This capability would help to meet the project goals to model a range of climate and infrastructure scenarios. In addition, it was critical to have software that was able to model 3D hydrodynamics, including gravitational circulation, and thermal- and salinity-driven stratification, all of which are present in the Bay-Delta system. CASCaDE's hydrodynamic team dedicated large amounts of effort working closely with Deltares to develop and apply Delft3D-FM software that could be used to achieve the project's modeling needs for the Bay-Delta. This work is outlined in the Research and Development portion of this report.

Research and Development

Software Verification

Deltares developed Linux and parallel computing capability to accommodate multiple simulation capability, speed up simulation times and improve modeling performance on computing clusters. The hydrodynamics team applied numerous versions of this software to the Bay-Delta model to assess its ability to accurately reproduce Bay-Delta hydrodynamics quickly and efficiently. Project hydrodynamic modeler Rosanne Martyr spent considerable effort on the compilation and application of Delft3D-FM on numerous computing platforms to assess the software's speed and ability to reproduce computations across computing platforms. Platforms included a Windows-based personal computer, USGS Linux blade cluster named Swift, and NSF-funded supercomputers Gordon and Stampede, located at San Diego Supercomputer Center (SDSC) and University of Texas' Texas Advanced Computing Center (TACC), respectively. These supercomputers are part of the XSEDE project (<http://xsede.org>). The hydrodynamic team was awarded computer research time at Gordon and Stampede through the successful submission of research proposals showing, first, that the parallel solver of the hydrodynamic model, a key component for the parallelization of the software, and subsequently the entire software with the Bay-Delta model, was scalable up to a large number of computational processors. This was critical in proving

that the model could take advantage of the supercomputer resources at the SDSC and TACC.

An important portion of this work included the profiling of parallel processes within the software itself. Profiling analysis highlights the parts of the software that have the longest computing times, as well as the time spent computing by each computing processor. This work, done by Martyr, helped developers at Deltares find software bugs and areas to improve the parallel computing performance of the code. An example of profiling analysis figure for 16 processors is shown below. This example shows that, while the overall software takes the same amount of time on each processor (top figure), the parallel computing framework per processor can vary in computing time, creating potential bottlenecks for the entire software.

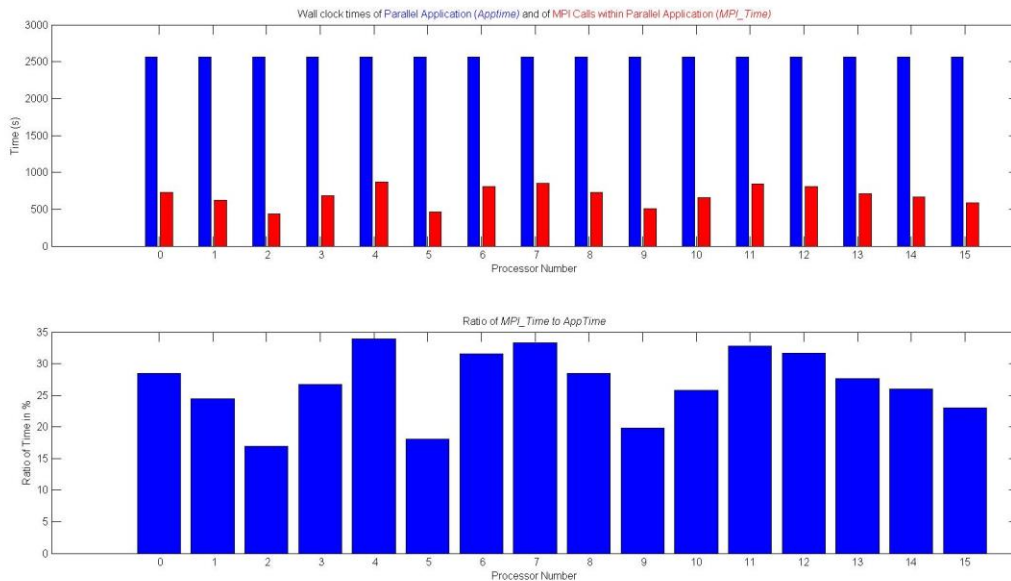


Figure 4-1. The time spent by individual processors on parallel processing work in seconds (above) and as a percentage of the entire runtime (below).

Subsequently, once the 3D, parallel version of Delft3D-FM was available and installed, Martyr performed full model testing of the Bay-Delta model on the 3D-capable version of the hydrodynamic software. Full model testing was performed on each machine, the USGS's Swift, SDSC's Gordon, and TACC's Stampede. Runtimes on individual machines can differ based on hardware configuration, compilers, software optimization for particular compilers, and the computational problem size per computing processor.

Nonetheless, the goal is for the software to show a decrease in runtime that is proportional to the number of cores or processors used. The following figure shows that Delft3D-FM, with the Bay-Delta model, indeed decreases runtime with increasing number of processors. Model runtimes are faster on XSEDE machines than on the USGS cluster due to improved hardware, optimized compilers and increased memory.

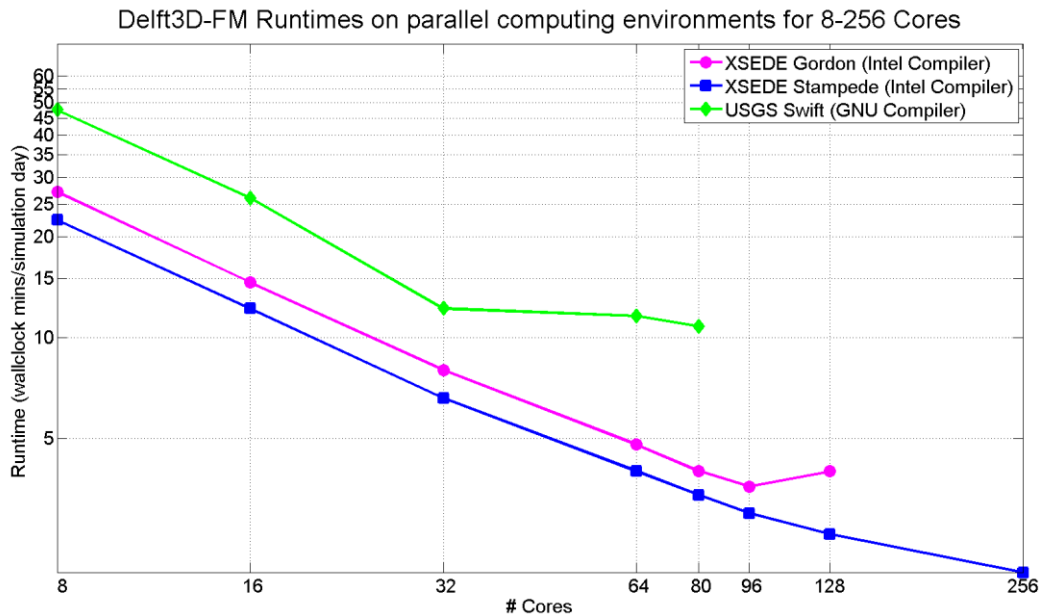


Figure 4-2. The runtimes of the hydrodynamics software on the San Francisco Bay model on different computing platforms.

Finally, Martyr worked closely with model developers at Deltares to improve model accuracy in the San Francisco Bay-Delta domain. This included a month-long visit to Delft, Netherlands in 2014. Software capabilities that were key to the CASCaDE project had been added and/or modified. Model developers included faster implementations of the 3D momentum and salinity advection schemes, and made overall improvements in code structure to decrease model runtime. Model accuracy has also increased due to improvements in 3D discharge routines to handle flow reversal, full functionality of diffusivity and viscosity coefficients, and modifications in the unstructured grid to improve flow connectivity between bays and channels.

Unstructured Grid

The unstructured grid, developed by Mick van der Wegen, includes the San Francisco Bay and Delta, large portions of the Sacramento and San Joaquin Rivers and many of

their distributaries, the Yolo Bypass floodplain, gates and barriers for water conveyance, and many narrow, sinuous channels. The model domain includes depiction of South, Central and North Bays, lower Yolo floodplain up to Fremont Weir, numerous channels of the north, central and south delta, as well as flooded islands of Frank's Tract and Mildred Island. The northern boundaries of the grid were extended to account for increased upstream tidal propagation due to sea level rise. As such, the domain now includes the Sacramento River up to Verona, the American River eastward to Fair Oaks, the Mokelumne River eastward to Woodbridge, the San Joaquin River southward to Vernalis, and Napa, Sonoma, and Petaluma River outlets to the North Bay. Van der Wegen has updated the bathymetry on this new grid using a compiled bathymetry and topography dataset provided by Jaffe and Fregoso at the USGS.

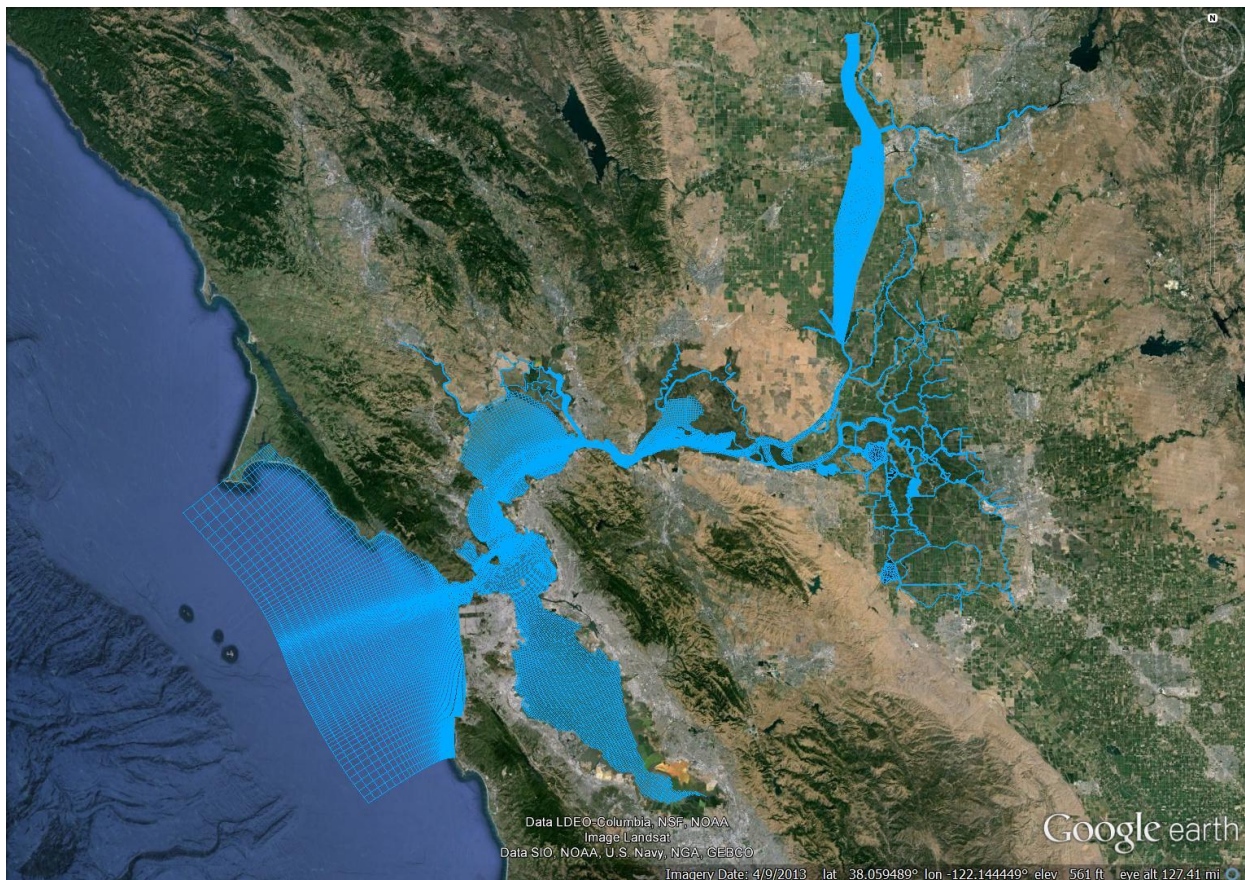


Figure 4-3. The unstructured grid of the Bay-Delta domain

The model utilizes a combination of grid triangles, rectangles and pentagons which allows for alignment along main flow directions, more natural depictions of irregular

coastlines, and numerical efficiency. Model resolution is lower in the open ocean near Point Reyes, and higher in the inner channels of the Delta and within the San Francisco Bay where drivers and response gradients are large.

Software 3D Development

Software 3D hydrodynamics were introduced in early 2014. Shortly after, 3D salinity was included, while 3D temperature was introduced in late 2014. As mentioned previously, Delft3D-FM uses a finite volume scheme and unstructured grid approach for the horizontal domain, defined by the aforementioned grid, while the vertical structure uses a finite difference method. Delft3D-FM has two approaches, the sigma layer method and the z layer method, to discretize the vertical structure of the domain. The sigma layer method uses a prescribed number of vertical layers which are subsequently kept constant in space and time, leading to thicker layers in deep regions and thinner layers in shallow regions. Sigma layer thickness is uniform with depth, and varies in time to accommodate changes in water surface elevation. In contrast, the z layer method uses a prescribed layer thickness, so that the number of vertical layers is smaller in shallow regions and larger in deep regions. The number of layers also varies in time due to changes in water levels. Similar to the sigma approach, layer thickness in the z-layer approach is uniform with depth. Martyr worked closely with van der Wegen and others in Delft to assess the feasibility of these two vertical discretization approaches for the Bay-Delta domain. The sigma layer approach was provided in early 2014, while the z layer approach became available in early 2015.

Both vertical approaches were extensively tested on the Bay-Delta domain for runtime stability, reproducibility of calculations across computing platforms, and for accuracy when compared to measurements throughout the Bay and Delta. Initial tests with 3D salinity in the Bay-Delta domain revealed a number of numerical instabilities. The hydrodynamics team worked alongside developers at Deltares on repeated testing of updated code versions to obtain software that was stable for long simulations over a range of hydrological conditions. Furthermore, salinity and temperature were tested and calibrated separately, as the temperature capabilities became available in late 2014, after salinity calibration had begun.

Finally, in early 2015, 3D boundary conditions became available for Delft3D-FM. This capability allows for the specification of a vertically varying profile of velocity, salinity and temperature at the boundaries, which are important for climate change scenarios. The hydrodynamics team will soon conduct tests of these boundary conditions.

Findings

Water levels, Flows, and Salinity Calibration

3D water levels, flows, and salinity were calibrated over the period December 16, 1999 to September 30, 2000. This period was chosen to correspond with initial calibration work of 2D water levels and flows done by van der Wegen, spanning the period December 16, 1999 to February 15, 2000. The calibration period includes highly variable hydrologic conditions, including an above average wet period in February, March and April, 2000. Model setup uses the sigma layer approach with 10 vertical layers, variable friction values that are inversely proportional to depth, and a host of other parameters chosen with guidance from Deltares. The following sections highlight the latest calibration results.

The hydrodynamics team notes the following major findings regarding the Delft3D-FM software:

1. Model runtimes range between 7 and 11 minutes per simulation day, and are dependent on the frequency of file writing and the computing platform.
2. The z layer approach produces more landward salt transport and less vertical mixing than the sigma layer approach. However, the z layer approach was not stable during periods of high and varying hydrologic conditions.
3. The sigma layer version is more vertically diffusive than the z layer approach. In addition, the software is unable to use more than 10 sigma layers, leading to increased vertical mixing due to the relative increased thickness of the layers in deeper areas.
4. Bottom friction is shown to be a major contributor to vertical mixing and diffusion. Application of bottom friction values that are inversely proportional to water depth

(i.e. low in deep areas and high in shallow areas) leads to an increase in landward salt transport, and increased salinity-driven stratification.

Daily freshwater discharge was specified at the Sacramento, San Joaquin, American, Mokelumne, Napa, and Petaluma Rivers, based on USGS measurements at nearby stations. Hourly water levels were prescribed at the Pacific Ocean boundary, based on NOAA measurements of water levels at Point Reyes. Daily surface and bottom salinity were prescribed at the Pacific Ocean boundary based on USGS measurements of upper salinity at the Farallon Islands. Almost all freshwater flows were prescribed initial and boundary salinity conditions of 0. The San Joaquin River is the exception to this, for which a daily salinity was prescribed at the Vernalis boundary based on conductivity measurements at a nearby station.

Delft3D-FM software supports the inclusion of weirs, pumping stations, and temporary installations of gates and barriers. Pumping stations at Tracy, Clifton Court, and North Bay Aqueduct were included for calibration. The Delta Cross Channel Gates and temporary barriers at Middle River, Old River, and Grant Line Canal were included in calibration simulations. Work is ongoing for the inclusion of the Sacramento Weir and Suisun Marsh Salinity Control Gates.

The team noted model spinup times of approximately 2.5 months; as such error statistics are calculated for the period March 1 to October 1, 2000. The following is a summary of model error and skill for water levels, discharges, and salinity. Modeled water levels had an average RMSE of 0.14m. Modeled discharges had an average RMSE of 56 m³/s, which is dominated by errors at Freeport, Jersey Point, and Rio Vista. The average modeled salinity RMSE for time series stations was 1.7 in the lower water column, and 1.2 in the upper water column. This error was dominated by errors at Crockett. The average cruise salinity RMSE error was 1.5, and the average profile station error was also 1.5. The cruise and profile station errors were dominated by errors at Pinole Shoal. The mean unbiased RMS difference (ubRMSD), bias, RMSE, and Skill are provided in the table below.

	Water levels m	Discharges m ³ /s	Lower Salinity	Upper Salinity	Salinity Profile by Station	Salinity Profile by Cruise
ubRMSD	0.133	53.553	1.496	1.102	1.093	1.134
Bias	0.005	1.387	0.124	-0.272	0.899	0.899
RMSE	0.139	56.261	1.734	1.239	1.534	1.542
Skill	0.976	0.943	0.926	0.901	0.907	0.989

Table 4-1. Performance metrics for water level, discharge, and salinity for the calibrated 3D model.

Water levels

Modeled water levels were compared to hourly water levels at ten stations throughout the domain, shown in the figure below.

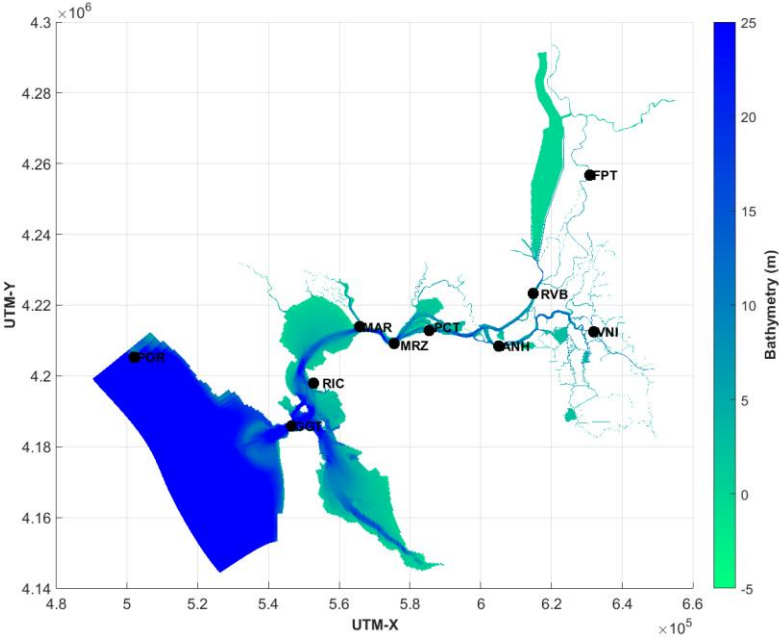


Figure 4-4. Locations of water level calibration stations

Overall, a mean model RMSE of 0.140m and bias of 0.005m is achieved. The highest RMSE occurred at Freeport (0.29m), and the lowest RMSE occurred at Point Reyes (0.02m). Bias was very small, from 0.033m at Antioch to 0.15m at Freeport.

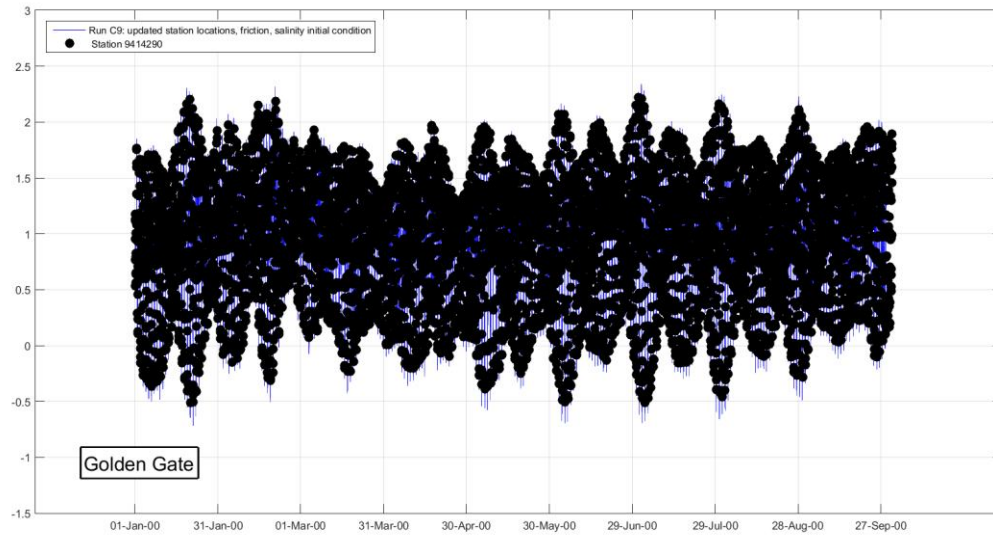


Figure 4-5. Modeled (in blue) and measured (in black) water levels at the Golden Gate Bridge from January to September, 2000.

Water levels and discharges at Freeport are lower than measurements during February and March. This may be attributed to modeled flow overtopping at Sacramento Weir into the Yolo floodplain. Work is underway to explicitly define Sacramento Weir to prevent this excessive overtopping.

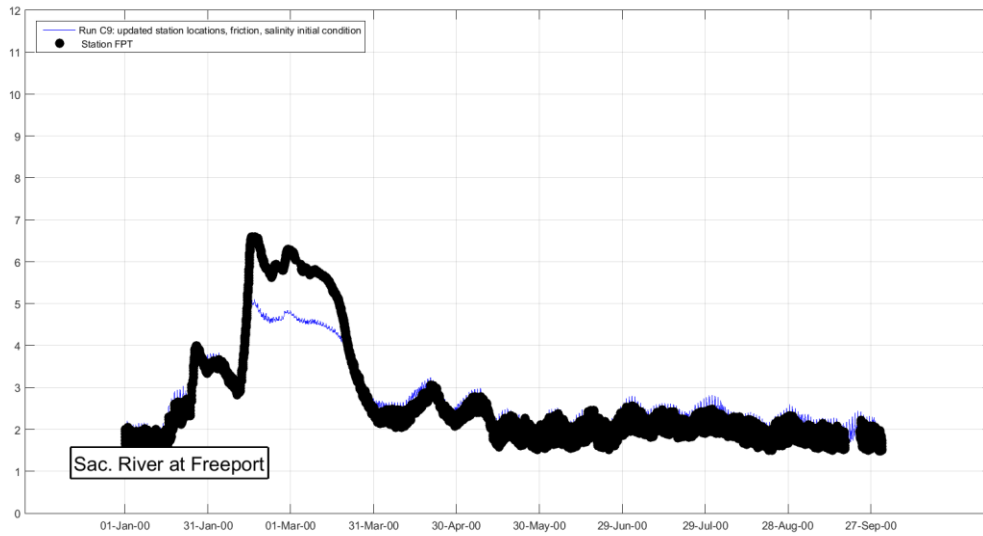


Figure 4-6. Modeled (blue) and measured (black) water levels at the Sacramento River at Freeport from January to September, 2000.

Model skill was very high, from 0.93 at Freeport to 1.0 at Point Reyes. Normalized bias and normalized, unbiased RMSD of measurements and model are shown in the target diagram below. Model RMSD is larger than the measured RMSD for almost all stations, indicating that the range of modeled water levels was larger than the measurement range for the calibration period.

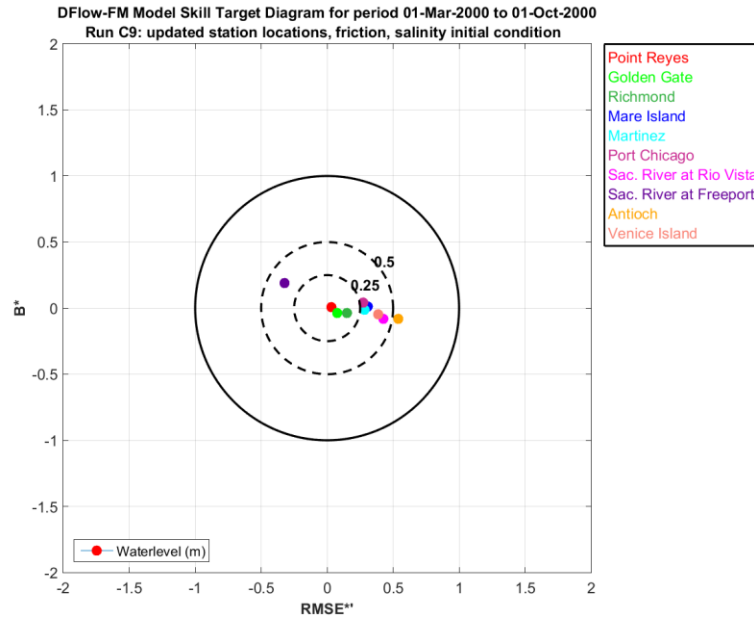


Figure 4-7. Water level target diagram shows the modeled normalized, unbiased RMSE on the horizontal axis, and modeled normalized bias on the vertical axis. Decreasing distance from the center shows increasing agreement with measurements.

Discharges

Modeled discharges were tidally filtered and compared to daily measurements of tidally filtered discharges at 9 stations throughout the domain.

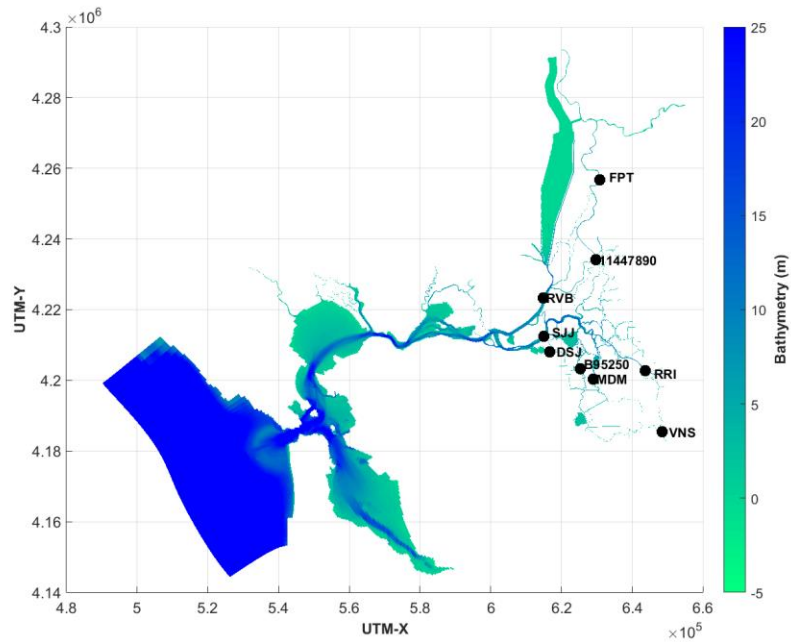


Figure 4-8. Locations of discharge calibration stations.

The mean modeled RMSE was $56\text{m}^3/\text{s}$. The lowest RMSE occurred at Dutch Slough ($6.4\text{m}^3/\text{s}$), while the highest RMSE occurred at Freeport ($120\text{m}^3/\text{s}$). Mean model bias was $1.4\text{m}^3/\text{s}$, with a maximum bias of $22\text{m}^3/\text{s}$, and a minimum bias of $-19\text{m}^3/\text{s}$. Model skill was also high, ranging from 0.86 at Dutch Slough to 1.0 at Vernalis.

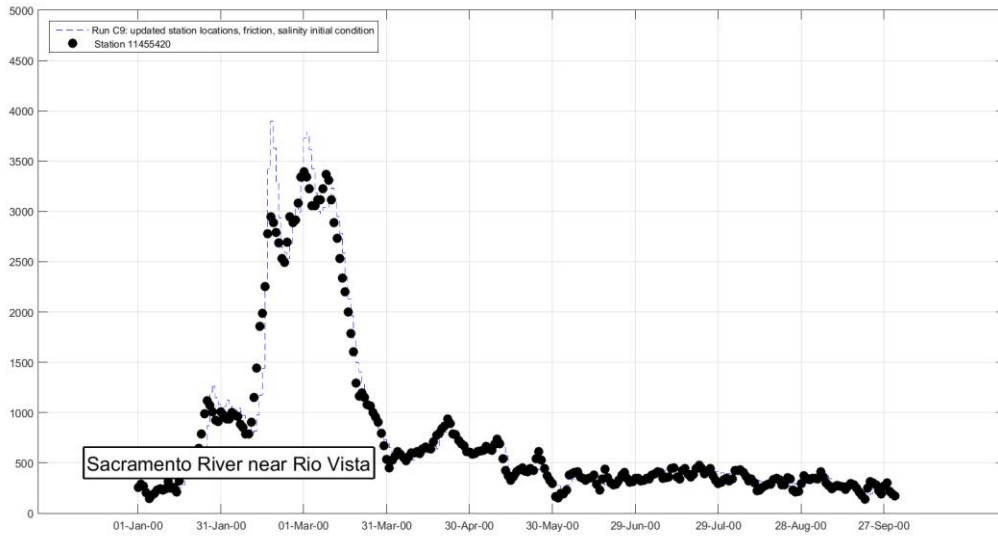


Figure 4-9: Modeled (blue) and measured (black) tidally filtered discharge at the Sacramento River near Rio Vista from January to September, 2000.

Based on the target diagram, the model showed good agreement with the variability of the measurements. Many stations exhibited little bias and small RMSE. Approximately half of the stations had smaller RMSD than the measurements.

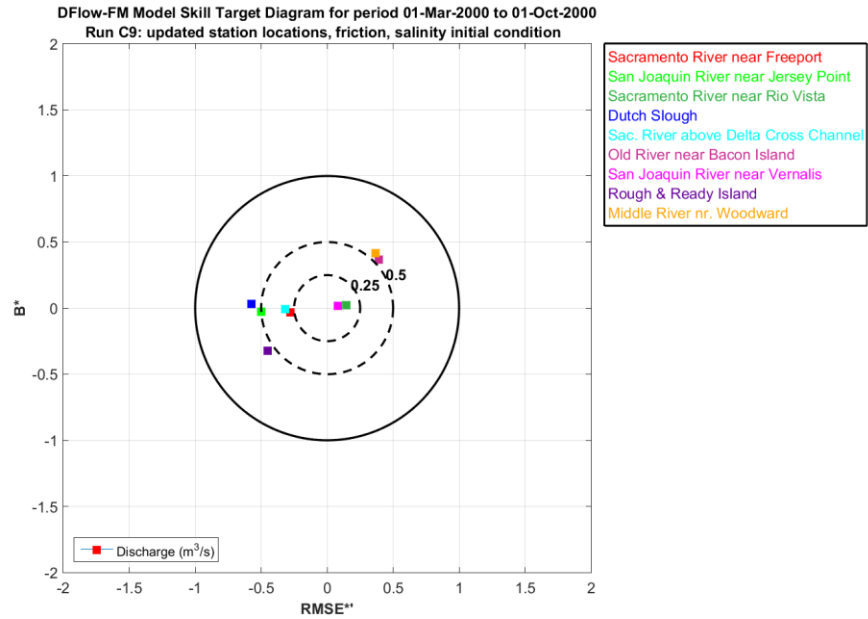


Figure 4-10. Discharge target diagram of modeled normalized, unbiased RMSE and normalized bias

Salinity

Modeled salinity was compared to continuous time series measurements at fixed upper and lower water column locations throughout the Bay-Delta, and to vertical profiles of salinity in Central, San Pablo, and Suisun Bays. Salinities at USGS-maintained gauges (denoted by 8 digit labels) are recorded every 15 minutes while salinities reported through CDEC repository (denoted by three-letter labels) are provided hourly. USGS vertical profiles of salinity are collected monthly.

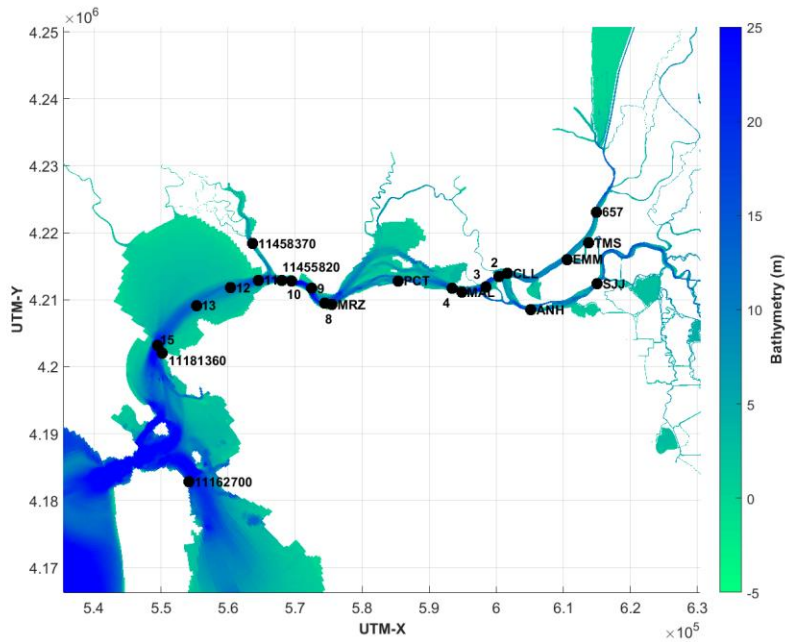


Figure 4-11. Calibration station locations for continuously recorded upper and lower salinity, and monthly recorded vertical salinity profiles.

Continuous Time Series

Modeled and measured salinity (shown in blue and black, respectively) in the lower water and upper water columns are plotted as a function of time from Jan 1, 2000 to Oct 1, 2000. Error statistics are calculated over the period Mar 1, 2000 to Oct 1, 2000. Three locations showing salinity in San Pablo Bay, Carquinez Strait, and Suisun Bay are provided as examples. Overall, the model closely follows the trends of the data and is able to replicate seasonal patterns of salinity variation. Close agreement of modeled lower and upper salinity also indicate that the model is able to replicate salinity-driven stratification at various locations within the Bay.

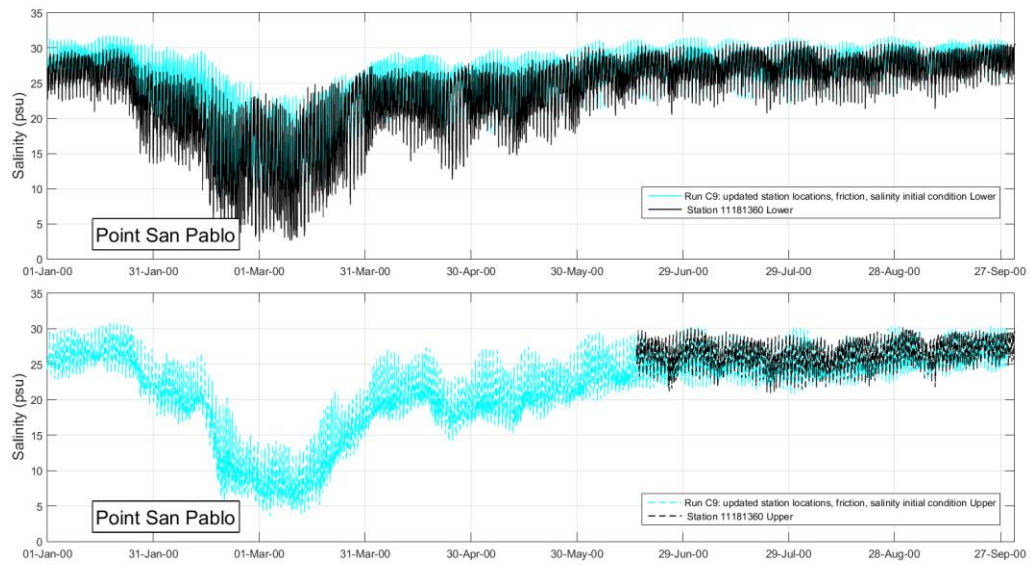


Figure 4-12. Modeled (blue) and measured (black) salinity in the lower water column (shown above) and in the upper water column (shown below).

The mean RMSE for upper salinity was 1.2, while the mean RMSE for the lower water column was 1.7. The lowest RMSE values for upper salinity occurred at Emmatton and Jersey Point (0.09 and 0.1, respectively), while the highest RMSE values occurred at Martinez and Crockett (2.5 and 3.5, respectively).

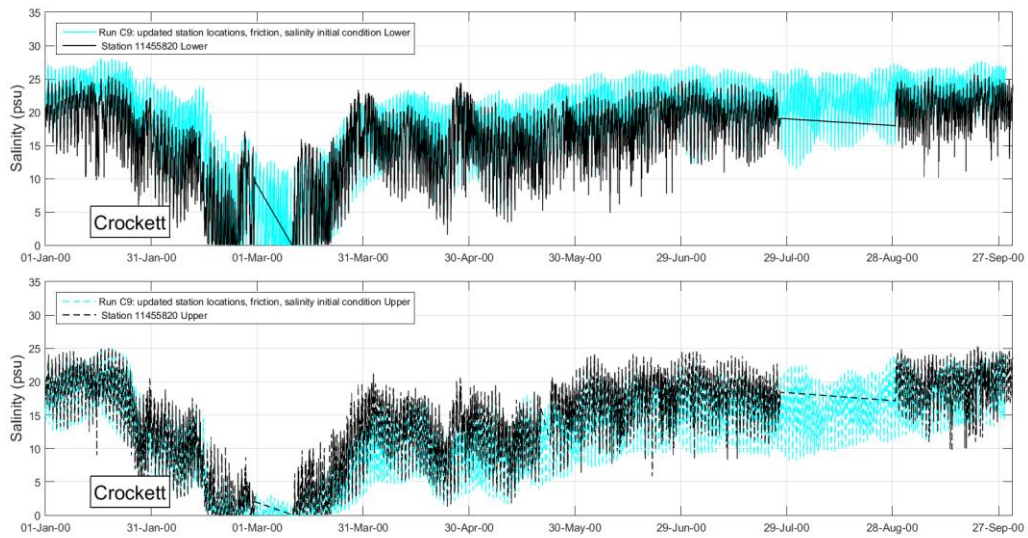


Figure 4-13: Modeled (blue) and measured (black) salinity in the lower water column (shown above) and in the upper water column (shown below).

For bottom salinity, the lowest RMSE values occurred at Emmatton and Collinsville (0.12 and 0.42, respectively), while the highest RMSE occurred Crockett and Mare Island Strait in the southern Napa River (3.4 and 2.7, respectively). Measurements of salinity in the lower water column are unavailable for Three Mile Slough, Jersey Point, and Antioch.

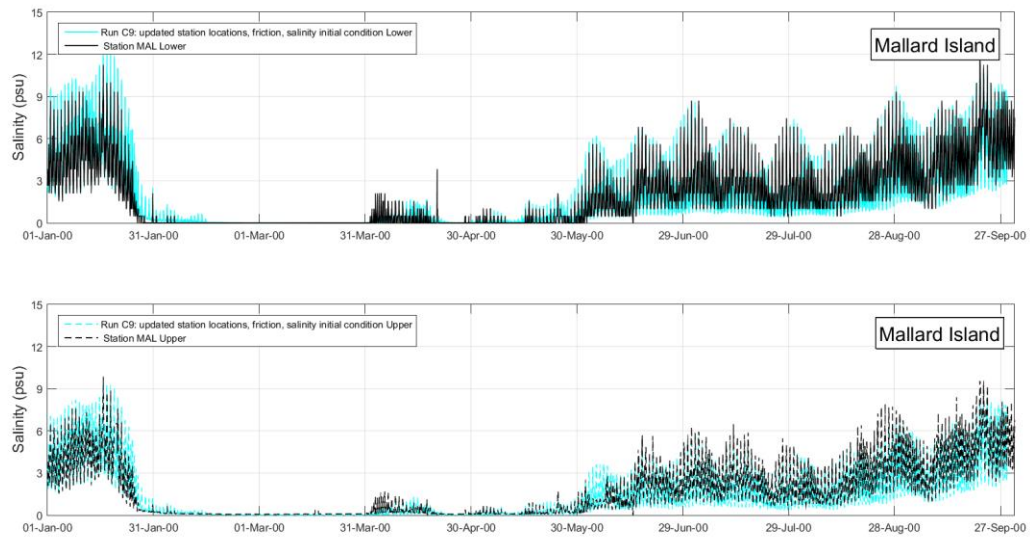


Figure 4-14. Modeled (blue) and measured (black) salinity in the lower water column (shown above) and in the upper water column (shown below).

Mean model skill was 0.93 and 0.90 for lower and upper salinity, respectively. Almost all stations fall within the unit circle of the target diagram, showing good agreement with measurement trends and variability. Model agreement with salinities at Three Mile Slough is poor (outside the unit circle); this may be attributed to this location's small salinity magnitude and variation in spite of the model's relative agreement with measurements (mean measured salinity of 0.11 versus mean modeled salinity of 0.08).

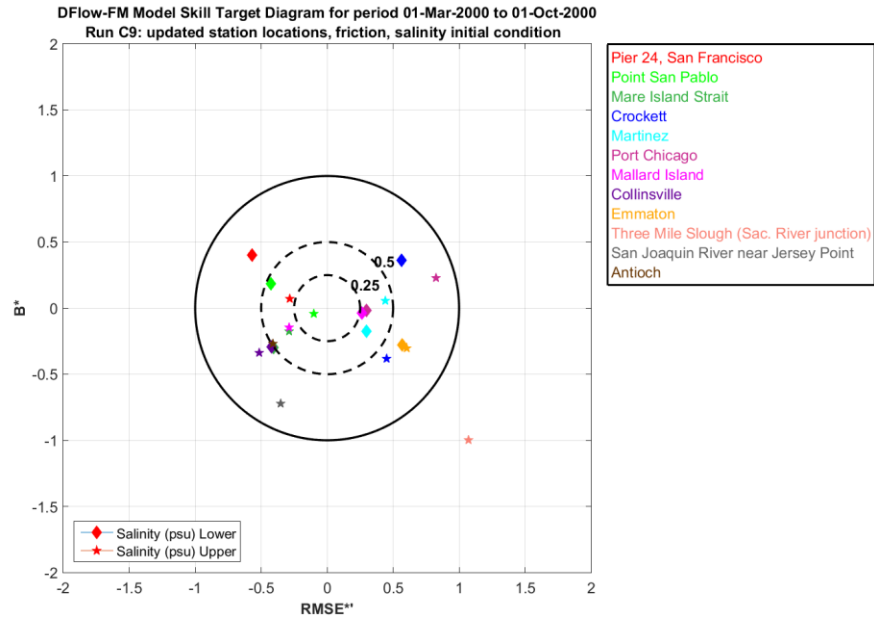


Figure 4-15. Continuous salinity target diagram of modeled normalized, unbiased RMSE on the horizontal axis and normalized based on the vertical axis.

Cruise profiles

Modeled vertical profiles of salinity were compared to monthly measured vertical profiles throughout the North Bay (i.e. San Pablo Bay, Carquinez Strait, and Suisun Bay) for 7 distinct dates and times. The model captures the range of salinity as well as the vertical profile shape for many stations, and captures the variability in regional salinity across seasons.

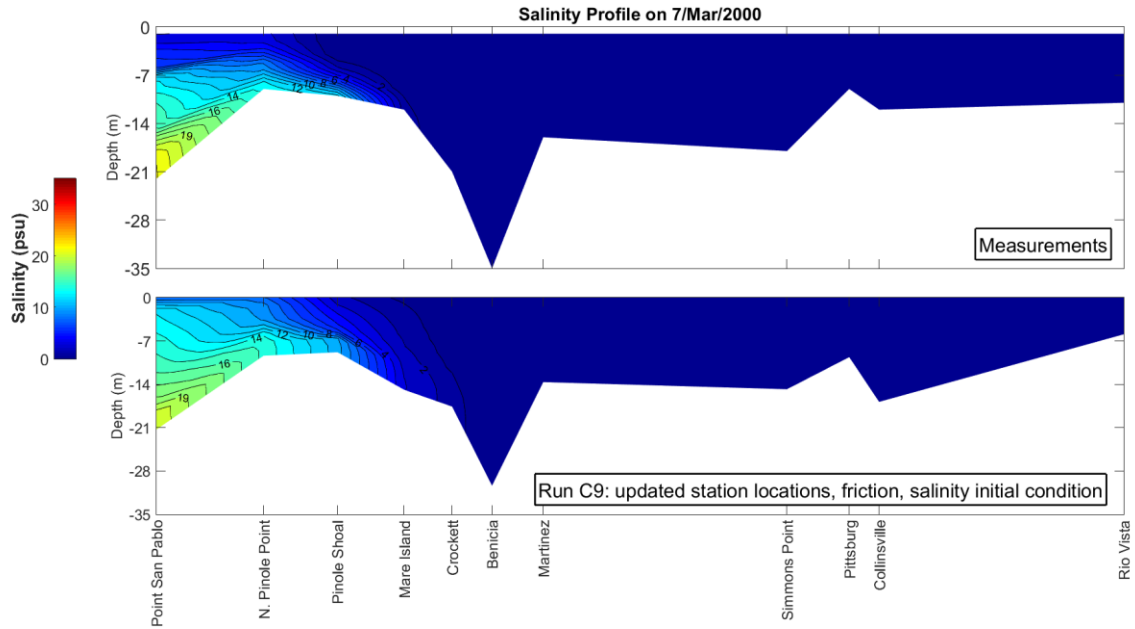


Figure 4-16. Measured (shown above) and modeled (shown below) vertical salinity profiles of Northern San Francisco Bay.

Cruise RMSE was highest in May (3.0) and lowest in September (0.5), with a mean RMSE of 1.5. Station RMSE was highest at Pinole Shoal (3.0) and lowest at Collinsville (0.447), with a mean station RMSE of 1.5. Station model skill ranged from 0.73 at Collinsville to 0.98 at Crockett and Benicia. It is noted that average model RMSE at Crockett was lower (1.8) than the time series RMSE (approximately 3.0).

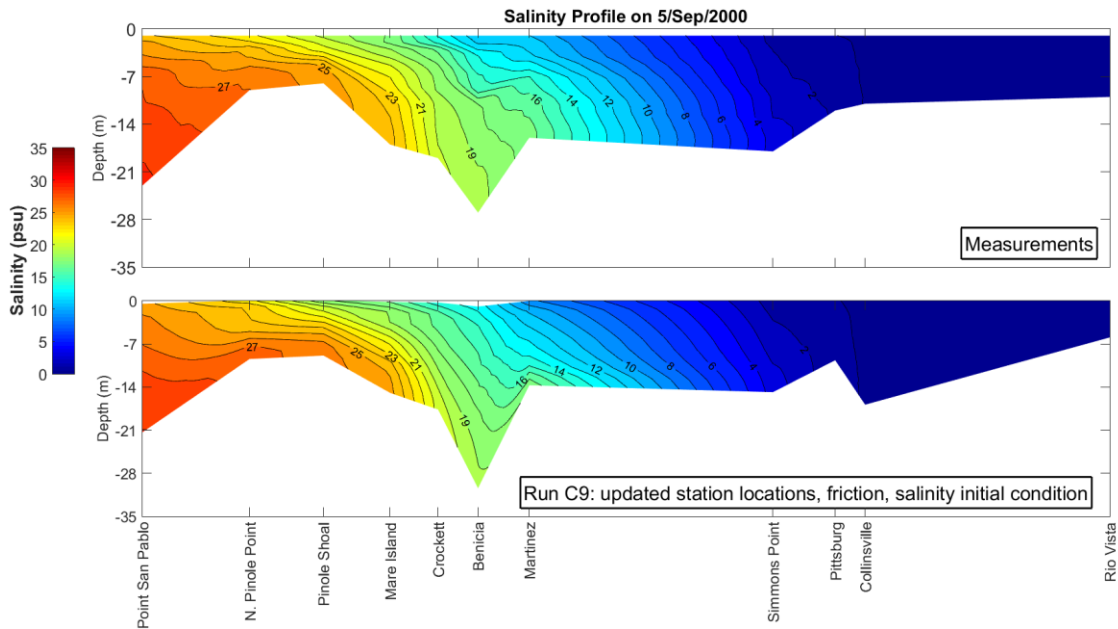


Figure 4-17. Measured (shown above) and modeled (shown below) vertical salinity profiles of Northern San Francisco Bay.

Both cruise (shown below) and station (not shown) target diagrams show good model agreement with the measurements. Overall modeled salinity profiles appear saltier than the measurements throughout the calibration period based on the normalized bias, but model-to-measurement agreement is very close by the end of the calibration period.

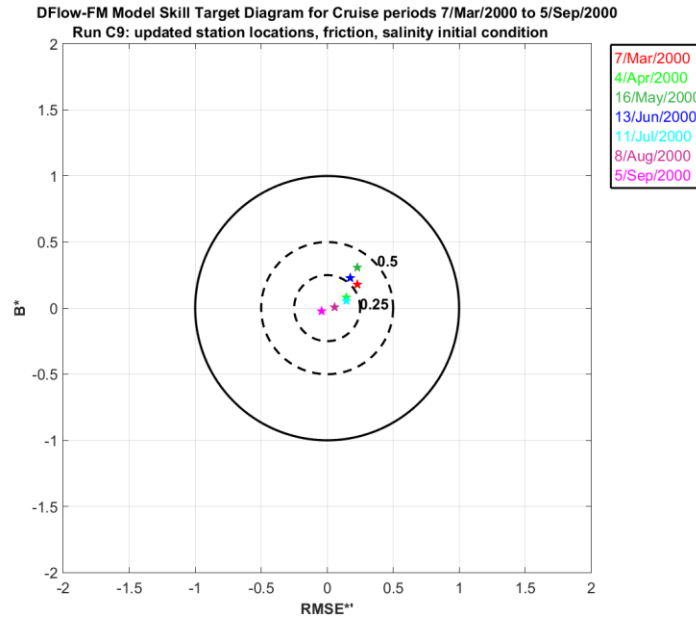


Figure 4-18. Cruise salinity vertical profile target diagram from March to September, 2000.

Recent Improvements

As previously mentioned, work was underway for the inclusion of the Sacramento Weir gates and Suisun Marsh salinity gates in the model setup. The Sacramento Weir gates have been included and have resulted in greater model agreement to measured flows and water levels at Freeport during both low and high flow periods.

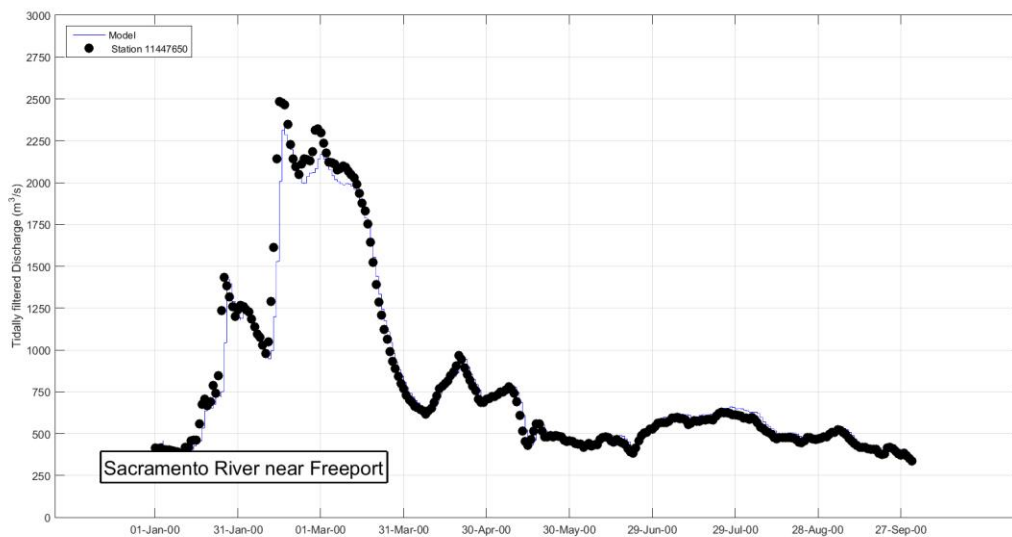


Figure 4-19. Measured (black) and modeled (blue) tidally filtered discharges at the Sacramento River at

Freeport. Modeled discharges more closely match measurements due to the inclusion of the Sacramento Weir gate operations.

This addition to the model setup also improved model-measurement agreement at the Delta Cross Channel and to a smaller extent at other locations in the Western Delta, and has led to an overall reduction of model discharge RMSE, and an increase in model discharge skill. Statistical analysis of modeled water levels and discharges now yields the following metrics:

	Water levels m	Discharges m ³ /s
ubRMSD	0.125	34.463
Bias	0.007	6.013
RMSE	0.133	37.233
Skill	0.978	0.961

Table 4-2. Modeled unbiased RMSD, RMSE, bias, and skill for March to September, 2000. Inclusion of Sacramento Weir gate operations decreased modeled RMSE and increased model skill in water levels and discharges.

Initial investigation shows no negative effects on model performance of salinity with the inclusion of the Sacramento gate operations; further statistical analysis on salinity is ongoing.

Temperature Calibration

As mentioned previously, temperature modeling capability was added to Delft3D-FM in late 2014. Thus calibration efforts were done separately from hydrodynamics and salinity efforts which started earlier in 2014. The aim of the project is to deliver a calibrated 2D and 3D temperature model with emphasis on the Delta region. Various Delft3D-FM related models have been set up and were calibrated to investigate the influence of climate change scenarios on the ecology in the San Francisco Bay and Delta region. This part concerns the progress made in water temperature data analysis and model configuration and calibration of coupling the DFM model (www.d3d-baydelta.org) with an atmospheric heat flux model forced by spatial fields of relative

humidity, air temperature and cloudiness to obtain water temperature dynamics. This effort was led by Mick van der Wegen.

Van der Wegen and others developed the temperature model initially in 2D mode for WY 2011 and did preliminary tests in 3D mode. In addition sensitivity analysis was performed on model parameters like relative humidity, air temperature and cloudiness (HAC), in terms of their value in time (constant, hourly or daily varying) and in terms of their spatial distribution. The hydrodynamic runs included Yolo bypass, and operations of the water export pumping, delta cross channel and temporary dams in the Delta. The results of the 2D configuration are discussed here.

In initial runs, the wind speed and direction, the relative humidity, the air temperature and the cloudiness measured at Stockton were applied uniformly to the model domain. These time series have an interval of one day. For the cloudiness the observed cloud cover, on a scale from 0 to 8, was multiplied by a factor 10 to represent the cloudiness in percentage form. For the rivers and the sea, a uniform temperature of 5°C was used.

The complexity of the model was gradually increased, first by applying measured temperatures at all boundaries, and later on by using spatially and hourly varying humidity, air temperature and cloudiness fields (MACA data, <http://maca.northwestknowledge.net/>, see also figure below). The Yolo Bypass, smaller rivers/pumps and dams were included in the model while the project was progressing.

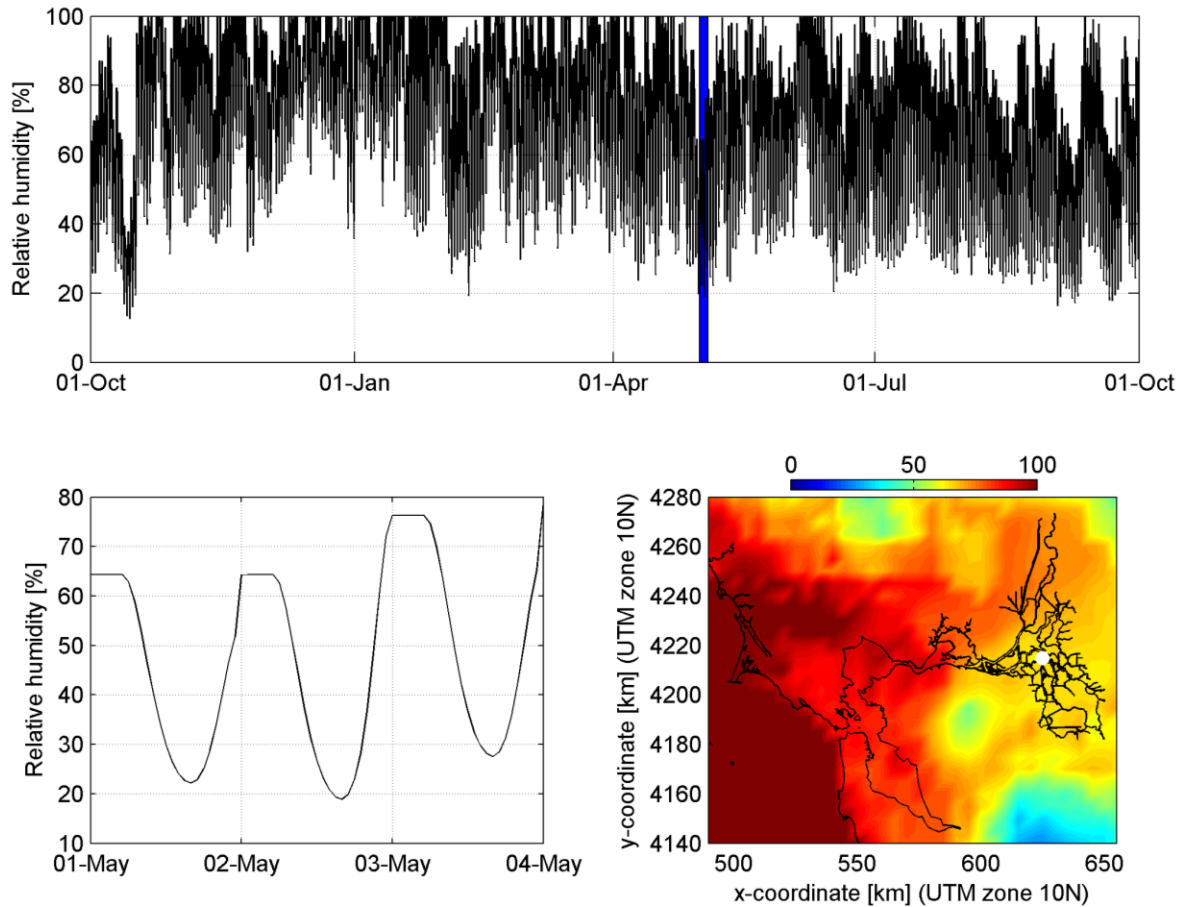


Figure 4-20. Input data of relative humidity in the centre of the Delta region, indicated with a white dot in the lower right panel, for water year 2011 (top panel), in May to visualize daily variation (lower left panel) throughout the model domain on 1 Oct 2010 (lower right panel).

Data analysis of regional measurements shows relatively constant water temperature at the ocean but more seasonally varying temperatures for more inland located stations. Delta temperatures are slightly lower than ocean temperatures in winter.

2D model results (best performing run June 11, 2015), including initially uniform temperature of 15 °C, spatially varying wind fields and hourly varying HAC fields, show that seasonal trends and absolute values are reproduced fairly well despite differences in daily varying temperatures.

In general model results are warmer and shows less variation than observations (see also target diagram below). Sensitivity analysis and input data analysis suggests that

the wind field is quite uncertain (coarse data, assumed spatial variation) and have a high impact on the model results. Using the wind-field (mainly magnitude) as a calibration parameter may considerably improve model results.

Comparison of these 2D runs with preliminary 3D runs shows only limited differences, which is attributed to effective tide induced vertical mixing, allowing for stratification only in deeper areas with limited flow velocities.

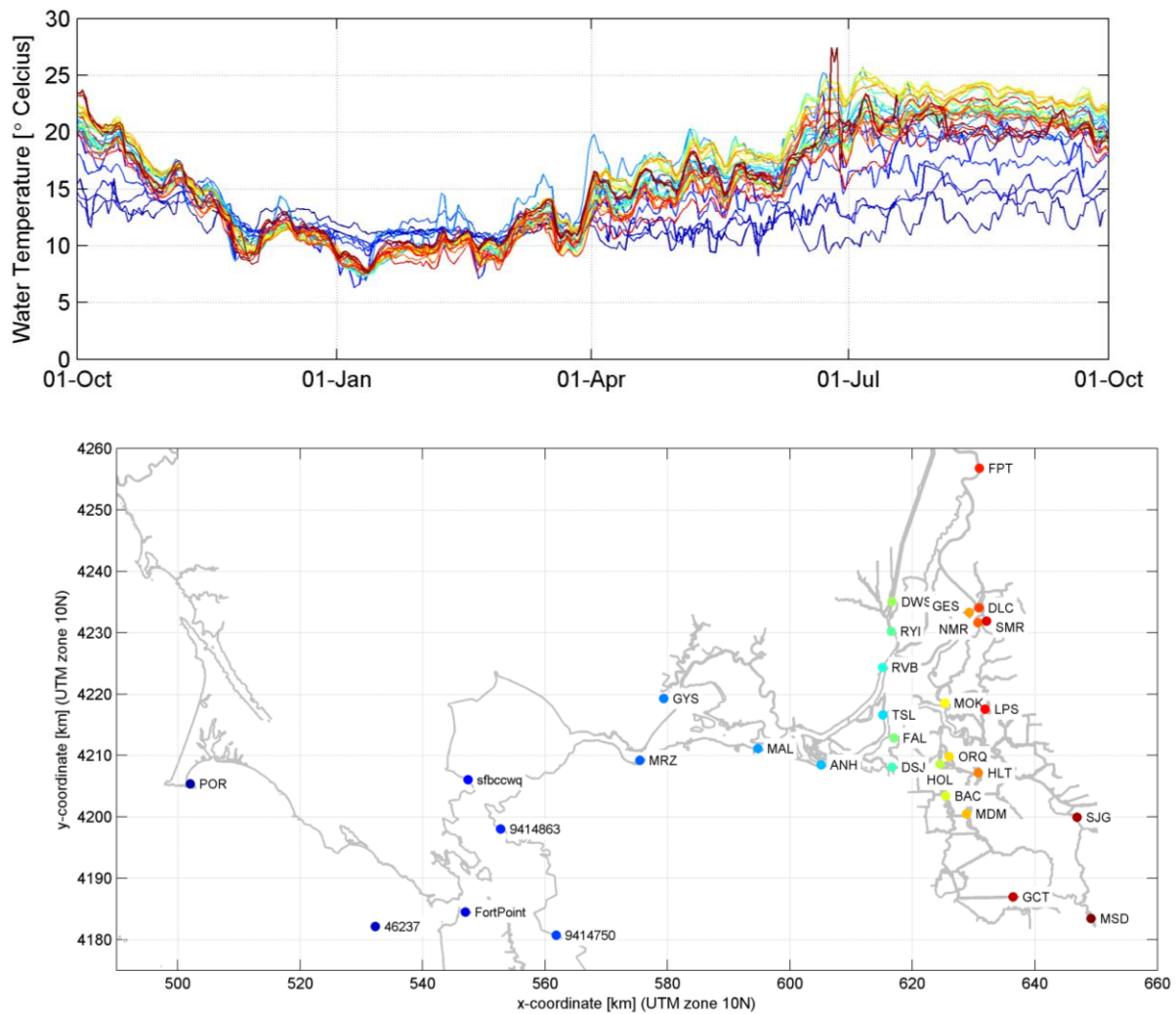


Figure 4-21: Observed daily averaged water temperature at all stations used for model calibration for water year 2011 (1 Oct 2010-30 Sep 2011). Colors in the top panel match the station locations in the lower panel. Sources: www.cdec.water.ca.gov, <http://co-ops.nos.noaa.gov>, data.cencoos.org

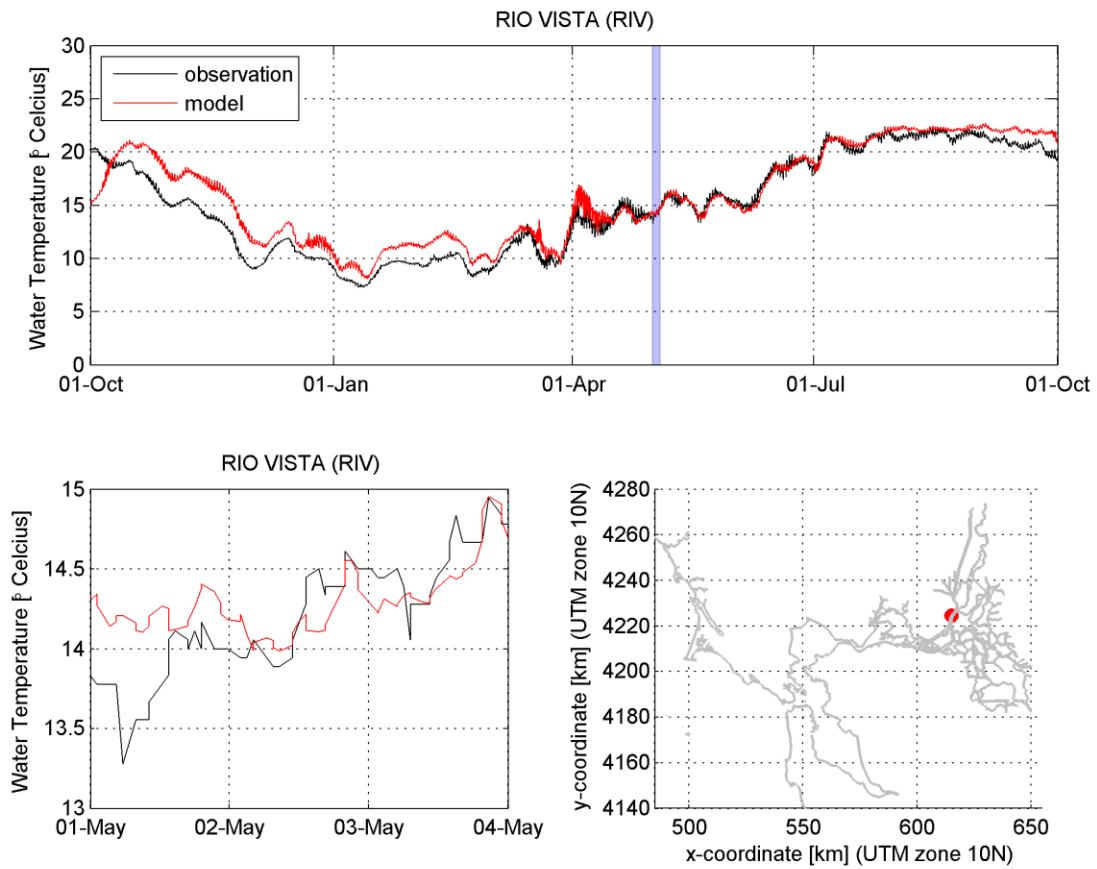


Figure 4-22. Time series of computed (red) and observed (black) water temperatures for station Rio Vista (RIV).

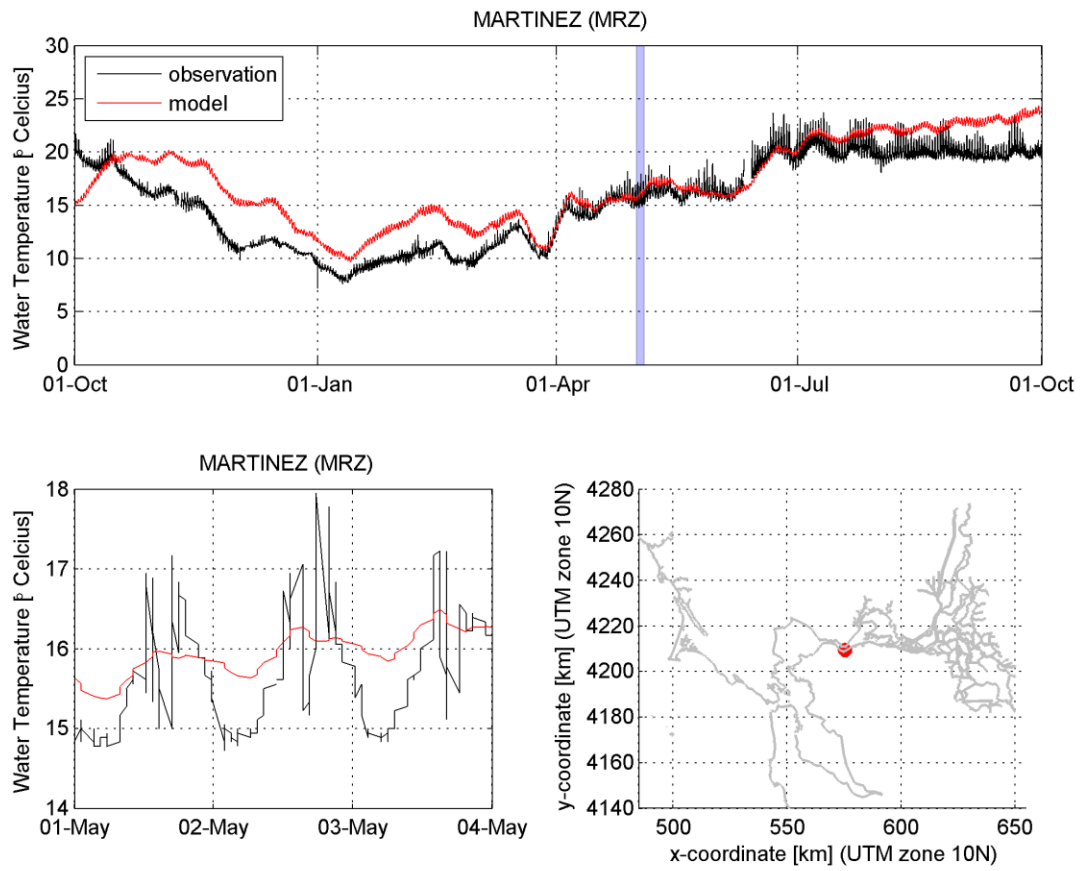


Figure 4-23. Time series of computed (red) and observed (black) water temperatures for station Martinez (MRZ).

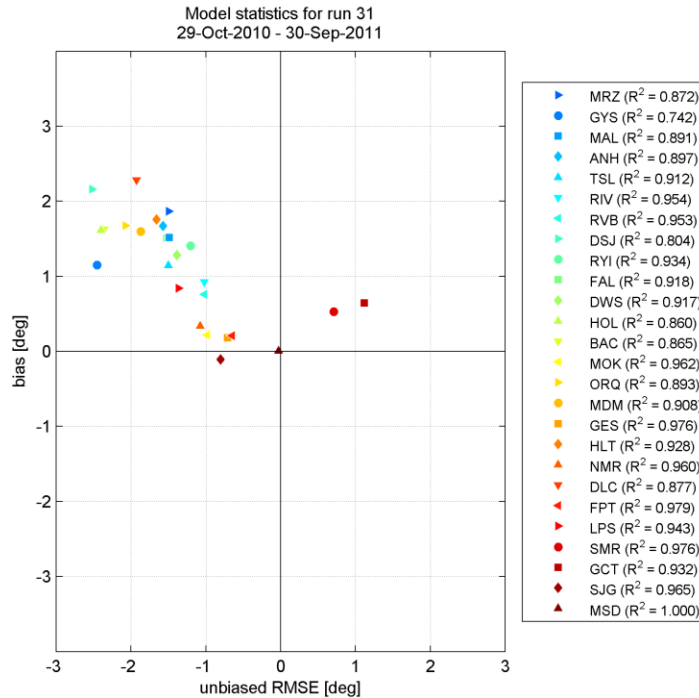


Figure 4-24. Target diagram for WY 2011. Station colors are equal to colors in Figure 4-21. On the vertical axis the bias is plotted, and the horizontal axis represents the unbiased root-mean-square-error. If the uRMSE is negative (positive), the variation in the model is smaller (larger) than in the observations.

The model results show that temperature dynamics can be modeled with significant skill despite uncertainties in atmospheric forcing. This means that we can assess the impact of temperature gradients on salinity intrusion and explore possibilities to minimize salt intrusion by water temperature management through gate operations. In addition the model will provide input to ecological model runs related to bivalves, phytoplankton and fish habitat to better explore these dynamics and assess the impact of climate change and pumping scenarios.

Task Hurdles

Considerable work was spent on software stability and scaling on computing clusters. Numerous code versions were tested, and errors reported to Deltares to help with software improvements. This work was necessary to pursue long-running simulations and to ensure accurate calculations. Scalable 3D hydrodynamic software became available in mid-2014, thus causing delays in the start of model calibration and

validation. Once model calibration work had started, instabilities in the salinity scheme were observed. This was not discovered during the verification phase due to the short length of the verification runs, and the high variability of hydrologic conditions in the calibration run. Finally, 3D discretization of the domain using sigma layers showed excessive numerical diffusion. We spent many months testing numerous parameters to reduce numerical vertical diffusion. In early 2015, software developers were able to develop the z-layer approach to vertical discretization, however this approach proved to be unstable during high flow conditions. As such, we optimized the sigma layer approach to achieve the most accurate, stable model calculations feasible with this scheme. Temperature capability was added to the software in late 2014, so temperature calibration work had to be pursued separately from, and later than, other 3D calibration. As such, this work is still ongoing.

Task Accomplishments

The hydrodynamic team has achieved a number of accomplishments regarding the modeling software. Through our work, we now have functional software on multiple operating systems that can be used for serial and parallel computations. The software is suitable for use on a variety of computing environments, from personal computers to computing clusters and supercomputers. The team has created an unstructured grid with representative Bay-Delta bathymetry, including numerous bays, the lower Yolo floodplain, many Delta channels, and a number of freshwater rivers. The model includes the major regional pumping stations, the Delta Cross Channel gates and temporary barriers throughout the Delta. The 3D model calibration for water levels, discharges, and salinity is nearly complete, and shows excellent agreement throughout the Bay-Delta for a wide range of hydrologic conditions. 3D calibration work for the hydrodynamic model was presented at the Bay-Delta Science Conference in October, 2014.

The software development of 3D boundary conditions is complete, and ready to be tested on the Bay-Delta domain. The calibration of temperature has made significant strides, and will soon be ready to be combined with the calibrated 3D model for testing a full Bay-Delta model incorporating 3D hydrodynamics, salinity and temperature.

Task 4 team (hydrodynamics) shared initial 3D hydrodynamics and salinity calculations with Thompson and Parchaso of Task 9 and Brown and Wulff of Task 10 as input for the bivalve and habitat models. A number of post-processing tools were developed by Deltares to convert hydrodynamic calculations into a format suitable for these models. Through these conversion tools, spatially varying, depth-averaged salinity was used as an input parameter to assess habitat suitability for fish. This was a successful proof-of-concept exercise and shows significant promise for further work.

Next Steps

Work is ongoing to incorporate the Suisun Marsh Salinity Control Gate and Sacramento Weir in the model. Calibration work with 3D temperature is ongoing: more extensive 3D runs will be done, and will include 3D boundary definitions (including vertical velocity, temperature and salinity profiles). Model validation of hydrodynamics and salinity for WY2011 will begin in July, 2015. At this point, 3D temperature will be coupled with 3D hydrodynamics and salinity to assess model runtime and stability. WY2011 model output will be shared with other teams (Tasks 5, 6, 9, 10) to serve as input to their modeling efforts. The validated model will be applied to climate and infrastructural change scenarios. Knowles, Lucas and others at the CASCaDE II user meeting of August, 2014 whittled the early projections of scenario based simulations thought possible to 16-20 production runs spanning 1.5 simulation years. This work will start in early fall of 2015.

Task 5: Phytoplankton

Lisa Lucas, Wim Kimmerer, and Jan Thompson, in collaboration with Hans Los, Tineke Troost, and Valesca Harezlak, Deltares (submitted 11-20-15)

This task is comprised of two primary activities: (1) the development and application of simple numerical models of phytoplankton production and consumption, leading to a publication by Lucas and Thompson (2012); (2) the development of a 2D/3D San Francisco Bay-Delta phytoplankton model, through which scenarios of climate and infrastructural change will ultimately be run.

Activity 1: Using simple models to revise entrenched paradigms

How to “make” more phytoplankton (Lucas and Thompson 2012, *Ecosphere*)

Background

Although the question “What controls phytoplankton biomass and productivity?” is of universal interest to aquatic scientists and resource managers, our motivation for this study was sparked by (1) the particular importance of that question (and its answers) to management of the Delta; and (2) increasing evidence that widely held conceptual models attempting to explain Delta primary productivity— and guiding management plans— were flawed. Based on our previous research in the SF Bay-Delta, these flaws appeared significant enough that management plans based on these conceptual models could ultimately result in restoration actions that yield unexpected, and perhaps disappointing, results.

Many physical, biological, and chemical factors interact to influence phytoplankton biomass and productivity in natural systems and, as we show in Lucas & Thompson (2012), the major drivers must be considered in concert. During the time this research was conducted and published, the Bay-Delta Conservation Plan (BDCP) was being developed with the goals of co-equally managing California’s water supply and restoring the health of the Delta’s ecosystem. One explicit BDCP objective was to increase the productivity of the Delta’s foodweb, starting with its base—the phytoplankton.

Extending our team’s previous field- and modeling-based research (Lucas et al. 2002, 2009a,b; Lopez et al. 2006; Thompson et al. 2008), this new paper directly tested two

intuitive, widely accepted conceptual models helping guide the BDCP. Those conceptual models are: (1) shallower aquatic habitat is more productive than deeper habitat (because depth-averaged light, and thus phytoplankton growth rate, is greater in shallower habitat); and (2) habitat with a longer hydraulic residence time is more productive than short-residence time habitat (because a longer residence time is expected to provide phytoplankton more time to grow and accumulate). We refer to these two conceptual models as the “shallower is greener” and “slower is greener” hypotheses, respectively (Fig. 5-1). A major aim of this paper was to provide Delta scientists, resource managers, and planners an accessible assessment of whether those conceptual models should be expected to hold in the Delta and, thus, whether restoration based on those rules-of-thumb should be expected to result in a more productive ecosystem.

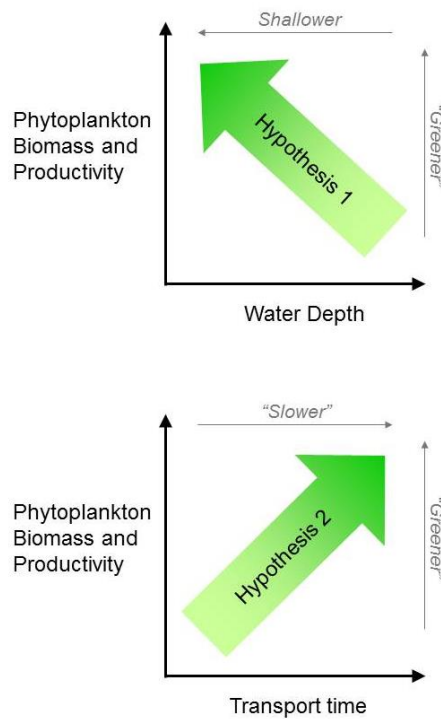


Figure 5-1. Schematics of the two hypotheses tested by Lucas and Thompson (2012).

Approach

To test the “shallower is greener” and “slower is greener” hypotheses, eliminate unnecessary complexity and extraneous process, and communicate findings in the

clearest possible way, we designed 2 extremely simple, stripped-down numerical models. The model for testing hypothesis #1 (coded in Fortran) describes time-dependent phytoplankton dynamics in a vertically well-mixed water column, including the following processes: light-limited phytoplankton growth, respiration loss, zooplankton grazing, and benthic (clam) grazing. Phytoplankton biomass and net primary productivity were computed across a range of water depths and benthic grazing rates, with all parameters reflecting values or ranges representative of the Delta. The objective was to explore quantitatively how water depth influences phytoplankton dynamics in a light-limited water column, and how that influence varies with benthic grazing strength.

The model for testing hypothesis #2 (coded in Matlab) describes steady-state phytoplankton biomass and productivity in a vertically well-mixed habitat as a function of transit time through the habitat. The effective phytoplankton growth rate (algal growth rate minus respiration and grazing losses) was computed for a range of benthic grazing rates. (Effective growth rate is positive if growth is faster than collective local losses, resulting in a habitat that is a net “source” of algal biomass; effective growth rate is negative if collective losses are faster than growth, resulting in a habitat that is a net “sink” for algal biomass.) Simple analytical expressions for habitat-averaged algal biomass and productivity (derived in this study) were evaluated across a range of transit times and effective growth rates.

In addition to the model-based computations described above, measurement-based analyses were also performed. For example, an extensive data set of measured benthic biomass, water clarity, solar irradiance, and water depth from 2001-2003 (previous CALFED-funded research) was used to calculate effective growth rate across the Delta. This μ_{eff} “map” was used as an indicator of the applicability of the models’ findings.

Results/Findings

Hypothesis #1: Shallower is Greener

Our model-based test of Hypothesis #1 indicates that the “shallower is greener” assumption can fail if benthic grazing is significant. Such is the case in much of the

Delta, due to the voracious grazing of the exotic freshwater clam *Corbicula fluminea*. The expectation that a shallower habitat will have higher phytoplankton biomass and productivity than a deeper habitat (a prevalent assumption in early drafts of the BDCP) is rooted in the assumption that the “bottom-up” process of light-limited algal growth is the only depth-dependent process governing phytoplankton biomass. Certainly, light-limited net algal growth rates (growth minus respiration) are higher in shallower water columns than in deeper ones, due to the fact that irradiance decreases exponentially with depth (Fig. 5-2A & B). So if there are no other local loss processes, phytoplankton biomass would also be expected to increase with decreasing water depth (Fig. 5-2E, dark blue line).

But growth is not the only process that, in the depth-averaged sense, varies with water column depth. The depth-averaged rate of algal biomass loss to benthic consumers (benthic grazing rate/water depth)—a potentially large loss term—also varies inversely with water depth (Fig. 5-2C). In other words, the shallower the habitat, the faster a given population of clams can filter through the overlying water column and deplete it of algal biomass. So, two of the most dominant biological processes influencing phytoplankton biomass in the Delta (light-limited growth and benthic consumption) are, in the depth-averaged sense, strong non-linear functions of water depth and fastest in shallow water. The combined effect of these processes—the effective phytoplankton growth rate—is a complex function of habitat depth and benthic grazing rate that is not necessarily more positive as the water column gets shallower (Fig. 5-2D). The result of these combined processes is that algal biomass and net productivity may be increased or decreased with a decrease in habitat depth, depending on the benthic grazing rate (Fig. 5-2E & F). The range of possible biomass and productivity outcomes at the low end of the depth spectrum is particularly broad, depending on grazing rate (i.e. whether and how many clams show up). Given that we do not yet know how to predict habitat colonization by *C. fluminea*, this broad range of possible outcomes translates into significant restoration uncertainty. Thus, shallower habitat may not necessarily be associated with higher phytoplankton biomass or productivity if colonization by bivalves is possible.

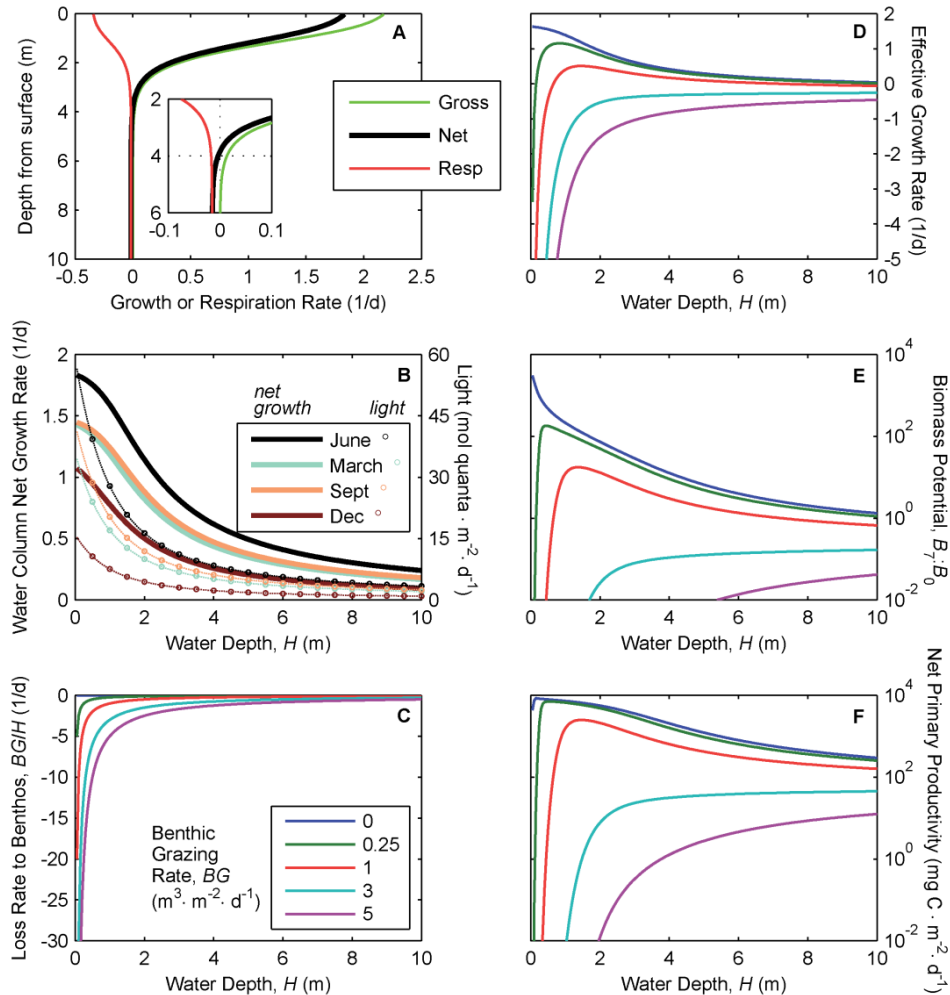


Figure 5-2 (reprinted from Lucas & Thompson, 2012): (A) Vertical profiles of calculated day-averaged phytoplankton gross growth rate, net growth rate, and respiration rate (shown as negative here, since it is a loss process). (B) Calculated day-averaged, depth-averaged phytoplankton net growth rate for day 1 of the simulation (solid curves) and daily depth-averaged irradiance as PAR (dotted curves with circles; calculated following Cloern et al. 1995) as functions of water depth. (C) Calculated depth-averaged rate of phytoplankton biomass loss to benthic grazing versus water depth for five values of benthic grazing rate. (D) Calculated phytoplankton effective growth rate versus water depth for day 1 of the simulation. (E) Phytoplankton biomass potential as represented by $B_7:B_0$, the calculated biomass at 7 days normalized by biomass at time=0, as a function of water depth for five values of benthic grazing rate. (F) Calculated net primary productivity at 7 days versus water depth for five values of benthic grazing rate. (D)-(F) share the same legend as (C).

These model-based findings were corroborated with previously published data from the Delta, which showed very similar patterns of observed phytoplankton biomass and measurement-based productivity as functions of habitat depth and *Corbicula* colonization status (Lopez et al. 2006; Fig. 5-3 herein). Both observations and modeling

thus indicate that, if bivalve colonization is possible, depth is not by itself a good predictor of phytoplankton biomass or productivity, especially in the shallower depth range. In a system such as the Delta, “the shallower is greener” expectation should therefore be abandoned.

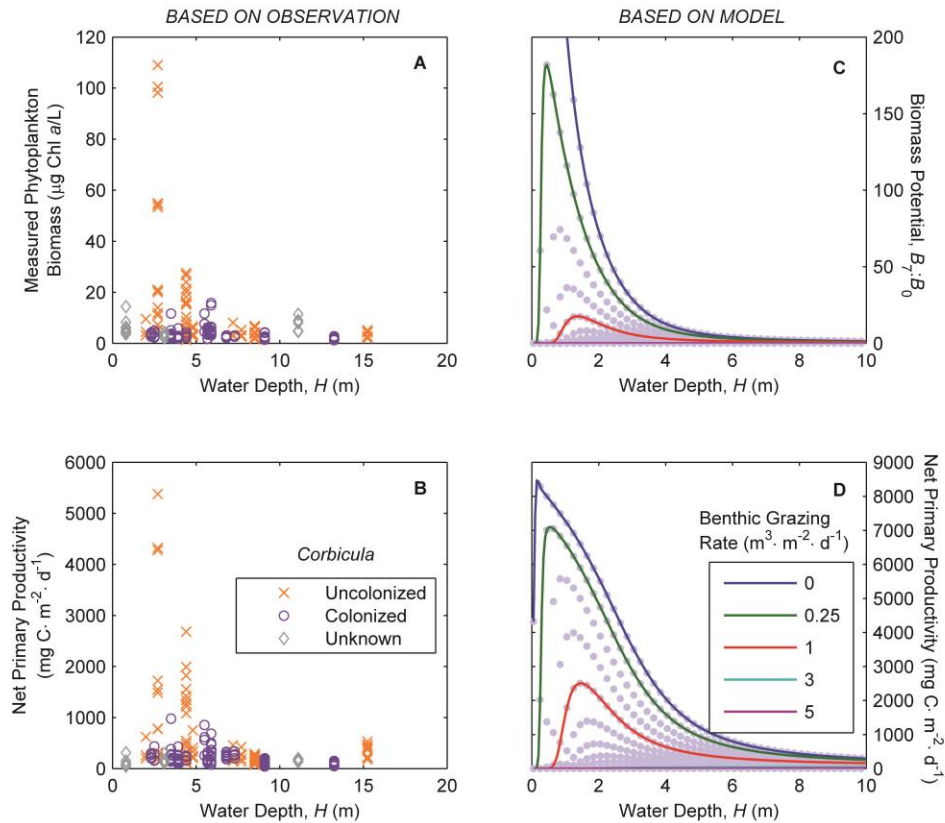


Figure 5-3 (reprinted from Lucas and Thompson, 2012): (A) Measured phytoplankton biomass and (B) calculated measurement-based net primary productivity versus water depth for habitats across the Delta and a range of seasons. Orange x’s represent habitats where *Corbicula* was rare or absent (“uncolonized”) at the time of sampling. Purple o’s represent habitats where *Corbicula* was abundant (“colonized”) at the time of sampling. Gray diamonds represent habitats where the clam colonization status at the time of sampling is unknown. Data from Lopez et al. (2006) and Sobczak et al. (2002, 2005). (A) and (B) are an updated and modified version of Fig. 4 in Lopez et al. (2006). (C) Model-calculated phytoplankton biomass potential ($B_7:B_0$) versus water depth. (D) Model-calculated net primary productivity at 7 days versus water depth. (C) and (D) are a reprise of Fig. 5-2E-F, but plotted on linear scale and with additional dots representing values for 20 different benthic grazing rates between 0 and $10 \text{ m}^3 \cdot \text{m}^{-2} \cdot \text{d}^{-1}$, a realistic range for the Delta.

Hypothesis #2: Slower is Greener

Our model-based test of Hypothesis #2 indicates that the “slower is greener” assumption can also fail if benthic grazing is significant. The expectation that longer

transport times, or slower flow, will result in higher phytoplankton biomass and productivity (another prevalent assumption in early BDCP drafts) is implicitly rooted in the assumption that the bottom-up process (algal growth) dominates over in situ loss processes. It has been shown with a precursor model (Lucas et al. 2009a), however, that if loss dominates over growth phytoplankton biomass in a vertically well-mixed habitat will *decrease* with increasing transport time. That early model was extended in this study and applied to calculate habitat averaged biomass and productivity across a range of benthic grazing rates and transport times. (One can roughly think of “transport time” as “residence time,” or time spent by a blob of phytoplankton-containing water within a defined habitat). The model indicates that if benthic grazing is sufficiently weak such that growth dominates over loss (i.e., effective growth rate is positive), then slower transport/higher transport time indeed results in higher algal biomass and productivity (Fig. 5-4A & B, green curves). However, if benthic grazing is sufficiently strong to overpower growth, resulting in a negative effective growth rate, biomass and productivity decrease with slower transport (Fig. 5-4A & B, red curves). Although this latter behavior may not be immediately intuitive, it does make sense: the longer a phytoplankton population is exposed to net loss conditions as it advects through a habitat, the more depleted it will become by the time it exits the habitat. The range of possible biomass and productivity responses is particularly broad at the long transport time end of the spectrum, depending to a large degree on benthic grazing rate. Again, because we do not yet know how to predict bivalve colonization of Delta habitats, this broad range of possible outcomes translates into significant uncertainty with respect to realized phytoplankton biomass and productivity of Delta habitats.

To explore the applicability of the full range of conditions (and thus biomass and productivity responses) represented in the theoretical curves of Fig. 5-4, we calculated effective growth rate for 135 cases where all necessary measurements were available to estimate effective growth rate in the Delta (Fig. 5-5A). All three habitat functionalities (growth dominated [green], loss dominated [red], and approximately balanced growth and loss [yellow]) have substantial representation within the dataset. Thus, the full range of algal biomass and productivity response as a function of increasing transport time (increasing strongly to decreasing strongly and everything between) is to be

expected in the Delta. This collection of measurement-based effective growth rates is characterized by a broadened envelope at shallower depths, a narrower envelope at deeper ones, and large negative values for large clam grazing rates (Fig. 5-5B); this is consistent with the model-based behavior of μ_{eff} in Fig. 5-2D, lending further credence to the model. Transport time scales such as “residence time” or “flushing time” should therefore not be taken as predictors of, or “surrogates” for, primary productivity or food availability at the base of the Delta’s foodweb.

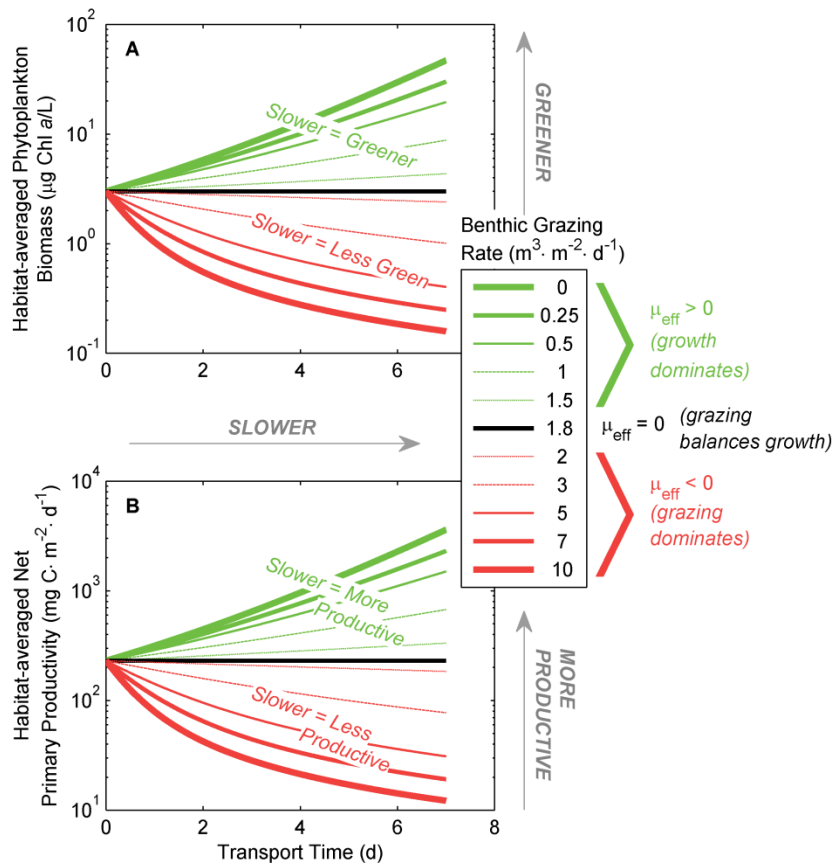


Figure 5-4 (reprinted from Lucas and Thompson, 2012): Model calculations of steady-state average phytoplankton biomass (A) and net phytoplankton primary productivity (B) versus transport time in a flowing habitat for a range of benthic grazing rates typical of the Delta. These calculations were performed for a 3m deep habitat with the characteristic net growth rate shown in Fig. 5-2B for June conditions.

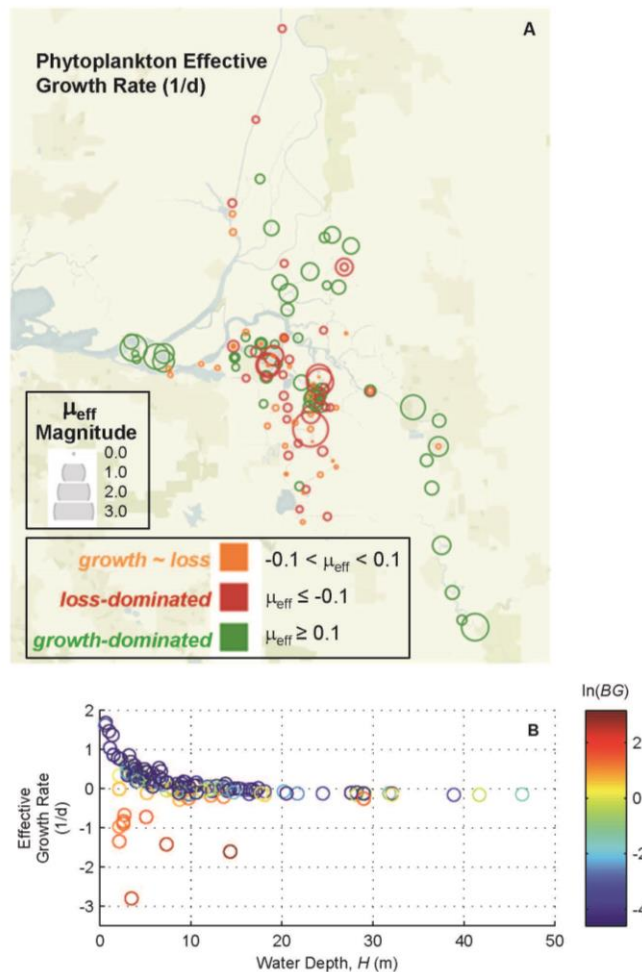


Figure 5-5 (reprinted from Lucas and Thompson, 2012): (A) Map of phytoplankton effective growth rate across the Delta calculated based on parameters measured during field studies in spring-summer 2001-2003. Symbols are color-coded to depict positive (green), negative (red), and approximately zero (yellow) effective growth rate. (B) Phytoplankton effective growth rate versus habitat depth for the cases mapped in panel (A). Color bar is coded to represent $\ln(BG)$, where BG (benthic grazing rate) is in $\text{m}^3 \cdot \text{m}^{-2} \cdot \text{d}^{-1}$. For plotting purposes, minimum BG was set to $0.01 \text{ m}^3 \cdot \text{m}^{-2} \cdot \text{d}^{-1}$.

In summary, benthic bivalves can upend the common, intuitive conceptual models that we commonly expect to govern primary productivity in aquatic habitats. In particular, this study demonstrated that in ecosystems invaded with bivalve grazers, neither shallow nor hydrodynamically slow (long residence time) habitats can be expected to produce significant amounts of phytoplankton for the pelagic food web. Colonization of new habitats is therefore a significant source of uncertainty surrounding the ultimate

outcomes of Delta habitats intended to be “food producers.” Furthermore, this study demonstrated (1) the critical importance for ecosystem management of simultaneously considering all major stressors—abiotic and biotic, and (2) the valuable role of simple models in illuminating and communicating complex process interactions and implications for ecosystem management.

Management Implications

The invasive clam *Corbicula fluminea* was shown capable of negating the expected food-production benefits of planned restored aquatic habitats. This study highlighted how exotic species can complicate ecosystem restoration, and demonstrated the importance of basing productivity estimates on not just one isolated factor (e.g. water depth or residence time), but rather on the interactive effects of many simultaneously acting processes.

We gave several presentations on this work to Bay-Delta and international audiences. After the paper’s publication, new BDCP drafts heavily referenced its cautionary lessons and acknowledged the large uncertainties associated with restoration of habitats subject to bivalve colonization. ICF consultants performing BDCP analyses expressed great interest in the work and contacted the authors as they developed approaches for incorporating clam grazing into their estimates of productivity for the future Delta. The paper was also cited in:

- the USEPA’s review of the BDCP (<http://www2.epa.gov/sites/production/files/documents/july3-2013-epa-comments-bdcp-adeis.pdf>);
- the report “Workshop on Delta Outflows and Related Stressors, Panel Summary Report”, intended to guide the State Water Resources Control Board in developing Delta outflow objectives (<http://deltacouncil.ca.gov/sites/default/files/documents/files/Delta-Outflows-Report-Final-2014-05-05.pdf>);
- a review of current knowledge of the role of tidal marsh restoration in SFB fisheries management (<https://escholarship.org/uc/item/1147j4nz>);

- ongoing work by the IEP Tidal Wetlands Project Workteam, which is developing conceptual models in support of the FRPA (Fish Restoration Plan Agreement) monitoring plan;
- an *Estuary News* article highlighting the work (<http://www.sfestuary.org/estuary-news/clams-muddle-delta-restoration/>).

Activity 2: Developing a 2D/3D San Francisco Bay-Delta Phytoplankton Model

Progress/Status/Next Steps

A multi-dimensional model of phytoplankton dynamics is being developed for the full San Francisco Bay-Delta (SFBD) domain (see Fig. 4-3). The software being used for this purpose is called “BLOOM”, which is a powerful phytoplankton competition model developed by Dr. Hans Los (Deltares, the Netherlands; Los 2009) and implemented in aquatic ecosystems all over the world. BLOOM is run as a component of Deltares’ DELWAQ water quality suite, which includes modules for other interacting state variables and processes such as grazers, dissolved oxygen, detritus, heavy metals, and more. BLOOM computes phytoplankton biomass of user-specified algal groups as a function of nutrient- and light-limited growth, respiration, grazing, settling, mortality, and hydrodynamic transport. Transport terms (velocity, stage, turbulent diffusivity) are generated by the Delft3D-FM hydrodynamic model, saved, and then read in by DELWAQ to provide the physical foundation for driving the phytoplankton model (i.e. BLOOM is run “offline” relative to the hydrodynamic model, for greater overall efficiency).

To our knowledge, this is the first attempt to build a phytoplankton model of the full Bay-Delta system. As such, the present effort is treated as the first stage of a phased approach, to be followed by later stages of refinement and incorporation of broader collections of processes driving phytoplankton variability and linking algal dynamics to other ecosystem components. This phase therefore focuses on incorporating the three core processes solidly established as historically driving and limiting phytoplankton biomass and productivity in the SFBD (Cloern and Jassby, 2012; Cloern 1996): (1) light availability, (2) grazing, and (3) hydrodynamics and transport. Although the BLOOM

software contains the infrastructure for modeling nutrient dynamics, incorporation of nutrient effects on phytoplankton growth is not taken up in this stage. As an extension of the current phase, the modeling effort associated with the San Francisco Bay Nutrient Management Strategy coordinated by the San Francisco Estuary Institute (<http://www.sfei.org/search/node/nutrient%20management%20strategy>) is collaborating with the CASCaDE 2 team, building its nutrient modeling capability on the tools being developed in CASCaDE 2 (in particular, the hydrodynamic and phytoplankton models). For the present phase, nutrients are assumed to never limit phytoplankton growth, which is consistent with measurements indicating that nutrient limitation is rare in the SFBD (Cloern and Jassby, 2012; Jassby et al. 2002; Cloern 1999). Moreover, although our model domain includes the full SFBD and coastal ocean, the focus here is on the Delta and northern SFB and model evaluation in this phase will emphasize those regions.

There are multiple philosophies and approaches associated with ecosystem modeling. Many scientists elect to incorporate significant complexity from the outset. Others choose to begin a new modeling effort with as simple a model as possible. We have decided to follow the latter path. As such, we have elected to: (1) eliminate modeled state variables for which site-specific data for driving relevant processes and validating computed quantities is severely limited or non-existent (e.g. detritus); (2) avoid finer levels of detail in our characterization of the phytoplankton community than those for which we can confidently specify model parameters (e.g., Cloern and Dufford [2005] stated that, although cryptophytes can be an important component of the Bay's phytoplankton, we know very little about their growth rates). In our view, advantages of this simpler path include an enhanced ability to *understand* one's model results, as well as increased confidence that the processes and linkages influencing those results are relatively well-understood and well-constrained for the modeled ecosystem (in other words, when you get the *right answer*, you're getting it for the *right reasons*). Our approach is, and has been in the past, to incrementally learn from models and measurements in combination, discern any critical processes that may be "missing" from a model and limiting the model's skill in characterizing reality, and then design the next phase of model refinement to incorporate those critical processes. We have thus

grouped the phytoplankton community into 3 relatively coarse groups (see Table 5-1) and eliminated all other modeled state variables and non-essential processes via a step-by-step approach of model simplification and testing, ensuring at each step that the model does not “break.”

The major components of the current-phase phytoplankton model are described in Figure 5-6. In the following sections, we describe the specific approach, status, and next steps for each component.

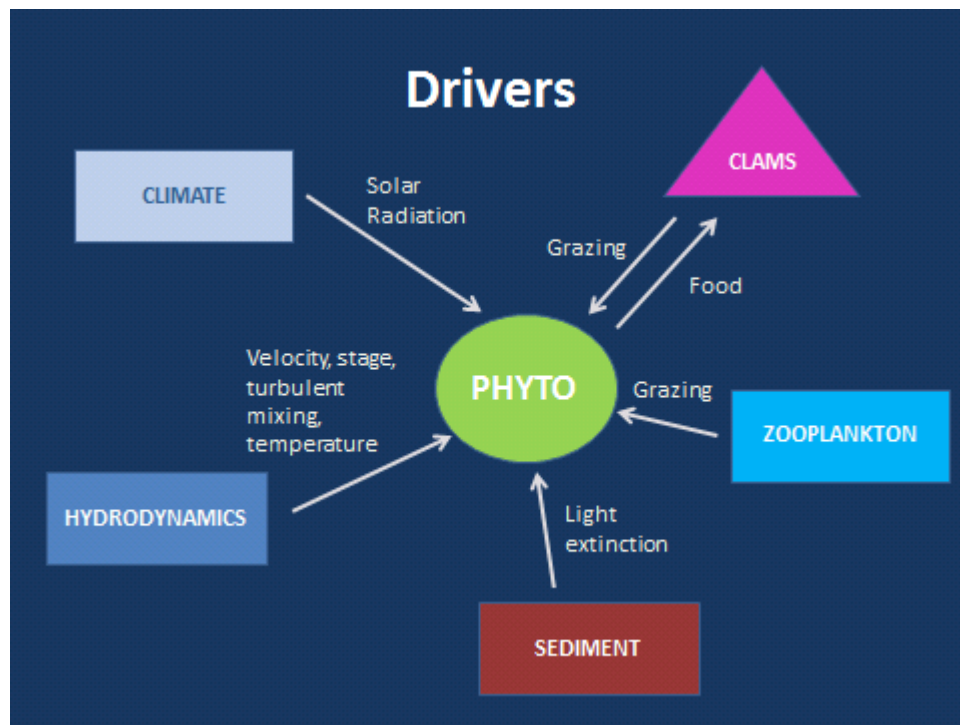


Figure 5-6: Processes driving phytoplankton dynamics in the model under development.

Phytoplankton

The BLOOM model allows for the simulation of multiple, competing phytoplankton groups or species. Typically, if nutrient limitation is considered, each phytoplankton group or species has multiple “types”, with each type defined by the primary growth-limiting agent (e.g. nitrogen, phosphorus, light). Since in the present phase we are neglecting nutrient limitation, each modeled phytoplankton group has only one “type” — the light-limited one. After extensive literature review and SFBD data analysis, we have elected to limit the granularity of our modeled phytoplankton community to just three

groups: (1) large diatoms (>5 μm), (2) large non-diatoms (>5 μm), and (3) small non-diatoms (<5 μm). The rationale is to keep this first model phase as simple as possible, while allowing for potentially important distinctions among phytoplankton with respect to grazing vulnerability, sinking, and growth rate. The large non-diatom group includes cryptophytes, green algae, and dinoflagellates. The small non-diatom group includes cyanobacteria such as *Microcystis aeruginosa*, as well as flagellates. We are not distinguishing between marine and freshwater species, and thus have elected in this stage to not activate BLOOM's salinity dependent mortality capability.

Table 5-1 shows distinctions between phytoplankton groups for major processes and parameters. Analysis of SFSU and USGS data did not reveal obvious relationships between phytoplankton functional groups and maximum growth rates in this system. For that reason, we have elected to begin specifying values for algal growth, respiration, and other related parameters that are generally based on the standard values used in BLOOM for other studies (e.g., see Smits and Van Beek 2013).

Phytoplankton Groups & Parameters							
Group	Who's included	Size	Sinking speed	Microzoo grazing	Mesozoo grazing	Benthic grazing	Growth rates and algal parameters
Large diatoms		> 5 um	O(0.5)-O(10) m/d	not grazed	grazed	grazed	Use Smits & Van Beek 2013 (Diatom-E-type)
Large non-diatoms	Crypto's, Greens, Dino's	> 5 um	0	grazed	grazed	grazed	Use Smits & Van Beek 2013 (Green-E-type)
Small non-diatoms	Microcystis & other cyanos & flag's	< 5 um	0	grazed	not grazed	zero or some small fraction grazed	Use Smits & Van Beek 2013 (Microcystis-E-type)

Table 5-1: Parameters describing three modeled phytoplankton groups.

Climate

The primary direct linkage between climate models and the phytoplankton model is via incident solar radiation at the water surface, which is attenuated in the water column

and drives photosynthesis by the phytoplankton. Total solar radiation at the water surface is provided by the user and adjusted in the model to represent only the photosynthetically active portion of the radiation (PAR). Solar radiation used in the phytoplankton model has, up until now, been specified as a constant value for testing purposes; however, we will soon implement the same MACA dataset being used to drive the water temperature model (Multivariate Adapted Constructed Analogs; Abatzoglou and Brown, 2012; <http://maca.northwestknowledge.net/>). The MACA data is downscaled GCM output that varies in time and space, and covers both the historical period and the remainder of this century. The MACA solar radiation is provided on a daily time step.

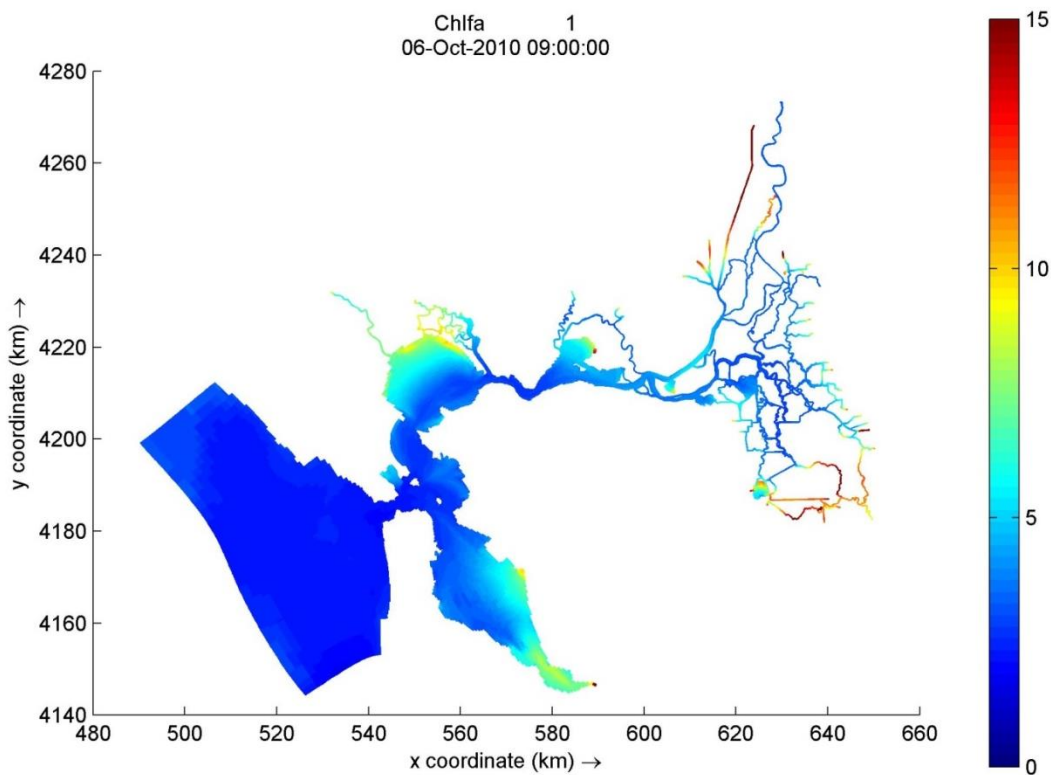


Figure 5-7: Computed phytoplankton biomass (as ug chlorophyll a/L) for a test run of the 3D SFBD phytoplankton model. Image represents chlorophyll a in the top layer of grid cells.

Hydrodynamics

As described under Task 4, calibration and validation of the hydrodynamic model for stage, flows, and salinity is nearly complete. 3D water temperature calibration is

underway. For the last several months, BLOOM runs have been conducted with an older version of the grid and with outputs from an older version of the hydrodynamic model, waiting until those components cease incurring major changes. In the meantime, BLOOM has been shown to run successfully in 3D over the full SFBD domain, driven by Delft3D-FM hydrodynamic quantities (see Fig. 5-7 for sample output). Once the 3D temperature model is fully calibrated and merged with the latest 3D hydrodynamics and salinity computations, modeled temperatures from that model will be used in computing algal growth rates and zooplankton grazing rates. Some important milestones in Deltares tool development allowed us to get to this point: (1) 3D DELWAQ with flexible mesh numerical capability (summer 2014), and (2) the “stitching tool” (AKA “ddcouplefm”), which allows for the reassembly of parallel hydrodynamic output for separate subdomains into a single data set on the large combined domain, which can then be used by DELWAQ (fall 2014).

Suspended Sediment

Suspended sediment concentration (SSC) is a major source of light attenuation in the SFBD. As described under Task 6, the 2D SSC model for the Delta is calibrated and published (Achete et al. 2015); the 3D SSC model for the Bay-Delta is under development. A Fortran tool has been provided by Deltares to convert SSC model outputs into a readable input file for BLOOM. This tool has been tested and the phytoplankton model can successfully read in spatially and temporally variable SSC's across the domain as a basis for computing light attenuation coefficients.

Other constituents contribute to light attenuation as well, including dynamically changing phytoplankton biomass (chl), detritus, and dissolved substances. Typically, a linear (or multiple linear) regression model is used to relate these parameters to light extinction. Currently, we are using an empirical light extinction relationship depending only on SSC and chl based on measurements in the central Delta (Lopez et al. 2006). We are currently developing a new, more general empirical light extinction relationship for the SFBD, to be used in BLOOM for representing the broader Delta and northern Bay. We plan to limit the empirical model of light attenuation to including just SSC and, perhaps, chl.

Zooplankton Grazing

Pelagic (zooplankton) grazing on phytoplankton includes components due to microzooplankton and mesozooplankton. We treat these very differently in the model because of the way they happen and the way they are measured.

Microzooplankton includes protists and larval stages of some mesozooplankton, but we focus here on the former only. This group includes ciliates, flagellates, and other heterotrophic, single-celled organisms. Their size ranges overlap substantially with those of phytoplankton, making any practical separation of living samples unfeasible. They are also very difficult to identify to species, and a lot of the species are unidentified. In addition, they can grow as fast as phytoplankton, and probably a lot faster when phytoplankton are light-limited, as they are in the San Francisco Estuary (Cloern 1987). Therefore they are capable of maintaining extremely high grazing rates on phytoplankton, at times exceeding that of benthic bivalves (York et al. 2011, Kimmerer and Thompson 2014).

Because of these characteristics of microzooplankton grazing, it is most often estimated through a dilution method (Landry and Hassett 1982, Calbet and Landry 2004) which simultaneously estimates phytoplankton growth rate and microzooplankton grazing rate in whole or size-fractionated water samples. Application of this method in the SFE (York et al. 2011) gave a result consistent with those from other estuaries, in that microzooplankton grazing is roughly 60% of phytoplankton growth.

Because of the consistency in this finding and the lack of information on which to base a single-taxon model of microzooplankton, we have chosen to represent microzooplankton grazing as a constant penalty term proportional to phytoplankton growth rate. This penalty is applied to both large and small non-diatoms. However, we apply no penalty term on large diatoms, which are assumed to not be grazed by microzooplankton because diatom frustules are expected to inhibit microzooplankton grazing on large diatoms.

Mesozooplankton in the SFE consists mainly of copepods. To describe mesozooplankton grazing on phytoplankton in the model, the grazing module

“CONSBL” is implemented. CONSBL’s approach is largely a Michaelis-Menten style approach, but with multiple corrections and adjustments (e.g. for temperature, food availability, grazer growth rate and mortality, etc). An extensive data and literature search was conducted to determine appropriate model parameters for this component. Parameter values have been altered from the model default values to better reflect the species and conditions found in the SFE. The new parameter values (discussed below) will soon be incorporated into the model and tested.

- *Fraction of algae egested* This is $1 - \text{assimilation efficiency (AE)}$, i.e., the fraction retained. Assimilation efficiency is highly variable and depends on the species of zooplankton and its food and the food concentration. The default value of 0.5 is in the middle of the range of values from the literature (e.g., Besiktepe and Dam 2002).
- *Preference for each algal group* This parameter is misnamed; a given grazer will consume different algal species in or out of proportion to their relative abundance as a function of size, shape, motility, and possibly smell of the alga and feeding mode of the copepod, although some preference can be evident when copepods actively reject particles (Kiørboe 2011). This parameter is difficult to establish a priori and should be determined by iteration to get consumption rates in line with literature values (e.g., Bouley and Kimmerer 2006, Kayfetz 2014 MS Thesis, SFSU). The default value of 1, meaning that both larger-celled algal groups are consumed equally, is a good starting point. The value of zero is applied to the small non-diatom group.
- *Fraction of egested material that is sedimented* There is no a priori way to determine this parameter because particles tend to be kept in suspension by turbulence and the sedimentation rate would be difficult to measure. The default value is 0.
- *Maximum filtration rate* This is actually a biomass-specific clearance rate (volume per mass per time). Since clearance rate is almost exactly proportional to carbon mass of copepods and other grazers, this is a constant. Fig. 1A in Kiørboe (2011) gives a value of $\sim 20 \text{ m}^3 \text{ gC}^{-1} \text{ d}^{-1}$ for this parameter.

- Maximum growth rate at 20°C This has been estimated for the abundant estuarine copepod *Pseudodiaptomus forbesi* at $\sim 0.4 \text{ d}^{-1}$ at 20°C (Kimmerer et al. 2014, Ignoffo et al. in prep.).
- Scaling factor for calibration This is a tuning parameter
- Maximum mortality rate at 20°C Mortality rate depends on the causes of mortality - e.g., predation depends on the number and kinds of predators, alternative prey, and temperature. These are not generally amenable to modeling except as a fixed proportion or as a damping function to prevent oscillations. However, mortality must roughly balance reproduction over a long enough time period, otherwise the population goes extinct or grows without bound. The value (0.17 d^{-1}) was taken from Table 3 in the review of mortality by Hirst and Kiørboe 2002. However, note that mortality is a local, not a global parameter, so adjustment may be necessary.
- Half saturation constant Half-saturation for an *Acartia* sp. was ~ 0.25 , that for *Eurytemora affinis* ~ 0.3 but with very small algae (Berggreen et al. 1988, Barthel 1983). Thus we will use 0.2 to reflect that copepods in the SF Estuary may be adapted to low food concentrations.
- Growth respiration fraction at 20°C This is the daily fractional loss of mass due to respiration associated with growth. Kiørboe et al. (1985) give values for a single species at 18°C. Respiration was determined at zero and maximum growth rates as set by food supply. This is for *Acartia tonsa*, which is common in the saline end of the SF Estuary and similar in size (though rather different in biology) to the other copepods in our system. This value (0.20 d^{-1}) may differ somewhat for early life stages.
- Maximum uptake rate This should be a power function of body size but the size range of copepods in the SF Estuary is rather narrow. Value of 1.7 d^{-1} is from Fig. 4 in Saiz and Calbet (2011).
- Maintenance respiration fraction at 20°C A value of 0.04 d^{-1} will be used. See above for growth respiration (Kiørboe et al. 1985).
- Temperature correction for filtration rate This has been altered to 0.12 deg C^{-1} to be similar to that for growth.

- Temperature correction for growth This coefficient is $\sim 0.12 \text{ deg C}^{-1}$ for two common copepods in the upper SF Estuary (Sullivan and Kimmerer 2013).
- Temperature correction for mortality As for mortality, this value (0.071 deg C^{-1}) is based on Hirst and Kiørboe 2002.
- Temperature correction for growth respiration Value to be used is 0.06 deg C^{-1} . Q10 for respiration is 1.82 - i.e., the factor by which respiration increases for a 10°C change in T (Ikeda 1985). The reference does not distinguish the two kinds of respiration.
- Temperature correction for uptake rate This has been altered to be similar to that for growth (0.12 deg C^{-1}).
- Temperature correction for maintenance respiration As for growth respiration above.

Benthic Grazing

A realistic depiction of benthic grazing rates is absolutely essential to any reasonable model characterization of phytoplankton dynamics in the SFBD. There are two general approaches to be implemented for providing a clam grazing term in the phytoplankton model: (1) imposing maps of clam grazing rate, based on measurements of benthic biomass for historical simulations, and (2) dynamic bivalve modeling for simulations of future scenarios.

Historic runs: imposing clam grazing rates based on measurements. The translation methodology for approach #1 has recently been developed by collaborators (T. Troost, V. Harezlak, H. Los) at Deltares and is shown in Fig. 5-8. The first step is the calculation of clam grazing rates from measurements of benthic biomass by J. Thompson (Task 9). The biomass data for northern SFB and the Delta are from the biannual DWR GRTS benthos sampling program (<http://www.water.ca.gov/bdma/grts/>). After grazing rate calculations are made, a map of discrete values of clam grazing rate is generated (Fig. 5-9). Step 2 is the interpolation of this discrete data onto a Cartesian grid within the Habitat software (Fig. 5-10). Step 3 is translation of the Cartesian interpolated field to the flexible mesh (“FM”) computational grid used by the water quality and hydrodynamic models. Finally, that translated, interpolated field is run through a Fortran utility (developed by Deltares), which writes the grazing rate map to a

file readable by the BLOOM phytoplankton model. BLOOM is currently able to run with benthic grazing maps processed as described in Figs. 5-8 through 5-10. Thorough testing continues to ensure BLOOM is properly utilizing grazing rates provided in this manner.

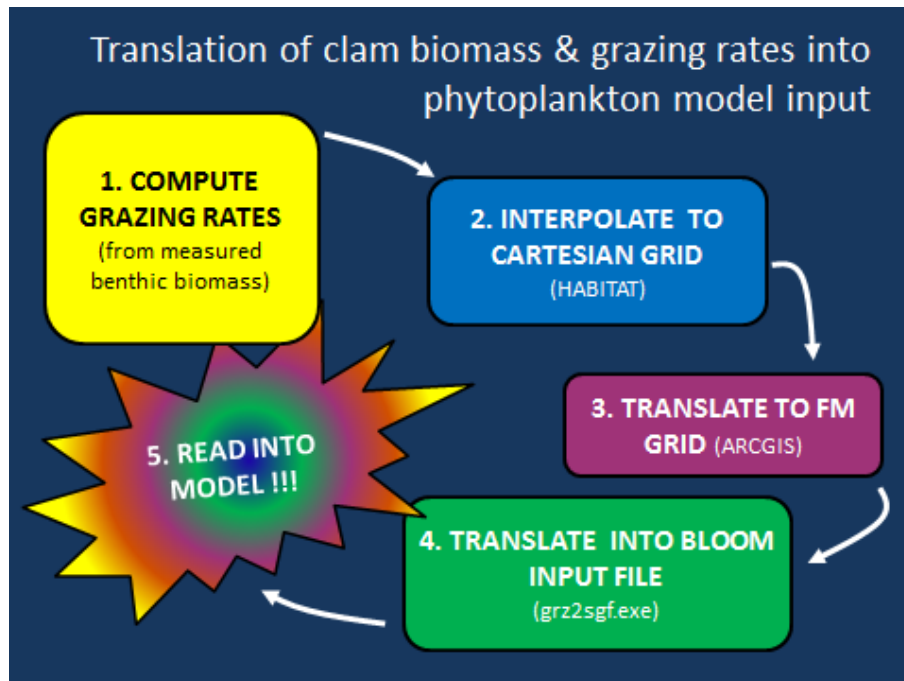


Figure 5-8: Methodology for translating discrete benthic biomass measurements into continuous maps of bivalve grazing rate for use in the phytoplankton model.

Generating clam grazing rates for future scenarios. In order to run phytoplankton simulations for future climate and infrastructure simulations, prescription of historical grazing rates (as in the first approach, Fig. 5-8) will not alone suffice. A methodology for providing bivalve grazing rates *in the future* is needed. The current plan is to develop a dynamic clam (DEB) model that couples to the phytoplankton model (see Task 9). In such an arrangement, 2-way communication would occur between models: the modeled phytoplankton would provide food for the modeled clam populations, and the modeled clams would graze on the modeled phytoplankton. A coupled dynamic bivalve-phytoplankton model is an ambitious and challenging goal that has not been attempted previously for the SFB. To begin development of such a model, the phytoplankton model must first be calibrated and validated as working well with prescribed historic

grazing rates (Approach #1 above). Due to the magnitude of this challenge, unknown hurdles may lie ahead, and alternatives may need to be considered.

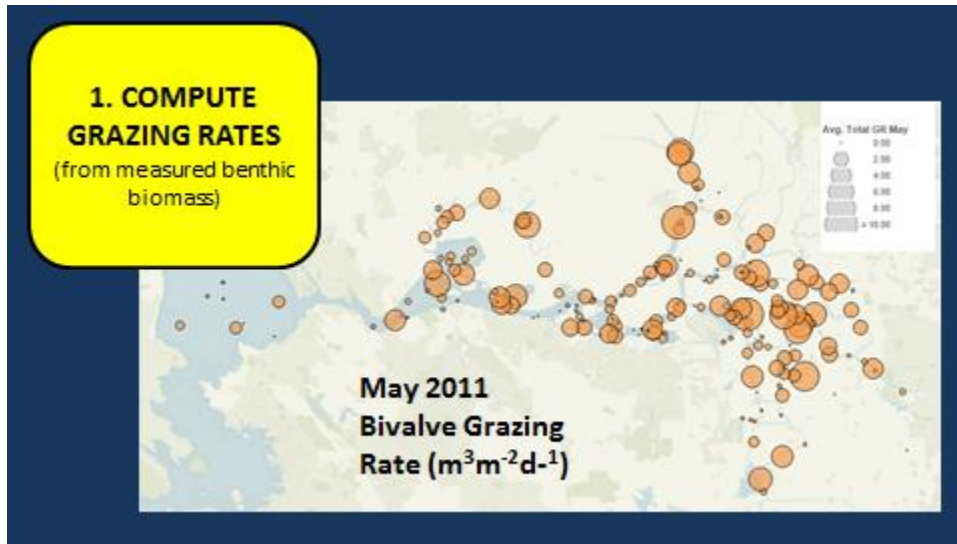


Figure 5-9: Example map of bivalve grazing rates based on DWR-GRTS benthic biomass measurements. Grazing rate calculations by J. Thompson (USGS).

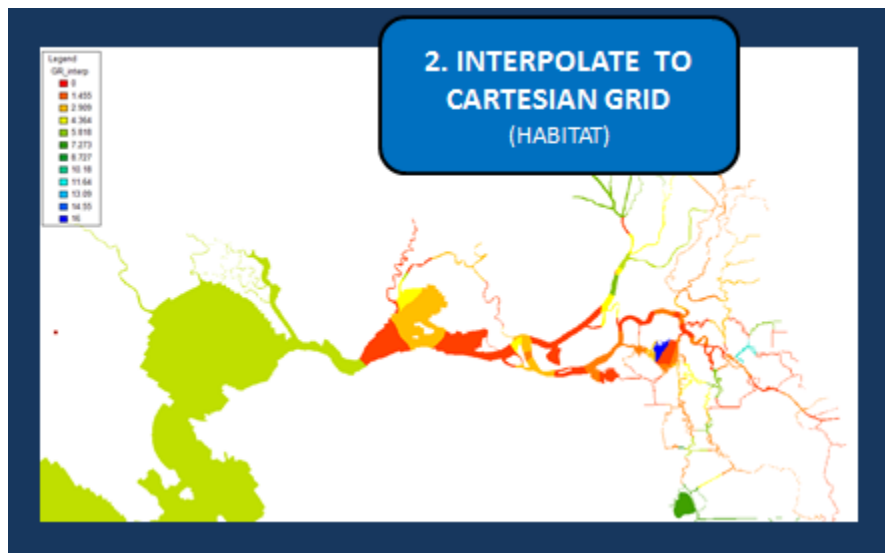


Figure 5-10: Interpolated benthic grazing rates on Cartesian grid, generated with Deltares' Habitat software. These are then distributed across the flexible mesh grid, converted further, and read into the BLOOM model.

Management implications

Even at their most idealized (Fig. 5-6), phytoplankton represent a nexus of multiple simultaneous and interacting processes, some of which can work to increase biomass and productivity, and others which can work to do the opposite. The net effect of these physical and biological processes will determine if algal biomass and productivity increase or decrease. Who cares?

Understanding the processes governing phytoplankton biomass and productivity in the contemporary SFBD—and how algal biomass and productivity may respond to major forces of change—is essential to building reasonable expectations of ecosystem function and health in the future. Phytoplankton is known to be a critical source of food at the base of the pelagic food web supporting fish in the Delta (Sobczak et al. 2002), even though algal biomass and productivity have declined over the the last few decades and annual production has been among the lowest of the world's tidal systems (Jassby et al. 2002, Jassby 2008). Recent research has identified linkages between fish declines in the SFBD and food limitation (Hammock et al. 2015). The fundamental importance of food production and availability at the base of the SFBD foodweb—and, specifically, the role of phytoplankton—has been and continues to be widely acknowledged in SFBD planning documents (e.g. BDCP, DSP Interaction Science Action Agenda—Action Area 6). The work performed under this task and continued from this point directly addresses these concerns and questions.

Next steps

As described above, many of the required pieces, inputs, procedures, and linkages necessary for running simulations of phytoplankton dynamics in the SFBD are now established or nearly so. Some have not yet been implemented or fully tested. The next major step will involve incorporating all of these developments and inputs (e.g., latest grid, calibrated/validated hydrodynamic model outputs, dynamic computed sediment concentrations, micro- and mesozooplankton grazing, measurement-based clam grazing rates, downscaled solar radiation) into a single simulation set-up for WY 2011. Testing of components individually and in concert will be performed and completed. We may choose to initially focus on running 2D depth-averaged phytoplankton simulations.

This would provide greater computational efficiency and may provide a reasonable characterization for the Delta. Calibration and validation of the model will be performed via comparison with historical measurements of chlorophyll *a* in the SFBD. Once the model is deemed able to reasonably characterize SFBD phytoplankton dynamics, this task will work with Task 9 scientists to begin developing a coupled, dynamic phytoplankton-bivalve model. That (or an alternative, if necessary) will be used to conduct simulations of future scenarios.

References

- Abatzoglou, J. T., and T. J. Brown. 2012. A comparison of statistical downscaling methods suited for wildfire applications. *Int. J. Clim.* **32**(5): 772-780.
- Achete, F. M., van der Wegen, M., Roelvink, D., and Jaffe, B.: A 2-D process-based model for suspended sediment dynamics: a first step towards ecological modeling, *Hydrol. Earth Syst. Sci. Discuss.* **12**:1507-1553, 10.5194/hessd-12-1507-2015, 2015
- Barthel, K. G. 1983. Food uptake and growth efficiency of *Eurytemora affinis* (Copepoda Calanoida). *Mar. Biol.* **74**: 269-274.
- Berggreen, U., B. Hansen, and T. Kiørboe. 1988. Food size spectra, ingestion and growth of the copepod *Acartia tonsa* during development: implications for determination of copepod production. *Mar. Biol.* **99**: 341-352.
- Besiktepe, S., and H. G. Dam. 2002. Coupling of ingestion and defecation as a function of diet in the calanoid copepod *Acartia tonsa*. *Mar. Ecol. Progr. Ser.* **229**: 151-164.
- Bouley, P., and W. J. Kimmerer. 2006. Ecology of a highly abundant, introduced cyclopoid copepod in a temperate estuary. *Mar. Ecol. Progr. Ser.* **324**: 219-228.
- Calbet, A., and M. R. Landry. 2004. Phytoplankton growth, microzooplankton grazing, and carbon cycling in marine systems. *Limnol. Oceanogr.* **49**: 51-57.
- Cloern, J. E. 1987. Turbidity as a control on phytoplankton biomass and productivity in estuaries. *Cont. Shelf Res.* **7**: 1367-1381.
- Cloern, J. E. 1996. Phytoplankton bloom dynamics in coastal ecosystems: a review with some general lessons from sustained investigation of San Francisco Bay, California. *Rev. Geophys.* **34**:

- Cloern, J. E. 1999. The relative importance of light and nutrient limitation of phytoplankton growth – a simple index of coastal ecosystem sensitivity to nutrient enrichment. *Aquat. Ecol.* **33**(1): 3-16.
- Cloern, J. E., and R. Dufford. 2005. Phytoplankton community ecology: principles applied in San Francisco Bay. *Mar. Ecol. Progr. Ser.* **285**:11-28.
- Cloern, J. E., and A. D. Jassby. 2012. Drivers of change in estuarine-coastal ecosystems: discoveries from four decades of study in San Francisco Bay. *Rev. Geophys.* **50**, RG4001, doi:10.1029/2012RG000397.
- Hammock, B. G., J. A. Hobbs, S. B. Slater, S. Acuña, S. J. Teh. 2015. Contaminant and food limitation stress in an endangered estuarine fish. *Sci. Tot. Env.* **532**: 316-326.
- Hirst, A. G., and T. Kiørboe. 2002. Mortality of marine planktonic copepods: global rates and patterns. *Mar. Ecol. Progr. Ser.* **230**: 195-209.
- Ikeda, T. 1985. Metabolic rates of epipelagic marine zooplankton as a function of body mass and temperature. *Mar. Biol.* **85**: 1-11.
- Jassby, A. D. 2008. Phytoplankton in the Upper San Francisco Estuary: Recent biomass trends, their causes and their trophic significance. *San Francisco Estuary and Watershed Science* **6**(1): 2.
- Jassby, A. D., J. E. Cloern, and B. E. Cole. 2002. Annual primary production: patterns and mechanisms of change in a nutrient-rich tidal ecosystem. *Limnol. Oceanogr.* **47**: 698-712.
- Kimmerer, W. J., T. R. Ignoffo, A. M. Slaughter, and A. L. Gould. 2014. Food-limited reproduction and growth of three copepod species in the low-salinity zone of the San Francisco Estuary. *J. Plankton Res.* **36**: 722– 735.
- Kimmerer, W. J., and J. K. Thompson. 2014. Phytoplankton growth balanced by clam and zooplankton grazing and net transport into the low-salinity zone of the San Francisco Estuary. *Estuaries Coasts* **37**: 1202-1218.
- Kiørboe, T. 2011. How zooplankton feed: mechanisms, traits and trade-offs. *Biol. Rev.* **86**: 311-339.
- Kiørboe, T., F. Mohlenberg, and K. Hamburger. 1985. Bioenergetics of the planktonic copepod *Acartia tonsa*: relation between feeding, egg production and respiration, and composition of specific dynamic action. *Mar. Ecol. Progr. Ser.* **26**: 85-97.
- Landry, M. R., and R. P. Hassett. 1982. Estimating the grazing impact of marine microzooplankton. *Mar. Biol.* **67**: 283-288.

- Lopez, C. B., J. E. Cloern, T. S. Schraga, A. J. Little, L. V. Lucas, J. K. Thompson, and J. R. Burau. 2006. Ecological values of shallow-water habitats: implications for restoration of disturbed ecosystems. *Ecosystems* **9**: 422-440.
- Los, F. J. 2009. Eco-hydrodynamic modelling of primary production in coastal waters and lakes using BLOOM. Ph.D. thesis, Wageningen University.
- Lucas, L. V. and J. K. Thompson. 2012. Changing restoration rules: exotic bivalves interact with residence time and depth to control phytoplankton productivity. *Ecosphere* **3**(12): 117. <http://dx.doi.org/10.1890/ES12-00251.1>
- Lucas, L. V., J. E. Cloern, J. K. Thompson, and N. E. Mosen. 2002. Functional variability of shallow tidal habitats in the Sacramento-San Joaquin Delta: restoration implications. *Ecol. App.* **12**(5):1,528-1,547.
- Lucas, L. V., J. K. Thompson, and L. R. Brown. 2009a. Why are diverse relationships observed between phytoplankton biomass and transport time? *Limnol. Oceanogr.* **54**: 381-390.
- Lucas, L. V., J. R. Koseff, S. G. Monismith, and J. K. Thompson. 2009b. Shallow water processes govern system-wide phytoplankton bloom dynamics: a modeling study. *J. Mar. Sys.* **75**:70-86.
- Saiz, E., and A. Calbet. 2011. Copepod feeding in the ocean: scaling patterns, composition of their diet and the bias of estimates due to microzooplankton grazing during incubations. *Hydrobiologia* **666**: 181-196.
- Smits, J.G.C., and van Beek. 2013. ECO: A generic eutrophication model including comprehensive sediment-water interaction. *PLoS ONE* **8**(7): e68104, doi:10.1371/journal.pone.0068104.
- Sobczak, W. V., J. E. Cloern, A. D. Jassby, and A. B. Muller-Solger. 2002. Bioavailability of organic matter in a highly disturbed estuary: the role of detrital and algal resources. *Proc. Nat. Acad. Sci.* **99**:8101-8105.
- Sullivan, L. J., and W. J. Kimmerer. 2013. Egg development times of *Eurytemora affinis* and *Pseudodiaptomus forbesi* (Copepoda, Calanoida) from the upper San Francisco Estuary with notes on methods. *J. Plankton Res.* **35**: 1331-1338.
- Thompson, J. K., J. R. Koseff, S. G. Monismith, L. V. Lucas. 2008. Shallow water processes govern system-wide phytoplankton bloom dynamics: a field study. *J. Mar. Sys.* **74**:153-166.
- York, J. L., B. A. Costas, and G. B. Mcmanus. 2011. Microzooplankton grazing in green water—results from two contrasting estuaries. *Estuaries Coasts* **34**: 373-385.

Task 6: Turbidity and geomorphology

Bruce Jaffe, Mick van der Wegen, Fernanda Achete, Theresa Fregoso and Dano Roelvink
(submitted 06-22-15)

This task is comprised of two components: (1) creation of a seamless bathymetric/topographic DEM for use in modeling of hydrodynamics, Task 4, and turbidity and geomorphology, this task, and (2) creation and application of a calibrated process-based model to explore present-day and future turbidity and geomorphology of the Delta. Each component is summarized below, including the results and findings, management implications, and recommendations for next steps in this research.

Summary of progress/status

Overview of creation of seamless bathymetric/topographic DEM for use in modeling

A seamless bathymetric/topographic DEM is required for running hydrodynamic/sediment transport/geomorphic models. By seamless, we mean that the DEM does not have discontinuities at the water-land boundary. The bathymetric and topographic data in the CASCaDE II models is represented by a flexible mesh, unstructured grid that changes resolution depending on the complexity of the natural processes and geomorphology. The CASCaDE II modelers requested an already created and vetted, standard cell sized grid that they could then use to create their flexible mesh. Modelers wanted as much of a modern day grid as possible, complete with areas without data in existing DEMs, expanded data coverage areas as needs were realized over the course of the project, and shoreline and levee elevations that eventually became part of a seamless bathymetric / topographic DEM.

There were four phases that built towards the current seamless bathymetric / topographic surface. Phase 1 involved evaluating the USGS 2005 DEM created by Amy Foxgrover and others, 2003, for areas that needed new data, or still lacked data. Then, following the methodology established during the creation of the original USGS DEM, updating the DEM with new data added to a California Department of Water Resources (DWR) soundings file (CSDP bathymetry data) that compiled all known

available delta bathymetric surveys. The final part was updating the shoreline to better reflect the modern Delta. The second phase involved extending the DEM north along the Sacramento and American Rivers, incorporating newer multibeam data sets, and creating a levees file complete with elevations. In the third phase we began working directly with DWR to assess a seamless bathymetric / topographic DEM that they created of the Delta, and applying updates and corrections to it based on our assessment and project needs. The final phase was obtaining the necessary data to add the Yolo Bypass into the DEM, which resulted in the current working DEM. Details for each of the four phases are presented after the results/finds from the turbidity and geomorphology modeling.

Turbidity and geomorphology modeling

The numerical model applied in the turbidity and geomorphology modeling is Delft3D Flexible Mesh (D3D FM). D3D FM is a process-based unstructured grid model developed by Deltares (Deltares, 2014). It is a package for hydro- and morphodynamic simulation based on a finite volume approach solving shallow-water equations applying a Gaussian solver.

The average cell size of the Bay-Delta model ranges from 1200m x 1200m in the coastal area, to 450x600m in the Bay area, down to 25x25m in Delta channels. In the Delta, each channel is represented by at least 3 cells in the across-channel direction (Figure 6-1). The grid flexibility allows including the entire Bay-Delta in a single grid containing 63,844 cells of which about 80% are rectangles which keeps the computer run times at an acceptable level. On an 8-core desktop computer, it takes 6 real days to run 1 year of hydrodynamics simulation and an additional 12 hours to run the sediment module using the outputs of the hydrodynamic simulation. More information on the model can be found at <http://www.d3d-baydelta.org/>.

D3D FM allows straightforward coupling of its hydrodynamic modules with a water quality model, DELWAQ. Delwaq calculates sediment dynamics based on the DFM flow field and couples hydraulic and sediment dynamics with the phytoplankton model or the habitat (ecological) model (Achete et al., 2015).

The DELWAQ sediment model has been calibrated in detail against measured suspended sediment concentration (SSC) levels, including a sensitivity analysis on model parameters. The sediment model provides a yearly sediment budget, depositional patterns and assessment of model results in terms of turbidity levels for an entire year, Water Year 2011.

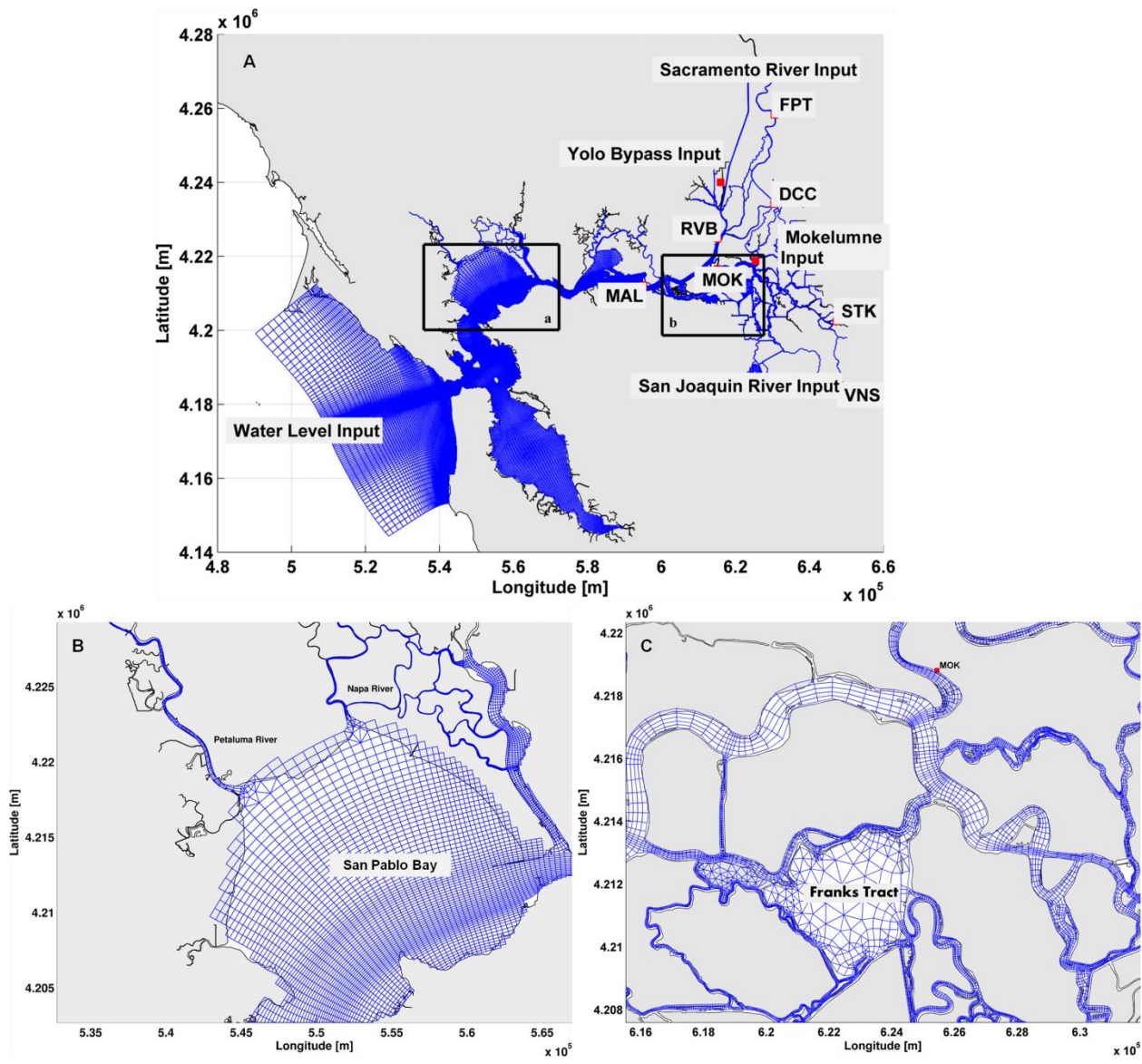


Figure 6-1. Numerical mesh for the D3D FM model. Red dots indicate the calibration stations. (<http://san-francisco-bay-delta-model.unesco-ihe.org/>). Zoom in of the computational grid, A) San Pablo Bay connecting to the Petaluma and Napa Rivers, B) Delta channels

Overall, the model reproduces the SSC peaks and event timing and duration in the wet season as well as the low concentration in dry season throughout the Delta, except at Mallard where the water column is stratified due to salt intrusion. Stratification issues are not solved in a 2D model. For this reason we are working on a 3D model in order to include the Bay area, leading to a unique source to sink model.

Results/findings

Turbidity and geomorphology modeling

Our focus has been to represent realistic SSC levels capturing the peaks, including their timing and duration, and to develop a sediment budget to assess sediment trapping in the Sacramento-San Joaquin Delta. We analyze the results based on a) SSC levels in the Sacramento-San Joaquin Delta (Delta), b) sediment budget and c) translation of SCC to turbidity levels using a two dimensional horizontal, averaged in the vertical (2DH), model. This process-based model is able to quantify high-resolution sediment budgets and SSC, both in time (~ monthly/yearly) and space (~10s-100s of m).

The results shown below are derived from an extensive calibration process where the different sediment fraction parameters (w_s , τ_{cr} and M) were tested. Our initial models used multiple sediment fractions as was done in previous work (van der Wegen et al., 2011; Ganju and Schoellhamer, 2009). However, tests with a single mud fraction proved to be consistent with the data, representative of the sediment budget, and allow a simpler model and better understanding of the SSC dynamics. With a single fraction it was possible to reproduce more than 90% of the sediment budget for the Delta when compared with the sediment budget derived from discharge and SCC observations (Figure 6-2).

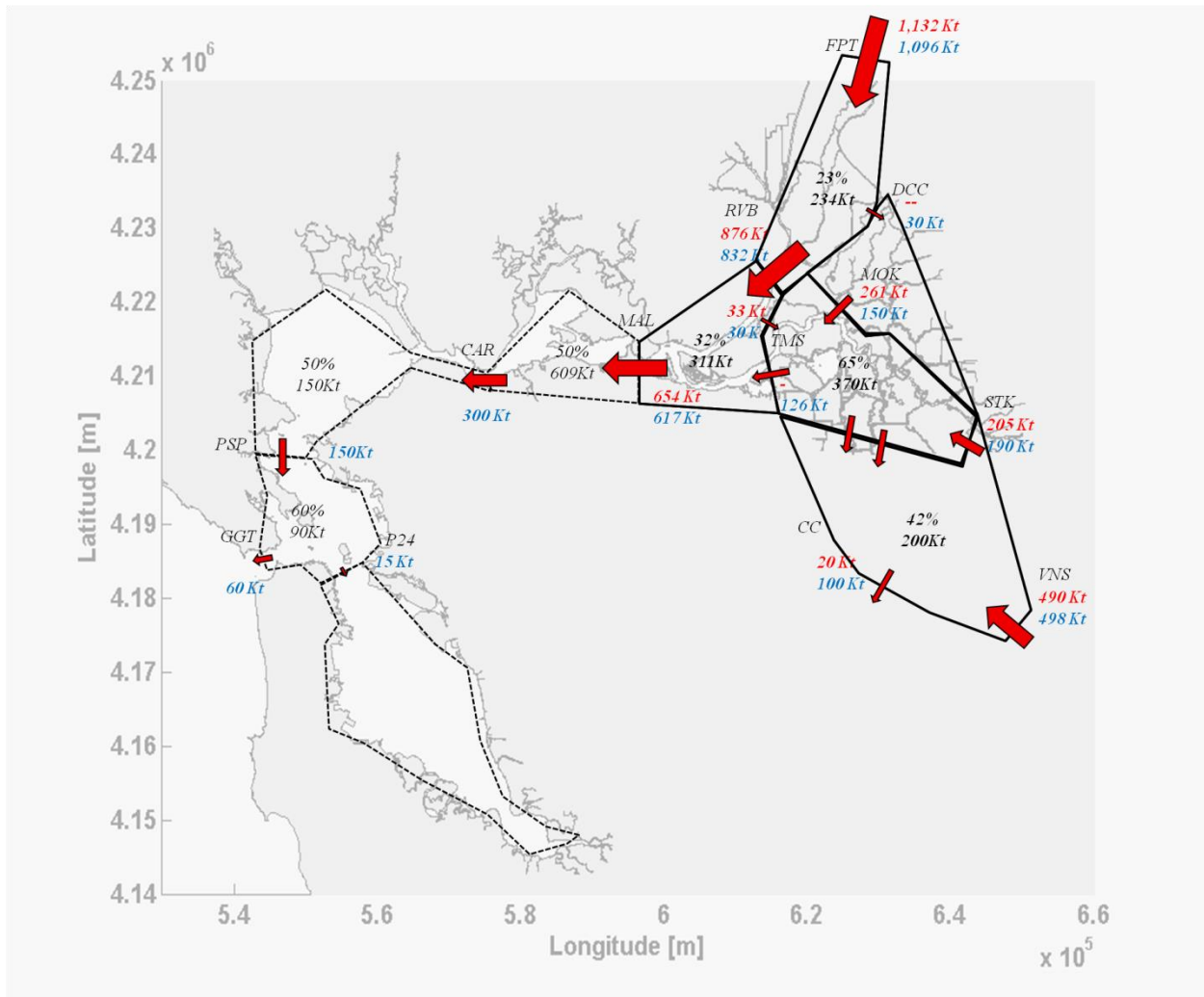


Figure 6-2. Sediment pathway model. The arrows represent the sediment fluxes through the cross sections. Area of the arrow is proportional to the flux. Sediment fluxes from observations are in red and from the model are in blue.

Sediment trapping differs by region in the Delta. Model results show that Northern Delta (the least efficient) traps ~ 23%; Central/Eastern Delta traps 32%, Central/Western 65%, and the most efficient is the Southern Delta region that traps 67% of the sediment input. Regions with the highest trapping efficiencies contain islands inundated through levee breaching.

Sedimentation occurs in flooded islands areas, such as Frank Tract and the Clifton Court. The 2D model is sufficient for such areas (Figure 6-3). More downstream near Carquinez Strait a 3D model would be needed to account for flow stratification and

density effects resulting from salinity and temperature gradients. The focus, however, of this study is on the Delta. The San Joaquin River downstream of Stockton experiences high deposition. The constant dredging needed to maintain the Stockton navigation channel supports this finding. The river discharge modulates the deposition pattern in the main channels. In the Sacramento, deposited sediment is gradually washed away and transported to the mud flats at the channel margins, until the next peak. At flooded island the sedimentation process is gradual and steady, erosion is not observed in these areas. The deposition pattern provides insight into the best areas for marsh restoration.

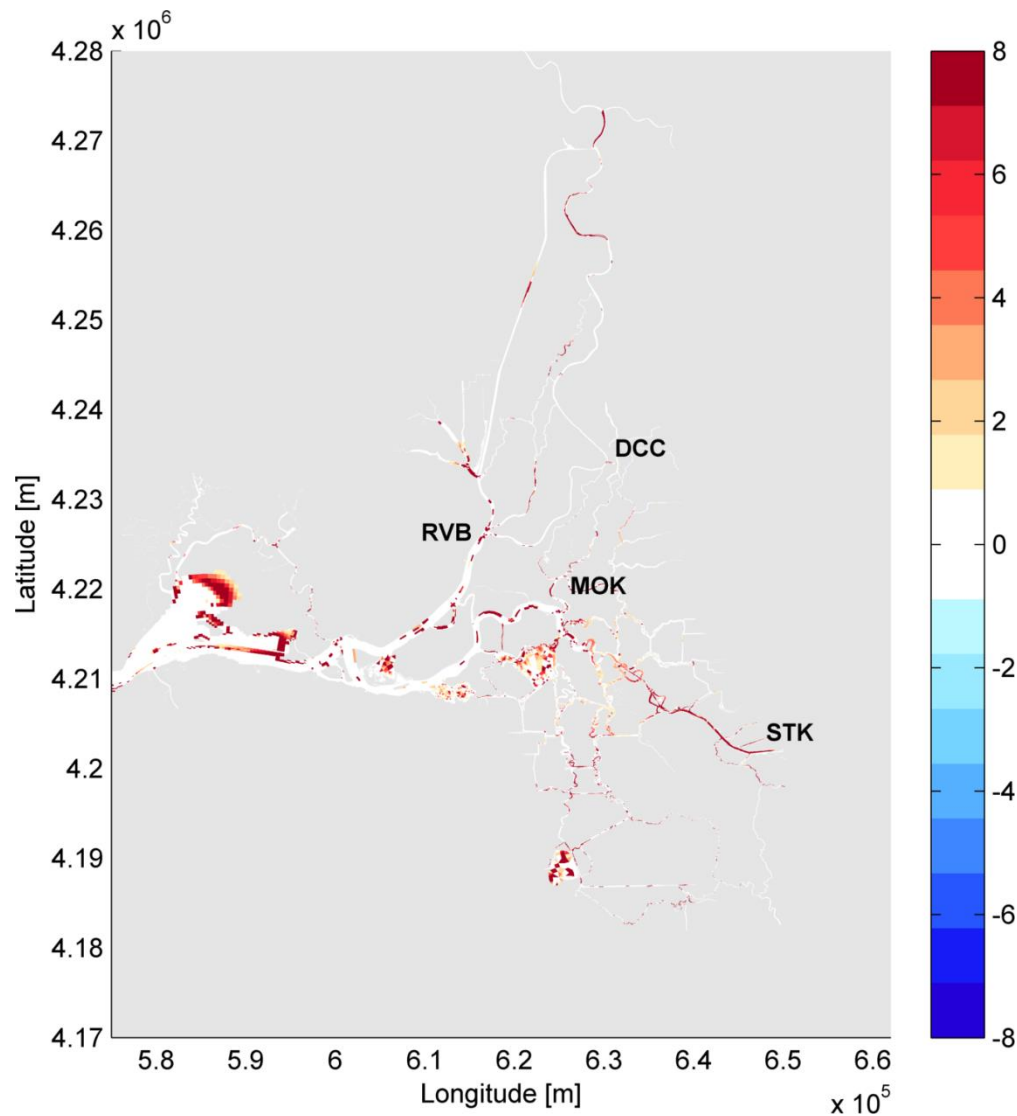


Figure 6-3. Modeled deposition for a 1-year period. The color bar indicates deposition (red shades) and erosion (blue shades) in mm.

To further investigate the influence of the channel network in the sedimentation pattern, we applied the same forcing for 4 different channel configurations ranging from a full Delta network to a schematization of the main river (Fig. 6-4). A higher degree of network schematization leads to higher peak sediment export. However, the sedimentation area is similar for all configurations because it is mostly driven by the geometry and bathymetry (Achete et al, submitted).

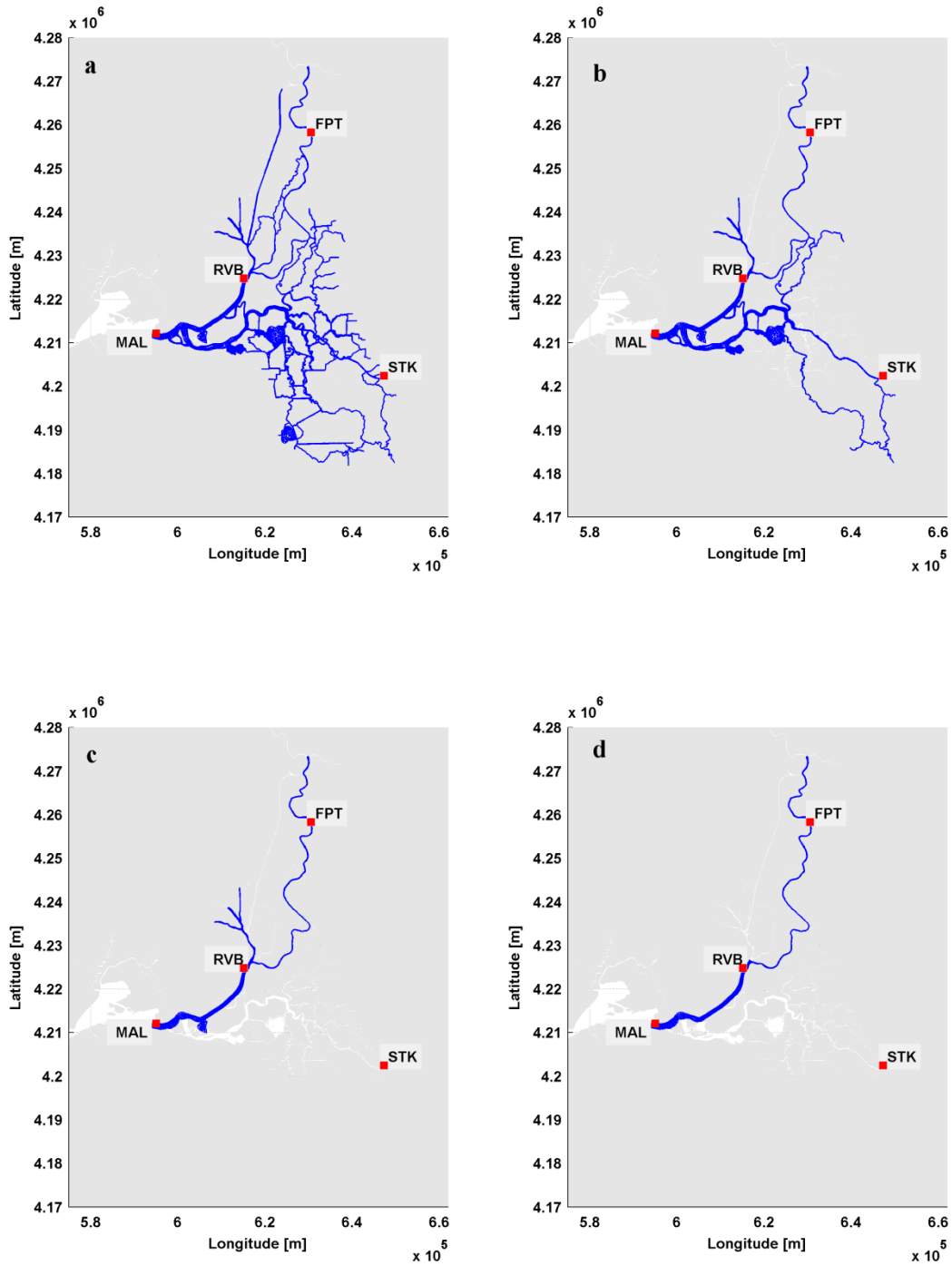


Figure 6-4. Grid of each schematization, "Delta"(A), "2 Rivers"(*B); "Sacra ext" (C); "Sacra" (D).

Deposition patterns develop as the result of peak river flows after which, during low river flow conditions, the tidal currents are not able to significantly redistribute deposited

sediment. Deposition is quite local and mainly takes place at the junction in the region where the Sacramento River, the Sacramento River Deep Water Ship Channel and Yolo Bypass merge (Fig. 6-5). This is probably a deep region subject to dredging to maintain shipping to Sacramento. We could not confirm this with data. The limited impact of tidal flows is confirmed by runs without a seaward tidal forcing showing similar hydrodynamics and sediment dynamics. No-tide runs lead to lower trapping efficiencies because the tidal movement enhances sediment suspension.

More schematized networks under equal forcing lead to remarkably similar deposition patterns. Excluding smaller channels in the network decreased mass storage by about 15%. A higher level of schematization also leads to higher tide residual velocities, more sediment export and a lower trapping efficiency. These results allow modelling of less measured estuaries where not all the small channels have bathymetric data, and still are able to calculate mass storage and trapping efficiency.

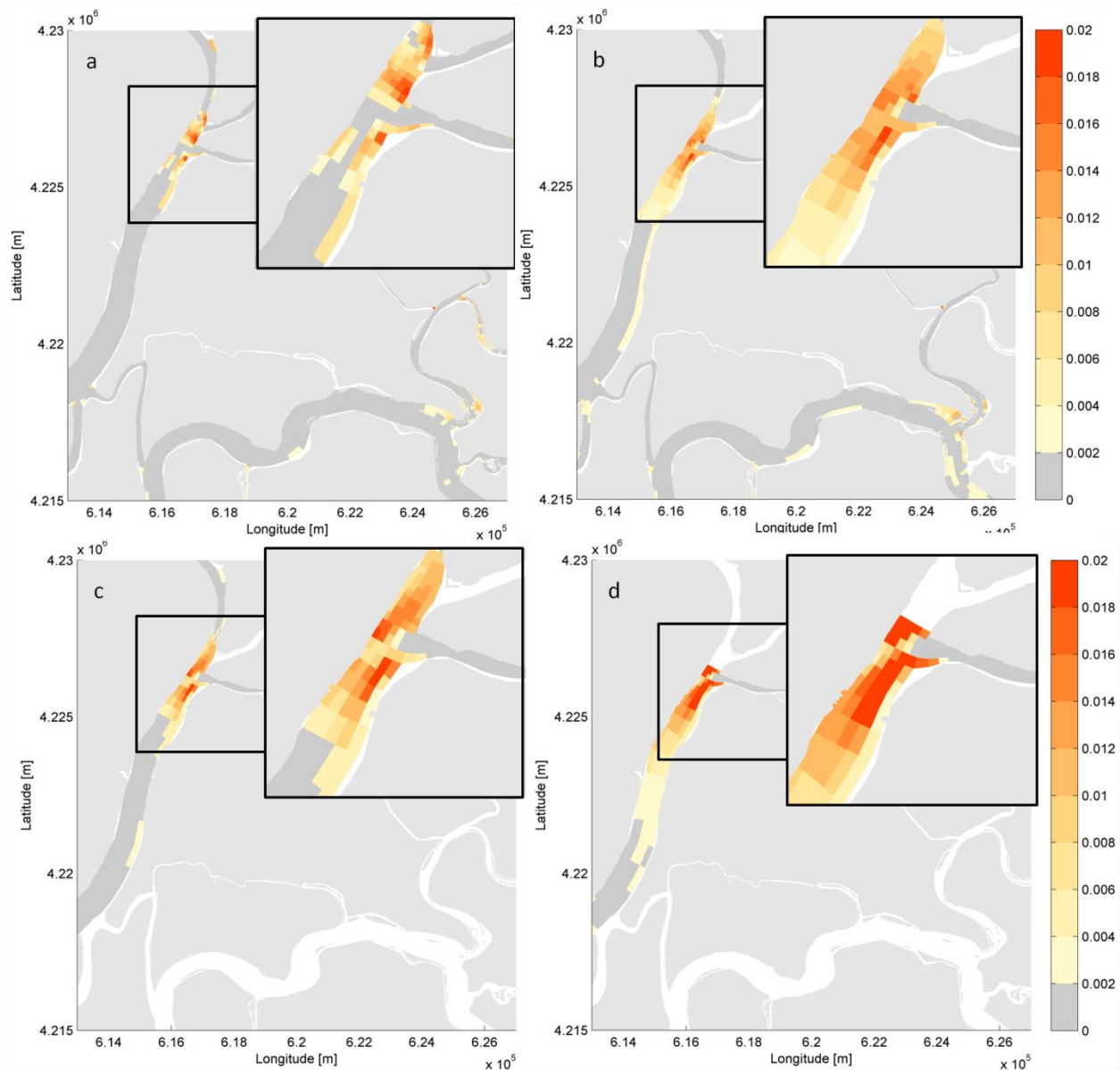


Figure 6-5. Deposition maps at the last time step. The color bar indicates mm of deposited sediment and in darker gray is the relative grid, (a) "delta", (b) "2 rivers", (c) "Sacra ext", (d) "Sacra", (e) "Sacra linear" and (f) "delta no tides".

Ecological analysis is often based on turbidity levels. SSC and turbidity are correlated by rating curves as $\log_{10}(\text{SSC}) = a \cdot \log_{10}(\text{Turb}) + b$, where a and b are local parameters empirically defined for each Delta area. For the Northern area $a=0.85$ and $b=0.35$; Central/Western area $a=0.91$ and $b=0.29$, Central/Eastern $a=0.72$ and $b=0.26$; Southern $a=1.16$ and $b=0.27$; Eastern $a=0.914$ and $b=0.29$ (USGS Sacramento, personal communication 2014).

We present average values for turbidity within a specific Delta region as well as its seasonal and daily variations (Figure 6-6). Generally, the mean turbidity levels and spatial variations are higher during the wet season than during the dry season. During the wet season, the Southern area had the highest mean value (50 NTU), and deviation (15 NTU), caused by a combination of large sediment supply and low flow velocities. The Northern region is the second most turbid area (45 ± 10 NTU), where sediment transported by the Sacramento River flows in the channels, increasing the turbidity levels. The Central West region is the least turbid area (5 ± 2 NTU) and, as previously shown, it has the highest trapping efficiency of the entire Delta. In the dry season the mean turbidity daily variation decreases in the entire Delta. The opening of the DCC during the dry season lets sediment from the Sacramento River enter these areas, increasing the mean turbidity level. The spatial distribution of the most turbid areas is the same as in the wet season. The daily deviation is primarily proportional to the turbidity level and to the distance from the sea. In the Southern and Western areas the daily variation is higher during the dry season. It shows that there is a strong tidal signal in these parts of the Delta.

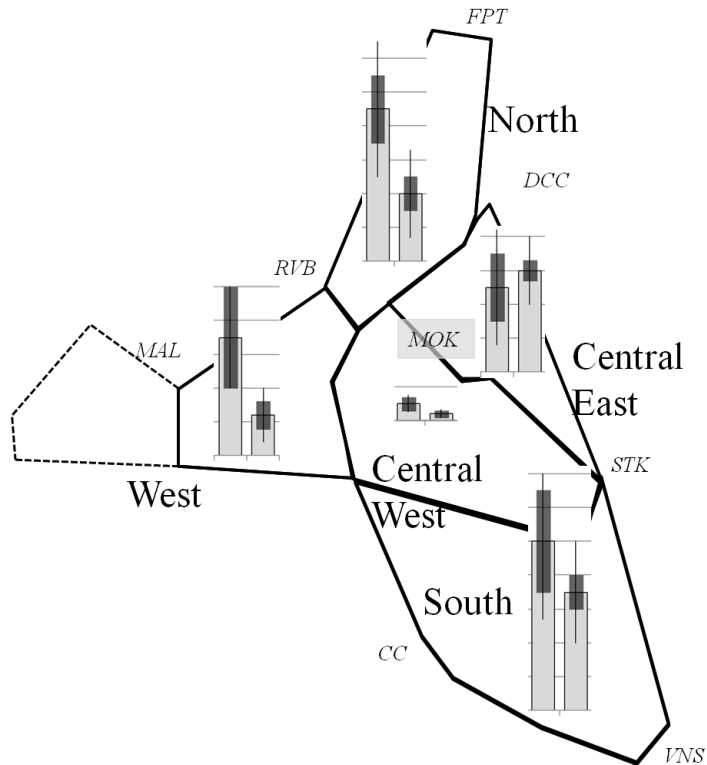


Figure 6-6. Turbidity in each Delta region. For each region, the left bars indicate the average value for the wet season and the right bars the dry season. The light gray bars indicate the mean turbidity over the region, the darker bars are the spatial deviation and the lines the daily deviation. Each horizontal line represents 10 NTU.

Detailed explanation of the creation of seamless bathymetric/topographic DEM for use in modeling

In Phase 1, evaluation of the original USGS bathymetric DEM released in 2005 revealed a DEM made up of bathymetric surveys spanning from 1933 to 2002 and collected by DWR, the Army Corp of Engineers (COE), and the National Oceanic and Atmospheric Administration (NOAA). Significant areas without surveys were identified including Mildred and liberty Islands, and areas of older data were highlighted. Checking the DWR data file (CDSP Bathymetry data) that compiled the surveys for the original DEM revealed an update in 2007 that added in five new surveys. These surveys were added to the files that created the DEM, and in cases where the new data was dense enough, older surveys were completely replaced. The most time intensive part of this update was editing the shoreline to better fit the modern delta. Previously the shoreline

was based off of images taken in the 1990's at a scale of 1:12,000. The current software agreement with ESRI allows access to their satellite imagery of the USA with a resolution of up to a half a meter (ESRI 2014). Images used for this update were collected in 2007 and 2008. In addition to the satellite images, use was made of the NOAA shoreline data explorer (NOAA 2015); shorelines were obtained from images taken in 1983, 2003, and 2007. The updated shoreline was a conglomerate of all these data sources, including the original shoreline, with the goal to best represent the modern geography of the delta and the extents of the data. The completion of the shoreline, and edits and adjustments made to the files that create the bathymetric DEM, resulted in an updated Delta Bathymetric DEM and a starting point for the modelers (Figure 6-7). Comparing the interpolated DEM with the original bathymetric soundings shows a mean difference of -14.5 cm and a standard deviation of 78 cm that indicates that on average, the DEM is slightly shallower than the sounding data.

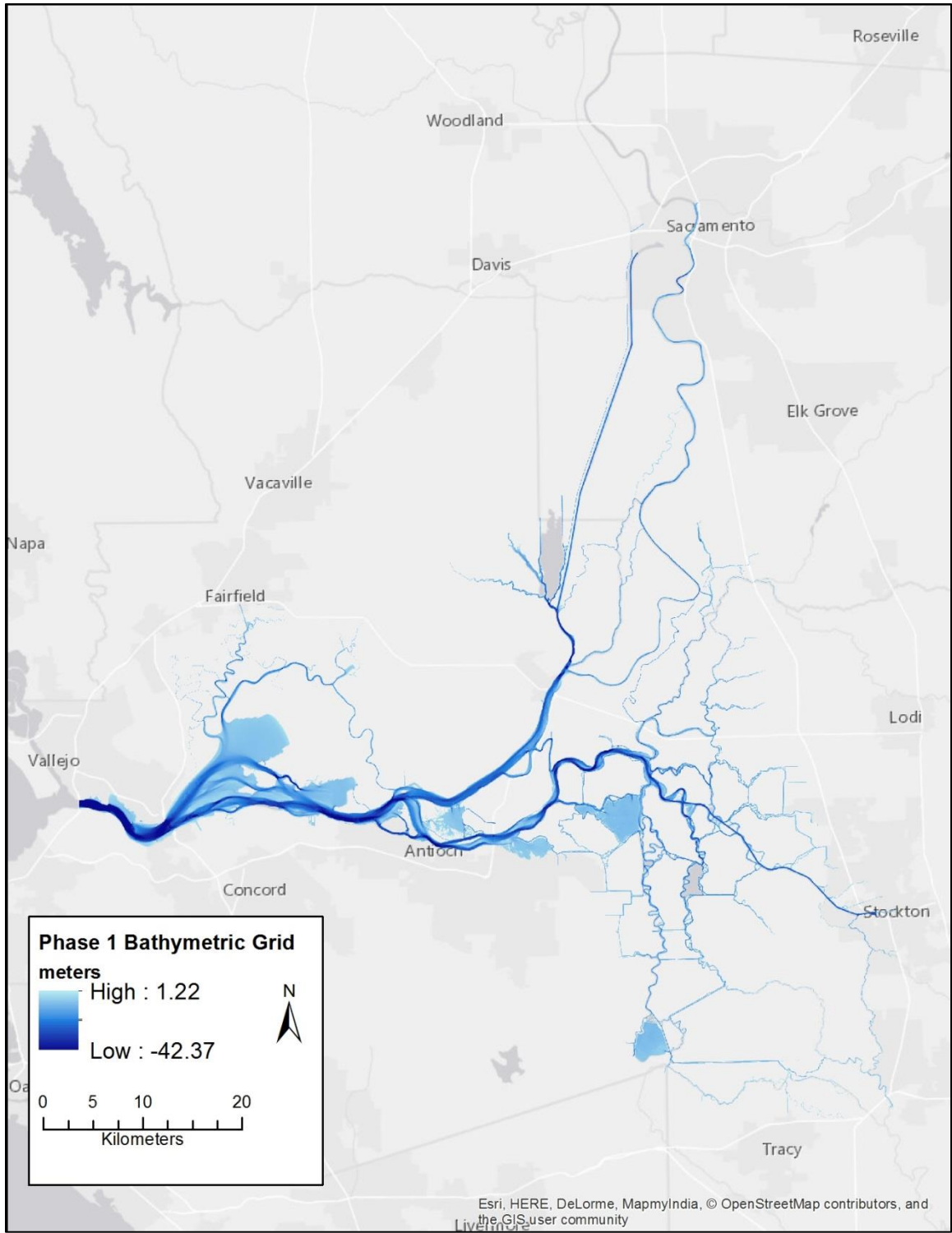


Figure 6-7. Updated bathymetric DEM resulting from Phase 1 activities. See text for details on changes made to the USGS 2005 bathymetric DEM.

In Phase 2 it was determined that the northern boundary conditions of the DEM were not sufficient. Bathymetric data needed to be located that would extend the Sacramento River north to Verona and the Fremont Weir, and north east along the American River to the Nimbus Dam. Through contacts at DWR, data from the Central Valley Floodplain Evaluation and Delineation Program (CVFED) was obtained in the form of recently collected multibeam and single beam bathymetric surveys, and topographic data in the form of LiDAR surveys. The data was collected by a variety sources-- private consulting firms and DWR led survey teams with collection dates as early as 2008 for the LiDAR flights and as late as 2011 for some of the bathymetric surveys. This new data included coverage of the Sacramento River from Walnut Gove up to Verona that was collected during two multibeam surveys with soundings every 3-feet in the horizontal, a survey collected by DWR's Urban Levees program in 2008, and one from 2011 collected by contractors for DWR. The Urban Levees data also included a 5-mile reach of the American River from its confluence with the Sacramento River. This data was resampled to 1-meter resolution than to 10-meter resolution for merging with the USGS 2011 Delta bathymetric DEM. Coverage of the American River came via a 2002 Comprehensive Study of the Sacramento and San Joaquin Rivers by the Army Corp of Engineers that used data from surveys that were conducted in 1997 of both topographic and bathymetric data. This new data was then merged into the existing Phase 1 Delta bathymetric DEM. In the Sacramento River, the new multibeam dataset far exceeded what had been used in the first DEM, so that portion of the river was removed. In the case of the other new datasets, there were also areas of overlap. In all cases the newer datasets took preference, but areas of overlap were left in order to create smoother transitions between the datasets. The last part of Phase 2 was to create Delta levee polygons for use by the modelers. A total of 84 polygons were created that contained statistics for elevation for every five meters along the perimeter of each polygon. The bathymetric update (Figure 6-8) for this phase began a relationship with DWR and access to future bathymetric updates to refine the USGS delta bathymetric product.

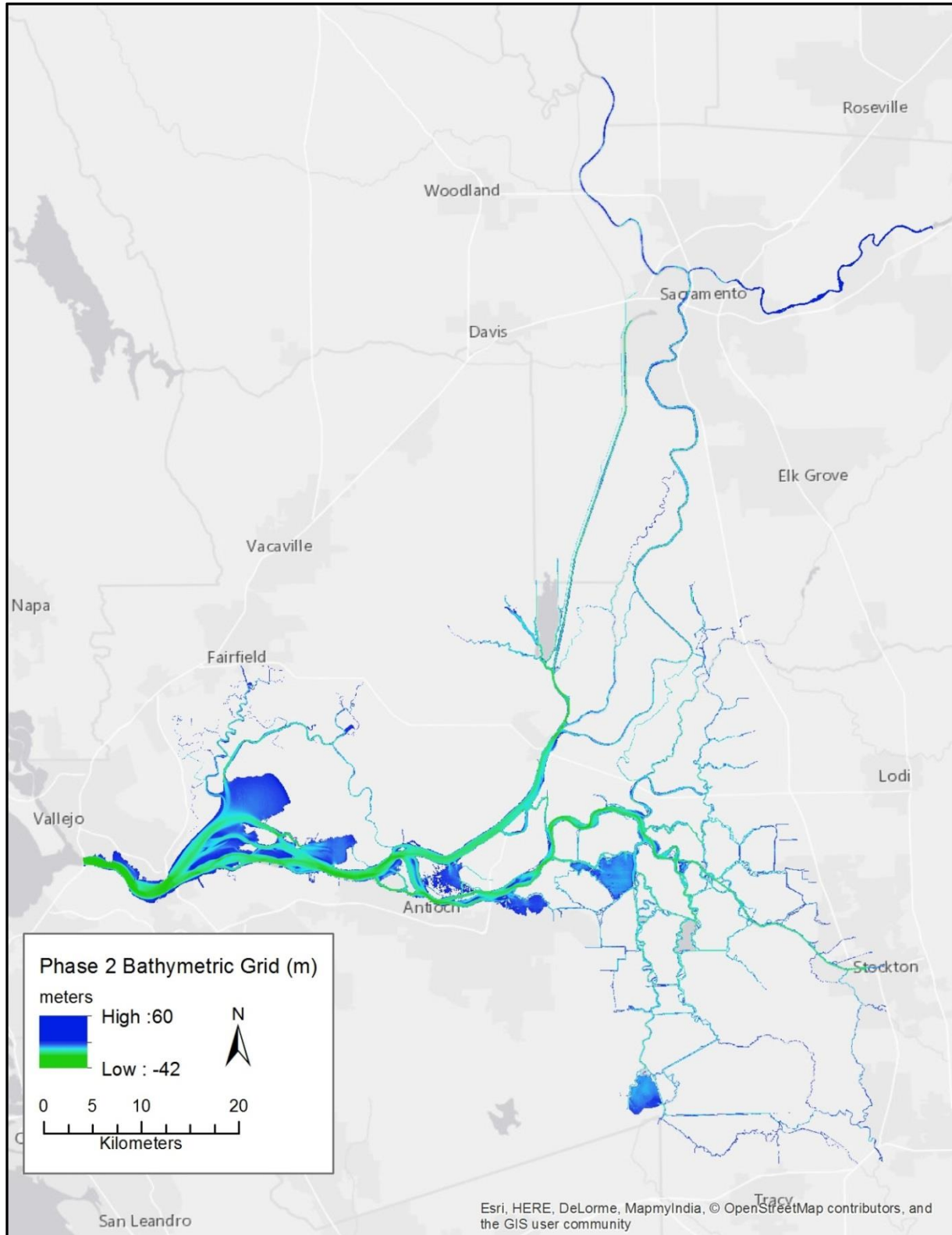


Figure 6-8. Updated bathymetric DEM resulting from Phase 2 activities. See text for details on changes made to the Phase 1 bathymetric DEM.

Building from the relationship established with DWR in Phase 2, in Phase 3 contact was made with a group within DWR led by Eli Ateljevich and Rueen-Fang Wang that are working on their own seamless bathymetric / topographic DEM product. At the time of first contact, they had just released a version of their product that they made available to the USGS to critique and refine for the mutual benefit of all (Rueen-Fang and Ateljevich, 2012). Figure 6-9 shows the initial comparison between the USGS and DWR bathymetric DEMs. Examination revealed that they had used the 2005 USGS Delta Bathymetric DEM and methods as their starting point for their efforts, which made it easier to compare the two DEMs and determine the areas of change. As part of their report they also provided a data sources file that clearly indicated source and location for the new surveys. Analysis showed that they had done a very careful and thorough job combining all the bathymetric and topographic data sets into one surface. The only issue that was discovered was that instead of always replacing older single beam data sets with newer more recent surveys, DWR would combine the datasets for an average surface, their thinking being that they did not want to bias the model with signals from possible extreme events. The result of such averaging can create wider channels and shallower depths, which reports a false geomorphic signal that would be perpetuated throughout a model based on that data. Discussion led DWR to believe that combining data sets when newer surveys were sufficient to replace older areas was not the better option. It was decided that since the USGS needs were more pressing than DWR's current timeline of updating their DEM, that the USGS would regrid some areas of the DWR DEM using only the most recent survey and the resulting newly gridded areas would be shared. The USGS also refined the Mildred Island bathymetry that DWR used with the USGS data collected in 2002 and passed on the results. The decision was also made to replace western areas of the DWR DEM that were based on an older NOAA product with a newly released higher resolution USGS EROS seamless bathymetric / topographic product. The addition of the topographic data into the DEM added a huge amount of new data to play with. The ability to have the shore and levees directly into the DEM was very helpful for the modelers, but they did not want the entirety of the DWR product. A subsection of the DWR DEM was taken that included all of the bathymetric data and at least 100 meters of topographic data that is directly adjacent to

shore and includes at minimum, levee profiles. This subsection along with the newly refined pieces developed by the USGS became the Phase 3 version of the Delta bathymetric and now topographic DEM (Figure 6-10).

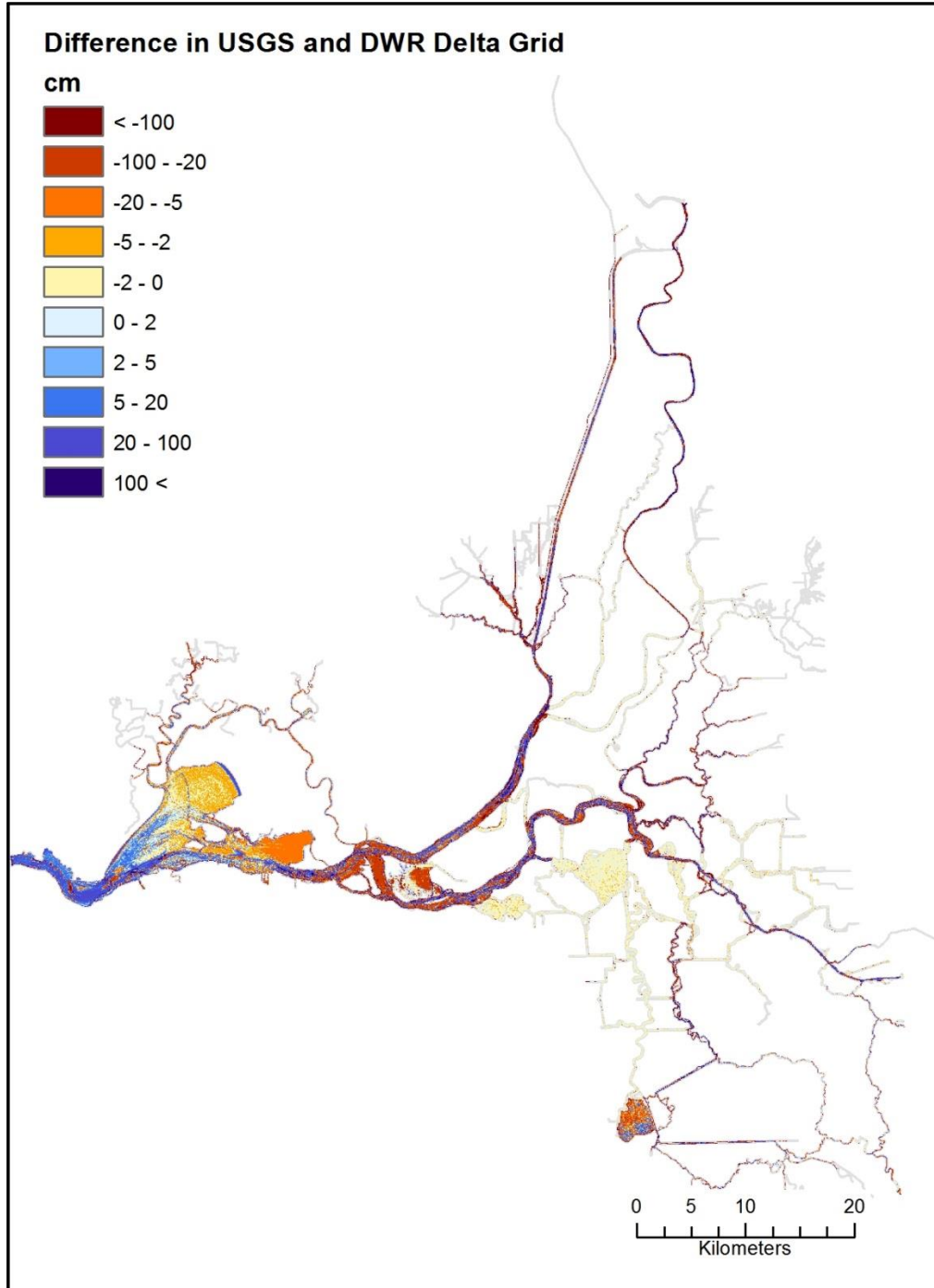


Figure 6-9. Initial comparison between the USGS and DWR bathymetric DEMs

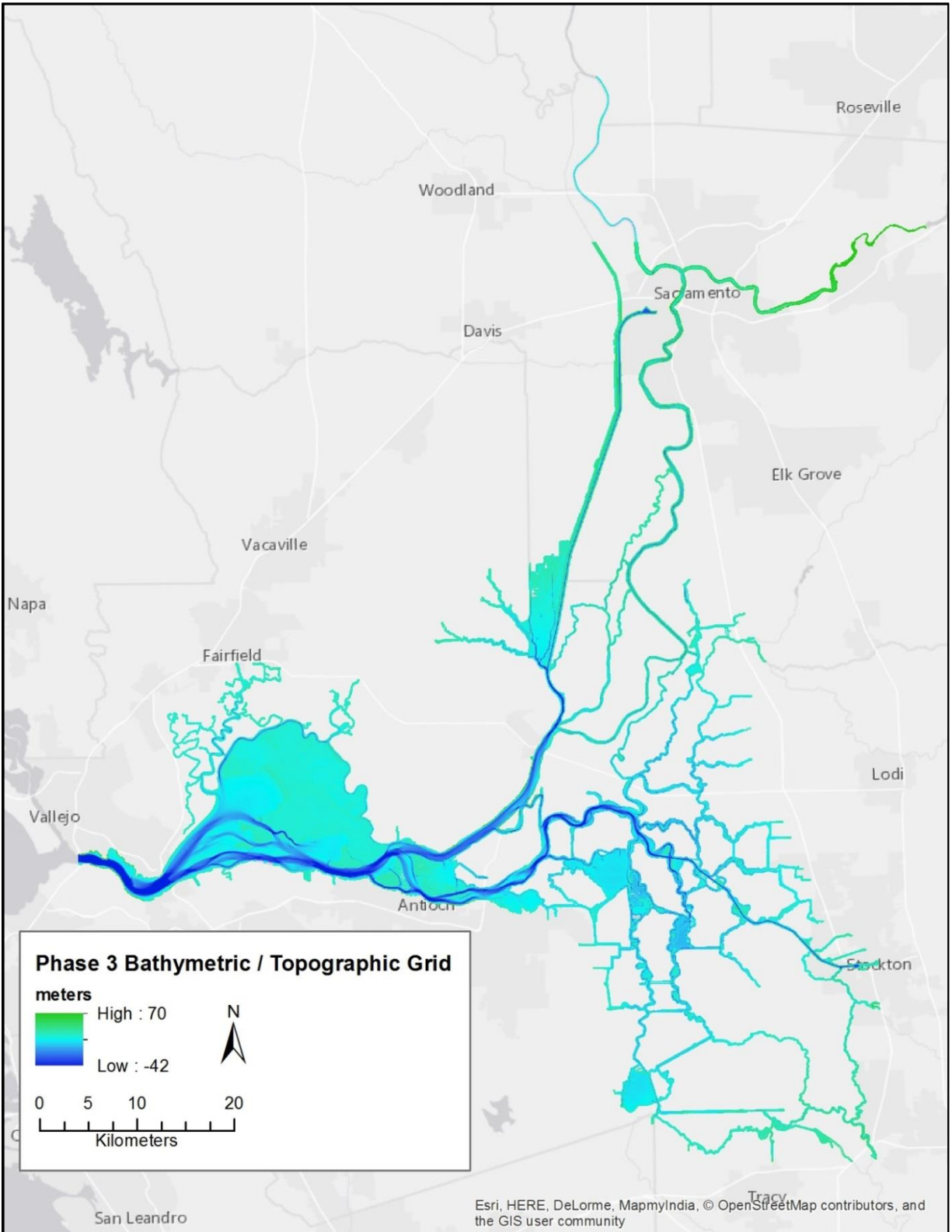


Figure 6-10. Updated bathymetric/topographic DEM resulting from Phase 3 activities. See text for details on changes made to the Phase 2 bathymetric DEM.

Phase 4 (Figure 6-11) began with the sole purpose of adding the Yolo bypass into the DEM. The necessary LiDAR files were extracted from the CVFED data files then mosaicked together and resampled from a 1 meter resolution to the 10 meter resolution used by the DEM. The LiDAR was inspected for any weird artifacts and areas of standing water, represented by a mostly flat surface, were removed with holes left in the data. Additional bathymetric survey data for Tule Canal that runs along the eastern boarder of the Yolo bypass from the Fremont Weir to the beginning of the Toe Drain was pulled from the CVFED data and provided direct to the modelers at their request. This was done in large part because the width of the Tule Canal ranges from 5 – 215 meters and the cell size of the USGS gridded data is 10 meters and would have been unable to define the true shape of the canal. Adding in the Yolo Bypass also allowed the use of a 2011 bathymetric survey collected by the USGS in the Sacramento starting at the confluence of the Sacramento and Feather rivers at Verona (Finlayson and others 2011). There was a missing chunk in the multibeam data between the USGS survey and the CVFED survey along the Sacramento just before Verona. Single beam sounding data from the CVFED data was interpolated to fill this gap. The bathymetric and topographic data for this new area is not seamless, it was deemed unnecessary to spend more time on this when the modelers' process of creating their mesh would allow them to easily bridge the missing data gaps between the topographic and bathymetric data, and every moment spent working on this would be a lost moment that the modelers could have spent working with the data and validating their model.

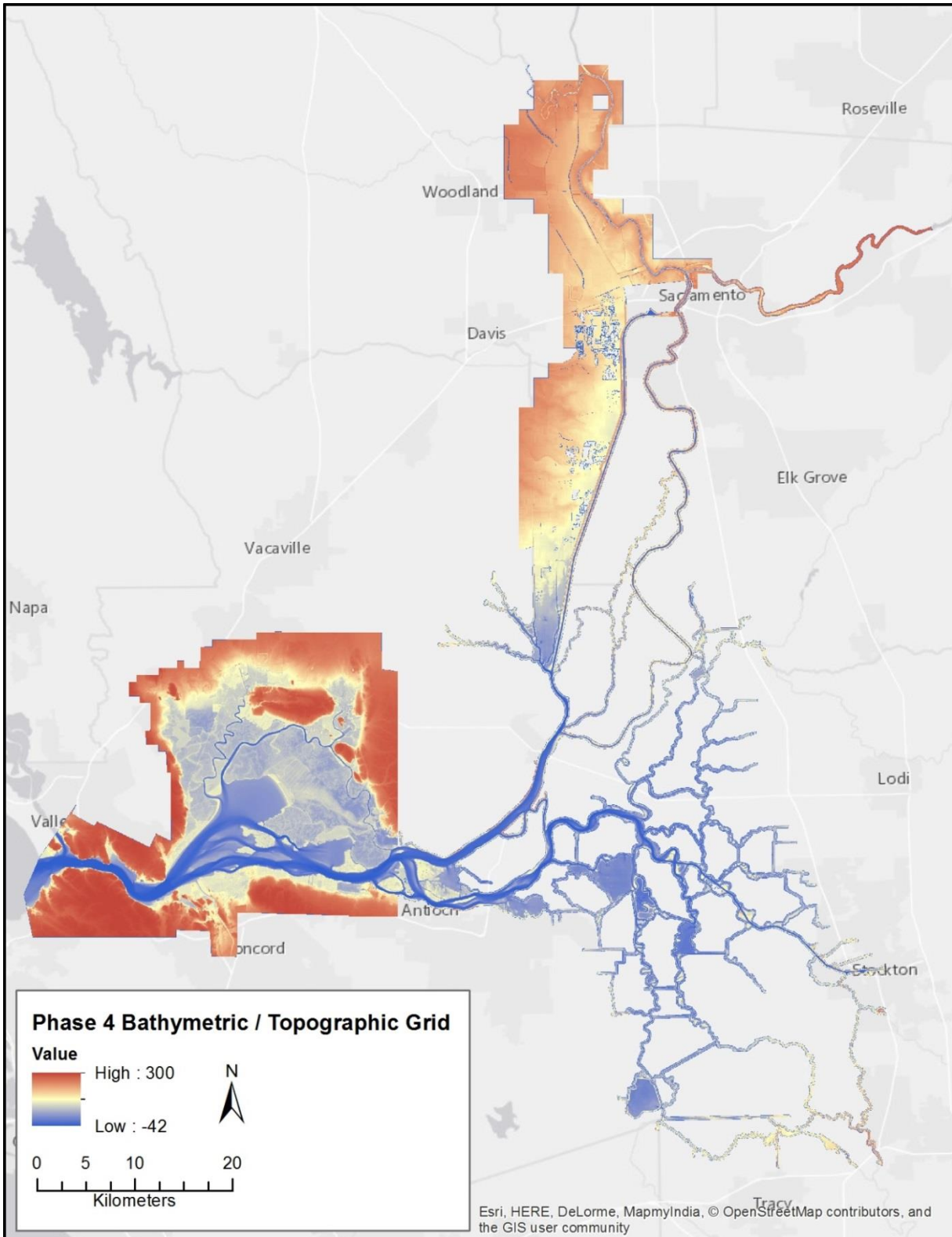


Figure 6-11. Final bathymetric/topographic DEM produced in Phase 4. See text for details on changes made to the Phase 3 bathymetric/topographic DEM.

The current surface is a combination of the DWR seamless bathymetric / topographic product and USGS updates (Figure 6-12). The DWR team is planning on continuously updating their product and will be working in the USGS contributions.

There are still areas of older data that would benefit from new surveys (Figure 6-13). DWR will continue to collect additional surveys in the Delta that will be made available to the USGS for possible further updates of the USGS bathymetric/topographic DEM.

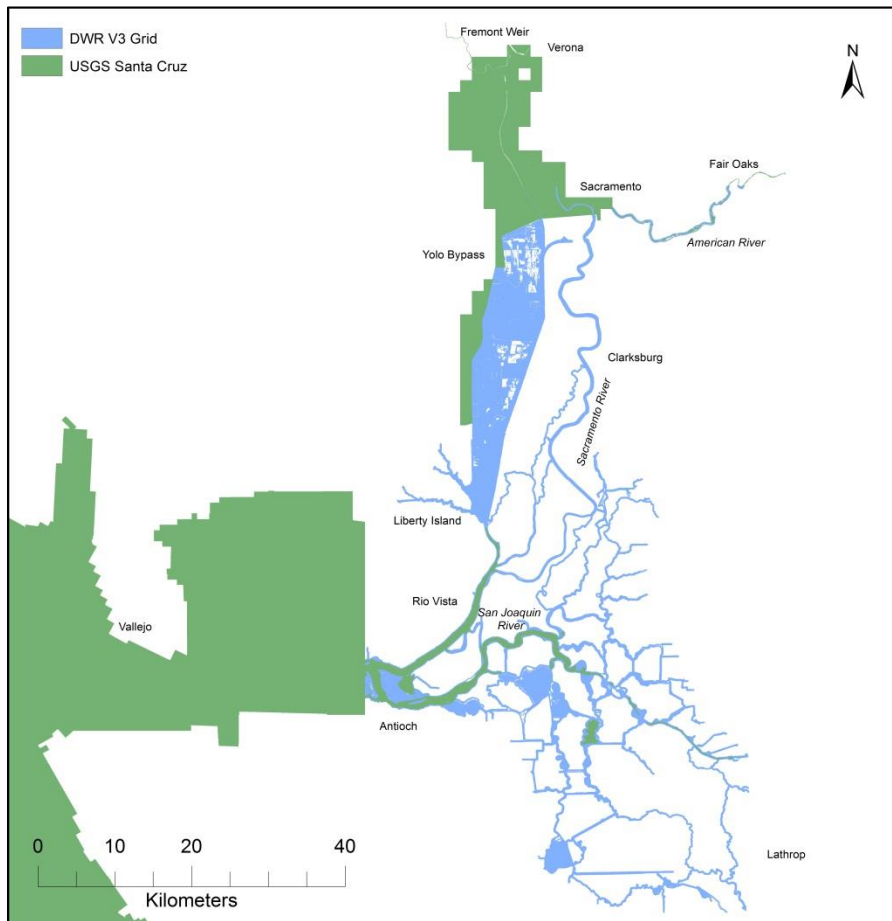


Figure 6-12. Phase 4 contributions to the updated bathymetric / topographic DEM by the USGS and DWR.

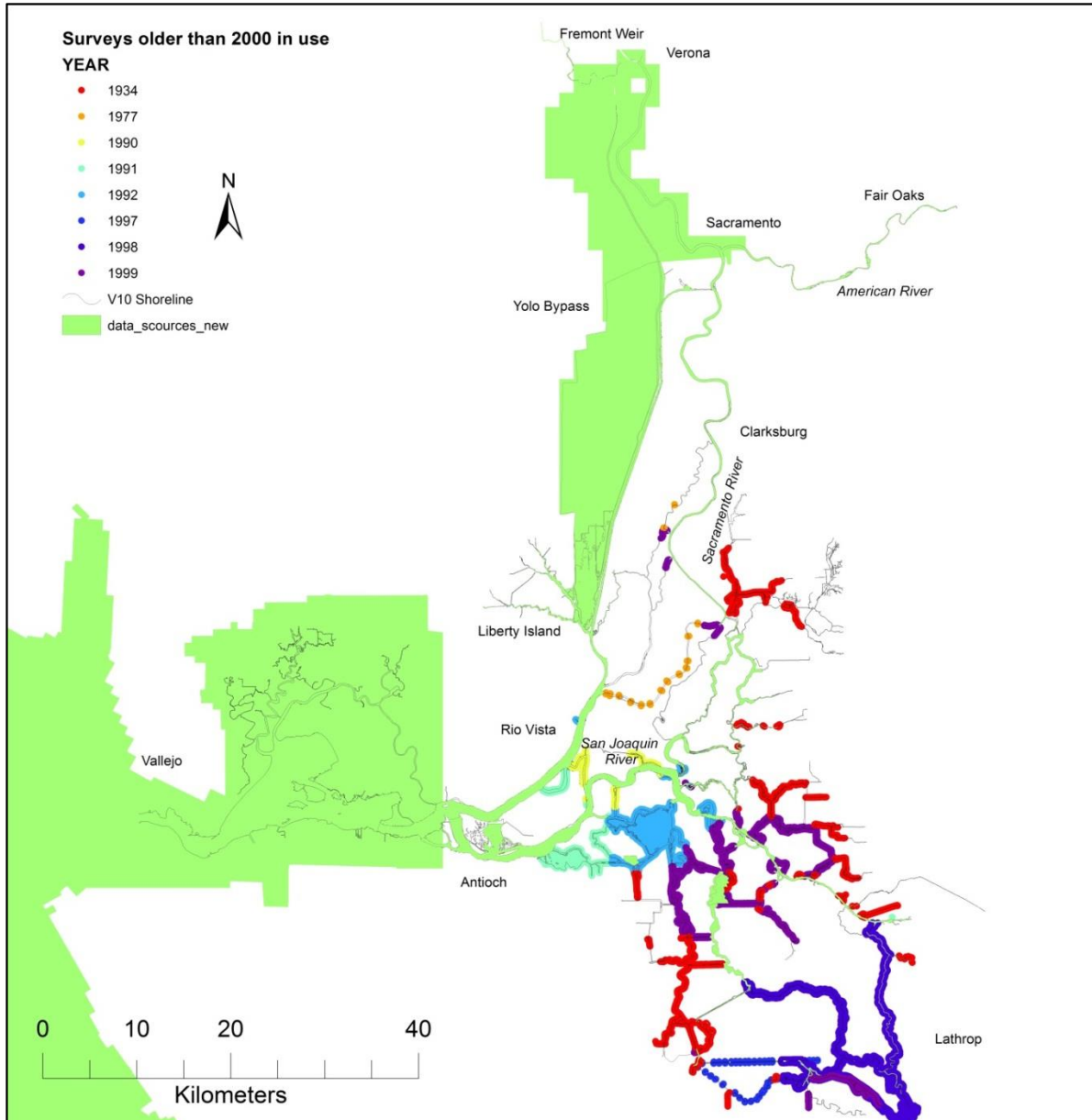


Figure 6-13. Areas with the most recent bathymetric data older than 2000. Areas where data from the 1930s is the most recent data are shown in red.

Management implications

With simple sediment settings of one fraction at the input boundary and a simple distribution of bed sediment availability, it is possible to reproduce seasonal variations as well as construct a yearly sediment budget with more than 90% accuracy when compared with a data derived budget. Our research shows that it is extremely important to have discharge and SSC measurements at least at the input boundaries and close to

the system output in order to be able to calibrate the model settings applied for hydrodynamics and suspended sediment.

Next steps

Overall, the model reproduces the SSC peaks and event timing and duration (wet season) as well as the low concentration in dry season throughout the Delta, except at Mallard where the water column is stratified due to salt intrusion. Stratification issues are not solved in a 2D model. For this reason we are working on a 3D model in order to include the Bay area, leading to a unique source to sink model.

Bathymetry used the bathymetric/topographic DEM is as old as the 1930s. Surveying these areas and updating the DEM is advisable to ensure that in changes in channels since collection of the old data are reflected and the best available representation of current conditions are used in modeling.

Change analysis on areas of the Delta where multiple surveys have been conducted would improve understanding of the causes for geomorphic change. Such a dataset would be invaluable for verifying geomorphic models and decrease uncertainty in forecasts of potential Delta response to changing conditions.

The present model opens the possibility for forecast and operational modeling. The forecast scenarios may include changing in river sediment supply, pumping and temporary barriers operations as well as sea level rise scenarios.

The modeling approach applied allows for direct coupling of the suspended sediment concentration results into an ecology model.

References

Achete, F., Van der Wegen, M., Roelvink, D., and Jaffe, B.E., 2015, A 2D Process-Based Model for Suspended Sediment Dynamics: a first Step towards Ecological Modeling, Hydrology and Earth Systems Sciences, 2837-2857. doi:10.5194/hess-19-2837-2015, <http://www.hydrol-earth-syst-sci.net/19/2837/2015/>.

Achete, F., Van der Wegen, M., Roelvink, D., and Jaffe, B.E., submitted, Suspended Sediment Dynamics in a tidal channel network under Peak River Flow, Ocean Dynamics.

Army Corp of Engineers, 2002, Comprehensive Study of the Sacramento and San Joaquin Rivers

Central Valley Floodplain Evaluation and Delineation Program.

<http://www.water.ca.gov/floodsafe/docs/CVFED.pdf>.

CSDP bathymetry data, 2007, Retrieved from the Bay-Delta Office, California Department of Water Resources.

<http://baydeltaoffice.water.ca.gov/modeling/deltamodeling/models/csdp/csdp.cfm>

Deltares, 2014, D-Flow Flexible Mesh, Technical Reference Manual, Deltares, Delft, 82 pp.

ESRI Imagery.

<http://www.arcgis.com/home/item.html?id=c03a526d94704bfb839445e80de95495>

Finlayson, D.P., Jaffe, B.E., Reis, T., 2011, Bathymetry and Acoustic Backscatter: Sacramento River near Woodland California. (USGS Field Activity ID: S-03-11-CA)

Foxgrover, A., Smith, R.E., & Jaffe, B.E., 2003, Suisun Bay and Delta Bathymetric Surveys: Field Data Collection. <http://sfbay.wr.usgs.gov/sediment/delta/index.html>

Ganju, N. K. and Schoellhamer, D. H., 2009, Calibration of an estuarine sediment transport model to sediment fluxes as an intermediate step for simulation of geomorphic evolution, Cont. Shelf. Res., 29, 148–158, doi:10.1016/j.csr.2007.09.005.

NOAA Shoreline Data Explorer. <http://www.ngs.noaa.gov/NSDE/>

USGS EROS Data Center (2013) 2 m Coastal National Elevation Dataset.

http://topotools.cr.usgs.gov/topobathy_viewer/

Van der Wegen, M., Jaffe, B. E., and Roelvink, J. A., 2011, Process-based, morphodynamic hindcast of decadal deposition patterns in San Pablo Bay, California, 1856–1887, J. Geophys. Res.- Earth, 116, F02008, doi:10.1029/2009jf001614.

Task 7a: Trend in sediment supply from the Central Valley to the Delta

Dave Schoellhamer and Tara Morgan-King (submitted 06-16-15)

Progress/status

We have published journal articles on the geomorphic adjustment of the San Francisco estuary and watershed to reduced sediment supply (Schoellhamer et al. 2013) and on a step decrease in suspended-sediment concentration in the Delta in 1983 associated with El Nino storms (Hestir et al. 2013). Schoellhamer collaborated with colleagues at Portland State University to develop new estimates of historical flows and sediment supply to San Francisco Bay. A journal article by Mofkakhari et al. describing those results is being revised as suggested by the journal's reviewers. A journal article describing trends in watershed sediment supply and erosion of river cross sections since the early 1900s is being written by Morgan-King and Schoellhamer.

Results/findings

In the San Francisco Estuary, suspended sediment has been declining over the past 30 years as a result of declining sediment supply, contributing to dramatic changes in the ecology and geomorphology of the estuary. However, the decline has not been gradual. Recent observations of an abrupt decrease in suspended sediments in the San Francisco Bay have been explained by a model that suggests that the step change has occurred due to exceedance of a sediment regulation threshold that triggered the change from a sediment transport regime to a supply-limited system. We investigated structural changes in the historical record of total suspended solids (TSS) concentration measured in the upper estuary to verify the model predictions. TSS in the upper estuary exhibited an abrupt step decrease in 1983 corresponding to the record-high winter and summer flows from the 1982 to 1983 El Niño event. After this step change, TSS concentrations had a significant declining trend despite subsequent near-record high flows. The abrupt change in TSS followed by the declining trend provides evidence for the hypothesis of sediment supply limitation in the San Francisco Estuary.

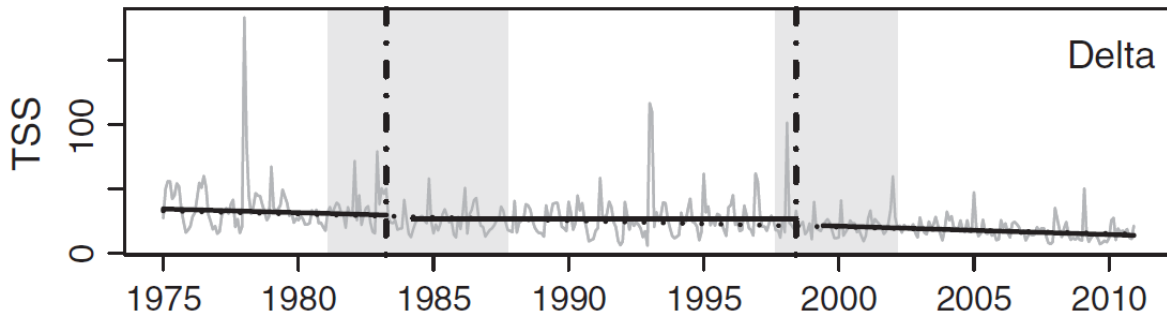


Figure 7a-1. Mean total suspended solids from 6 monthly sampling stations in the Delta, 1975-2010. Dates corresponding to a significant break point are indicated with a vertical dashed line. The 95% confidence interval around the break point is represented by the shaded gray area. The dotted lines indicate the overall trend for the period of record (1975–2010), and the solid lines indicate the trends for the periods separated by breakpoints. For periods with no significant trend, the trend is graphically represented by the mean. Data from <http://www.water.ca.gov/bdma/meta/discrete.cfm>. See Hestir et al. (2013) for more details.

Schoellhamer et al. (2013) present a conceptual model of the effects of increasing followed by decreasing sediment supply that includes four sequential regimes, which propagate downstream: a stationary natural regime, transient increasing sediment supply, transient decreasing sediment supply, and a stationary altered regime. The model features characteristic lines that separate the four regimes. Previous studies of the San Francisco Estuary and watershed are synthesized in the context of this conceptual model. Hydraulic mining for gold in the watershed increased sediment supply to the estuary in the late 1800s. Adjustment to decreasing sediment supply began in the watershed and upper estuary around 1900 and in the lower estuary in the 1950s. In addition to the step change in the early 1980s, large freshwater flow in the late 1990s caused a step adjustment throughout the estuary and watershed. It is likely that the estuary and watershed are still capable of adjusting but further adjustment will be as steps that occur only during greater floods than previously experienced during the adjustment period. Humans are actively managing the system to try to prevent greater floods. If this hypothesis of step changes occurring for larger flows is true, then the return interval of step changes will increase or, if humans successfully control floods in perpetuity, there will be no more step changes.

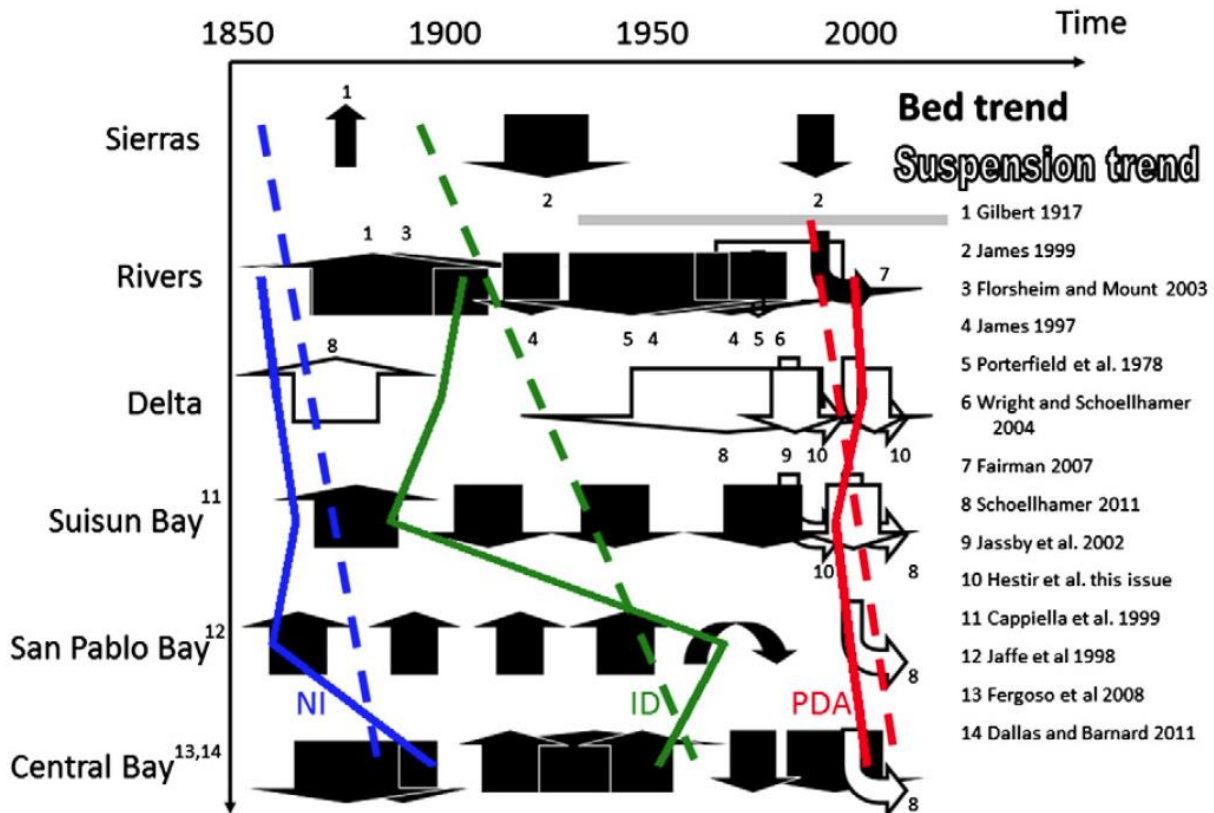


Figure 7a-2. Temporal and longitudinal summary of studies related to the hydraulic mining sediment pulse and subsequent adjustment and characteristic lines. Up and down arrows indicate increasing and decreasing trends, not magnitudes. Other arrows indicate peaks and step changes. Solid arrows are for bed elevation data, empty arrows for water column data (suspended sediment concentration or discharge). The width of the arrows indicates the time period over which the observation was made. The gray horizontal line between Sierras and Rivers in the 20th century indicates our assumption that dam construction halted sediment transport from the Sierras to the rivers. Straight dashed lines approximate the natural to increasing supply (NI, blue) characteristic line, increasing to decreasing supply (ID, green) characteristic line, and possible decreasing to altered equilibrium (PDA, red) characteristic line if a stationary adjusted regime was reached at the end of the 20th century. Solid lines are the same characteristic lines from the quantitative conceptual model. See Schoellhamer et al. (2013) for details.

In a recent study, Moftakhari et al. (in revision) recovered historic archival records and used a rating curve approach to propose the first instrumental estimate of daily delta inflow (1849 – 1929) and historic sediment loads to San Francisco Bay, to provide a better understanding of the changes in the inputs and related adjustments. The total

sediment load is constrained using bathymetric survey data to produce continuous daily sediment transport estimates for 1849 to 1955, the time period prior to sediment load measurements. We estimate that 58+7% of the sediment delivered to the estuary between 1850 and 2011 was the result of anthropogenic alteration in the watershed that increased sediment supply. The timing of sediment flux events has shifted over time because significant spring-melt floods have decreased, causing estimated springtime transport (April 1st to June 30th) to decrease from ~25% to ~15% of the total. By contrast, wintertime sediment loads (December 1st to March 31st) have increased from ~70% to ~80%. An approximately 25% reduction of annual flow since the 19th century along with decreased sediment supply has resulted in a ~60% reduction in annual sediment delivery.

Management implications

El Nino conditions in 1983 and in the late 1990s created the largest flows observed in the Sacramento Valley during the adjustment period and were the likely drivers of step adjustments (Hestir et al., 2013; Schoellhamer, 2011). Flood peaks in rivers were at channel capacity and in 1998 relatively large flows that persisted into the dry season greatly increased seaward sediment transport in the estuary (Ganju and Schoellhamer, 2006). In addition, McKee et al. (2013) found that sediment supply from local tributaries that drain directly to San Francisco Bay experienced a step decrease around 1999.

We hypothesize that the San Francisco Estuary and Watershed have not achieved a stationary adjusted regime and are still capable of adjusting but the adjustment has become a series of steps that occur only during greater floods. Smaller floods with a magnitude that has occurred during the adjustment period are capable of mobilizing only relatively small amounts of sediment. Larger flows that have not previously occurred during the adjustment period remain capable of transporting relatively large quantities of sediment and causing a step change in system variables. These large flows cause simultaneous adjustment throughout the watershed and estuary which creates vertical characteristic lines in our conceptual model.

Human efforts to reduce flood flows in the Sacramento Valley currently suppress the large flows that are capable of causing adjustment. The large flows in the late 1900s were at the upper limit of what the Sacramento Valley flood control system is designed to allow. Thus, humans are actively managing the system to try to prevent larger flows. If flood control is successful in perpetuity, there would be no more adjustment and a stationary adjusted regime would be attained. Porter et al. (2011), however, found that a flood with a 500 year or greater return period would overwhelm the Sacramento Valley flood control system. If flood control is not successful, there will be future adjustments. In this case, the return interval of adjustment floods is likely to increase as larger and larger flows would be needed to cause adjustment.

When the return interval of adjustment floods becomes greater than ecological response times, ecological variables will adjust to the prevalent environmental conditions as if a stationary adjusted regime exists. For example, consider the simple case of a tidal marsh in an estuary with a prevalent condition of 1) an inadequate sediment supply rate to maintain elevation relative to rising sea level and 2) episodic floods that deposit much greater quantities of sediment. The marsh survives as long as the return interval of these nourishing floods is less than the time for marsh drowning under prevalent conditions. If the nourishing floods are too infrequent, the marsh will drown between them. In the San Francisco Estuary, large flows in the late 1900s decreased subsequent suspended-sediment concentrations and some aspects of the ecosystem have adjusted to clearer waters.

In San Francisco Bay, suspended sediment limits light in the water column which limits phytoplankton growth (Cloern, 1987). Thus, a decrease in SSC would increase phytoplankton. In San Francisco Bay beginning in 1999 when SSC decreased (Schoellhamer, 2011), chlorophyll concentrations increased, and autumn blooms occurred for the first time since at least 1978 (Cloern et al., 2007). Both SSC and chlorophyll indicate that the Bay crossed a threshold and fundamentally changed in 1999. San Francisco Bay has been transformed from a low-productivity estuary to one having primary production typical of temperate-latitude estuaries. Cloern et al. (2007) also state that a shift in currents in the Pacific Ocean, improved wastewater treatment,

reduced sediment inputs, and introductions of new species may be responsible for the chlorophyll increase.

Reduced SSC may be one of several factors contributing to a collapse of several San Francisco Bay estuary fish species that occurred around 2000 (Sommer et al., 2007; Mac Nally et al., 2010). Abundance of some fish species increases in more turbid waters (Feyrer et al., 2007). The population collapse has had the most serious consequences for delta smelt which require turbid water for successful feeding and predator avoidance.

Coverage of invasive submerged aquatic vegetation (SAV) has expanded in the Delta during the latter half of the 20th century. Brazilian waterweed (*Egeria densa*) is the dominant submerged aquatic plant species in the Delta and comprises 85% of the SAV community biomass (Hestir et al., unpublished data). Decreasing turbidity and increasing water column light are likely explanatory factors for this invasion.

E. densa expanded in the Delta from the 1960s to late 1990s and reached nuisance levels in the 1990s (Jassby and Cloern, 2000). *E. densa* is an unusual plant in that it functions as an ecosystem engineer, changing the basic properties and functions of an ecosystem (Jones et al., 1994a,b). With respect to sedimentation processes, *E. densa* is capable of increasing sedimentation rates in channels and reducing turbidity and flow velocity in the water column (Champion and Tanner, 2000; Wilcox et al., 1999). These changes in the physical environment are particularly pronounced when *E. densa* grows to the top of the water column during the height of the growing season (mid-summer to fall).

The Mofstakhari et al. (in revision) time series of daily Delta outflow and sediment supply to the estuary from 1849-2011 are likely the best available estimates of these quantities for simulating historical conditions and evaluating water and sediment inputs to the Delta prior to hydraulic mining and large-scale water resources development.

Next steps

Suspended sediment has trended downward following step decreases in the Delta in 1998 and Suisun Bay in 1983 (Hestir et al., 2013). Two factors, SAV and suspended-sediment regulation, may account for the decreasing trend after a step decrease. These factors may prevent establishment of a stationary altered regime or of prevalent conditions that appear stationary between adjustment floods.

SAV may be an example of an ecosystem factor that can begin to control prevalent sedimentation conditions as the return interval of adjustment floods increases. Delta TSS experienced a step decrease in 1983, no trend 1983–1998, a step decrease in 1998, and a significant decreasing trend 1998–2010 (Hestir et al., 2013). The 2000s TSS decrease may be caused by SAV trapping sediment and acting as an internal sediment sink independent of the watershed factors decreasing sediment supply. This may indicate that forcing mechanisms other than the hydraulic mining sediment pulse and subsequent adjustment to decreased supply are beginning to control sedimentation in the Delta and can be expected to increase in importance in the future. Studies of the effect of SAV on sedimentation in the Delta at the local and landscape scales are needed to determine the role SAV plays in altering the Delta ecosystem.

Another possible factor that could cause a decreasing trend of suspended sediment following a step decrease is that the step decrease shifted the system from transport to supply regulation (Hestir et al., 2013; Schoellhamer, 2011). Under transport regulation which may have been present before the observed step decreases, degradation by prevalent conditions that would have decreased the size of the erodible sediment pool would not affect the quantity of suspended sediment because of the excess supply of sediment. As the erodible sediment pool decreases and the system shifts from transport to supply regulation, degradation by prevalent conditions would decrease the erodible sediment pool that in turn would decrease suspended sediment. Continued monitoring and analysis of flow and SSC data are needed to evaluate changing sedimentation in the Delta.

The erodible pool of sediment in the Delta has decreased in recent decades and thus the erodibility of the bed has decreased. Numerical models of sediment transport are most sensitive to erosion and deposition. Long-term monitoring and analysis and tidal

cycle studies of erodibility and settling velocity, the primary deposition characteristic, would quantify future changes in erodibility and help develop more accurate numerical models for simulation pelagic habitat, effects of restoration, and effects of climate change.

References

Cappiella, K., Malzone, C., Smith, R., Jaffe, B., 1999. Sedimentation and Bathymetry Changes in Suisun Bay, 1867–1990. United States Geological Survey Open-File Report 99–563 (<http://pubs.er.usgs.gov/usgspubs/ofr/ofr99563>).

Champion, P.D., Tanner, C.C., 2000. Seasonality of macrophytes and interaction with flow in a New Zealand lowland stream. *Hydrobiologia* 441, 1–12.

Cloern, J.E., 1987. Turbidity as a control on phytoplankton biomass and productivity in estuaries. *Continental Shelf Research* 7, 1367–1381.

Cloern, J.E., Jassby, A.D., Thompson, J.K., Heib, K.A., 2007. A cold phase of the East Pacific triggers new phytoplankton blooms in San Francisco Bay. *Proceedings of the National Academy of Science* 104, 18561–18565.

Dallas, K.L., Barnard, P.L., 2011. Anthropogenic influences on shoreline and nearshore evolution in the San Francisco Bay coastal system. *Estuarine, Coastal and Shelf Science* 92, 195–204.

Fairman, D., 2007. A Gravel Budget for the Lower American River. Department of Geology, California State University, Sacramento (M.S. thesis, 158 pp. <http://www.csus.edu/indiv/h/hornert/Dave%20Fairman%20thesis%20gravel%20budget%20American%20River.pdf>).

Feyrer, F., Nobriga, M.L., Sommer, T.R., 2007. Multidecadal trends for three declining fish species: habitat patterns, and mechanisms in the San Francisco Estuary, California, USA. *Canadian Journal of Fisheries and Aquatic Sciences* 64, 723–734.

Florsheim, J.L., Mount, J.F., 2003. Changes in lowland floodplain sedimentation processes: predisturbance to post-rehabilitation, Cosumnes River, CA. *Geomorphology* 56, 305–323.

Fregoso, T.A., Foxgrover, A.C., Jaffe, B.E., 2008. Sediment deposition, erosion, and bathymetric change in central San Francisco Bay: 1855–1979. US Geological Survey Open-File Report 2008-1312 (41 p. <http://pubs.usgs.gov/of/2008/1312/>).

Ganju, N.K., Schoellhamer, D.H., 2006. Annual sediment flux estimates in a tidal strait using surrogate measurements. *Estuarine, Coastal and Shelf Science* 69, 165–178.

Gilbert, G.K., 1917. Hydraulic mining debris in the Sierra Nevada. U.S. Geological Survey Professional Paper 105. (<http://pubs.usgs.gov/pp/0105/report.pdf>).

Hestir, E.L., Schoellhamer, D.H., Morgan, T.L., and Ustin, S.L., 2013. A step decrease in sediment concentration in a highly modified tidal river delta following the 1983 El Niño floods: *Marine Geology*, v. 345, p. 304-313.

Jaffe, B.E., Smith, R.E., Torresan, L.Z., 1998. Sedimentation and bathymetric change in San Pablo Bay, 1856–1983. US Geological Survey Open-File Report 98-759 (<http://pubs.er.usgs.gov/usgspubs/ofr/ofr98759>).

James, A., 1997. Channel incision on the lower American River, California, from streamflow gage records. *Water Resources Research* 33(3), 485–490.

James, A., 1999. Time and the persistence of alluvium: river engineering, fluvial geomorphology, and mining sediment in California. *Geomorphology* 31, 265–290.

Jassby, A.D., Cloern, J.E., 2000. Organic matter sources and rehabilitation of the Sacramento–San Joaquin Delta (California, USA). *Aquatic Conservation: Marine and Freshwater Ecosystems* 10, 323–352.

Jassby, A.D., Cloern, J.E., Cole, B.E., 2002. Annual primary production: patterns and mechanisms of change in a nutrient-rich tidal ecosystem. *Limnology and Oceanography* 47(3), 698–712.

Jones, C.G., Lawton, J.H., Shachak, M., 1994a. Organisms as ecosystem engineers. *Oikos* 69, 373–386.

Jones, C.G., Lawton, J.H., Shachak, M., 1994b. Positive and negative effects of organisms as physical ecosystem engineers. *Ecology* 78, 1946–1957.

Mac Nally, R., Thomson, J.R., Kimmerer, W.J., Feyrer, F., Newman, K.B., Sih, A., Bennett, W.A., Brown, L., Fleishman, E., Culberson, S.D., Castillo, G., 2010. Analysis of pelagic species decline in the upper San Francisco Estuary using multivariate autoregressive modeling (MAR). *Ecological Applications* 20, 1417–1430.

McKee, L.J., Lewicki, M., Schoellhamer, D.H., Ganju, N.K., 2013. Comparison of sediment supply to San Francisco Bay from Coastal and Sierra Nevada watersheds. *Marine Geology* 345, 47–62

Moftakhari, H.R., Jay, D.A., Talke, S.A., and Schoellhamer, D.H., submitted, Estimation of historic flows and sediment loads to San Francisco Bay, 1849-2011: *Journal of Hydrology*.

Morgan-King, T.L., and Schoellhamer, D.H., in prep., Trend in sediment supply from the Sacramento River and implications for future supply: journal article

Porter, K., Wein, A., Alpers, C., Baez, A., Barnard, P., Carter, J., Corsi, A., Costner, J., Cox, D., Das, T., Dettinger, M., Done, J., Eadie, C., Eymann, M., Ferris, J., Gunturi, P., Hughes, M., Jarrett, R., Johnson, L., Dam Le-Griffin, H., Mitchell, D., Morman, S., Neiman, P., Olsen, A., Perry, S., Plumlee, G., Ralph, M., Reynolds, D., Rose, A., Schaefer, K., Serakos, J., Siembieda, W., Stock, J., Strong, D., Sue Wing, I., Tang, A., Thomas, P., Topping, K., Wills, C., 2011. Overview of the ARkStorm scenario. U.S. Geological Survey Open- File Report 2010-1312 (183 pp. <http://pubs.usgs.gov/of/2010/1312/>).

Porterfield, G., Busch, R.D., Waananen, A.O., 1978. Sediment transport in the Feather River, Lake Oroville to Yuba City, California. U.S. Geological Survey Water-Resources Investigations Report 78-20 (79 pp.).

Schoellhamer, D.H., 2011. Sudden clearing of estuarine waters upon crossing the threshold from transport- to supply-regulation of sediment transport as an erodible sediment pool is depleted: San Francisco Bay, 1999. *Estuaries and Coasts* 34, 885–899.

Schoellhamer, D.H., Wright, S.A., and Drexler, J.Z., 2013, Adjustment of the San Francisco estuary and watershed to reducing sediment supply in the 20th century: *Marine Geology*, v. 345, p. 63-71.

Sommer, T., Armor, C., Baxter, R., Breuer, R., Brown, L., Chotkowski, M., Culberson, S., Feyrer, F., Gingras, M., Herbold, B., Kimmerer, W., Mueller-Solger, A., Nobriga, M., Souza, K., 2007. The collapse of pelagic fishes in the upper San Francisco estuary. *Fisheries* 32, 270–277.

Wilcox, R.J., Champion, P.D., Nagels, J.W., Croker, G.F., 1999. The influence of aquatic macrophytes on the hydraulic and physico-chemical properties of a New Zealand lowland stream. *Hydrobiologia* 416, 203–214.

Wright, S.A., Schoellhamer, D.H., 2004. Trends in the Sediment Yield of the Sacramento River, California, 1957–2001. *San Francisco Estuary and Watershed Science* 2(2). (<http://repositories.cdlib.org/jmie/sfews/vol2/iss2/art2>).

Task 7b: Projecting future sediment supply from the Sacramento River

Lorraine Flint, Michelle Stern, Toby Minear, Scott Wright, and Alan Flint (submitted 06-12-15)

Progress/status

The main objective of this task (7b) is to develop a spatially distributed flow and sediment transport model of the Sacramento River Basin for application to a hydrodynamic model of the Bay Delta (task 6). To help answer the overarching question of how will future changes in physical configuration and climate change affect water quality, ecosystem processes, and key species in the Delta, a watershed and sediment transport model was developed to impose future climate scenarios to determine the watershed response to climate change. Outputs from this watershed model are used as inputs to a hydrodynamic model of the Bay Delta which simulates sediment supply through the Bay Delta and has major implications regarding turbidity, geomorphic change, and wetland stability. A watershed model of the Sacramento River Basin (Figure 7b-1) was developed to simulate streamflow and suspended sediment for the period (1958-2008) using the Hydrological Simulation Program – FORTRAN (HSPF) (Bicknell et al., 2001). Extensive care was taken to compensate for sparse calibration data in this large model domain by employing spatially distributed meteorological data, and using spatially distributed properties throughout the domain to guide the calibration process.

Data used for the HSPF model include: the 2006 land use data from the National Land Cover Database (NLCD) (mrlc.gov/nlcd2006.php) (Fry et al., 2011), elevation data from the National Elevation Dataset (NED) (ned.usgs.gov/) (Gesch et al., 2009), and the hydrology and stream network from the USGS National Hydrography Dataset (NHD) (nhd.usgs.gov/) (Simley and Carswell, 2009). Extensive soils data was obtained from the Soil Survey Geographic (SSURGO) (Soil Survey Staff,

websoilsurvey.ncrs.usda.gov/) database, including erosion potential (k-factor), texture (percent sand silt and clay), hydrologic soil group, available water supply, surface texture, and geology. Time series data including meteorological station data, streamflow, snow water equivalent, and suspended sediment and sediment loads were collected for the time period 1958-2008. Station data for the meteorological development was collected from National Weather Service (NWS) Cooperative Observer Program (COOP, www.ncdc.noaa.gov/), Remote Automated Weather Stations (RAWS, www.raws.dri.edu/), and California Irrigation Management Information System (CIMIS, www.cimis.water.ca.gov/) stations within the study area. Snow calibrations compared data to the California Data Exchange Center (CDEC, cdec.water.ca.gov) snow stations.

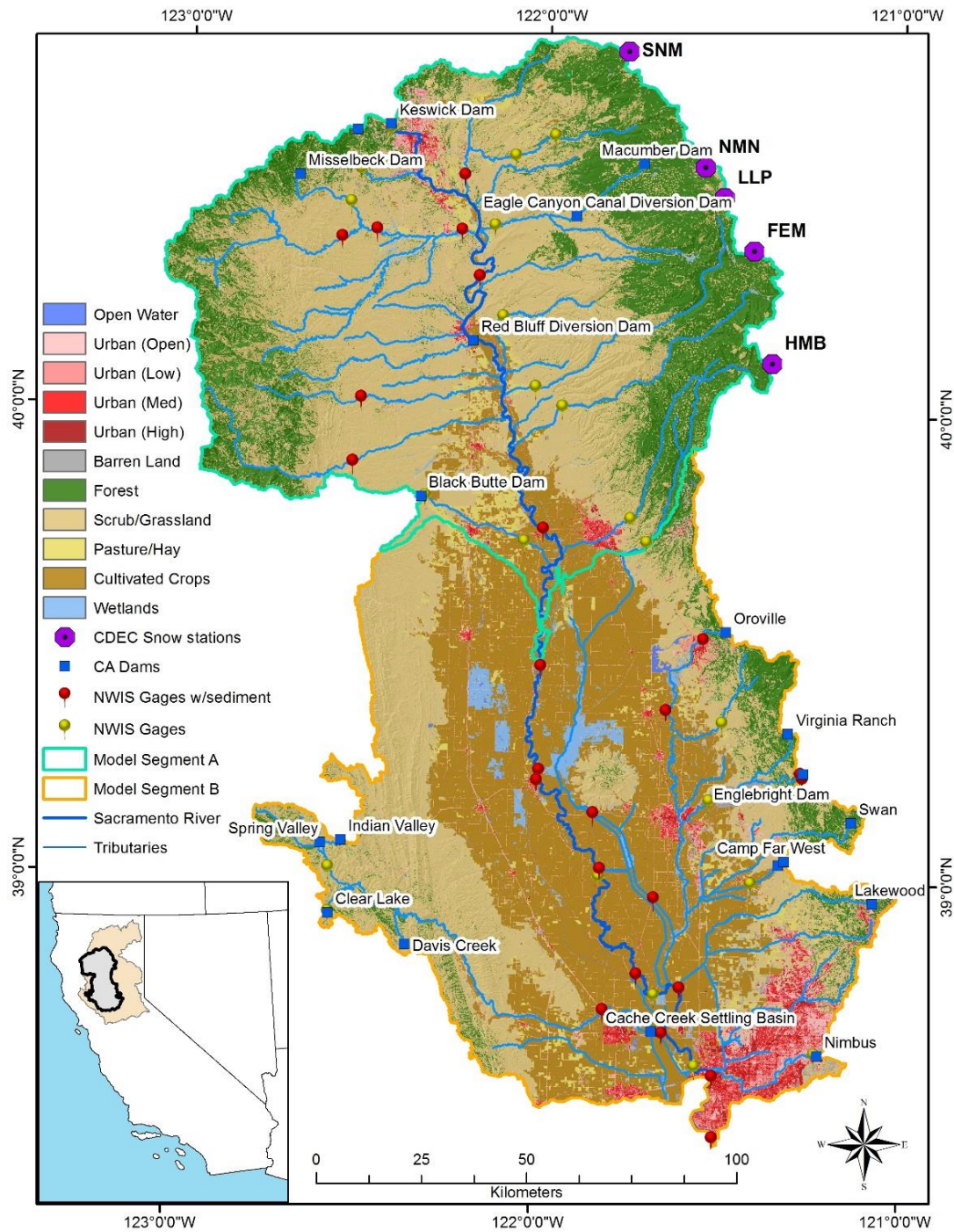


Figure 7b-1: Location map of the Sacramento River Basin model domain, CA indicating: land use, snow stations, major California dams/diversions, hydrologic and sediment gages, and the model reaches. Total drainage area of the Sacramento River is indicated (orange of inset). California Data Exchange Center (CDEC) snow stations (purple) are abbreviated as: SNM = Snow Mountain, NMN = New Manzanita Lake, LLP = Lower Lassen Peak, FEM = Feather River Meadow, HMB = Humbug.

The streamflow and sediment boundary conditions for the period of 1958 to 2008 were developed using available continuous streamflow data, locations of large dams, and natural watershed boundaries. Modeled stream reaches were chosen from the Sacramento River and the main contributing tributaries below large dams. Considering the size of the model domain, there is a limited amount of long-term data available to use for calibration. Gages with a complete hydrologic record (1958-2008) were used as boundary conditions when located on the model boundary. Other gages located within the domain were used during calibration. A series of selection criteria were developed to select dams to use as flow boundaries and that allowed negligible sediment to pass downstream. Dams used as boundary conditions in this model were chosen on the basis of trap efficiency, watershed size, and sediment yield. When continuous daily time series data was not available, the surrounding watershed above the dam was modeled.

HSPF has been shown to do a reasonable job of predicting hydrology, sediment, water quality, and pollutant loads, however the inability of meteorological stations to cover the spatial variations of precipitation and the uncertainty of managed flow data (diversions and return flows) are major limiting factors of more accurate predictions (Chen and Herr, 2002). A better representation of watershed rainfall was found to have the greatest impact on model accuracy (Fo et al., 1999). HSPF typically assigns data from meteorological stations directly to each sub-basin (Thiessen polygons). These meteorological stations are sparsely located in areas and are not all active on any given day. The objective of the meteorological development in this project is to enhance the spatial distribution of daily meteorological data and therefore increase the accuracy of modeled stream flow and suspended sediment. Incorporating gridded meteorological data as an input to HSPF has been successfully demonstrated (Nigro et al., 2010; Hayashi et al., 2004) and was shown to have increased the accuracy of the hydrologic results (Nigro et al., 2010). Precipitation is the key driver of the rainfall-runoff process in HSPF, and a more accurate spatially distributed precipitation estimate results in improved simulation results (Nigro et al., 2010).

The method used to interpolate station point data throughout the model grid is the Gradient Inverse Distance Squared (GIDS) spatial interpolation (Nalder and Wein,

1998). Spatial interpolation of meteorological data can be inaccurate when there are few stations and large distances between each station. The GIDS method provides accuracies at least as good as established kriging (another spatial statistical interpolation method) techniques without the complexity and subjectivity of kriging and the required station density (Nalder and Wein, 1998; Flint and Flint, 2012). For every active station, GIDS develops regressions for each day including the variables northing, easting, and elevation to interpolate to each 270-meter grid cell. This approach provides a detailed and localized incorporation of topographic and regional influences on precipitation.

Precipitation was summed and air temperature was averaged to transform the daily maps into monthly maps. PRISM data (Parameter-elevation Regressions on Independent Slopes Model) (prism.oregonstate.edu/) are recognized as high-quality spatial climate data sets (Daly et al., 2008) and were used for comparison to match the measured data trend and to keep the regional monthly structures intact. A ratio was developed for each grid cell using monthly PRISM values. The daily GIDS maps were multiplied by the PRISM ratio to produce daily meteorological values that sum or average to exactly match PRISM monthly values (Figure 7b-2). This method was applied to precipitation and air temperature data, and then the data was spatially distributed to each sub-basin. This method is an improvement to the typical distribution of meteorological stations because the measured data trend is preserved and the regional monthly structures are incorporated spatially.

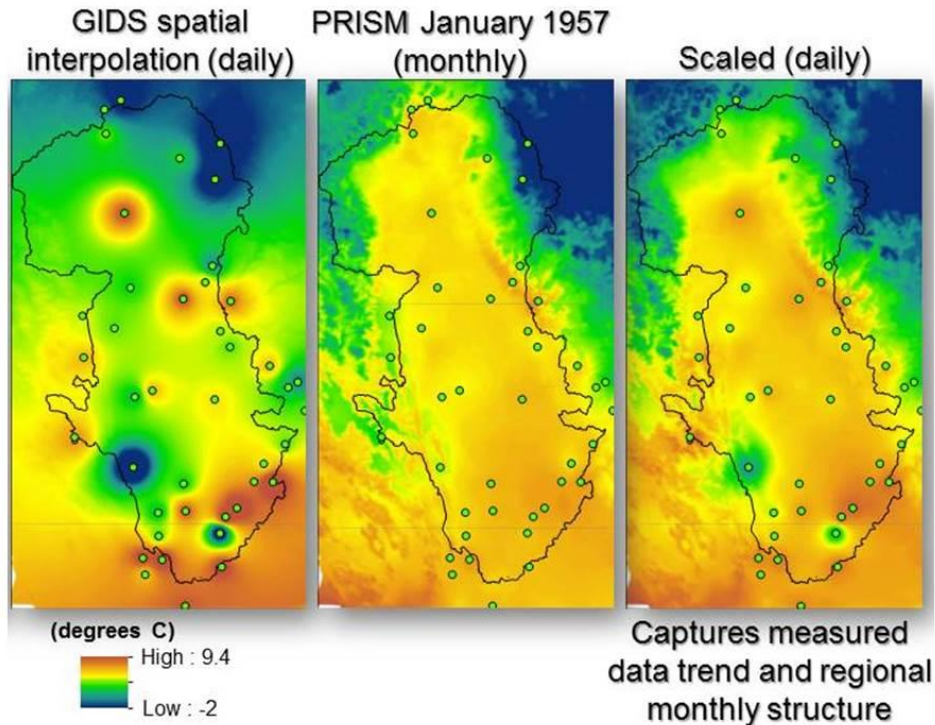


Figure 7b-2: Meteorological development (Minimum air temperature) for January 12, 1957 (42 active stations out of 78) using the GIDS interpolation and PRISM data.

Potential evapotranspiration (PET) is important because it drives the water balance equation in the model. PET can be calculated directly by HSPF or pre-processed and applied as a daily time series for each sub basin. For this project, PET was calculated using the Priestley-Taylor equation (Priestley and Taylor, 1972) based on hourly solar radiation, topographic shading, atmospheric parameters, and cloudiness. The PET estimates using the Priestley-Taylor equation were calibrated to all CIMIS stations in California and then distributed daily to each sub-basin. This process is different and an improvement over internal HSPF calculations that use pan evaporation measurements with an adjustment factor or other temperature based equations. It more accurately reflects local conditions and matches projected future PET estimates. Other formulas that use a linear relationship of PET to air temperature severely overestimate future potential evapotranspiration (Milly and Dunne, 2011). . The Priestley-Taylor equation is temperature based but employs a non-linear relationship of PET to temperature that is far more accurate when extrapolating PET into the future. Many hydrologic models

employ empirical formulas, frequently use air temperature as a key input, and do not consider the energy balance in the computation of PET (Milly and Dunne, 2011).

Basins were delineated using a small watershed file containing 8-digit USGS Hydrologic Unit Codes (HUC-8) (NHD), where adjacent HUC-8's with similar soil and hydrologic characteristics were combined or split up. The outermost watershed boundary was delineated by the aforementioned major dams, complete gage records, or natural watershed boundaries. The National Land Use Cover Database (NLCD) 2006 land use data was used to calculate the proportion of each model segment that corresponded to each land use type. NLCD land use from 2006 (mrlc.gov/nlcd2006.php) was simplified from 15 to eight categories to decrease the total number of modeled land segments. HSPF uses a hydraulic function table (FTABLE) to represent the geometric and hydraulic properties of stream reaches and reservoirs (Bicknell, et al., 2001). FTABLEs were developed to characterize the volume-dependent discharge from a stream based on stage, surface area, volume and discharge. It is essential to develop FTABLEs that accurately reflect the major hydrological processes and water quality constituents like sediment in order to ensure a realistic and unique simulation of the Sacramento River Basin. To enable a better simulation of suspended sediment, FTABLEs were developed using hydraulic geometry.

Hydrologic parameters for each sub basin were initially determined in BASINS, or Better Assessment Science Integrating point and Non-point Sources, which is a multipurpose environmental system that integrates GIS, watershed data and modeling tools.

Parameters were based on spatial layers of physical properties such as land use, erosion potential (k-factor), soil texture, slope, and hydrologic soil group. BASINS was used to generate a text-based user control input (UCI) file that was modified in a text editor to use gridded meteorological data, diversions, and to send files to WDMUtility (a program included in the BASINS package that is used to manage input and output time series and to convert text files to binary format). The calibration approach for this study was intended to maintain spatial relationships of physical properties used to estimate hydrologic parameters across the domain in order to compensate for sparse calibration data. This requires spatially distributed values corresponding to physical properties that

can be scaled up or down during the calibration process yet still preserve the spatial characteristics of each sub basin. Each hydrologic parameter was initially assessed using the BASINS Technical Note 6: Estimating Hydrology and Hydraulic Parameters for HSPF (USEPA, 2000), with subsequent adjustments during the calibration process.

The model calibration was completed in segments due to the complexity and size of the study area. Outputs from the northern domain (Segment A, Figure 7b-1) were used as inputs to the southern half (Segment B, Figure 7b-1) of the model. The hydrologic calibration of the model was an iterative process where the main calibration parameters were adjusted while maintaining their spatial distribution. Because of the limited calibration data, the goal of this calibration approach was to maintain a consistent spatial distribution of the parameters that corresponded to mapped properties and provided a logical and consistent calibration across the entire landscape. During calibration, qualitative comparisons were performed using hydrographs, followed by statistical analyses (Table 7b-1).

Table 7b-1: Daily calibration statistics from the seven gages used in model segment A. Values in bold are located on the Sacramento River. cfs = cubic feet per second. *Model performance is based on guidelines from Donigian, 2002.

1958-2008							
Model reach number	Name	Correlation coefficient	Coefficient of determination (R ²)	Mean error (cfs)	Mean error (percent)	Model fit efficiency (NSE)	Model performance*
1	Cow C. Millville	0.77	0.60	79.6	-33.3	0.56	Poor
18	Cottonwood	0.87	0.75	653.7	-36.1	0.47	Good
22	Sac R Red Bluff	0.97	0.94	1,043.8	-8.1	0.92	Very good
27	Deer C Nr Vina	0.78	0.61	132.9	-19.3	0.53	Fair
31	Mill Creek	0.76	0.57	-37.8	44.6	0.56	Poor
46	Butte C Chico	0.87	0.76	-8.8	10.7	0.75	Good
49	Sac R Butte City	0.96	0.92	-1,281.5	-9.0	0.91	Very good
Calibration: 1998-2008							
Model reach number	Name	Correlation coefficient	Coefficient of determination (R ²)	Mean error (cfs)	Mean error (percent)	Model fit efficiency (NSE)	Model performance*
1	Cow C. Millville	0.76	0.57	52.3	-19.0	0.53	Poor
18	Cottonwood	0.84	0.70	528.5	-18.2	0.54	Good
22	Sac R Red Bluff	0.96	0.92	811.4	-5.9	0.92	Very good
27	Deer C Nr Vina	0.80	0.64	144.2	9.3	0.46	Fair
31	Mill Creek	0.78	0.61	-40.6	100.9	0.59	Fair
46	Butte C Chico	0.88	0.77	-2.8	63.7	0.77	Good
49	Sac R Butte City	0.95	0.91	-1,306.2	-11.0	0.90	Very good
Validation: 1980-1995							
Model reach number	Name	Correlation coefficient	Coefficient of determination (R ²)	Mean error (cfs)	Mean error (percent)	Model fit efficiency (NSE)	Model performance*
1	Cow C. Millville	0.81	0.65	74.2	-36.3	0.60	Fair
18	Cottonwood	0.86	0.74	617.9	-37.7	0.57	Good
22	Sac R Red Bluff	0.97	0.94	1,047.9	-9.2	0.93	Very good
27	Deer C Nr Vina	0.80	0.64	145.5	-15.5	0.56	Fair
31	Mill Creek	0.78	0.62	-21.2	51.2	0.60	Fair
46	Butte C Chico	0.90	0.81	5.2	5.4	0.80	Very good
49	Sac R Butte City	0.97	0.93	-1,480.6	-11.1	0.92	Very good

Visual comparisons were completed using hydrographs of modeled and observed (gage) data for the calibration (1998-2008) and validation (1980-1995) time periods. Overall the baseflows were closely matched on the Sacramento River; some peaks were modeled well and others underestimated the observed data.

The hydrologic calibration results showed a range of model accuracy for tributaries but calibration and validation of the Sacramento River ranged from “good” to “very good” performance (Table 1) based on published HSPF statistical guidelines (Donigian, 2001). The average daily and monthly flow R² values for the Sacramento River were 0.93 and 0.98, respectively. Sediment calibration resulted in a wide range of accuracy depending on location, although the model calibration to measured sediment loads were underestimated on average by 39% for the Sacramento River, and model calibration to suspended sediment concentrations were underestimated on average by 22% for the Sacramento River (Figure 7b-3).

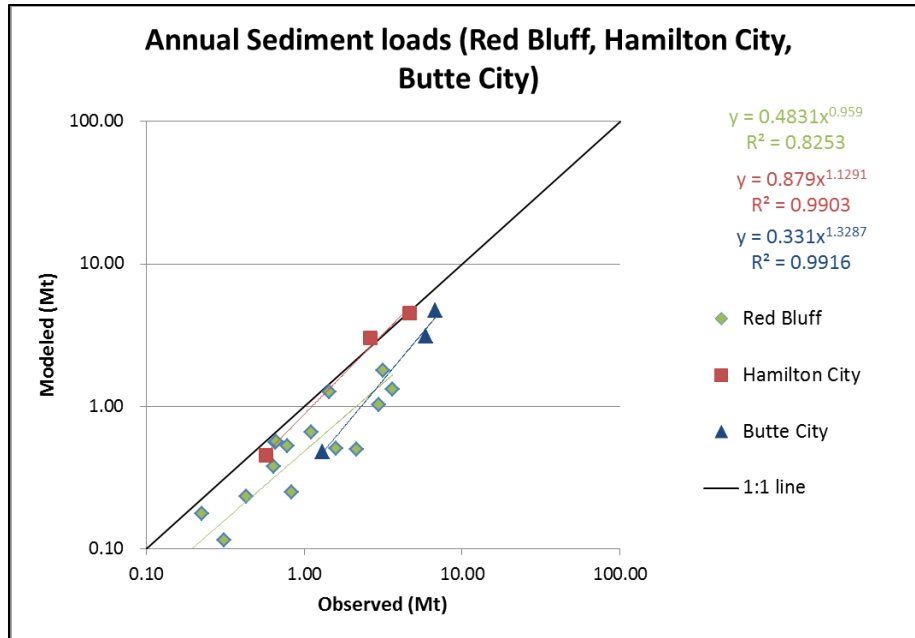


Figure 7b-3: Comparison of modeled and observed annual sediment loads (million metric tons, Mt) for gage locations of Sacramento River at Red Bluff, Hamilton City, and Butte City.

Results/findings

Sediment supply has decreased by half during the second half of the 20th century, observed in the sediment record at Sacramento River at Freeport (USGS gage 11447650) (Wright and Schoellhamer, 2004). The HSPF simulated historical annual flows at Sacramento River at Butte City gage (>160 km upstream from Freeport, southernmost point of model segment A) were separated into two flow regimes: upper and lower 50% of annual flows with corresponding annual sediment loads in million metric tons (Mt, Figure 7b-4). There was a slight decreasing trend in sediment loads ($p < 0.0025$) shown in the lower 50% flow regime.

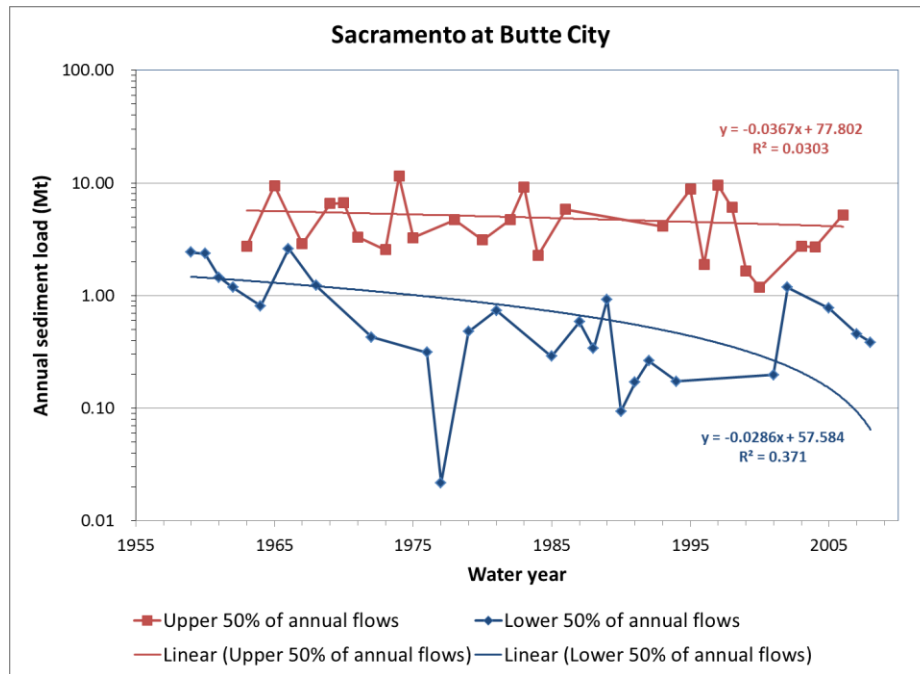


Figure 7b-4: Annual suspended sediment loads (Mt) for the upper 50% (red) and lower 50% (blue) of annual flow at Sacramento River at Butte City (end of model segment A).

These findings are important because the origin and main driving mechanism of the decrease in sediment supply to the delta are not fully known, yet the watershed model was able to replicate the trend in observed sediment data over 160 km upstream of the long-term gage. The modeled decline in sediment transport over the last 50 years was shown to be independent of any streamflow trend. Since the model area is downstream of all major impoundments in the watershed, the decline in sediment could likely be due at least partially to diminishing sediment supply from the foothills and the armoring of river channels below dams.

To further explore the results of this study without access to the climate scenarios, a preliminary sensitivity analysis was done using the Climate Assessment Tool (CAT). The CAT program allows a user to adjust temperature and precipitation to determine the watershed response. Several “wet” and “dry” hypothetical scenarios were imposed on the model base conditions and were chosen to emulate the consensus of simulations of air temperature and precipitation change for northern California over the next hundred years (Cayan et al., 2008). The Sacramento River at Butte City was most sensitive to a

moderate increase in temperature (1.5 degrees C) coupled with a 10% increase of storm volume and frequency. Increases in streamflow and mean sediment outflow of 17.5% and 93%, respectively, were seen in the wet and warm scenario, whereas decreases in both sediment and streamflow were seen in all of the dry scenarios.

Management implications

The results from the climate change sensitivity exercise revealed that the base hydrology was most sensitive to a moderate increase of 1.5 degrees and a 10% increase of storm intensity and frequency. This emphasizes the importance of not just the magnitude of precipitation change, but the timing and variability of the precipitation change in the future. Intense storms will generate an increased amount of runoff and consequently less recharge. More runoff will generate more flooding, and coupled with temperature increases can cause earlier melting of the snow and therefore create larger magnitude floods than previously experienced. The intense flooding could threaten a dated levee and flood control system which is already in need of reinforcing and repair.

The increases in flooding, runoff and sediment was partially offset by evapotranspiration in the warmest scenario, although the percent increases are similar in both scenarios that generate increases of precipitation in the form of storm intensity and frequency. Snowpack losses are projected to increase through the next century (Cayan et al., 2008), which will decrease snow pack accumulation and likely cause a shift in the hydrologic timing: snow will melt earlier in spring leaving less water during the summer months. The shift in hydrologic timing will cause problems for water managers who need to keep water in the reservoir as long as possible. Northern California is depends on spring snowmelt to fill the reservoirs and to sustain the entire state through the long dry season. Modeled sediment outflow was more sensitive to changes in climate than streamflow and runoff. The HSPF runs which include future climate scenarios will give managers an idea of how sediment supply could change in the next 100 years.

Next steps

Hydrologic calibration of model segment B is complete, sediment calibrations are nearly complete, and 20 future climate projections (10 models and 2 representative

concentration pathways) will be run through the HSPF model. Hydrologic inflows to the HSPF model (Task 3) are required for the future runs using the LOcalized Constructed Analogues (LOCA; Pierce et al., 2014) statistical downscaling approach for Global Climate Model projections. Future climate projections will be run and compared to the historical simulated values for each projection. Two journal articles are in preparation to be completed once the future climate/flow and sediment runs are finished. One article is focused on the model methodology and calibration, the other highlights the climate change results for future projected sediment transport. Draft manuscripts are planned for the end of 2015.

References

- Bicknell, B., Imhoff, J., Kittle, J., Donigian, A., & Johanson, R. (2001). Hydrologic Simulation Program - FORTRAN, user's manual for Version 12. 845.
- Cayan, D., Maurer, E., Dettinger, M., Tyree, M., & Hayhoe, K. (2008). Climate change scenarios for the California region. *Climatic Change*, 87, S21-S42.
- Chen, C., & Herr, J. (2002). Comparison of BASINS and WARMF models: Mica Creek Watershed. Palo Alto, CA and Research Triangle Park, NC: EPRI and NCASI.
- Daly, C., Halbleib, M., Smith, J., Gibson, W., Doggett, M., Taylor, G., et al. (2008). Physiographically-sensitive mapping of temperature and precipitation across the conterminous United States. *International Journal of Climatology*, 28, 2031-2064.
- Donigian, A. J. (2001). Watershed model calibration and validation: the HSPF experience. *Proceedings of the Water Environment Federation*. 30, pp. 44-73. National TMDL Science and Policy.
- Fo, A., Crawford, K., & Stensrud, D. (1999). Mesoscale precipitation fields Part II: hydrometeorologic modeling. *Journal of Applied Meteorology*, 38, 102-125.
- Gesch, D., Evans, G., Mauck, J., Hutchinson, J., & Carswell, W. (2009). The national map - elevation. U.S. Geological Survey Fact Sheet, 4.
- Hayashi, S., Murakami, S., Watanabe, M., & Bao-Hua, X. (2004). HSPF simulation of runoff and sediment loads in the Upper Changjiang River Basin, China. *Journal of Environmental Engineering*, 130(7), 801-815.

- Milly, P., & Dunne, K. (2011). On the hydrologic adjustment of climate-model projections: the potential pitfall of potential evapotranspiration. *Earth Interactions*, 15, 1-14.
- Nalder, I., & Wein, R. (1998). Spatial interpolation of climatic normals: test of a new method in the Canadian boreal forest. *Agricultural and Forest Meteorology*, 92, 211-225.
- Nigro, J., Toll, D., Partington, E., Ni-Meister, W., Lee, S., Guzierrez-Magness, A., et al. (2010). NASA-modified precipitation products to improve USEPA nonpoint source water quality modeling for the Chesapeake Bay. *Journal of Environmental Quality*, 39, 1388-1401.
- Pierce, D.W., Cayan, D.R., and Thrasher, B.L. (2014). Improved Statistical Downscaling using Localized Constructed Analogs (LOCA). [draft]
- Priestley, C., & Taylor, R. (1972). On the assessment of surface heat flux and evaporation using large-scale parameters. *Monthly Weather Review*, 100, 81-92.
- Simley, J., & Carswell, W. J. (2009). *The National Map - Hydrography*. 3054, 4.
- U.S. Environmental Protection Agency. (2000). Estimating hydrology and hydraulic parameters for HSPF: EPA BASINS Technical Note 6. Office of Water 4305, 32.
- Wright, S., & Schoellhamer, D. (2004). Trends in the sediment yield of the Sacramento River, California, 1957-2001. *San Francisco Estuary and Watershed Science*, 2(2).

Task 7c: Delta marsh sustainability

Judith Drexler and Kathleen Swanson (submitted 06-12-15)

Progress/Status

Task 7c has been completed and a paper has been published in *San Francisco Estuary and Watershed Science* on the results (Swanson et al. 2015).

Results/Findings

The purpose of task 7c was to address marsh sustainability in the context of future changes in climate in the Sacramento-San Joaquin Delta. A marsh was deemed sustainable if its elevation remained above mean low low water (~50 cm below mean sea level) through to 2100 CE. We used a one-dimensional marsh surface elevation model, the Wetland Accretion Rate Model of Ecosystem Resilience (WARMER), to explore the conditions that lead to sustainable tidal freshwater marshes. A sensitivity analysis of 450 simulations was conducted encompassing a range of porosity values, initial marsh plain elevations, organic and inorganic matter accumulation rates, and sea-level rise rates.

Our WARMER runs provided important information about marsh sustainability in the Delta. First of all, the most sensitive inputs to the model were sea-level rise and sediment. In fact, the interplay between these two inputs was especially important. More than 84% of the scenarios resulted in sustainable marshes with 88 cm of SLR by 2100. However, if SLR was increased to 133 cm and 179 cm, only 32% and 11%, respectively, of the scenarios resulted in sustainable marshes by 2100. Marshes situated in high-energy zones were marginally more resilient than those in low-energy zones because of their higher inorganic sediment supply. Overall, what we learned is that marshes at the upstream reaches of the Delta as well as high energy marshes will be more resilient to sea-level rise greater than 88 cm by 2100 than their downstream and low-energy counterparts. We also learned that in order to have greater certainty in marsh sustainability modeling, we need to constrain future rates of above- and belowground productivity under increased CO₂ concentration and increased flooding.

Currently, data are simply not available for dominant plant species in the Delta under these conditions.

Management implications

The Delta is a region in which there is substantial interest in wetland restoration by state agencies. Wetland restoration requires a huge outlay of resources both for planning, conducting the restoration, and post-restoration monitoring. In order for wetland restoration to be successful managers and scientists need to understand the energy environment in which restoration will take place and whether or not the sediment regime can support a wetland into the future. These are difficult factors to determine, however, our modeling showed that the rate of sea-level rise and sediment supply are crucial in determining whether or not a wetland can withstand the future pressures of climate change. Our data will help managers see that restoration in the upper reaches of the Delta and along main channels will likely lead to better long-term outcomes for restoration than in areas which will have greater flooding and lower sediment supply.

Next steps

Ultimately what is needed is to link marsh sustainability modeling to the hydrodynamics model being developed as part of CASCaDE II. Specifically what is needed is to bring in potential changes in salinity to the modeling of marsh sustainability. Managers and scientists who are planning restorations in the Estuary need a way to anticipate the future salinity as well as sediment supply and sea-level in order to better understand whether or not the types of wetland they seek to restore will actually be sustainable through time. For example, if managers are seeking to establish a slightly brackish marsh, which will provide important habitat for sensitive fish species, they need to know (1) whether that marsh will still be there in 50-100 years and (2) whether or not that salinity range may change dramatically within that time frame.

Another improvement would be to explore using other marsh sustainability models, such as MEM, which also incorporate changes in carbon storage through time (including estimating methane fluxes).

References

Swanson, K. M., J. Z. Drexler, C. C. Fuller, D. H. Schoellhamer. 2015. Modeling tidal freshwater marsh sustainability in the Sacramento-San Joaquin Delta under a broad suite of potential future scenarios. *San Francisco Estuary & Watershed Science* **13**(1). <https://escholarship.org/uc/item/9h8197nt>

Task 8: Contaminant biodynamics

Robin Stewart (submitted 11-15-15)

Background

Contaminants such as selenium (Se) have the potential to impede restoration of key fish species and the food webs that support them. The fate and impacts of contaminants in the SF Bay-Delta depends on a number of interlinked processes including: 1) physical transport; 2) biogeochemical transformation/degradation/biotransformation; 3) uptake into phytoplankton and/or partitioning onto particles, and; 3) physiological uptake and elimination by higher organisms. Biodynamic models have been developed for Se that have helped evaluate these processes and identify those that are most influential in controlling bioaccumulation in organisms in general. Yet, efforts to extend these models into dynamic estuarine environments are ongoing. For the SF Bay and Delta, identification of Se sources (local estuarine vs. riverine inputs) and key processes modulating uptake into the food web base has been confounded by limited bioaccumulation data in resident species and their food across a range of hydrodynamic and estuarine conditions. Further, sufficiently detailed computational models (hydrodynamic, sediment and phytoplankton) for quantifying complex estuarine processes at spatial and temporal scales relevant to Se biogeochemical cycling/bioaccumulation have not been available until now.

The contaminants sub-task addresses the following questions regarding the fate and effects of selenium (Se) in the Bay-Delta estuary:

- How does Se bioaccumulation vary with hydrologic conditions -- source water (Sac vs SJR), freshwater inflow and residence time?
- How does residence time alter the relative contributions of internal (refineries) vs. external (delta) sources of Se to clams?
- How will changes due to climate or delta configuration affect these relationships and what are the consequences for Se accumulation in predators?

Progress/Status

While the D3D-FM hydrodynamic model was under development during most of the project our progress focused on collecting additional field Se data including water and suspended particulates for Se model development and validation in Delwaq as well as evaluating critical processes that would be important in constructing and validating model runs and interpreting results of the model runs.

We further evaluated our existing 17-year time series of historical Se data to better understand spatial and temporal variability and how estuarine processes influence that variability. The knowledge gained from this analysis was published in 2013 (Stewart et al. 2013). This manuscript also included preliminary model runs using DELFT3D (predecessor to D3D-FM) that evaluated the distributions and patterns of Se loads from internal and riverine sources.

Availability of reliable Se data in biota and water has been limited to date. Part of the challenge is the cost and access to laboratories with the capability of running Se analysis. To address this need we developed a method for the analysis of Se in water, particulates and biota in Menlo Park. Our method utilizes isotope dilution hydride generation ICP-MS and yields highly accurate and precise measurements of small sample masses (~10 mg dry weight) with a low detection limit (0.02 µg Se/g dry weight or 0.03 µg Se/L). A draft manuscript of the method has been completed and we anticipate that the manuscript will be ready to submit to a peer-reviewed journal (Limnological Methods) within the next two months.

With the ability to analyze a large number of Se samples we continued our 17-year monthly Se time series (now 20 years) in *Potamocorbula* at 2 locations (station 4.1 near Pittsburg; station 8.1 near Carquinez Straits) and added an additional down estuary station in San Pablo Bay (station 12.5), which will be critical for model validation of sources of Se internal to the estuary (Figure 8.1). We also added the analysis of water and particulate at these stations where clams are collected to better link to model output for Se load distributions. All sample Se analyses of clams have been completed

through June of 2015 and water through February 2015. These data will be made available to the scientific community by the end of 2015 via an online data sharing.



Figure 8.1: Locations of selenium sampling locations in Northern San Francisco Bay for our long-term time series and drought study. Long-term time series stations – 12.5, 8.1, and 4.1. Drought study – 2.1, SACOL6, SACOL10, SACOL13, SR101b, SR104b, Hydro657, SR104, SJOL7-8, SJOL10 and SJOL14.

We received supplemental drought funding from the USGS in 2014 to collect additional samples of both invasive clams (*Potamocorbula amurensis* and *Corbicula fluminea*) to evaluate distributions of clams and Se exposures under changing salinities during the drought (Figure 8.1). These data expand upon earlier coincident sample collections of both species at station 2.1 near Chain Island. Sample analyses of the additional drought sites have been completed for *Potamocorbula* and *Corbicula*. These data will be utilized in future evaluations of drought scenarios and their impact on Se exposures. Preliminary results for this study were presented in a poster at the Bay-Delta Science conference in October 2014 (Kleckner et al. 2014).

With the newly developed method for Se analyses we took the opportunity to analyze additional samples of *Corbicula* collected coincident with *Potamocorbula*. The value of these measurements are to identify critical differences in processes of how these two different invasive bivalves respond to changes in food and Se exposures at different salinities such as those experienced during drought conditions. Predators utilize these clams differently and thus changes in their distributions could have implications for

exposures. We anticipate utilizing these data in evaluating the impact of future scenarios on Se exposures of Bay-Delta predators.

Results/Findings

Our manuscript combines a 17-year time series and preliminary results of a hydrodynamic 3D model (precursor to D3D-FM) to identify the biological and

physiochemical processes controlling selenium (Se)

bioaccumulation in *Potamocorbula amurensis* in San Francisco Bay. In

particular, we demonstrated that riverine inflows provide

a powerful modulating force on the source driven level of Se contamination (near Carquinez Strait), driving bioavailable concentrations up and down as inflows change seasonally and year to year (Figure 8.2).

Our preliminary model runs using DELFT3D illustrated that Se loading mid-estuary near Carquinez Strait is detected both down and up estuary as far as Chipp's Island. The model also indicated that during high flow (Sacramento River = $3200 \text{ m}^3 \text{ m}^{-\text{s}}$, San Joaquin River flow = $800 \text{ m}^3 \text{ m}^{-\text{s}}$), considerably less tracer Se would be accumulated at Stns

Figure 8.3: Relative Se tracer concentrations ($\mu\text{g l}^{-1}$) in mid-water near Stns 4.1, 8.1 and 12.5 following a 2 month simulation (Delft3D) of Se transport in northern San Francisco Bay under low-flow conditions (Sacramento River = $150 \text{ m}^3/\text{s}$, San Joaquin River = $50 \text{ m}^3/\text{s}$). Simulation specifies conservative transport of Se tracers and Se loading from 5 local area refineries.

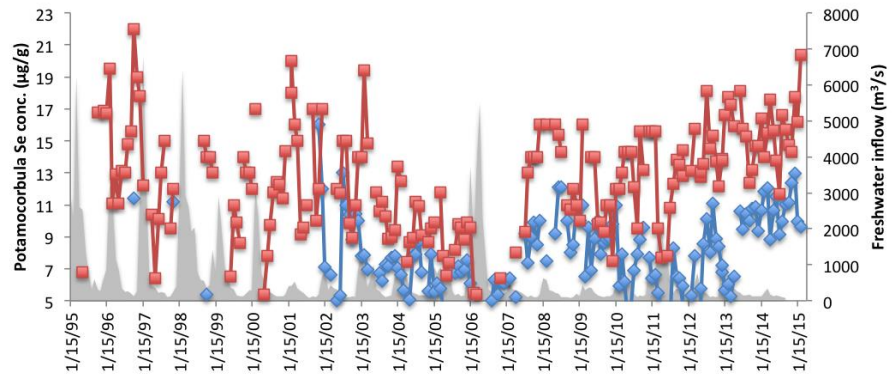
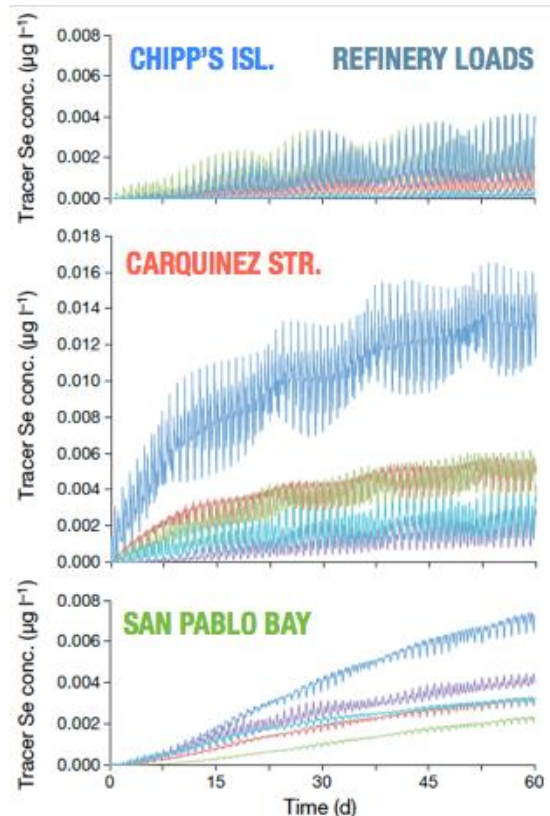


*Figure 8.2: Monthly selenium concentrations in *Potamocorbula amurensis* from 1995 through 2015 in the San Francisco Estuary plotted against freshwater inflow. Station 8.1 – red squares; Station 4.1*



8.1 or 12.5, and no refinery tracer Se is detected up-estuary at Stn 4.1 (data not shown). A 60 d simulation cannot assess the ultimate accumulation of Se concentrations in this system, but it does suggest that it is feasible that the relative distribution of Se among stations, as observed in the clams, could be explained by dispersion from a single source of input near Stn 8.1. Future model runs will re-evaluate distributions under different climate and management scenarios (Figure 8.3).

Our most recent results through 2015, which include drought conditions, indicate that Se concentrations in the clams are increasing to the highest levels recorded over the course of the 20-year history, and are remaining elevated throughout the entire year. In fact, a significant finding from this dataset is that selenium exposures are more linked to freshwater inflow than season (Figure 8.4). Spring Se concentrations in the clams, long thought to be low, are now equivalent to or higher than observed fall concentrations.

We anticipate that, as with earlier analyses of the time series, the elevated Se concentrations in the spring will be linked to lower freshwater inflows compared to earlier years. It is unclear without evaluation using the D3D-FM-DELWAQ model if elevated concentrations in the spring are influenced by additional source contributions from the rivers or by changes in residence time. These are specific questions that will be addressed using the model in 2016.

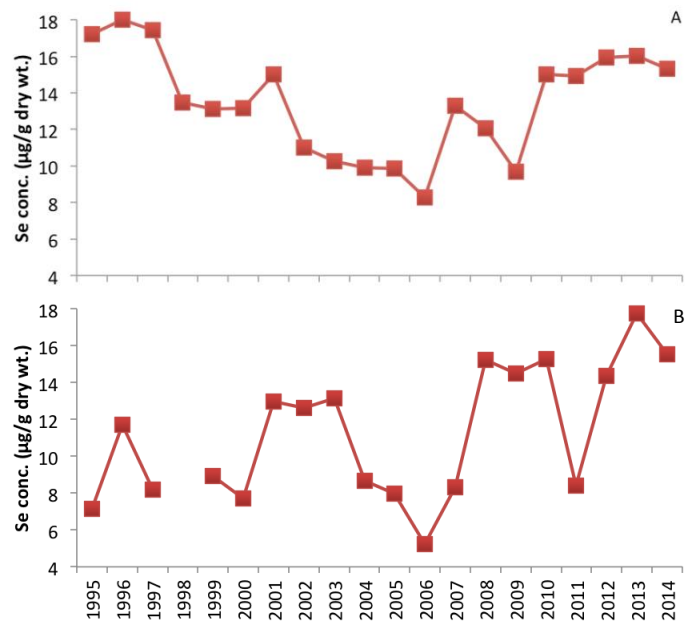


Figure 8.4: Selenium concentrations (µg/g dry wt) in *Potamocorbula amurensis* in the fall (A) and spring (B) months at Carquinez Strait (station 8.1). Fall months: September – December. Spring months: March – June.

An important question that we addressed in our drought study was if *Potamocorbula amurensis* expanded its distribution further up estuary and into the delta with increasing salinities would Se concentrations in the clams remain elevated or decline. Previous data collected for the freshwater invasive clam *Corbicula fluminea* indicated lower Se concentrations in this species in the central delta. Our drought sampling showed that as *Potamocorbula* expanded its distribution

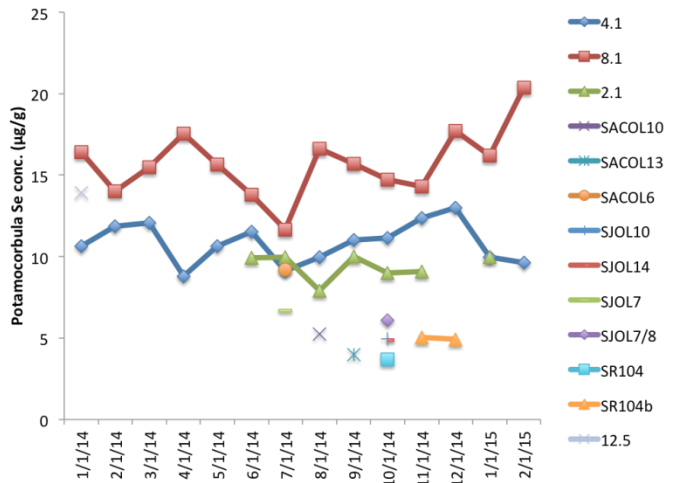
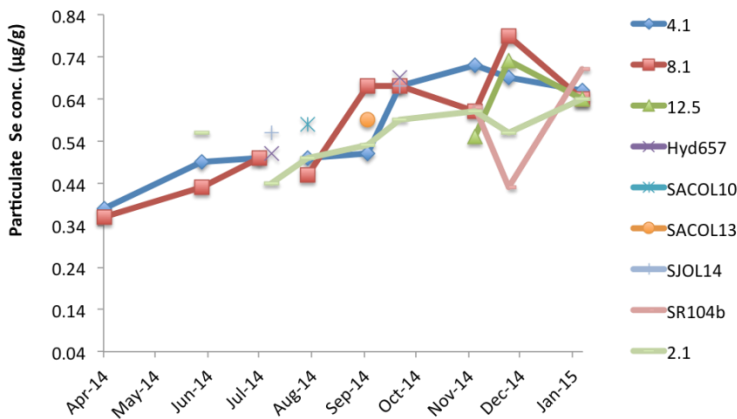
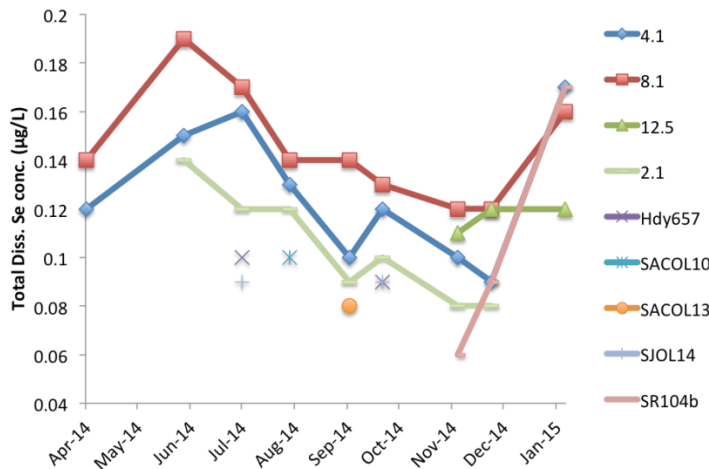


Figure 8.5: Selenium concentrations ($\mu\text{g/g}$ dry wt) in *Potamocorbula amurensis* during drought conditions in 2014. Station locations are shown in Figure 1.



up the Sacramento River toward Rio Vista and up the San Joaquin River tissue Se concentrations declined and were similar to those measured in *Corbicula fluminea* (Figure 8.5). These results suggest that the estuarine clam's physiology was not the only factor controlling Se concentrations, and that Se exposures were different between the Bay and Delta. Indeed, total dissolved Se

Figure 8.6: Total dissolved and particulate Se concentrations during drought conditions in 2014. Station locations are shown in Figure 1.

particulate, were highest in the Bay and declined towards the Delta (Figure 8.6).

Particulate Se measurements may be misleading since Se is associated predominantly with the organic fraction of the suspended particulate material which accounts for a very small mass relative to other particle types. The increase in particulate Se through time at all stations may reflect a change in the particle composition and not have a significant impact on Se exposures for the clams. For this reason it is important to track both the dissolved and particulate phases of Se to understand Se exposures in this estuary.

Management Implications

The management implications of our results thus far are broad and have been utilized by a range of groups. We have been consulted by US EPA region 9 in their development of site-specific criteria (water and fish tissue) for Se for North San Francisco Bay. Of particular interest was the range of Se concentrations observed in our historical data series of clams, which form a critical diet and pathway of exposure of Bay-Delta predators. Our drought results have yet to be released but will also be of interest to EPA. Our Se analytical method has been sought out and our lab contracted to analyze samples in support of the Regional Monitoring Program Selenium Working Group. This working group is conducting research in support of the development of a Se TMDL by the Regional Water Quality Control Board recently released for public comment (July 2015).

Next Steps

An update of our monthly Se time series initially published in 2010 (Kleckner et al. 2010) will be provided to the scientific community and accessible online by early 2016.

We anticipate engaging in model development in the fall of 2015 with the following objectives:

- Use D3D-FM hydrodynamic output from different hydrodynamic scenarios in DELWAQ to identify and evaluate distributions of dissolved Se related to sources (internal vs. external).

- Validate model results to field collected clam Se data
- Develop Se exposure/risk maps for predators under different scenarios that could be incorporated into the Habitat model.
- Begin collaborative studies to understand the influence of residence time on Se exposures in time and space.

References

Kleckner AE, Stewart AR, Elrick KA, Luoma SN (2010). Selenium concentrations and stable isotopic compositions of carbon and nitrogen in the benthic clam *Corbula amurensis* from Northern San Francisco Bay, California: May 1995–February 2010. U.S. Geological Survey Open-File Report 2010-1252, 34 p.

Stewart AR, Luoma SN, Elrick KA, Carter JL, van der Wegen M (2013) Influence of Estuarine Processes on Spatiotemporal Variation in Bioavailable Selenium. *Mar Ecol Prog Ser* 492:41-56

Task 9: Food web effects of invasive bivalves *Corbula*, *Corbicula*, and *Dreissena* spp

Jan Thompson and Francis Parchaso, in collaboration with Tineke Troost, Valesca Harezlak, Bert Jagers, Deltares (submitted 07-18-15)

The goal of this task was to develop a bivalve model that would dynamically link to the phytoplankton model and supply grazing rates to that model. Bivalve growth and phytoplankton grazing/loss rate need to be part of a feed-back loop for the carbon flow to be internally consistent. Our plans were to develop the model for *Corbicula fluminea* and *Potamocorbula amurensis* and to develop the parameters necessary to determine likely distribution patterns for *Dreissena bugensis*, and *Dreissena polymorpha*.

Progress/Status

The Biomass Based Stage-Structured Model (BBS) that we planned to use to “grow” the bivalves with input from the DELWAQ and phytoplankton models was discontinued by Delft during our first year, so we have had to change our plans. We will dynamically link the bivalve growth and grazing rate to the phytoplankton/DELWAQ model eventually using a Dynamic Energy Budget model (DEB, Kooijman 2010) (<http://www.bio.vu.nl/thb/deb/>) that is supported by Deltares. As previously planned, the DEB model will dynamically change bivalve growth and grazing rates to be internally consistent with the carbon produced by the phytoplankton. DEB models have been heavily used by European scientists since ≈2000 and its concepts have been well tested. DEB cannot run independent of the phytoplankton model because the parameters are tuned with the availability of consumable carbon so we do not yet have results from that model. As described in Next Steps below, we are looking into the use of an interim estimate of benthic grazing in the phytoplankton model. These benthic grazing rates will be based on field data and will allow us to more quickly move forward on the phytoplankton model.

We will establish the initial conditions (mostly initial distribution of each species) for the bivalve model using a Deltares public-domain spatial model, HABITAT (<https://publicwiki.deltares.nl/display/HBTHOME/Home>). This model uses Habitat

Suitability Indices (HSI) to predict distributions based on how habitat characteristics relate to a species requirements (e.g. the independent relationship of a species distribution to salinity, temperature, water depth, sediment composition etc. are analyzed concurrently to determine a species potential distribution). We have derived HSI's for *C. fluminea* and *P. amurensis* and we have summarized some published values for *Dreissena* spp. We show the derivation of the HSI's for both *C. fluminea* and *P. amurensis* and then show an example of the HABITAT program with a projected *Corbicula* distribution in the delta as a function of salinity, temperature, and depth. These indices need to be tested with field data and they will be tested against output from the hydrodynamic model for our calibration years when that is available.

Because of the delay in getting output data from the hydrodynamic (salinity, temperature and turbidity will be needed) and phytoplankton models, we leveraged our CASCADE PES funding (USGS Priority Ecosystem Science Program funds which were a match for CASCADE DSP funding) to collaborate with the Environmental Monitoring Program/California Department of Water Resources (EMP/DWR), the Bureau of Reclamation (BOR), and the Interagency Ecological Program (IEP) to analyze samples from the past to the present that have been collected as part of three studies in the EMP program in DWR. This collaboration has allowed us to further our knowledge of the distribution of both bivalves, and to use these data to create HSI's with more data than was otherwise available. Therefore our data and knowledge base on what factors control adult and larval/juvenile bivalve distribution of *C. fluminea* and *P. amurensis* have increased substantially. The added studies include: (1) A study of 170 stations sampled twice a year in May and October in the bay and delta to examine the spatial distribution of benthic species (methods described at <http://www.water.ca.gov/bdma/grts/>). We have extended the analyses of these samples to include an estimate of *Potamocorbula* and *Corbicula* biomass, recruit density, and grazing rate at all of the stations for the period 2007-2012, 2014; (2) DWR has been collecting benthic samples in the bay and delta since the late 1970's and at least one replicate of these station samples has been retained (methods described at <http://www.water.ca.gov/bdma/meta/benthic.cfm>). We collaborated with DWR to analyze these samples for bivalve biomass, recruit density, and grazing rate which is

giving us an invaluable time series for these properties for *Potamocorbula* and *Corbicula* at 13 stations in the ecosystem; and (3) As restoration plans are now concentrating on marsh or seasonally flooded habitat it has also become important that we understand this previously unsampled environment. Therefore we have again used CASCADE (PES) and BOR funding and collaborated with DWR to look at the recruitment and grazing rate of *Corbicula* in some seasonally flooded environments. These studies have been invaluable in furthering our understanding of where these bivalves thrive and where they may be limited.

We are now are looking into testing the HSI's with field data for the years that we have these spatially intensive bivalve data (2007-2012) and for which there are environmental data that can be used for the HABITAT analyses.

Finally, we have produced papers and products that have helped us understand the effect of the bivalves on this system: (1) we finalized the conceptual models for *Potamocorbula* and *Corbicula* and the *Potamocorbula* model is now on the DRERIP web site. We hope that the *Corbicula* model will follow soon; (2) J. Thompson has used this time to work with L. Lucas on a simplified phytoplankton/benthic grazing model. Work with L. Lucas and L Brown used these simplified models to explain when benthic grazing is a determinant in bloom development and when it is not (Lucas et al. 2009). (3) J. Thompson with L. Lucas continued this modeling work and developed more robust conclusions (Lucas and Thompson 2012). (4) J. Thompson worked with W. Kimmerer to examine how zooplankton grazing interacted with bivalve grazing to control the phytoplankton biomass in the northern bay (Kimmerer and Thompson 2014).

Results/Findings

HABITAT Model Indices and Findings:

The HABITAT model uses Habitat Suitability Indices (HSI) to estimate the distribution of species. These indices qualitatively describe the potential occurrence of a species by numerically describing the ability of the species to live in a specific environment. The HSI ranges from 0 (little chance a species would be found in those conditions) to 1 (a high probability that the species would occur with those conditions). When various HSI

are examined concurrently it is possible to locate areas which have the highest number and lowest number of favorable conditions and therefore to identify locations where the species are most likely and least likely to be found.

A series of curves (Figure 9-1) were produced for each bivalve for several environmental variables. Environmental data that were used are available at the DWR data website (<http://www.water.ca.gov/iep/products/data.cfm>). Bivalve data will be released within a data report by the end of this calendar year. Environmental variables were chosen because there is data available to evaluate the likelihood of species success against that variable and because they describe what is likely to be a condition that limits the distribution of the species. For example, salinity is a physiological limit for *Corbicula*, and therefore we would expect the index to be 0 at salinities over 12. However, it is possible for the index not to reflect physiological limits measured in the laboratory because other co-varying variables may be limiting the success of the species in the field.

There are a number of theories on the best way to estimate a HSI curve, but given our shortage of data for *Potamocorbula* from other locations in particular, we have chosen a conservative approach here.

As shown in Figure 9-1 we began by plotting all of the available bivalve biomass data against each environmental variable (using depth as an example here), we then converted the data to presence absence data and plotted the frequency of occurrence of the bivalve for each measurement interval of the environmental variable (e.g. in Figure 9-1, at stations which were 1.5m deep, 0.69 or 69% of the stations had *Corbicula* present in the sample). The final plot is a “smoothed” plot of the second plot which incorporates an assessment of the number of samples available for each depth increment (e.g. for the example above there were 271 samples available that were collected in 1.5m of water but only 7 samples were collected in 19.5m of water). If the number of samples in an environmental increment was small, they were combined with neighboring data and a generalized ratio was determined (e.g. the HSI at the largest depths are based on a combination of adjoining frequency data).

HSI curves were developed for *Potamocorbula* and *Corbicula*. The curves for *Corbicula* (Figure 9-2, Table 9-1) and *Potamocorbula* (Figure 9-3, Table 9-2) were based on data from the San Francisco Estuary and Delta. The indices for *Dreissena* (Table 9-3) were based on literature searches. The next step will include checking these curves against known distributions of bivalves with measured environmental parameters.

The variables found to have the most influence on the distribution of *Corbicula* and *Potamocorbula* were electrical conductivity (EC), depth, temperature, turbidity. *Potamocorbula* seemed most influenced by EC and temperature whereas *Corbicula* seemed most influenced by EC and depth. Turbidity and EC appeared to be oppositely limiting to *Corbicula* and *Potamocorbula*. The opposite relationship with EC was expected as *Potamocorbula* is an estuarine bivalve and *Corbicula* is a freshwater bivalve. The positive relationship with turbidity for *Potamocorbula* was not expected and may be accurate, or it may reflect a relationship with some other factor that is correlated with turbidity.

We have also used the HABITAT model to interpolate grazing rate data for calibration runs of the phytoplankton model. Figure 9-4 shows a map of the interpolated bivalve grazing rate that was generated from the data shown in the lower figure; the two data sets look consistent.

The mechanics of the HABITAT model is shown in a series of plots. Each plot requires interpolated environmental data and HSI curves for the species of interest. In the example here we use data from the hydrodynamic model (Task 4) to establish depths and salinity distributions (Figure 9-5) in order to look at *Corbicula*'s distribution. The third environmental variable, temperature, was based on limited field data that was interpolated within HABITAT (Figure 9-6, upper plot). The map of temperature has many fewer data points and therefore has a coarser grid resolution than the previous plots. When these three environmental variables were concurrently combined with the HSI curves for *Corbicula* the resulting distribution is produced as shown in the lower

map in Figure 9-6. In looking closely at this map we feel it is generally consistent with our experience with *Corbicula* distribution during the last 10 years.

Extending our knowledge of the spatial distribution of bivalves

The spatially intensive benthic study that is designed and executed by DWR each May and October produces a remarkable set of data that includes community composition data and counts of species. By measuring the bivalves in these samples we now have data on biomass, mean size, number of recruits ($\leq 2.5\text{mm}$), and grazing rate at each station in the study for *Potamocorbula* and *Corbicula*. Figure 9-7 and 9-8 show results of this work; grazing rate is shown for each species for a dry year (2009) and a wet year (2011). These data will be released in a data report before the end of the year. Some of our observations from looking at these data include: (1) *Potamocorbula* grazing rate is consistently low in spring and peaks in fall of all years. Seasonal patterns are less clear with *Corbicula*. We hypothesize that winter mortality/predation limit *Potamocorbula* to being an annual species in the shallow waters of the bay. (2) Grazing rate magnitude is seasonally opposite in *Potamocorbula* (fall is greater than spring) and *Corbicula* (spring is greater than fall). Recruit seasonality and food availability is the primary control on biomass distribution. Recruits are found throughout the year and peak in abundance in fall for both species. We hypothesize that biomass and therefore grazing rates reflect a higher food availability for *Corbicula* in spring of dry years, whereas *Potamocorbula* has more food in fall. (3) The two species overlap around X2 in the low salinity zone. The overlap zone was similar in location and size in spring of dry and wet years but was broader and differed in location in the dry and wet falls, possibly reflecting the management of X2 in spring by resource managers. (4) Wet years do not limit the bivalve biomass. In 2011 we were able to observe the effect of a very wet year on the distribution and biomass of *Corbicula* and *Potamocorbula* (Figure 9-8). *Corbicula* had higher biomass levels in spring and summer and *Potamocorbula* had slightly smaller biomass in both seasons but most small biomass values were in the confluence area where *Corbicula* increased in biomass and grazing rate (Figures 9-7 and 9-8). The wider distribution of *Corbicula* in the wet year is not due to a reduction in

salt water because most of this area is freshwater. The distribution may be a reflection of higher food availability with the increased flow. These data will be released in a data report before the end of the year and should be useful for modelers who want to test a scenario but don't have grazing rate data. By matching water years, they should be able to get approximate spatial distributions of benthic grazing rates.

Extending our knowledge of the long term trends in bivalve biomass

We expected to see seasonal patterns in biomass for both species of bivalve and we did observe that pattern. We had less of a feeling about long term trends which are shown as annual median biomass at stations as shown in Figure 9-10. We observed two temporal patterns in the benthic biomass data at the DWR monitoring stations (Figure 9-9). Some stations (like D4 in Figure 9-10) have shown a large increase in biomass over the study period. This was particularly true of stations in the bay that were invaded by *Potamocorbula* (Figure 9-9, stations D7, D41, D41a, and D6) and the single station in the Sacramento River (D24) which had a large increase in *Corbicula*. Other stations as shown by the D28 plot (Figure 9-10) have had a sharp decline in *Corbicula* biomass beginning in the early 2000's. This pattern was observed at D16, C9, and P8.

The recruitment data has shown us that *Corbicula* recruits are available during all seasons in this system. Although there are a few months and locations that did not have them, it will be safest to assume that they are always there. All of the monitoring station data will also be released in a data report before the end of the year.

Extending our knowledge of the distribution of bivalves in restoration sites

This was the first study to examine *Corbicula* in an ongoing and potential restoration site. The Cache Slough Complex (Figure 9-11) is likely to be fully restored with the plan that it will supply habitat for fish and that it will produce phytoplankton. Benthic grabs were collected at 93 stations and *Corbicula* were found at 72 of the stations. Biomass generally increased down bay or down river and biomass was relatively high (several stations greater than 100 g AFDW/m² and several in the 20-100 range) at the permanently flooded portion of the complex at the mouths of Cache and Lindsey Sloughs and in the southern Deepwater Ship Channel. This is consistent with the

findings of Morgan and Schoellhamer (2014) who show this area of the Cache Slough Complex to favor suspended sediment retention, which may be a proxy for pelagic food sources. Grazing rates and water column turnover rates were sufficiently high in the Toe Drain, Liberty and Prospect Islands and the Deepwater Ship Channel to reduce if not limit phytoplankton biomass. Recruits were found everywhere and were frequently found in similar numbers throughout the length of a slough.

Summary of publications

During this study we finalized the conceptual models for *Potamocorbula* and *Corbicula*. The models have recently been combined and rewritten as part of the Tidal Wetlands Monitoring Program. These models have helped define where and when monitoring of the benthic bivalves might be important.

J. Thompson has used this time to work with L. Lucas on a simplified phytoplankton/benthic grazing model. Earlier work with L. Lucas and L Brown used these simplified models to explain when benthic grazing is a determinant in bloom development and when it is not (Lucas et al. 2009). J. Thompson with L. Lucas have now extended this modeling work with more robust conclusions and analysis (Lucas and Thompson 2012). A thorough description of this paper can be found in Task 5.

A paper by W. Kimmerer and J.Thompson examines how zooplankton grazing interacted with the bivalve grazing to control the phytoplankton biomass in the northern bay (Kimmerer and Thompson 2014). We showed through a mass balance approach that included estimates of primary production and grazing by bivalves, microzooplankton, and mesozooplankton, that grazing exceeded net phytoplankton growth and that grazing by microzooplankton exceeded bivalve grazing in some seasons and locations. The mass balance approach allowed us to see that phytoplankton that is transported into the northern bay is the only way that the food web could be balanced. Most importantly for CASCADE, we concluded that “the influence of bivalve grazing on phytoplankton biomass can be understood only in the context of limits on phytoplankton growth, total grazing, and transport”.

Next Steps

We will continue our work with HABITAT and will use the large volume of bivalve biomass data that we continue to acquire from the GRTS studies to look at the validity of our HSI's with field data. If the GRTS data verify the distribution relationships of each bivalve in the important overlap zone (in and around X2), we will publish the results and the indices for others to use.

We recognize that it is important that the phytoplankton model be operational as soon as possible and we are concerned that the DEB model, not previously used in an estuary, may require some alterations. For that reason, we are now considering developing methods to set and import grazing rates into the phytoplankton model at specific time intervals. We will, at a minimum, allow for changes in distribution as a function of changing salinity and temperature and will adjust bivalve biomass to reflect food availability. This approach will at a minimum give us an initial understanding of how well the phytoplankton model is working.

Management Implications

The Lucas and Thompson (2012) and Kimmerer and Thompson (2014) papers highlight the importance of modeling grazing rates and transport if we are to understand phytoplankton growth dynamics in the estuary. Therefore we have confirmed that our modeling approach is still valid and necessary. Understanding the changing distribution of the bivalves with varying environmental conditions will be critical to the development of any model within the North Bay and Delta. Therefore approaches such as the HIS's, which are reasonably easy to use, could be important for conceptual and numerical models in the future.

Our collaborative field work in this study has taught us a few important lessons. First *Corbicula* are always available as recruits. We do not know if the recruits originate from local populations or from upstream (possibly even reservoir) populations. The ubiquitous recruits are an important observation for those who are restoring habitat with the objective being production of phytoplankton. The number of locations with baby *Corbicula* without accompanying adults is a sobering reminder that this is a species just waiting for something to change. The most obvious limiting environmental factor given

the range of habitats in which we have observed this age-skewed distribution, is likely to be food availability.

Potamocorbula recruits are to some degree available all year during dry years but are seasonally limited in wet years. Reproduction in normal years occurs in spring and fall and an animal that is released in spring is very likely to be mature enough to reproduce in fall. Adult *Potamocorbula* continue to live considerably upstream of the low salinity zone after dry years and they are able to persist at those now fresh locations through the wet season in many instances. The combination of adult reproduction and physiological plasticity in *Potamocorbula* means they will be difficult to manage with freshwater flow. If at all possible it would likely take more fresh water than we will routinely have available for such an environmental use.

Both bivalve species appear to be resource limited and to respond quickly to a change in resources; we observed rapid changes in size frequency histograms throughout the system that would indicate new food had been made available and the bivalves grew quickly in response to it.

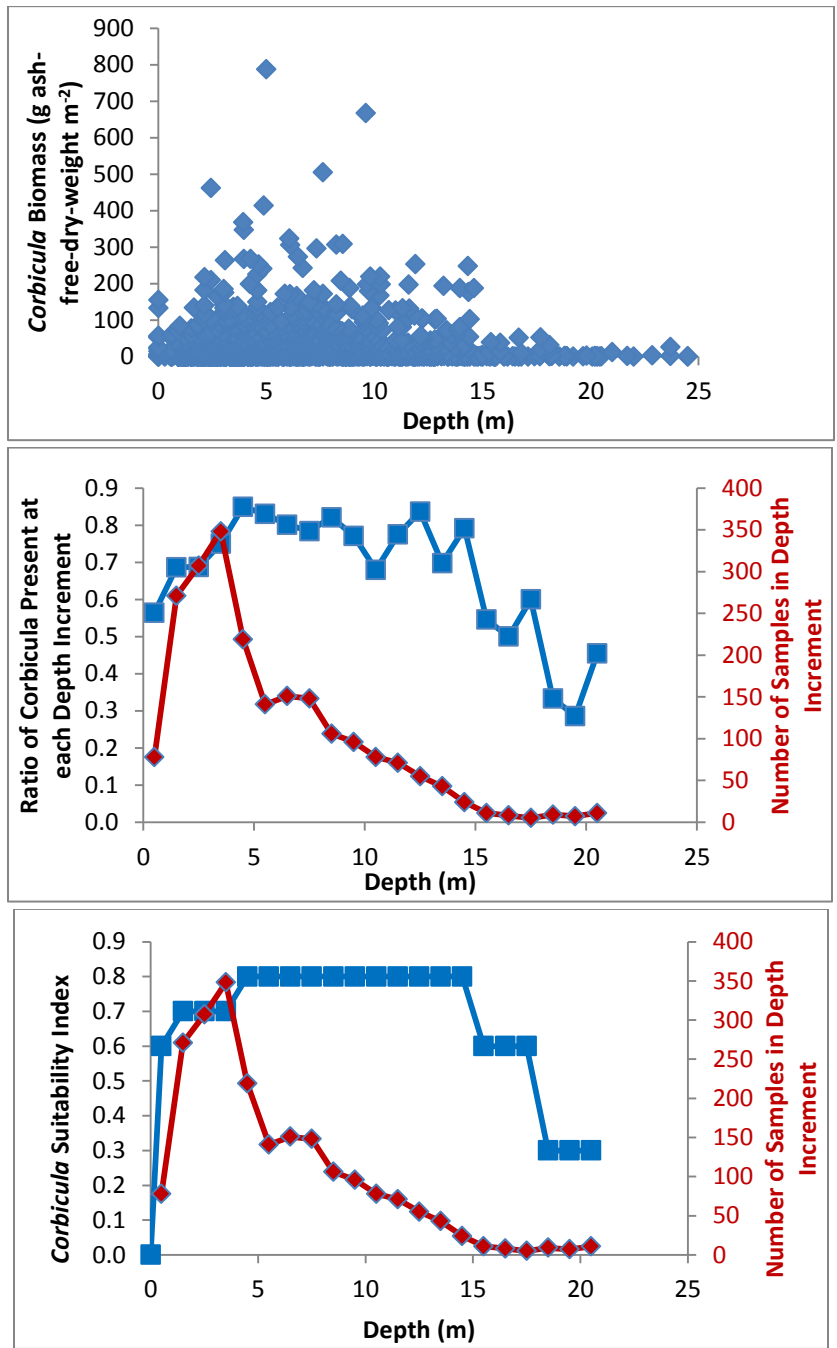


Figure 9-1. Technique for developing Habitat Suitability Indices. The first graph shows the raw biomass data plotted with water depth; the second graph shows that data converted to presence /absence and then binned by depth and plotted as the ratio of samples at that depth with *Corbicula* present; the third graph shows the resolution of the second plot to more generic distribution of values. Note the red lines show total number of samples available for each depth; these data were noted prior to the development of the third graph.

Ratio of Corbicula Present at each Environmental Parameter Increment

Number of Samples in Environmental Parameter Increment

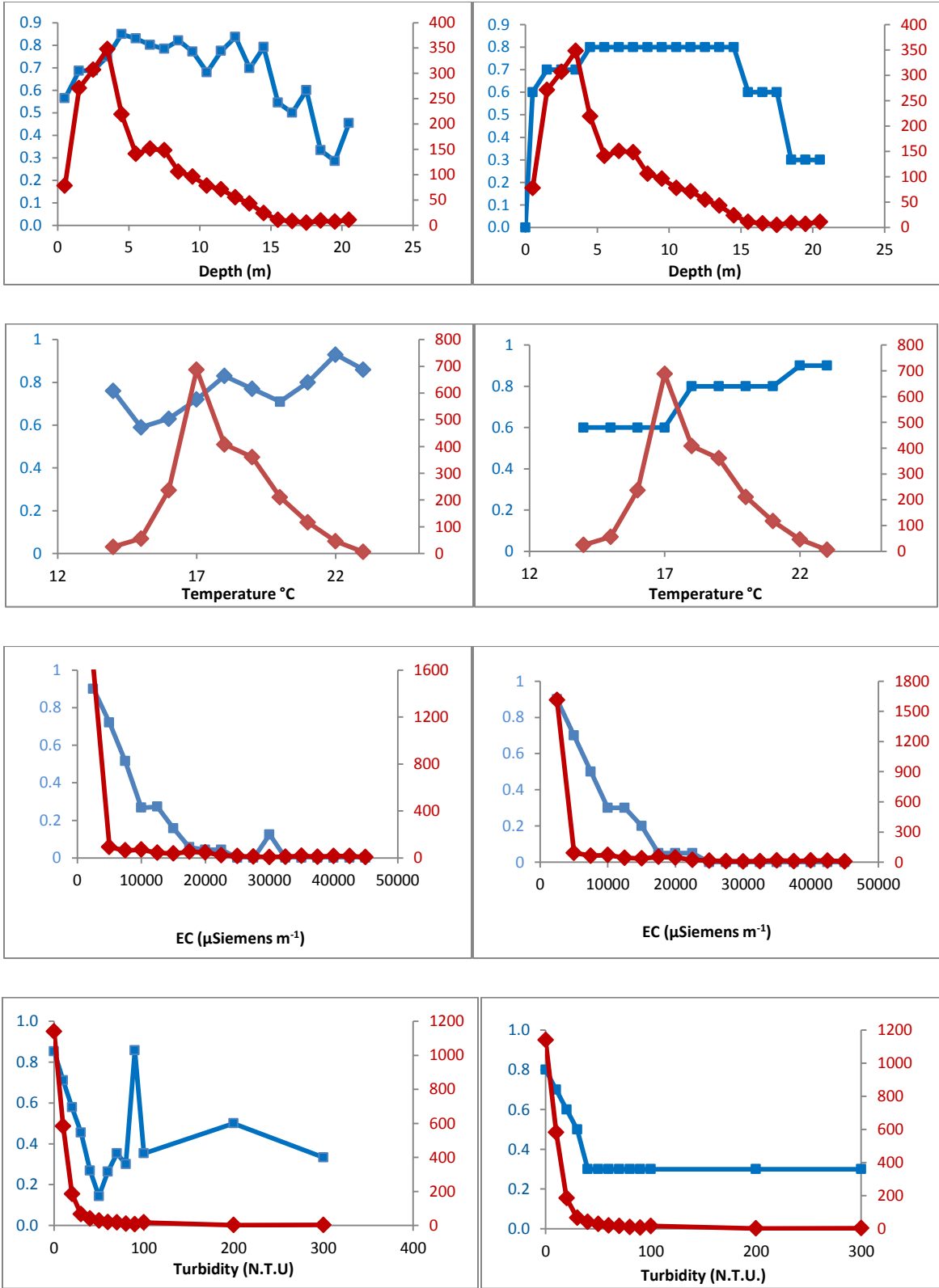
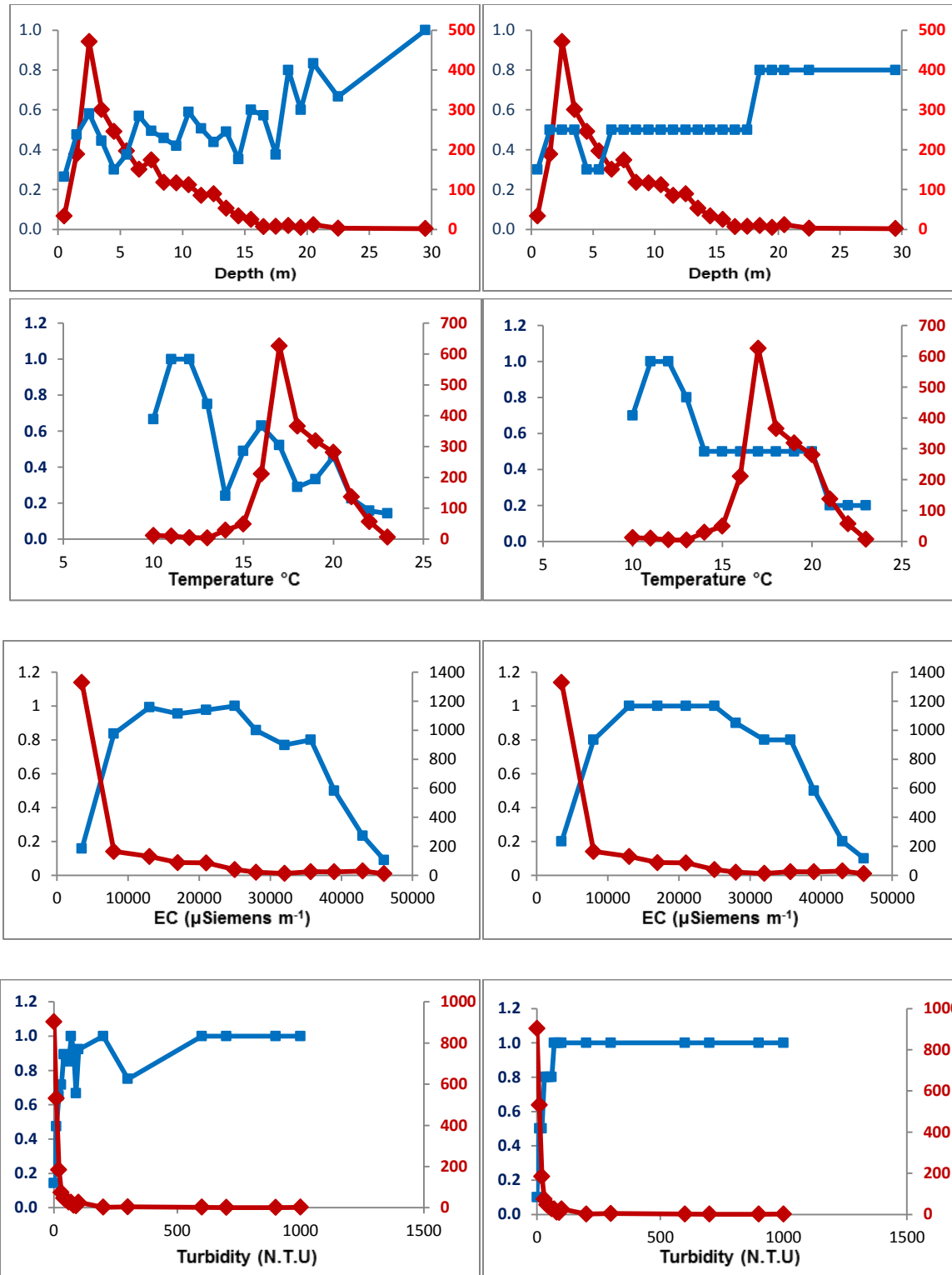


Figure 9-2. HSI curves for *Corbicula* ; left column shows frequency (ratio) of *Corbicula* occurring at each environmental increment (blue line). Right column shows smoothed line of the frequency data. Red line shows show total number of samples available for each environmental increment.

Ratio of Potamocorbula Present at each Environmental Parameter Increment



Number of Samples in Environmental Parameter Increment

Figure 9-3. HSI curves for *Potamocorbula*; left column shows frequency (ratio) of *Potamocorbula* occurring at each environmental increment (blue line). Right column shows smoothed line of the frequency data. Red line shows show total number of samples available for each environmental increment.

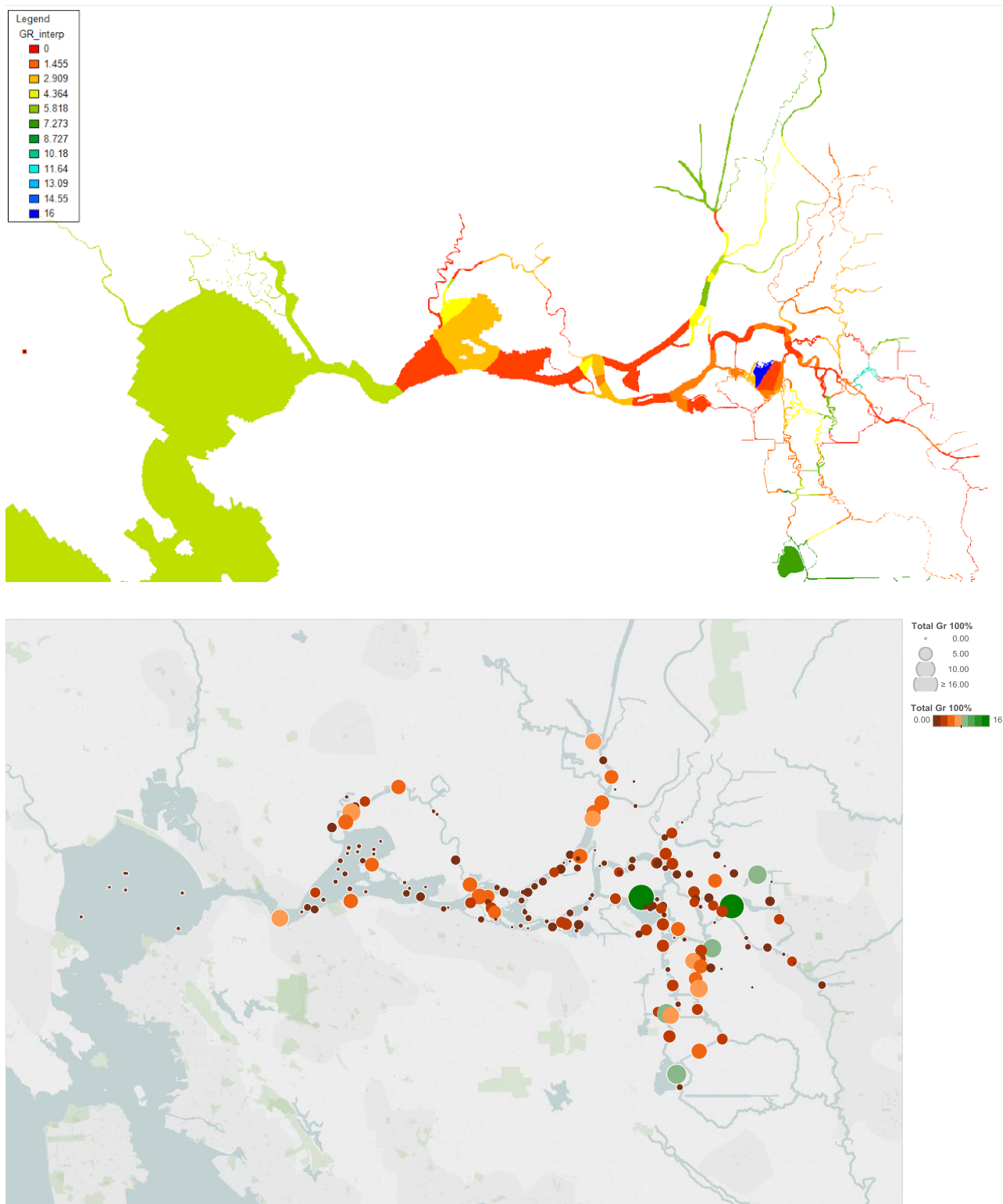


Figure 9-4. Example of HABITAT's interpolation of grazing rate data in the top map that is based on the raw data in the bottom graph. Note there is some difference in the color index for the two maps.

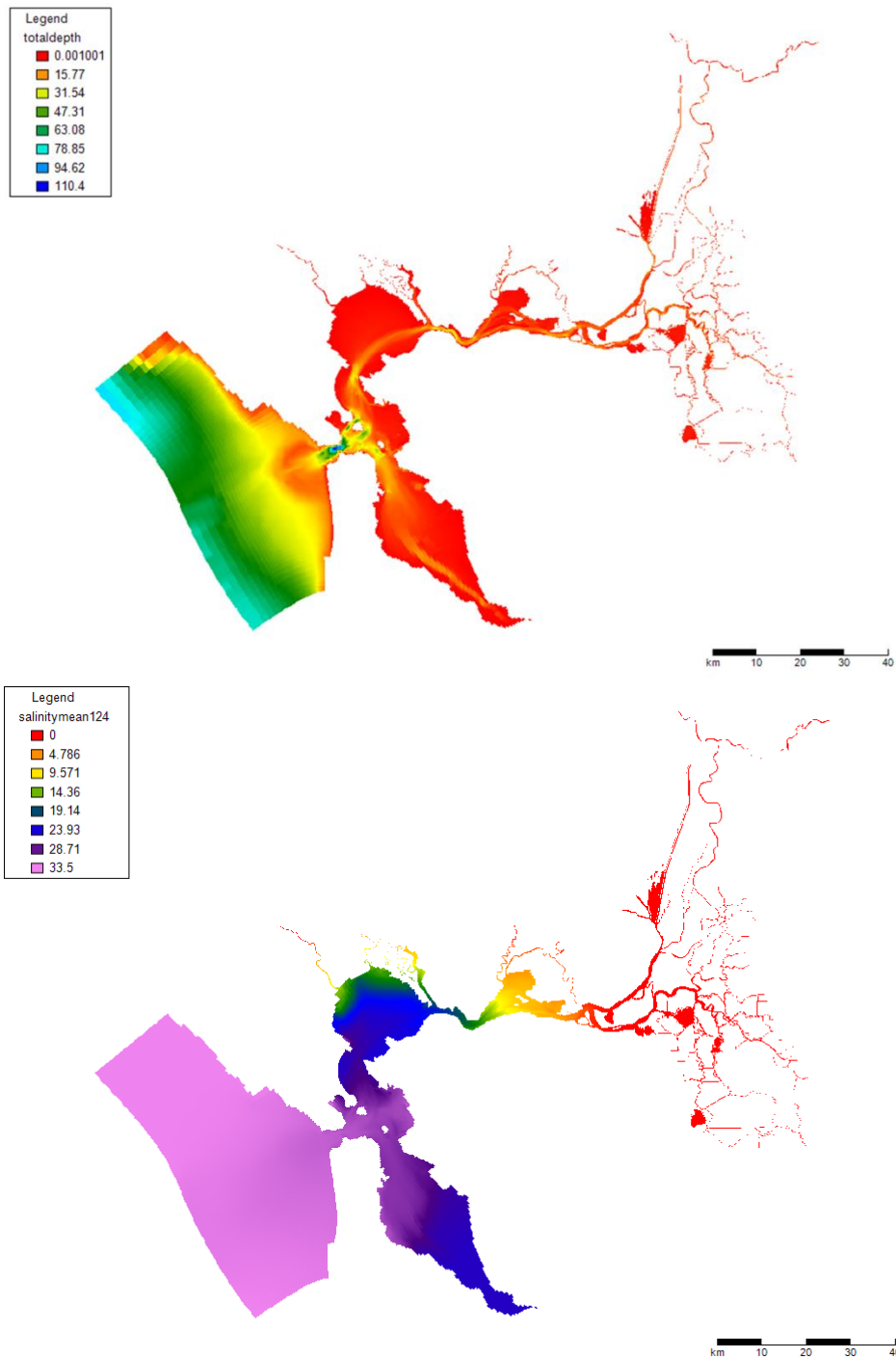


Figure 9-5. Depth and depth averaged salinity shown after HABITAT interpolated the model produced values acquired from the HYDRODYNAMIC Model.

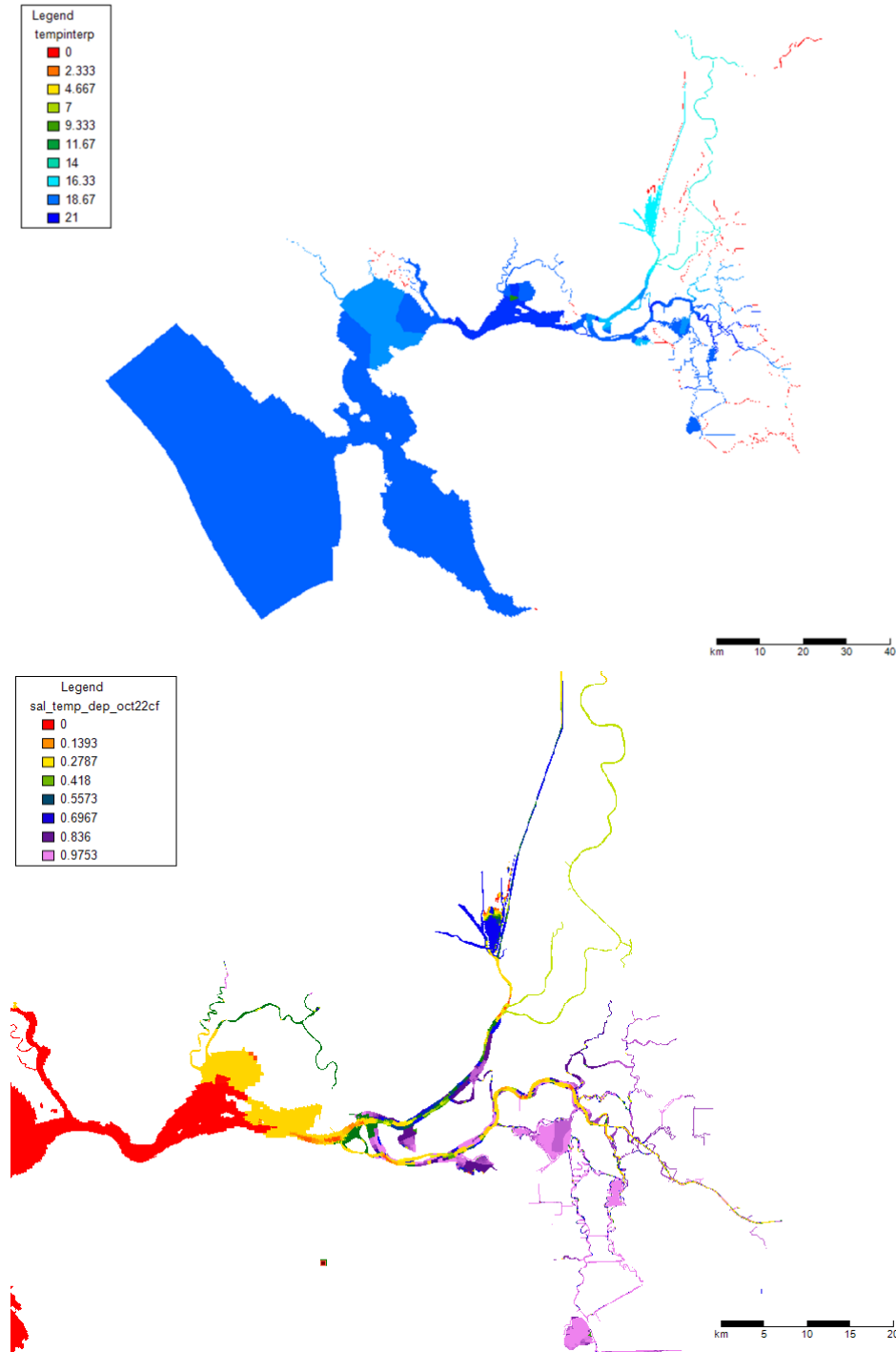


Figure 9-6. HABITAT interpolation of field temperature data. The spatial grain is much coarser than the model output shown in Figure 9-4. The bottom map is the result of HABITAT combining depth, salinity, and temperature. The distribution of *Corbicula* in this case is potentially limited in the bay (yellow and red), very common in the central and southern Delta (lavender and purple), and inconsistently distributed on the Sacramento River (blue, greens and yellow).

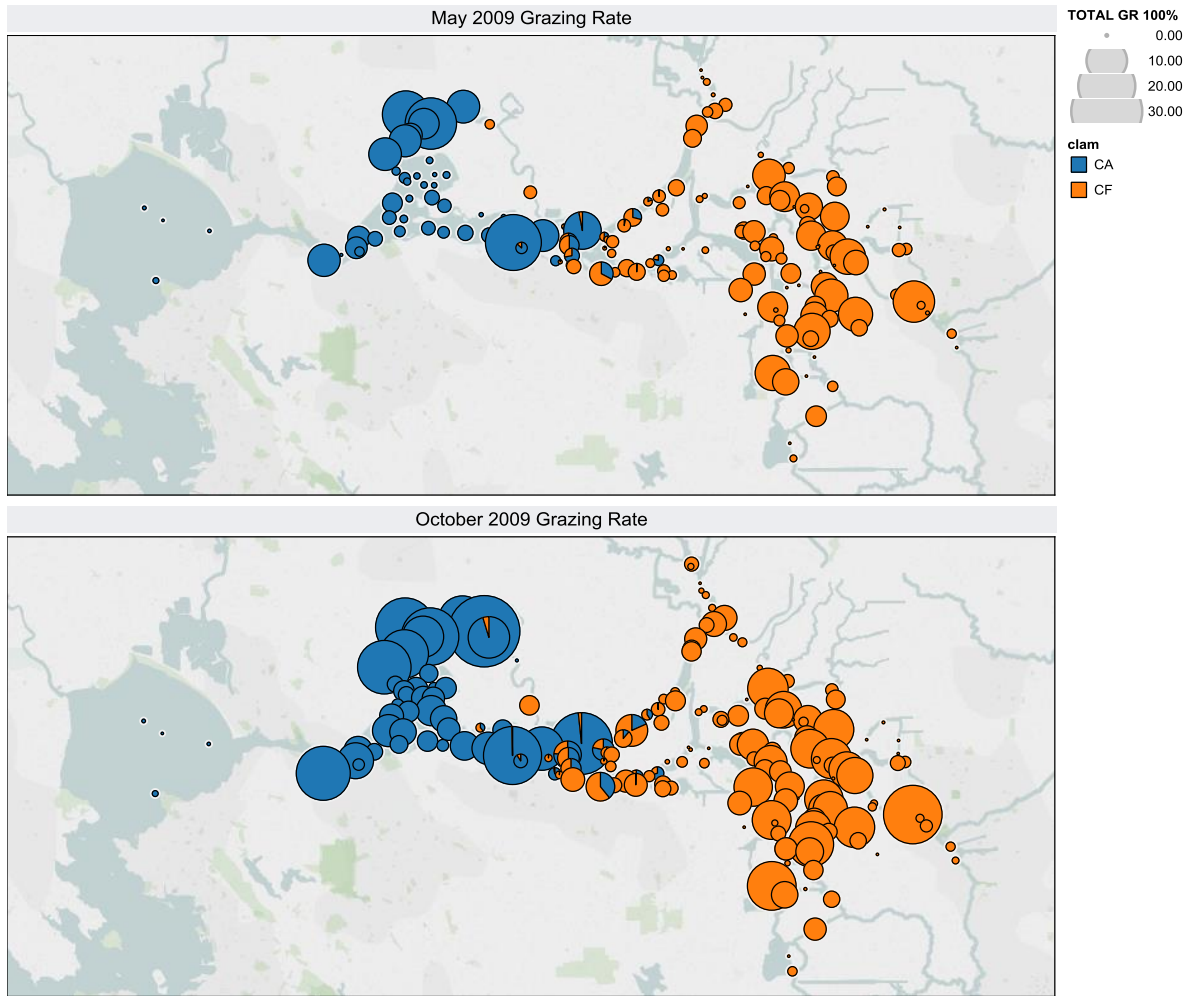


Figure 9-7. Example of grazing rate estimated in GRTS samples for a dry year (May and October 2009).

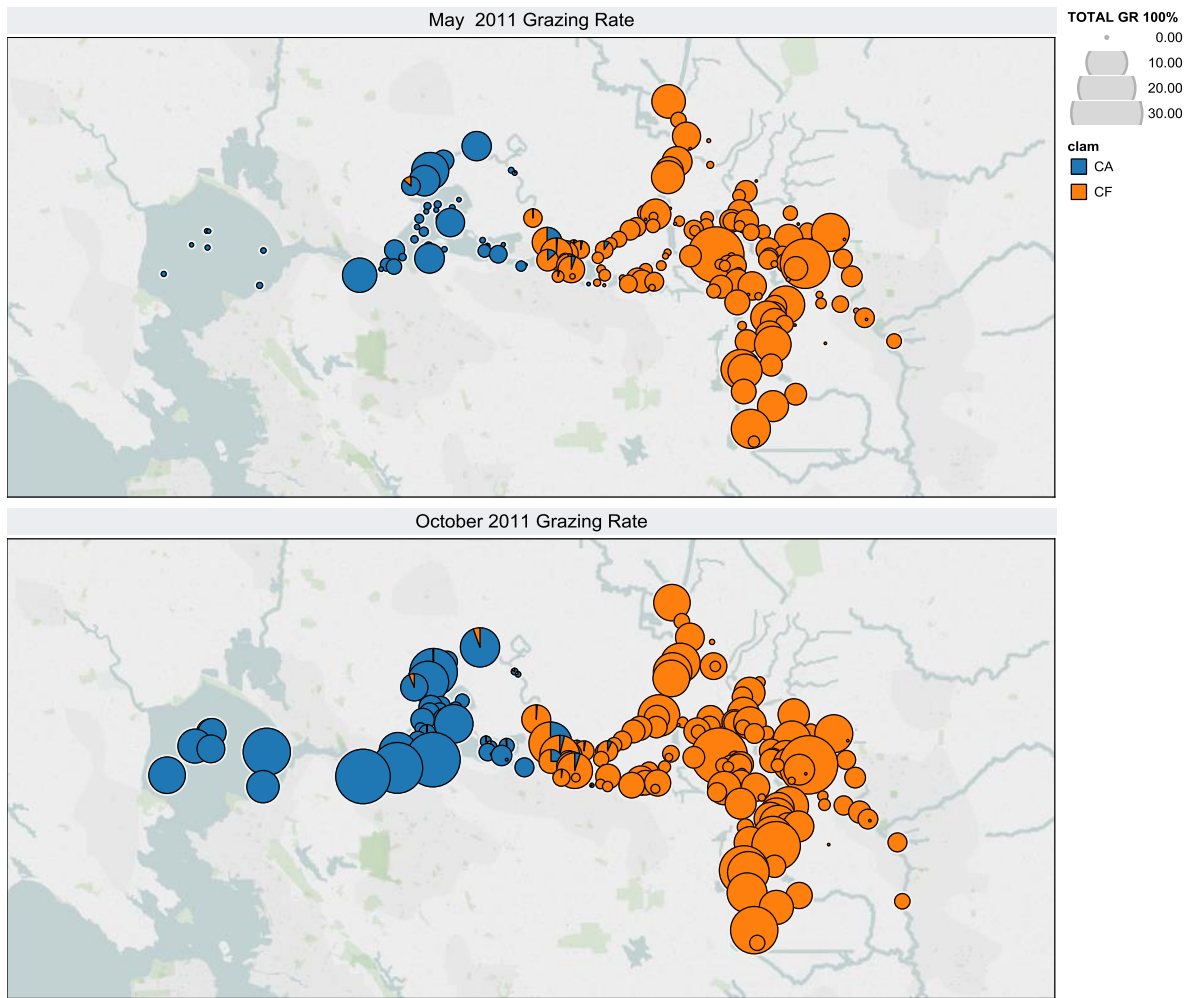
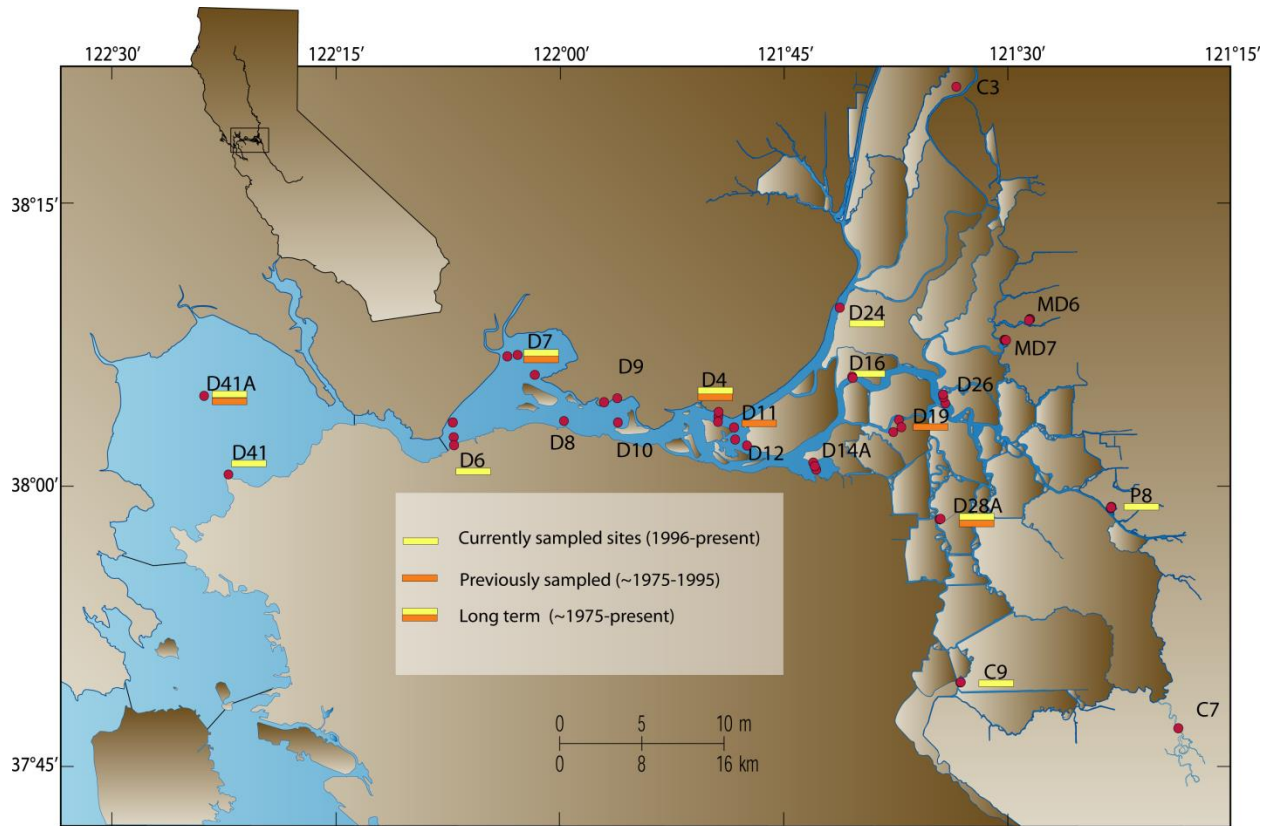


Figure 9-8. Example of grazing rate estimated in GRTS samples for a wet year (May and October 2011).



(courtesy of DWR)

Figure 9-9. DWR benthic sampling stations with period of sample collection shown for each station.

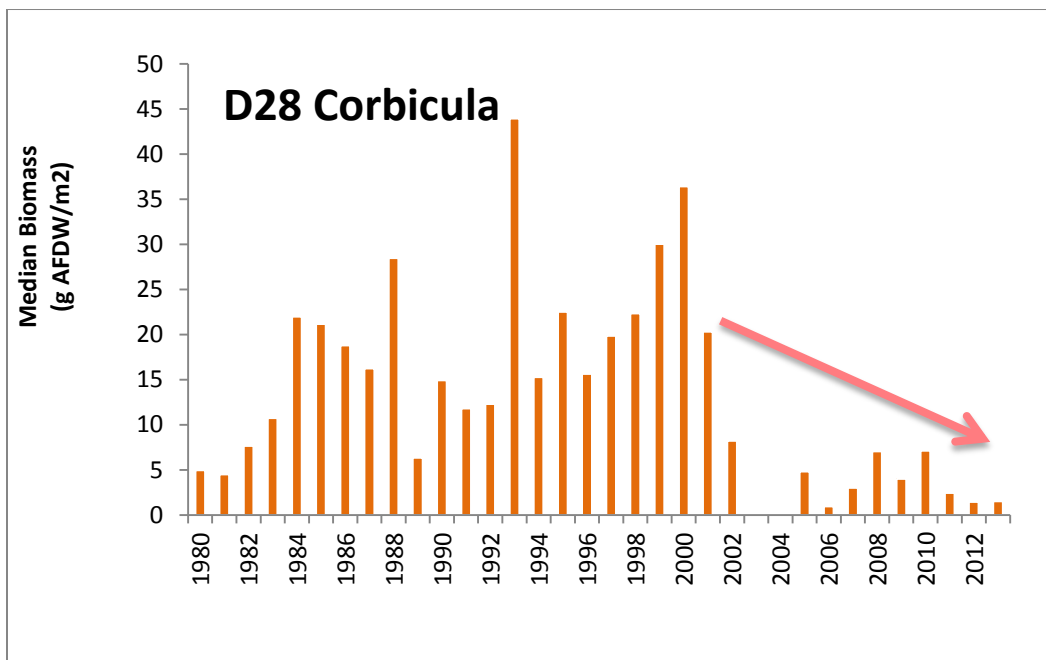
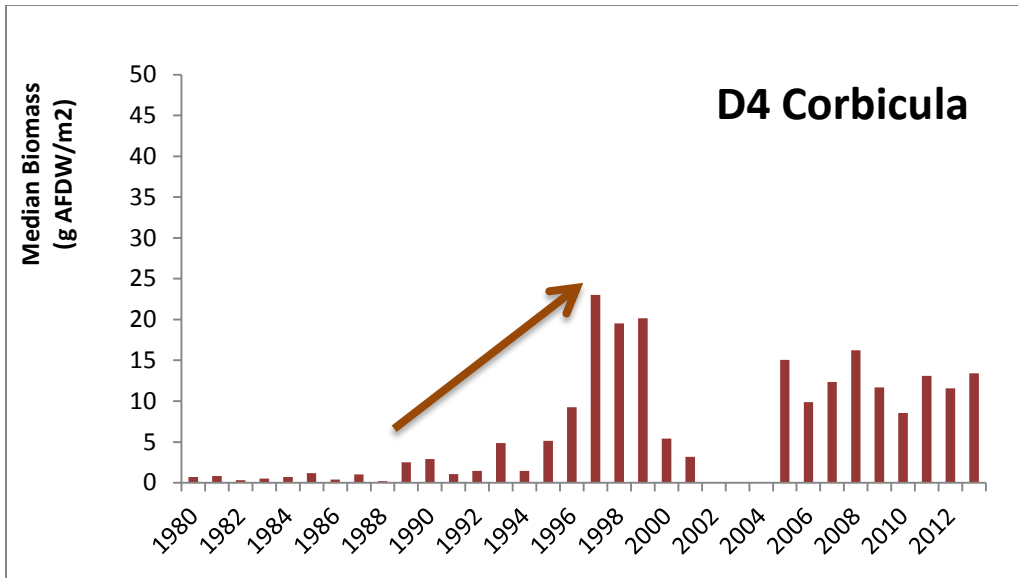


Figure 9-10. Median annual biomass (AFDW m⁻²) from two DWR monitoring stations. D4 is near the confluence of the Sacramento and San Joaquin Rivers and D28 is on Old River and both were sampled from 1980 to the present. Note samples were lost after enumeration in 2003 and part of 2004 so neither year is shown.

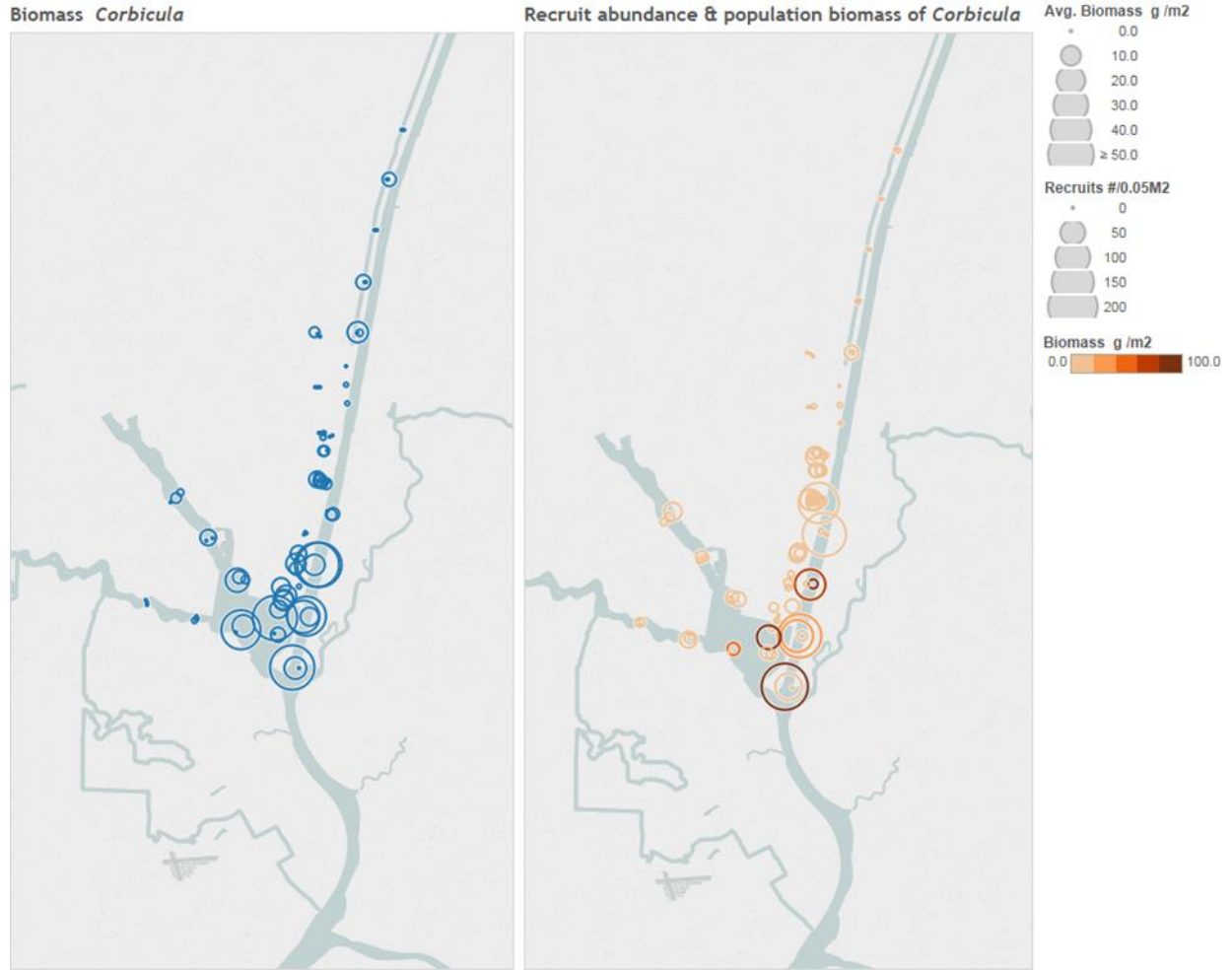


Figure 9-11. Cache Slough Complex sampling in October 2014 by DWR/USGS. Biomass (g AFDW m⁻²) of *Corbicula* shown on the left. The abundance of recruits (# 0.05m⁻²) is shown on the right with coincident color coding for *Corbicula* biomass magnitude at all locations where recruits were found.

Table 9-1. Untested Habitat Suitability Indices (HSI) for *Corbicula fluminea*

Depth (m)	HSI	Temp (°C)	HSI	EC ($\mu\text{Siemens m}^{-1}$)	HSI	Turbidity (NTU)	HSI
0	0	14	0.6	2500	0.9	0	0.8
0.5	0.6	15	0.6	5000	0.7	10	0.7
1.5	0.8	16	0.6	7500	0.5	20	0.6
2.5	0.8	17	0.6	10000	0.3	30	0.5
3.5	0.8	18	0.8	12500	0.3	40	0.3
4.5	1	19	0.8	15000	0.2	50	0.3
5.5	1	20	0.8	17500	0.05	60	0.3
6.5	1	21	0.8	20000	0.05	70	0.3
7.5	1	22	0.9	22500	0.05	80	0.3
8.5	1	23	0.9	25000	0	90	0.3
9.5	1			27500	0	100	0.3
10.5	0.9			30000	0	200	0.3
11.5	0.9			32500	0	300	0.3
12.5	0.9			35000	0		
13.5	0.9			37500	0		
14.5	0.9			40000	0		
15.5	0.7			42500	0		
16.5	0.7			45000	0		
17.5	0.7						
18.5	0.5						
19.5	0.5						
20.5	0.5						

Table 9-2. Untested Habitat Suitability Indices (HSI) for *Potamocorbula amurensis*

Depth (m)	HSI	Temp (°C)	HSI	EC ($\mu\text{Siemens m}^{-1}$)	HSI	Turbidity (NTU)	HSI
0.5	0.3	10	0.7	3500	0.2	0	0.1
1.5	0.5	11	1	8000	0.8	10	0.5
2.5	0.5	12	1	13000	1	20	0.5
3.5	0.5	13	0.8	17000	1	30	0.8
4.5	0.3	14	0.5	21000	1	40	0.8
5.5	0.3	15	0.5	25000	1	50	0.8
6.5	0.5	16	0.5	28000	0.9	60	0.8
7.5	0.5	17	0.5	32000	0.8	70	1
8.5	0.5	18	0.5	35700	0.8	80	1
9.5	0.5	19	0.5	39000	0.5	90	1
10.5	0.5	20	0.5	43000	0.2	100	1
11.5	0.5	21	0.2	46000	0.1	200	1
12.5	0.5	22	0.2			300	1
13.5	0.5	23	0.2			600	1
14.5	0.5					700	1
15.5	0.5					900	1
16.5	0.5					1000	1
17.5	0.5						
18.5	0.8						
19.5	0.8						
20.5	0.8						
22.5	0.8						
29.5	0.8						

Table 9-3. Untested Habitat Suitability Indices (HSI) for *Dreissena polymorpha* and *Dreissena bugensis*.

Depth (m) Lakes	HSI Zebra	HSI Quagga	Depth (m) Rivers	HSI Zebra	HSI Quagga	Temp (°C)	HSI Zebra	HSI Quagga
0	0.3	0.2	0	0.4		0	0	0
1.0	0.3	0.2	1.0	1		1	1	1
2.0	0.8	0.5	2.0	1		2	1	1
3.0	0.8	1	3.0	0.4		3	1	1
4.0	0.8	1	4.0	0.4		4	1	1
5.0	0.6	1	5.0	0.4		5	1	1
6.0	0.6	1	6.0	0		6	1	1
7.0	0.6	1	7.0	0		7	1	1
8.0	0.6	1	8.0	0		8	1	1
9.0	0.6	1	9.0	0		9	1	1
10.0	0.6	1	10.0	0		10	1	1
11.0	0.2	1	11.0	0		11	1	1
12.0	0.2	1	12.0	0		12	1	1
13.0	0.2	1	13.0	0		13	1	1
14.0	0.2	1	14.0	0		14	1	1
15.0	0.2	1	15.0	0		15	1	1
16.0	0.2	1	16.0	0		16	1	1
17.0	0.2	1	17.0	0		17	1	1
18.0	0.2	1	18.0	0		18	1	1
19.0	0.2	1	19.0	0		19	1	1
20.0	0.2	1	20.0	0		20	1	1
21.0	0.2	1	21.0	0		21	1	1
22.0	0.2	1	22.0	0		22	1	1
23.0	0.2	1	23.0	0		23	1	1
24.0	0.2	1	24.0	0		24	1	1
25.0	0.03	1	25.0	0		25	1	1
26.0	0.03	1	26.0	0		26	1	1
						27	1	1
						28	1	1
						29	1	1
						30	1	1
						31	1	1
						32	1	0
						33	1	0
						34	0	0

Spawn Temp (°C)	HSI Zebra	HSI Quagga	Salinity	HSI Zebra	HSI Quagga	Bottom Type	HSI Zebra	HSI Quagga
0	0	0	0	1	1	clay	0.47	0.75
1	0	0	1	1	1	loam	0.69	0.75
2	0	0	2	1	1	sand	0.74	0.75
3	0	0	3	1	1	peat	0.07	1
4	0	0	4	1	0.5	rock	0.88	1
5	0	1	5	1	0.5			
6	0	1	6	1	0.25			
7	0	1	7	1	0.25			
8	0	1	8	0.5	0.25			
9	0	1	9	0.5	0			
10	0	1	10	0.5	0			
11	0	1	11	0.5	0			
12	1	1	12	0.5	0			
13	1	1	13	0.5	0			
14	1	1	14	0.25	0			
15	1	1	15	0.25	0			
16	1	1	16	0	0			
17	1	1	17	0	0			
18	1	1	18	0	0			
19	1	1	19	0	0			
20	1	1	20	0	0			
21	1	1						
22	1	1						
23	1	1						
24	1	1						
25	0	0						
26	0	0						
27	0	0						
28	0	0						
29	0	0						
30	0	0						
31	0	0						
32	0	0						

Oxygen (mg/L)	HSI Zebra	HSI Quagga	Ca ²⁺ mg/L	HSI Zebra	HSI Quagga
0	0	0	0	0	0
1	0	0	8	0.5	0
2	0	0	12	1	0.5
3	0.25	0	16	1	1
4	0.25	0.25	20	1	1
5	0.5	0.5	24	1	1
6	0.5	0.5	28	1	1
7	1	1	32	1	1
8	1	1	36	1	1
9	1	1	40	1	1
			44	1	1
			48	1	1
			52	1	1
			56	1	1
			60	1	1
			64	1	1
			68	1	1
			72	1	1
			76	1	1
			80	1	1
			84	0	1
			88	0	1

Primary Reference: Nalepa and Schloesser (2014)

References

Kimmerer W and J K Thompson. 2014. Phytoplankton growth balanced by clam and zooplankton grazing and net transport into the low-salinity zone of the San Francisco Estuary. *Estuaries and Coasts*. 37:1202-1218.

Kooijman SALM. *Dynamic Energy Budget Theory for Metabolic Organisation*. Cambridge University Press; 2010.

Lucas, L.V., J.K. Thompson, and L.R. Brown. 2009. Why are diverse relationships observed between phytoplankton biomass and transport time? *Limnology and Oceanography* 54(1):381-390.

Lucas, LV and JK Thompson. 2012. Changing restoration rules: Exotic bivalves interact with residence time and depth to control phytoplankton productivity. *Ecosphere* 3(12): article 117. <http://www.esajournals.org/doi/pdf/10.1890/ES12-00251.1>

Morgan-King, TL and DH Schoellhamer. 2013. Suspended-sediment flux and retention in a backwater tidal slough complex near the landward boundary of an estuary. *Estuaries and Coasts* 36:300-318

Nalepa, T.F. and D. Schloesser (eds). 2014. *Quagga and zebra mussels: biology, impact, and control*. CRC Press, Boca Raton, FL. 775p

Task 10: Native and alien fishes

Larry Brown and Marissa Wulff, in collaboration with Tineke Troost, Valesca Harezlak, Bert Jagers, Deltares (submitted 06-10-15)

Progress/Status: HABITAT

Work with Previous CASCADE models

As CASCADE II began, we also continued to evaluate results from the previous iteration of CASCADE. We completed the publication of Brown et al. (2013). We also extended our analysis of the effects of future water temperature on delta smelt into the northern Delta (Brown et al. submitted), which was not possible in CASCADE I. This was possible because of other USGS monitoring that provided the water temperature records (minimum 2 years of daily measurements) needed to develop statistical water temperature models. We were also able to address the issues of vertical and horizontal temperature stratification, using measurements made under supplemental USGS funding for drought work in 2014. Through collaboration with UC Davis researchers, we were able to assess the possible effects of increasing water temperatures on delta smelt based on the most recent studies of delta smelt physiology. The overall conclusion of the study is that large portions of currently occupied habitat will become uninhabitable or physiologically stressful for long periods of the summer and early fall. This includes the northern Delta around Liberty Island and the Sacramento River Deepwater Ship Channel, where significant habitat restoration is being proposed to benefit delta smelt, Chinook salmon and other fishes.

Habitat Suitability Curves (Interim)

HABITAT model development began with development of habitat suitability index (HSI) curves for temperature, salinity and Secchi depth (turbidity indicator) for fish species occurring in the San Francisco Estuary. Development of HSI curves for species captured regularly in CDFW trawling programs were developed as described below. These species are generally tolerant of brackish and salt water. Freshwater and littoral species are less often captured in such geographically broad sampling programs; thus, HSI curves for those species will be determined from literature values (Table 10-1, attached). Depending on similarities in data among species, freshwater species may be

included in the habitat modeling as a small number of groups rather than individual species, for example, native coldwater species and invasive warmwater species. Currently, all HSI curves are interim versions and may change as knowledge of species biology and physiology improves and as we acquire DELWAQ results and learn more about applying the HABITAT tool.

Field data from the CDFW's fall midwater trawl (FMWT), Bay Study midwater and otter trawl (BS-MWT and BS-OT, respectively), and the summer townet survey (STN) were considered for development of HSI curves for fish habitat modeling. Data from each survey were considered separately because of differences in sampling gear and sampling protocols. For each survey we included the species that occurred in more than 5% of the samples. For some commonly occurring species (e.g. Delta smelt, longfin smelt) HSI curves were generated for multiple age classes. Because the Bay Study samples on a monthly schedule rather than a seasonal basis like FMWT and STN there is a question about whether non-occurrence results from the species not being in the system because it is avoiding the environmental conditions, is not captured by the gear because of size, or has left the area sampled by the survey for some other reason (e.g., seasonal migration). Thus, for the Bay study data we summarized species occurrence by month and then analyzed data for the months which included about 2% or more of the species occurrences during the sampling record. We assumed 2% represented sufficient occurrence to convey information about choice of environmental conditions. These species were primarily marine species known to utilize estuaries as nursery habitat for less than a year (Table 10-2, attached). These species were generally distributed in the seaward portions of the estuary, near the Golden Gate.

The initial step in determining the interim HSIs was to determine a single variable general additive model (GAM) for each environmental variable for each species or species age class. Data included species presence, specific conductance (converted to salinity for our purposes), water temperature and Secchi depth. For the midwater and townet survey trawls, surface values of variables were reported and used for analysis. For the bottom trawls, bottom salinity and water temperature were also reported; however, there were fewer bottom measurements than surface measurements because

of logistic constraints. Thus we calculated GAMs using both surface and bottom measurements to determine if there were major differences in the relationships that might suggest a problem with using the bottom values to define HSI curves. The GAM models should be similar. We also included Secchi depth GAMs for the otter trawl; however, we recognize that the otter trawl is generally deep enough that light levels are low and visibility is not greatly affected by suspended particles; however, strong relationships with Secchi depth would suggest that we have not considered some major environmental factor and need to do consider mechanisms that might produce such a relationship. Analysis was limited to the range of values the organism experienced (based on the data) as defined by the minimum and maximum value in the data set for that species. The GAMS were run using the R-package MGCV (<http://cran.r-project.org/web/packages/mgcv/mgcv.pdf>) using the “bam” routine for large data sets, assuming a binomial distribution. Predicted values of species occurrence were determined for each environmental variable. Outputs were predicted occurrence of a species across the values of environmental variables within which the species was observed and a graph of each relationship including the 95% confidence interval. In total we developed over 300 GAM models (Table 10-2, attached). All GAM models were statistically significant at $P < 0.05$. All GAM models by survey, species, and size class are listed in Table 10-2. Total deviance explained by each model is also listed. A total deviance explained of around 20% would be considered a strong model. Table 10-2 also gives literature information on the salinity use of each species (defined as guilds) and species estuarine use.

The GAM curves were converted to interim HSI curves as follows. First, the GAM curve was examined for general shape and the 95% confidence intervals examined as an indicator of model accuracy. In some cases, outliers produced odd “tails” at the extreme values of an environmental variable (e.g., a very high salinity for a generally low salinity species) with wide confidence intervals. In these cases we truncated the GAM predictions near the point of inflection. The minimum predicted occurrence value was then subtracted from all values to standardize the minimum HSI value to zero. The standardized values were then divided by the maximum value to put the data on the 0 to 1 scale expected of an HSI curve. We then discretized the curves for input into

HABITAT by reporting HSI values at each 0.5 salinity unit, each 0.5 degree ° centigrade for water temperature, and each 0.1 meter for Secchi depth. As mentioned previously, we consider these results as interim.

Deltares HABITAT modeling

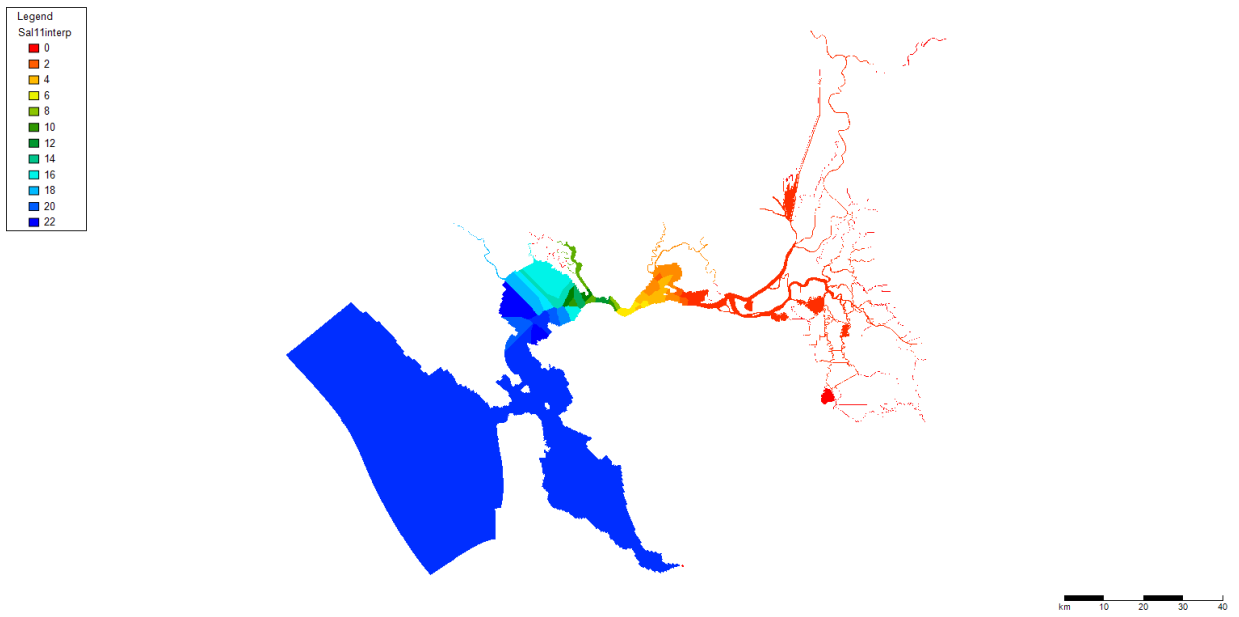
Modeling of habitat suitability for fish species in the estuary under future conditions depends on model outputs for water temperature, salinity, and turbidity (estimated from modeled suspended sediment concentration [SSC]) from the DELWAQ model. While awaiting these outputs, we wanted to make sure that the HABITAT program could produce appropriate results, thus we conducted a proof of concept model for habitat suitability for delta smelt occurrence. We used field data for water temperature, salinity, and Secchi depth from the CDFW Fall Midwater Trawl as our input data. We began by using HABITAT to interpolate field data across the entire estuary model grid to create salinity, Secchi depth and temperature maps (Figures 10-1, 10-2, and 10-3) that were used in place of DELWAQ outputs. These environmental parameter maps were then used in combination with interim delta smelt HSI curves (Figure 10-4) to produce total HSI maps for Delta Smelt for September 2011 (a good year for delta smelt abundance) and September 2014 (a poor year for delta smelt abundance) (Figure 10-5). The total HSI maps are based on the assumption that the minimum HSI of the three environmental variables determines the total suitability. For example, this method assumes that excellent conditions for water temperature and Secchi depth at a location will not mitigate the effects of undesirable salinity. As expected the good year of 2011, when delta smelt were relatively abundant, had better HSI values across a larger area than September 2014, which was a drought year.

The interpolated environmental variables had several discontinuities, especially in Suisun Bay (Figures 10-1, 10-2, and 10-3). This was caused by tidal aliasing both within and between days (i.e., sampling different phases of the tidal cycle). Tidal aliasing occurs in the FMWT data because all locations can't be sampled simultaneously. However, the modeled environmental data will not have such discrepancies because parameters in all grid cells will be computed simultaneously. To provide an example of the quality of the expected input files, we used some recently generated data to prepare

a more limited example. We used preliminary Delft3D-FM outputs from R. Martyr (Task 4; see step #2 in Fig. 10-7). Because the hydrodynamic model was run in parallel mode, the outputs (which were in separate files, each for its own subdomain/processor), those outputs then needed to be “stitched” together using the Deltares utility “DDCOUPLEFM” (step #3 in Fig. 10-7). These stitched hydrodynamic model output data were then run through a “dummy” DELWAQ (water quality) model run (step #4 in Fig. 10-7), which output them in the format needed for the next step. The DELWAQ outputs were then post-processed with another Deltares tool “DELWAQ2RASTER”, which takes the DELWAQ data on the flexible mesh grid and places it on a Cartesian grid, which is what HABITAT uses (step #5). (Note: DELWAQ2RASTER is a tool developed by collaborators at Deltares to meet the CASCaDE project’s specifications. It was completed in March 2015.) DELWAQ2RASTER also performs depth-averaging and allows the user to prescribe the mode of temporal processing of the Delft3D-FM/DELWAQ output maps (e.g. time-averaging, minimum or maximum over time, etc.). For example, if the user is interested in performing HABITAT analyses using maps of daily averaged of salinity or of minimum temperature over each month, that temporal processing is performed in this step. In the present test case case, 24-hour averaged maps of salinity and depth were generated. Once loaded in HABITAT, we were able to apply HSI curves and create output maps from actual Delft3D-FM/DELWAQ output (Figure 10-6). We created a pseudo HSI curve for depth that was developed as a turbidity indicator, for testing purposes only. This input will be replaced by suspended sediment concentration when model output becomes available. The resulting map is much smoother and does not have the discontinuities exhibited by the interpolated data. This is the quality of output we expect from our future applications of HABITAT.

Figure 10-1. Interpolated Fall Midwater Trawl salinity data for (a) 2011 and (b) 2014.

a.



b.

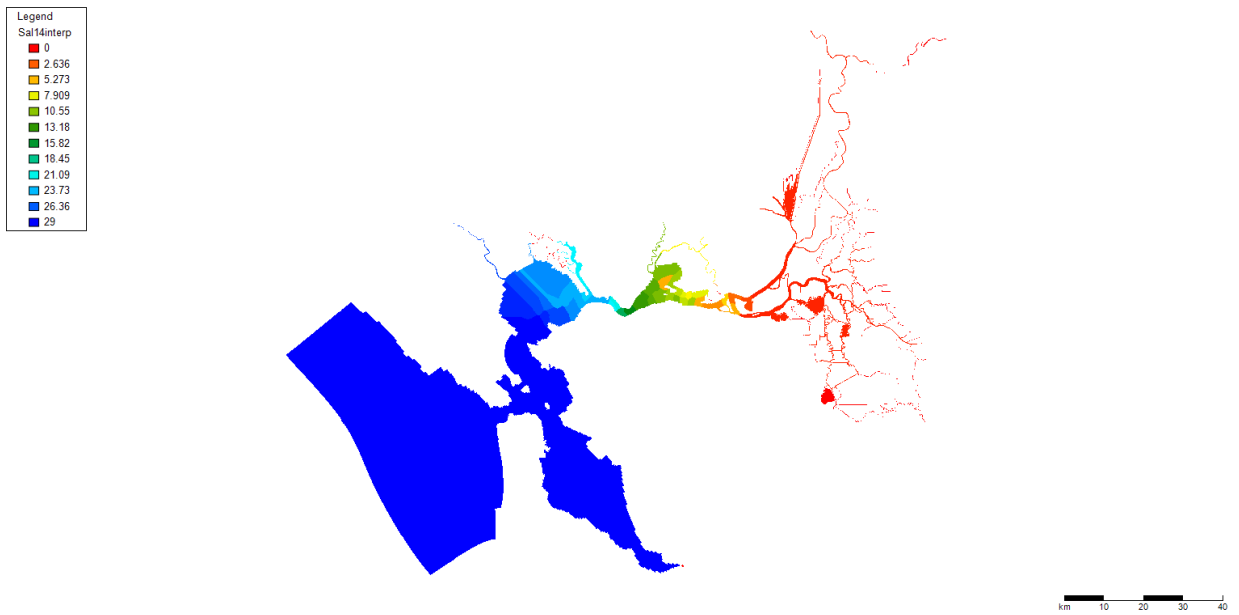
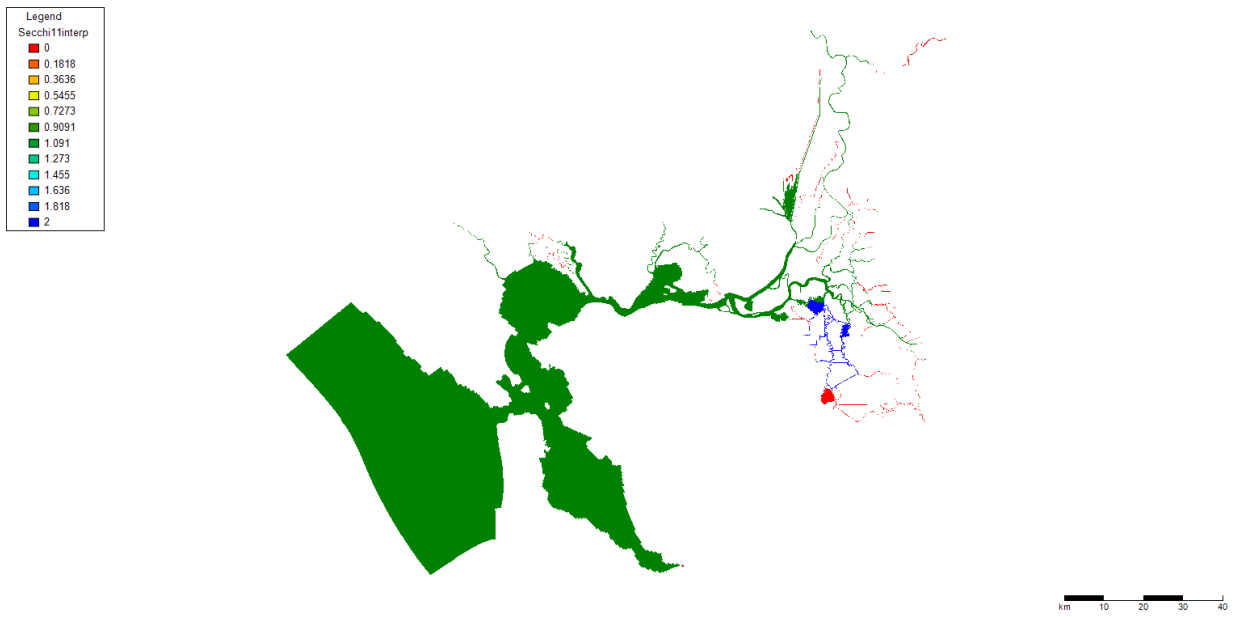


Figure 10-2. Interpolated Fall Midwater Trawl Secchi depth data for (a) 2011 and (b) 2014.

a.



b.

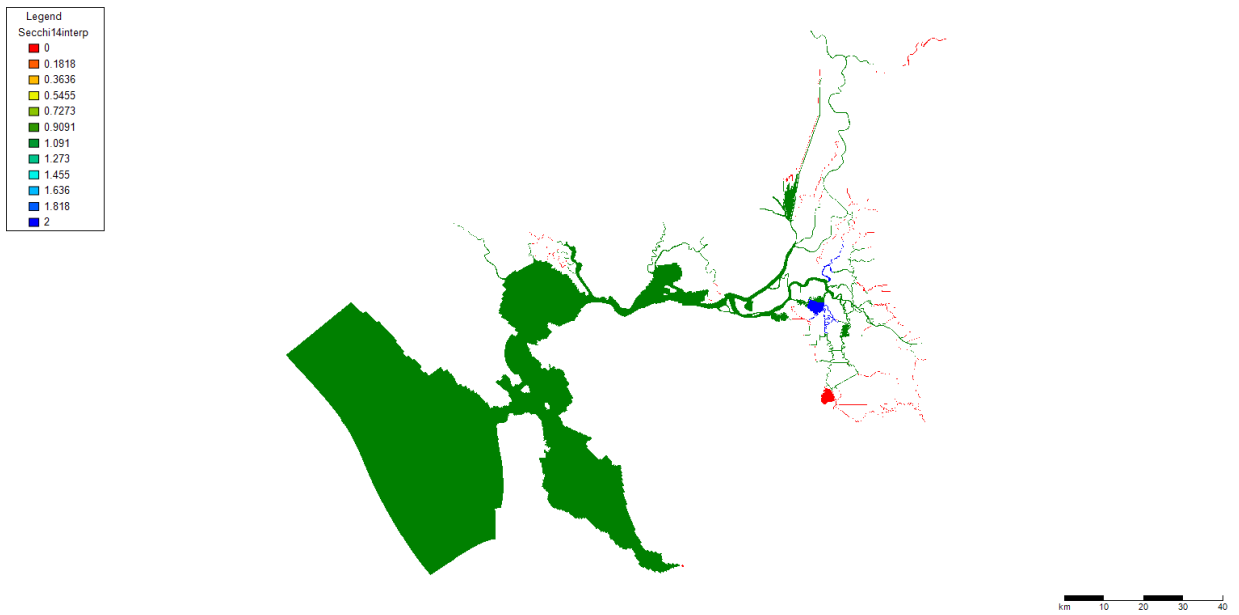
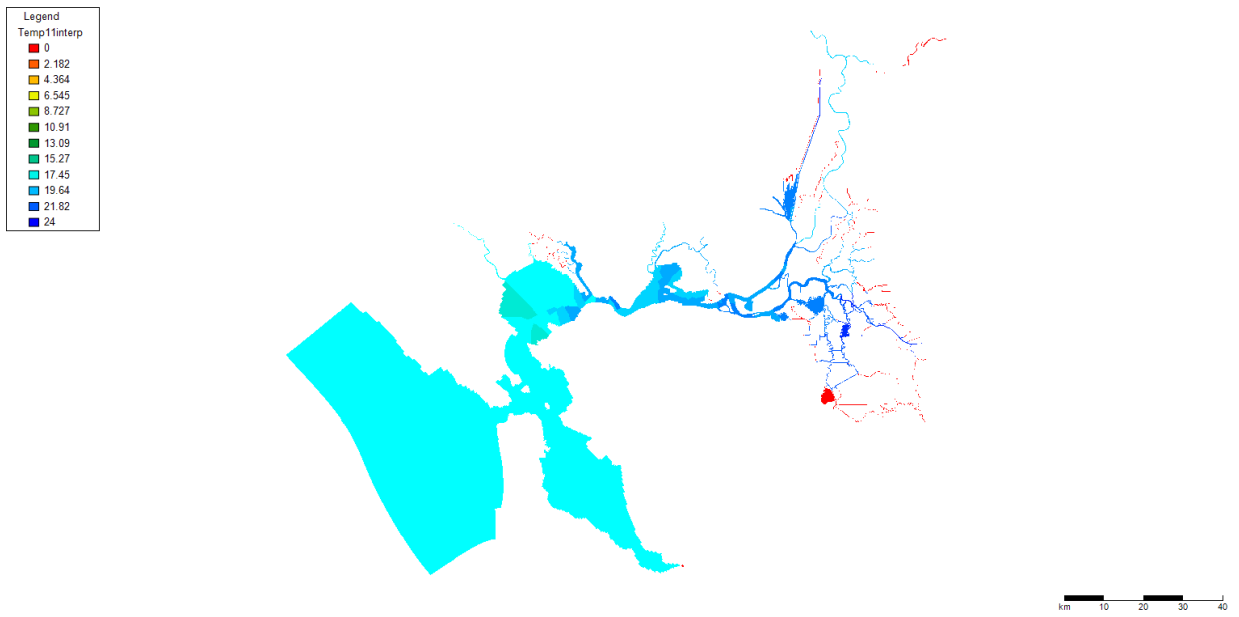


Figure 10-3. Interpolated Fall Midwater Trawl temperature data for (a) 2011 and (b) 2014.

a.



b.

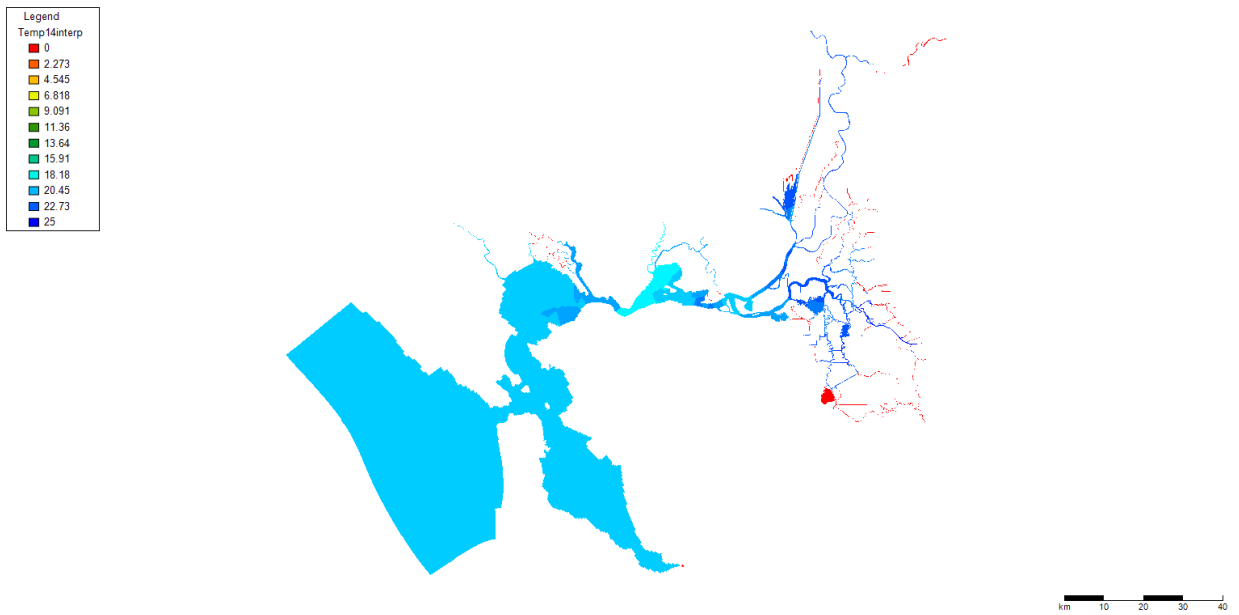
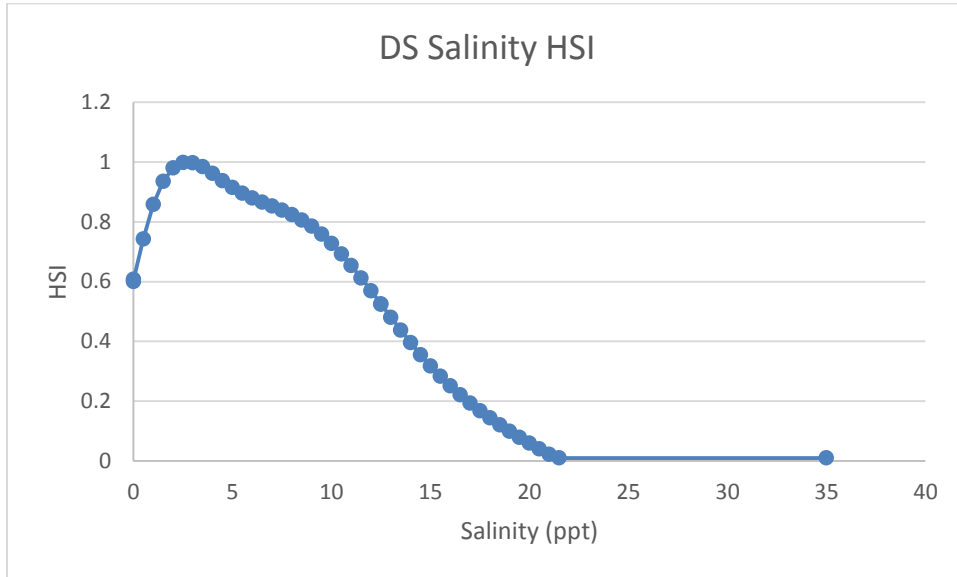
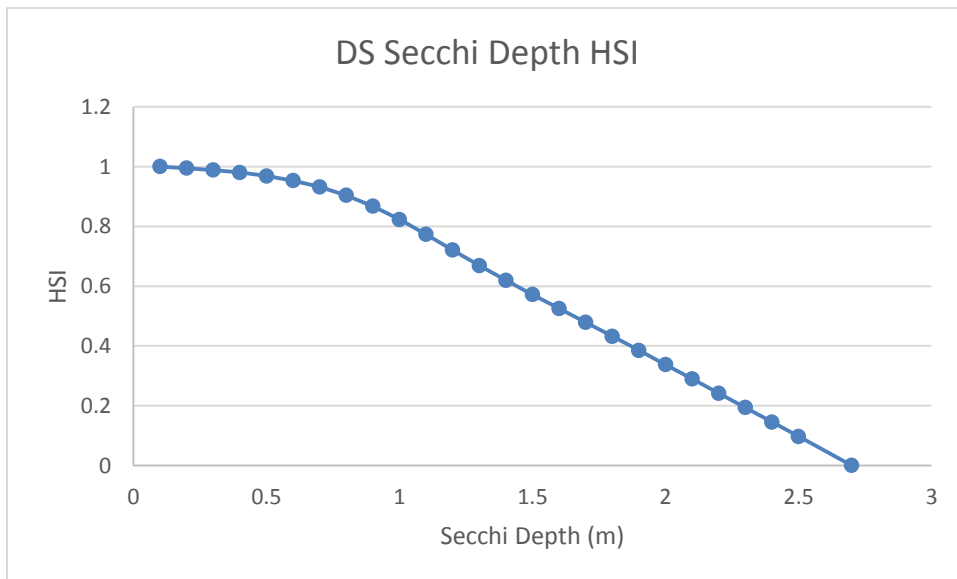


Figure 10-4. Interim habitat suitability index curves for Delta Smelt with respect to (a) salinity, (b) Secchi depth, and (c) temperature.

a.



b.



c.

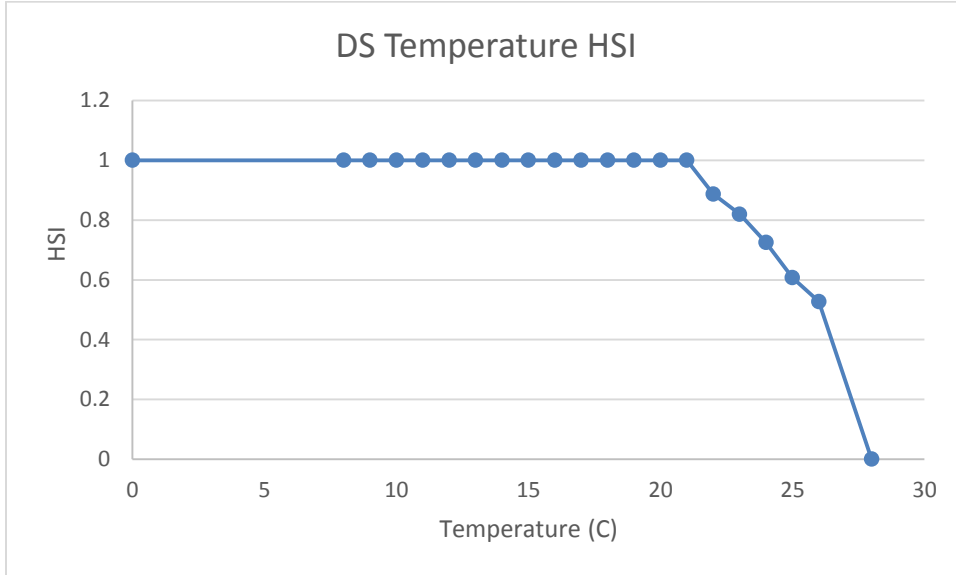
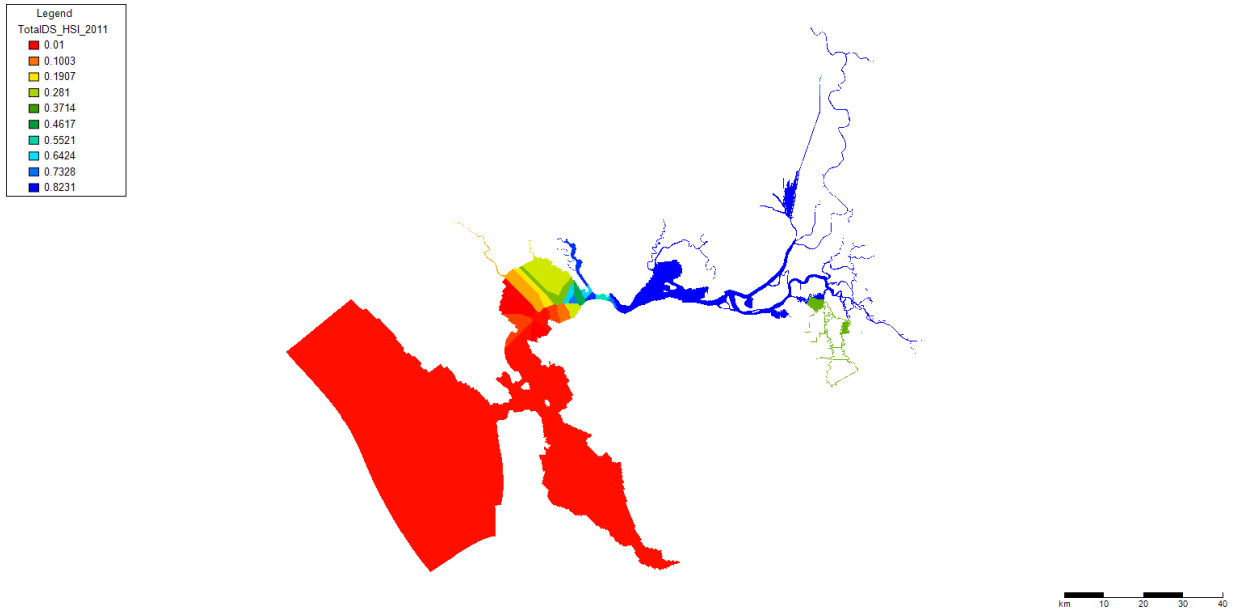


Figure 10-5. Total HSI maps for Delta Smelt in (a) September 2011 and (b) 2014.

a.



b.

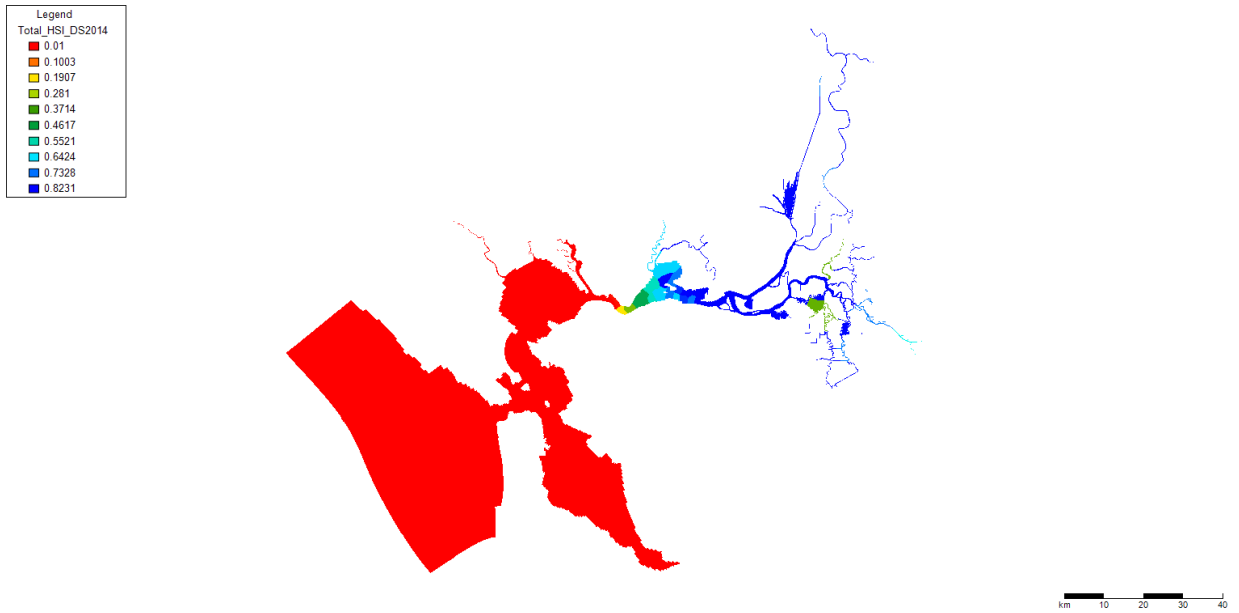
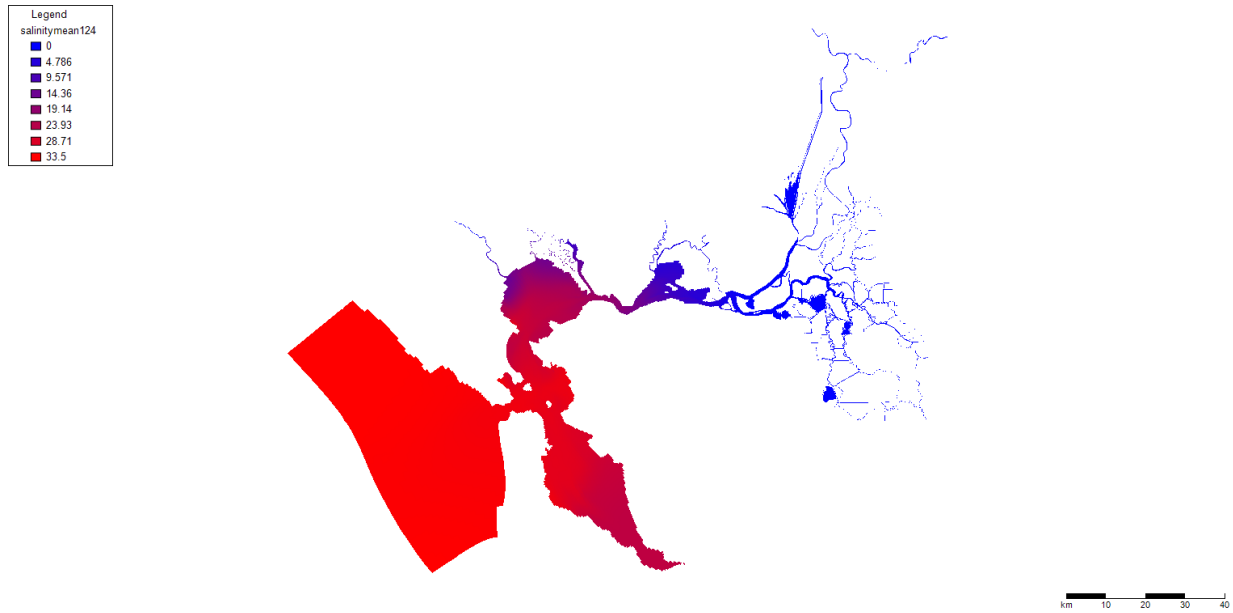
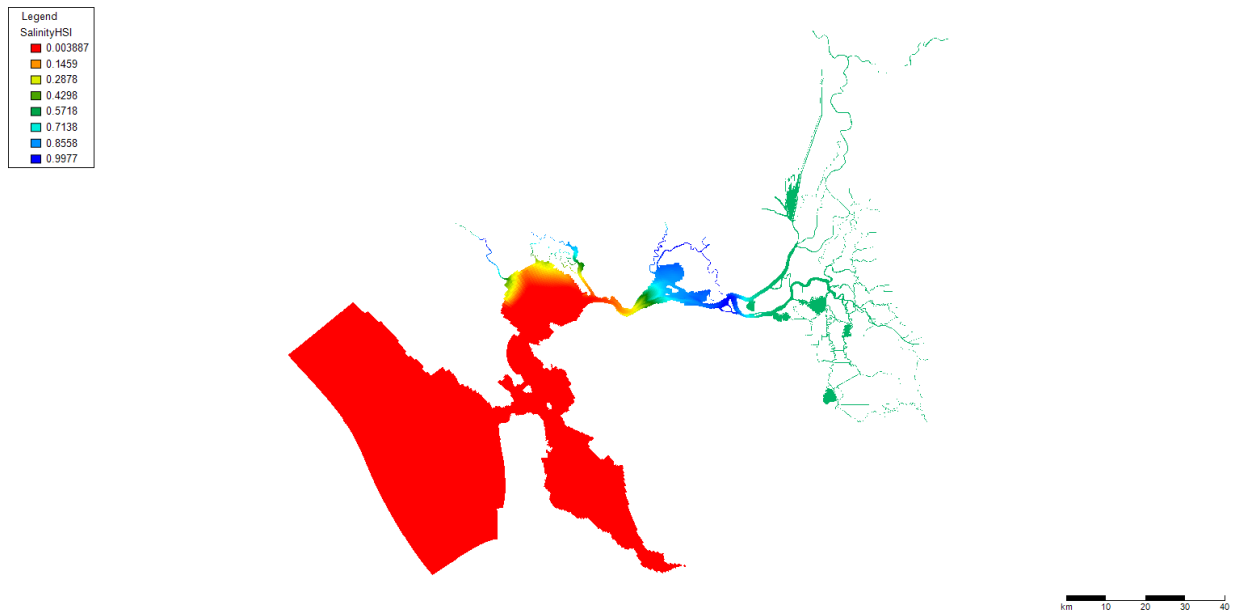


Figure 10-6. HABITAT results using 24-hr averaged Delft3D-FM hydrodynamic model outputs from a test run. Salinity input (a) and salinity HSI map (b), depth input (c) and depth HSI map (test turbidity indicator; d), and total HSI map for Delta Smelt (e).

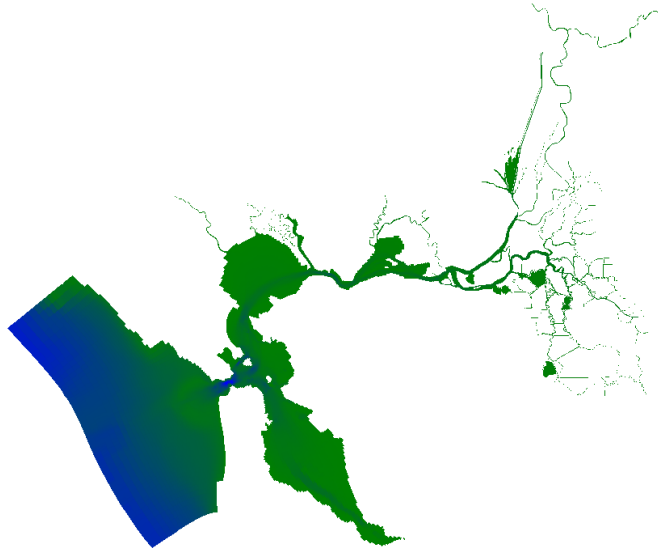
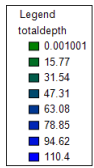
a.



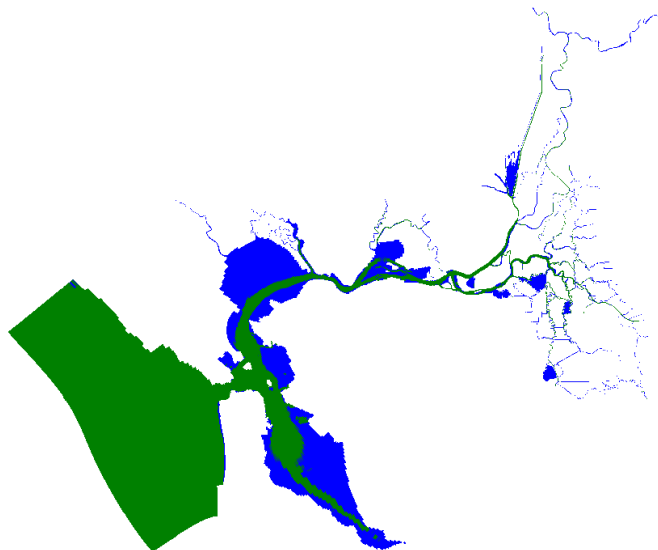
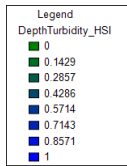
b.



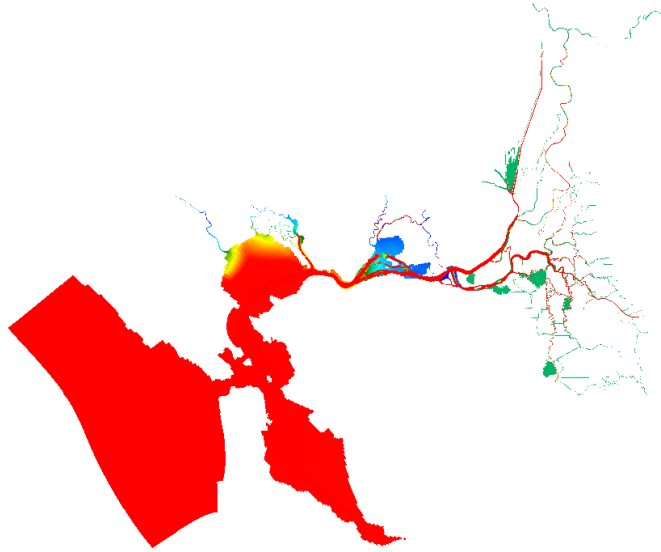
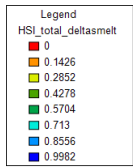
C.



d.



e.



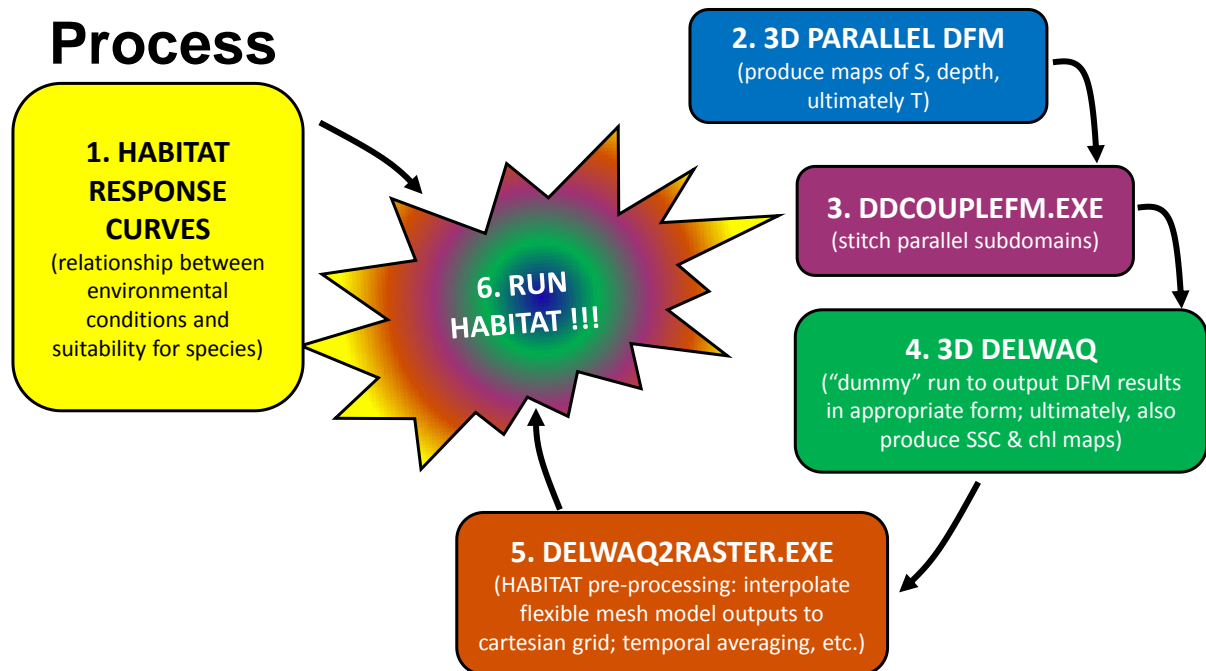


Figure 10-7. This schematic depicts the current process required for performing a HABITAT analysis in CASCaDE. First, HSI curves are generated. Then maps of relevant environmental parameters (e.g. salinity, temperature, depth) are computed by the Delft3D-FM hydrodynamic model (#2). If the hydrodynamic run was performed in parallel, the “stitching tool” DDCOUPLEFM must be used to re-stitch the outputs together into a single continuous map across the total domain (#3). The stitched maps must be run through a DELWAQ dummy simulation (#4). Alternatively, this step may consist of a real DELWAQ run for sediment or phytoplankton. The DELWAQ output must then be processed by DELWAQ2RASTER, a utility that translates mapped model outputs into a form readable by HABITAT.

Management implications

As demonstrated by the proof of concept modeling, HABITAT provides the capability to model the geographic location and distribution of appropriate physical habitat for any species for which we can develop HSI curves. When applied to the CASCADE II future scenarios, HABITAT will provide valuable information and the likely responses of species of interest. Such information will be invaluable to managers and policy makers responsible for managing aquatic resources in the Delta. Once the CASCADE II scenarios are address new modeling scenarios can be assessed using the same methods. The Results of HABITAT modeling should greatly reduce uncertainty about

the effects on species of concern of major changes in Delta infrastructure and operations and how those effects will evolve as climate change proceeds.

Next Steps

Our next steps with HABITAT are largely dependent on two factors. The first is locating a source of funding to continue the work. Without funding, making significant progress on next steps will be difficult. The second factor, is completion and validation of the other models supplying the data we use as input. Progress on the other models is detailed elsewhere in this report. The proof of concept models indicate the HABITAT program is functioning to the extent we have tested it thus far. However, several steps are still needed before we can apply HABITAT efficiently and with confidence.

1. HABITAT as we applied it in the proof of concept is fairly labor intensive because it works on a single time step and we are currently using it for single species. The program does include options for doing calculations for multiple species at selected time steps. We have not had the opportunity to test those capabilities yet and additional “debugging” may be necessary in collaboration with Deltares. An essential next step is to test these capabilities.

2. Finalize HSI curves for species of interest. As noted above, further refinement may be necessary based on new knowledge and preliminary applications.

3. We need to determine the best time averaging time interval to apply to model output for use as HABITAT input. We believe daily average values will be sufficient for HABITAT modeling purposes for fishes; however, we need to verify this with actual model test runs.

References

Aasen, K. D., & Henry Jr, F. D. (1981). Spawning behavior and requirements of Alabama spotted bass, *Micropterus punctulatus* Henshalli, in Lake Perris, Riverside County, California. *California Fish and Game*.

Allen, P. J., Hodge, B., Werner, I., & Cech, Jr, J. J. (2006). Effects of ontogeny, season, and temperature on the swimming performance of juvenile green sturgeon (*Acipenser medirostris*). *Canadian Journal of Fisheries and Aquatic Sciences*, 63(6), 1360-1369.

Armour, C. L. (1994). *Evaluating Temperature Regimes for Protection of Brown Trout*. NATIONAL BIOLOGICAL SERVICE FORT COLLINS CO MIDCONTINENT ECOLOGICAL SCIENCE CENTER.

Audet, C., FitzGerald, G. J., & Guderley, H. (1985). Salinity preferences of four sympatric species of sticklebacks (Pisces: Gasterosteidae) during their reproductive season. *Copeia*, 209-213.

Baker, S. C., & Heidinger, R. C. (1996). Upper lethal temperature tolerance of fingerling black crappie. *Journal of fish biology*, 48(6), 1123-1129.

Baxter, R., Hieb, K., DeLeon, S., Fleming, K., & Orsi, J. (1999). *Report on the 1980-1995 fish, shrimp, and crab sampling in the San Francisco Estuary, California*.

Beamish, R. J., & Levings, C. D. (1991). Abundance and Freshwater Migrations of the Anadromous Parasitic Lamprey, *Lampetra tridentate*, in a Tributary of the Fraser River, British Columbia. *Canadian Journal of Fisheries and Aquatic Sciences*, 48(7), 1250-1263.

Becker, G. C. 1983. *Fishes of Wisconsin*, Madison: University of Wisconsin Press.

Bjornn, T., & Reiser, D. W. (1991). Habitat requirements of salmonids in streams. *American Fisheries Society Special Publication*, 19(837), 138.

Black, E. C. (1953). Upper lethal temperatures of some British Columbia freshwater fishes. *Journal of the Fisheries Board of Canada*, 10(4), 196-210.

Brown, Larry R., William A. Bennett, R. Wayne Wagner, Tara Morgan-King, Noah Knowles, Frederick Feyrer, David H. Schoellhamer, Mark T. Stacey, and Michael Dettinger. "Implications for future survival of delta smelt from four climate change scenarios for the Sacramento–San Joaquin Delta, California." *Estuaries and coasts* 36, no. 4 (2013): 754-774.

Carlander, K. D. (1969). *Handbook of freshwater fishery biology*. Volume 1. Life history data on freshwater fishes of the United States and Canada, exclusive of the Perciformes.

Carveth, C. J., Widmer, A. M., & Bonar, S. A. (2006). Comparison of upper thermal tolerances of native and nonnative fish species in Arizona. *Transactions of the American Fisheries Society*, 135(6), 1433-1440.

- Castleberry, D. T., & Cech Jr, J. J. (1992). Critical thermal maxima and oxygen minima of five fishes from the upper Klamath basin. *California Fish and Game*, 78(4), 145-152.
- Cech Jr, J. J., & Doroshov, S. I. (2005). Environmental requirements, preferences, and tolerance limits of North American sturgeons. In *Sturgeons and paddlefish of North America* (pp. 73-86). Springer Netherlands.
- Cech Jr, J. J., Doroshov, S. I., Moberg, G. P., May, B. P., Schaffter, R. G., & Kohlhorst, D. M. (2000). Biological assessment of green sturgeon in the Sacramento-San Joaquin watershed (phase 1). *Final Report to the CALFED Bay-Delta Program. Project*.
- Cech Jr, J. J., Mitchell, S. J., Castleberry, D. T., & McEnroe, M. (1990). Distribution of California stream fishes: influence of environmental temperature and hypoxia. *Environmental biology of Fishes*, 29(2), 95-105.
- Cech Jr, J. J., Massingill, M. J., & Stern, H. (1982). Growth of juvenile sacramento blackfish, *Orthodon microlepidotus* (Ayres). *Hydrobiologia*, 97(1), 75-80.
- Chase, S. D. (2001). Contributions to the Life History of Adult Pacific Lamprey (*Lampetra tridentata*) in the Santa Clara River Of Southern California. *Bulletin of the Southern California Academy of Sciences*, 100(2), 74-85.
- Chittenden Jr, M. E. (1972). Responses of young American shad, *Alosa sapidissima*, to low temperatures. *Transactions of the American Fisheries Society*, 101(4), 680-685.
- Clemens, H. P., & Sneed, K. E. (1957). *The spawning behavior of the channel catfish Ictalurus punctatus* (No. 219). US Fish and Wildlife Service.
- Coble, D. W. (1975). Smallmouth bass. *Black bass biology and management. Sport Fishing Institute, Washington, DC*, 534, 44-53.
- Edwards, E. A., Gebhart, G., & Maughan, O. E. (1983). *Habitat suitability information: smallmouth bass*. OKLAHOMA COOPERATIVE FISH AND WILDLIFE RESEARCH UNIT STILLWATER.
- Eschmeyer, W. N., E. S. Herald, and H. Hamann. 1983. A field guide to Pacific coast fishes of North America. Houghton MifflinCo., Boston, xii + 336 pp.
- Fry, D. H. (1973). *Anadromous fishes of California*. State of California, Department of Fish and Game.
- Ganssle, D. (1966). Fishes and decapods of San Pablo and Suisun bays. *Ecological Studies of the Sacramento-San Joaquin Estuary, Part I (compiled by DW Kelley)*, 64-94.

Grant, G. C., & Maslin, P. E. (1999). Movements and reproduction of hardhead and Sacramento squawfish in a small California stream. *The Southwestern Naturalist*, 296-310.

Hokanson, K. E., Kleiner, C. F., & Thorslund, T. W. (1977). Effects of constant temperatures and diel temperature fluctuations on specific growth and mortality rates and yield of juvenile rainbow trout, *Salmo gairdneri*. *Journal of the Fisheries Board of Canada*, 34(5), 639-648.

Houston, A.H. 1982. Thermal effects upon fishes. Publication No. NRCC 18566, Environmental Secretariat, National Research Council of Canada. Ottawa. 200 pp.

Hubbs, C., H. B. Sharp, AND J. F. Scmneider. 1971. Developmental rates of *Menidia audens* with notes on salt tolerance. *Trans. Am. Fish. Soc.* 100: 603-610.

Jenkins, R. E., & Burkhead, N. M. (1994). *Freshwater fishes of Virginia* (p. 1079). Bethesda, Maryland: American Fisheries Society.

Keast, A. (1968). Feeding of some Great Lakes fishes at low temperatures. *Journal of the Fisheries Board of Canada*, 25(6), 1199-1218.

Kendall, A. W., & Schwartz, F. J. (1968). Lethal temperature and salinity tolerances of the white catfish, *Ictalurus catus*, from the Patuxent River, Maryland. *Chesapeake Science*, 9(2), 103-108.

Knight, N. J. (1985). *Microhabitats and temperature requirements of hardhead (Mylopharodon conocephalus) and Sacramento squawfish (Ptychocheilus grandis), with notes for some other native California stream fishes* (Doctoral dissertation).

Kohlhorst, D. W. 1976. Sturgeon spawning in the Sacramento River in 1973, as determined by distribution of larvae. *Calif. Fish Game*, 62, 32-40.

KRAMER, V. L., GARCIA, I. R., & Colwell, A. E. (1987). AN EVALUATION OF THE MOSQUITOFISH, *GAMBUSIA AFF/N/S*, AND THE INLAND SILVERSIDE, *MENIDIA BERYLLINA*, AS MOSQUITO CONTROL AGENTS IN CALIFORNIA WILD RICE FIELDS. *Journal of the American Mosquito Control Association*, 3, 626-632.

Kubicek, P.F. and D.G. Price. 1976. An evaluation of water temperature and its effect on juvenile steelhead trout in geothermally active areas of Big Sulphur Creek. *Transactions of California-Nevada Wildlife* 1976:1-24.

Lachance, S., Magnan, P., & FitzGerald, G. J. (1987). Temperature preferences of three sympatric sticklebacks (Gasterosteidae). *Canadian journal of zoology*, 65(6), 1573-1576.

Lambert, Thomas R., and James M. Handley. "SETTING AN INSTREAM FLOW REQUIREMENT FOR-S-'ALLMOUTH BASS (*Micropterus dolomieu*).*" Regulated rivers* (1984): 387.

Larimore, R. W. (1957). Ecological life history of the warmouth (*Centrarchidae*).*Illinois Natural History Survey Bulletin; v. 027, no. 01.*

Linares-Casenave, J., Van Eenennaam, J. P., & Doroshov, S. I. (2002). Ultrastructural and histological observations on temperature-induced follicular ovarian atresia in the white sturgeon. *Journal of Applied Ichthyology*, 18(4-6), 382-390.

Magee, A., Myrick, C. A., & Cech, J. J. (1999). Thermal preference of female threespine sticklebacks under fed and food-deprived conditions. *California Fish and Game*, 85(3), 102-112.

Marcy Jr, B. C., Jacobson, P. M., & Nankee, R. L. (1972). Observations on the reactions of young American shad to a heated effluent. *Transactions of the American Fisheries Society*, 101(4), 740-743.

Marine, K. R., & Cech Jr, J. J. (2004). Effects of High Water Temperature on Growth, Smoltification, and Predator Avoidance in Juvenile Sacramento River Chinook Salmon. *North American Journal of Fisheries Management*, 24(1), 198-210.

Matern, S. A. (2001). Using temperature and salinity tolerances to predict the success of the shimofuri goby, a recent invader into California. *Transactions of the American Fisheries Society*, 130(4), 592-599.

Matern, S. A. 1999. *The invasion of the shimofuri goby (*Tridentiger bifasciatus*) into California: establishment, potential for spread, and likely effects* Doctoral dissertation. University of California, Davis

Mayfield, R. B., & Cech Jr, J. J. (2004). Temperature effects on green sturgeon bioenergetics. *Transactions of the American Fisheries Society*, 133(4), 961-970.

McEnroe, M., & Cech Jr, J. J. (1985). Osmoregulation in juvenile and adult white sturgeon, *Acipenser transmontanus*. *Environmental Biology of Fishes*, 14(1), 23-30.

Meeuwig, M. H., Bayer, J. M., & Seelye, J. G. (2005). Effects of temperature on survival and development of early life stage Pacific and western brook lampreys. *Transactions of the American Fisheries Society*, 134(1), 19-27.

Middaugh DP, Shenker JM (1988) Salinity tolerance of young topsmelt, *Atherinops affinis*, cultured in the laboratory. *Calif Fish and Game* 74 (4):232-235

- Moss, S. A. (1970). The responses of young American shad to rapid temperature changes. *Transactions of the American Fisheries Society*, 99(2), 381-384.
- Moyle, P. B. (2002). *Inland fishes of California*. Univ of California Press.
- Moyle PB, Yoshiyama RM, Williams JE, Wikramanayake ED (1995) Fish species of special concern of California, 2nd ed. California Department of Fish and Game, Sacramento, California
- Moyle, P. B., Herbold, B., Stevens, D. E., & Miller, L. W. (1992). Life history and status of delta smelt in the Sacramento-San Joaquin Estuary, California. *Transactions of the American Fisheries Society*, 121(1), 67-77.
- Myrick, C. A., & Cech Jr, J. J. (2004). Temperature effects on juvenile anadromous salmonids in California's central valley: what don't we know?. *Reviews in Fish Biology and Fisheries*, 14(1), 113-123.
- Myrick, C. A., & Cech, J. J. (2002). Growth of American River fall-run Chinook salmon in California's Central Valley: temperature and ration effects. *California Fish and Game*, 88(1), 35-44.
- O'Leary, J. A., & Kynard, B. (1986). Behavior, length, and sex ratio of seaward-migrating juvenile American shad and blueback herring in the Connecticut River. *Transactions of the American Fisheries Society*, 115(4), 529-536.
- Propst, D. L., & Gido, K. B. (2004). Responses of native and nonnative fishes to natural flow regime mimicry in the San Juan River. *Transactions of the American Fisheries Society*, 133(4), 922-931.
- Richards, J. E., & Beamish, F. W. H. (1981). Initiation of feeding and salinity tolerance in the Pacific lamprey *Lampetra tridentata*. *Marine Biology*, 63(1), 73-77.
- Russell, J. E., Beamish, F. W. H., & Beamish, R. J. (1987). Lentic spawning by the Pacific lamprey, *Lampetra tridentata*. *Canadian Journal of Fisheries and Aquatic Sciences*, 44(2), 476-478.
- Smale, M. A., & Rabeni, C. F. (1995). Hypoxia and hyperthermia tolerances of headwater stream fishes. *Transactions of the American Fisheries Society*, 124(5), 698-710.
- Snyder, R. J., & Dingle, H. (1989). Adaptive, genetically based differences in life history between estuary and freshwater threespine sticklebacks (*Gasterosteus aculeatus* L.). *Canadian Journal of Zoology*, 67(10), 2448-2454.

- Sommer, T., Baxter, R., & Herbold, B. (1997). Resilience of splittail in the Sacramento–San Joaquin estuary. *Transactions of the American Fisheries Society*, 126(6), 961-976.
- Strange, R. J., Petrie, R. B., & Cech, J. J. (1993). Slight stress does not lower critical thermal maximums in hatchery-reared rainbow trout. *Folia Zoologica*, 42(3), 251-256.
- Swanson, C., Reid, T., Young, P. S., & Cech Jr, J. J. (2000). Comparative environmental tolerances of threatened delta smelt (*Hypomesus transpacificus*) and introduced wakasagi (*H. nipponensis*) in an altered California estuary. *Oecologia*, 123(3), 384-390.
- Swanson, C., Young, P. S., & Cech, J. J. (1998). Swimming performance of delta smelt: maximum performance, and behavioral and kinematic limitations on swimming at submaximal velocities. *The Journal of experimental biology*, 201(3), 333-345.
- Swift, C. C. 1989. *Biology and distribution of the tidewater goby, Eucyclogobius newberryi (Pisces: Gobiidae) of California*. Natural History Museum of Los Angeles County, 1989.
- Torgersen, C. E., & Close, D. A. (2004). Influence of habitat heterogeneity on the distribution of larval Pacific lamprey (*Lampetra tridentata*) at two spatial scales. *Freshwater Biology*, 49(5), 614-630.
- Van de Wetering, S. J., & Ewing, R. E. (1999). Lethal temperatures for larval Pacific lamprey, *Lampetra tridentata*. *Confederated tribes of the Siletz Indians. Siletz, Oregon*.
- Van Eenennaam, J. P., Linares-Casenave, J., Deng, X., & Doroshov, S. I. (2005). Effect of incubation temperature on green sturgeon embryos, *Acipenser medirostris*. *Environmental Biology of Fishes*, 72(2), 145-154.
- Vigg, S., & Kucera, P. A. (1981). Contributions to the life history of Sacramento perch, *Archoplites interruptus*, in Pyramid Lake, Nevada. *The Great Basin Naturalist*, 278-289.
- Vondracek, B., Wurtsbaugh, W. A., & Cech, J. J. (1988). Growth and reproduction of the mosquitofish, *Gambusia affinis*, in relation to temperature and ration level: consequences for life history. *Environmental Biology of Fishes*, 21(1), 45-57.
- Wang, J. C. 1986. Fishes of the Sacramento-San Joaquin estuary and adjacent waters, California: a guide to early life histories. Interagency Ecological Program Technical Report 9. 800 pp.
- Webb, M. A., Van Eenennaam, J. P., Doroshov, S. I., & Moberg, G. P. (1999). Preliminary observations on the effects of holding temperature on reproductive performance of female white sturgeon, *Acipenser transmontanus* Richardson. *Aquaculture*, 176(3), 315-329.

White, J. L., & Harvey, B. C. (1999). Habitat separation of prickly sculpin, *Cottus asper*, and coastrange sculpin, *Cottus aleoticus*, in the mainstem Smith River, northwestern California. *Copeia*, 371-375.

Wurtsbaugh, W. A., & Cech Jr, J. J. (1983). Growth and activity of juvenile mosquitofish: temperature and ration effects. *Transactions of the American Fisheries Society*, 112(5), 653-660.

Young, P. S., Swanson, C., & Cech Jr, J. J. (2004). Photophase and illumination effects on the swimming performance and behavior of five California estuarine fishes. *Copeia*, 2004(3), 479-487.

Table10-1: Physiological variables of selected fish species in the San Francisco Estuary.

Species	Upper Thermal Max	Lower Thermal Min	Stressful Temperatures
American shad	Upper lethal limit: 32-33°C (Moss 1970)	lower lethal: 4°C (Chittenden 1972)	
Bigscale logperch			
Black bullhead	35°C, 38°C in lab conditions (Smale and Rabeni 1995). 50% of fish in trial died in 24 hours: 35.0 °C, w/ aprox. acclimation temp of 23°C (Black 1953)		
Black crappie	>37-38C are usually lethal [M]. Rapid transfer protocols determined 24 LT-50 Values of 33.8, 35.1 and 31.5 ° C for age 0 size classes w/ mean TL of 30.2, 45.6 and 74.9 mm (Baker and Heidinger 1996).		> 31°C
Blue catfish	Can survive 37°C	Can survive 0°C	
Bluegill	Upper lethal tolerance 37-40°C depending on acclimation (Carveth et al. 2006) 40-41°C (short periods, when acclimated)	2-5°C	
Brook trout	26°C if acclimated	1°C	
Brown bullhead	Can survive 37°C	Can survive 0°C	
Brown trout	Thermal max 28-29°C, Thermal max depending on acclimation: 29, 33.4, 35°C (Cech et al. 1990)		
California roach			
Chameleon goby			
Channel catfish	36-38°C, 39°C is lethal.		Juveniles grown at 21-24C displayed decreased growth rates, impaired smoltification and increased predation vulnerability than fish grown at 13-16C. Fish grown at 17-20C had similar growth, variable smoltification impairment and higher predation vulnerability as fish at 13-16C (Marine and Cech 2004).
Chinook salmon	Can survive and grow at temps up to 24°C (Marine and Cech 2004).		
Common carp	Can survive high temps 31-36°C depending on acclimation temp and sudden temp changes.		

Table10-1: Physiological variables of selected fish species in the San Francisco Estuary.

Species	Upper Thermal Max	Lower Thermal Min	Stressful Temperatures
Delta smelt	Lethal limit of 29C. Embryo and larvae mortality likely increases above 18°C (Moyle 2002). Fish were acclimated to 17°C and freshwater (0 ppt). Delta smelt are able to tolerate 25.4°C (Swanson et al. 2000).	Fish were acclimated to 17°C and freshwater (0 ppt). Able to tolerate 7.5°C (Swanson et al. 2000).	
fathead minnow	Thermal max: 33°C (Moyle 2002). Thermal max: fathead (mean wt. 1.82g) mean 33.1+/-0.2C, range 31.8- 33.1C (Castleberry and Cech 1992). Upper lethal tolerance 36-38°C depending on acclimation temp (Carveth et al. 2006)		
Golden shiner	Can tolerate temps up to 36-37°C.		
Goldfish	Can survive 41°C.	Can survive 0°C	
Green sturgeon	Temps above 20°C are lethal to embryos (Cech et al)		
Green sunfish	Can survive temps up to 38°C. Upper lethal tolerance 39-41°C depending on acclimation temp (Carveth et al 2006)		
Hardhead			
Hitch	In lab fish acclimated to 30°C can withstand 38°C (CTM) for a short time.		
Inland silverside			
Kern brook lamprey			
Kokanee			
Largemouth bass	Can live at temps 36-37°C. Upper lethal tolerance 39.5°C depending on acclimation temp (Carveth et al 2006)		
Longfin smelt	Can withstand 20°C.		
Longjaw mudsucker	Can survive temps of at least 35°C.		
Misquitofish	Can occur to 42°C (Moyle). Upper lethal tolerance 40-42.5°C depending on acclimation temp (Carveth et al 2006)	Can occur as low as 0.5°C but temps less than 4C usually lethal (Moyle 2002).	
Pacific lamprey	Temps >28°C are lethal to ammocoetes (van de Wetering and Ewing 1999)		
Prickly sculpin			

Table10-1: Physiological variables of selected fish species in the San Francisco Estuary.

Species	Upper Thermal Max	Lower Thermal Min	Stressful Temperatures
Pumpkinseed	Thermal tolerance up to 38°C	Thermal tolerance down to 3-4°C. Feeding stops at temps below 6.5°C.	
Rainbow trout	Greater than 23°C can be lethal if not slowly acclimated. 24-27C are lethal, except for very short intervals. Lethal temps for large trout are 23-24C.	Less than 4°C can be lethal if not slowly acclimated.	Range of thermal maxima (29.4-30.0C) for all treatments (stress). The electroshocked group's thermal maxima (30.0C) was significantly higher than other groups (Strange et al. 1993).
Rainwater killifish			
Red shiner	Can tolerate up to 39.5°C. Upper lethal tolerance 39-41°C depending on acclimation temp (Carveth et al 2006)		
Redear sunfish			
Redeye bass			
Riffle sculpin	Temps over 30°C are usually lethal. Thermal max: 28, 29°C (Cech et al. 1990)		
River lamprey			
Sacramento pikeminnow	Reported temp max: 22.5, 24, 25°C depending on acclimation (Cech et al. 1990). Above 38°C is lethal. (Moyle).		
Sacramento blackfish	In a lab setting, juveniles can withstand temps up to 37°C		
Sacramento perch	Can acclimate to temps up to 30°C.		
Sacramento splittail	Fish acclimated to high temps can survive rapid changes and temps 29-33°C for a short time.		
Sacramento sucker	In a lab setting, 36C in the upper lethal temp for fish acclimated to warm water.		
Shimofuri goby	Can tolerate temps up to 37°C in the lab.		
Shiner perch	Depending on acclimation can survive in temps up to 30C.		
Smallmouth bass	Above 38°C is lethal.		Temps above 35°C are stressful,

Table 10-1: Physiological variables of selected fish species in the San Francisco Estuary.

Species	Upper Thermal Max	Lower Thermal Min	Stressful Temperatures
Speckled dace	Can survive as high as 34°C (sub-species specific). Upper lethal tolerance 36-37°C depending on acclimation temp (Carveth et al 2006)		
Spotted bass			
Staghorn sculpin	Juveniles tolerant of high temps (over 25°C)		
Starry flounder			
Steelhead	Critical thermal maximum: 27.5C when acclimated to 11C. 29.6 when acclimated to 19C.		
Striped bass	Temps over 30°C usually lethal.		Under stress once temps exceed 25°C
Threadfin shad		The northernmost overwinter survival--temperature recorded was 8.3 C.	
Threespine stickleback	Have been observed up to 25°C (Cowen 1991)		
Tidewater goby			
Topsmelt			
Tule perch	Temp max: 25.5, 27 °C depending on acclimation (Cech et al. 1990)		
Wakasagi	Lab Critical Thermal Max 27-29°C	Min 2-4.5°C	
Warmouth			
White catfish	Can survive temps of 29-31°C		
White crappie	>31°C is avoided.		
white sturgeon			
Yellowfin goby			

Table10-1: Physiological variables of selected fish species in the San Francisco Estuary.

Species	Prefered/Optimal Temperature	Salinity tolerance	Spawning Preferences
American shad	Optimal developmental temp: 17°C, Pref. 17-25°C	Young can live in salinities up to 20 ppt Have been collected at salinities up to 4.2 ppt.	Peak runs and spawning usually occur at 17-24 C in the Sac River and decrease significantly at temps above 20 C. At Millerton Reservoir peak spawning occurs at temps 11-17C usually in flows 20-60 cm/sec. Spawning occurs between 31-91 cm/sec.
Bigscale logperch		up to 13 ppt.	
Black bullhead			
Black crappie	Optimal summer temps: 27-29C	Salinity tolerance: up to 10 ppt.	Spawning temps: 14-20C
Blue catfish	Optimal growth: 27C	Up to 22 ppt. Optimal growth: less than 7- 8 ppt	Spawning takes place in early summer at temps between 21-25C.
Bluegill	Preferred temps/optimal growth: 27-32°C.	Prefer freshwater but have been found at 8 ppt. 12 ppt. is lethal.	Spawning temps: 18-21C.
Brook trout	prefer: 14-19°C poor growth above 19°C		
Brown bullhead	optimal growth temp 20-33°C.	Salinity tolerance 0-18 ppt.	
Brown trout	preferred: 12-20°C, optimal growth 17-18°C.		
California roach	Tolerant of 30-35C as well as cold, clear headwater streams.	Can survive salinities of 3 ppt. but die before salinity reaches 9-10 ppt.	Spawning is temperature dependent, usually occurring when temps are above 16C.
Chameleon goby	Thermal range 2-20C		
Channel catfish	Optimal growth: 24-30°C	Salinity to 10 ppt.	Spawning temp: 21-28C.
Chinook salmon	Food consumption and growth rates increased with temp over an 11-19C range (Myrick and Cech 2002). Egg & larval development -most successful between 6-12°C, dependent on acclimation temp (Myrick and Cech 2004).	anadromous Can survive salinities up to 16 ppt and are commonly found in estuaries of 10-12 ppt.	
Common carp	Optimal temp for growth ~24C, but are active in temp range 4-24C		Spawning occurs in spring and summer when temps > 15C with greatest spawning activity at 19-23C.

Table10-1: Physiological variables of selected fish species in the San Francisco Estuary.

Species	Prefered/Optimal Temperature	Salinity tolerance	Spawning Preferences
Delta smelt	Field collection: Temp 6-23°C, mean 15°C (Moyle et al. 1992). Found in a wide temperature range 6-28°C; Eggs hatch in 9-13 days when temps range between 14.8-16.5°C (Moyle 2002).	Most abundant in low salinity water associated with the mixing zone in the estuary, except when spawning - fish were captured in salinities of 0-14‰ (mean 2‰) (Moyle et al. 1992). Most often found in salinity range of 2-7 ppt. but can also be found in 0-18.4 ppt and can tolerate up to 19 ppt (Moyle 2002) Able to tolerate 19.1 ppt (acclimated to 17°C and freshwater (0 ppt) (Swanson et al. 2000)), and swim 43.3 cm/s v. 28.2 cm/s	Most spawning takes place at 7-15°C but observation suggests it can take place over 7-22°C (Moyle 2002).
fathead minnow	Temp preference: 22-23°C (Moyle 2002).		
Golden shiner			Spawning usually begins when temps reach ~20°C but has been recorded at temps as low as 14°C and rarely occurs above 27°C. Eggs hatch in 4-5 days at 24-27°C.
Goldfish	Prefer warmer temps 27-37°C		Spawning temp requirements; 16-26°C
Green sturgeon	Given access to abundant food and quality water, juveniles grow faster at 24°C and cycling of 24-19°C than at 19°C. Other stressors may change these results. Juvenile class studied (~0.1-10g) appear to be more temp tolerant than the egg, embryonic, larval, or larger juvenile stages (Allen). Optimal growth range for older juveniles; 15-19°C (Mayfield and Cech 2004). 17-18°C is probable upper limit of thermal optima for embryos, developmental abnormality rates increase significantly above these temps (Van Eenennaam et al. 2005).		March-July when temps are 8-14°C
Green sunfish	26-30°C is preferable	Low salinity tolerance and avoid salinities higher than 1-2 ppt.	Have been observed spawning at temps 15-28°C, spawning in CA usually doesn't occur until temps reach 19°C
Hardhead	Optimal temp. 24-28°C (Knight 1985).		Observed spawning April-May in water temperatures between 13-20°C (Grant and Maslin 1999).

Table10-1: Physiological variables of selected fish species in the San Francisco Estuary.

Species	Prefered/Optimal Temperature	Salinity tolerance	Spawning Preferences
Hitch	Prefer temperature range 27-29C	Ability to withstand salinity-- have been found in 7-9 ppt.	Spawning takes place in riffles with fine, clean gravel and temperatures 14-18C . Spawning has also been observed at 18-26C in low flow areas, and in ponds and reservoirs. Eggs hatch at 15-22C. Larval prefer swallow water with dense cover.
Inland silverside	Occur in water temps 8-34*C, but 20-25*C are probably optimal for growth.	Can survive salinities over 33 ppt. and commonly found at 10-15 ppt.	
Kern brook lamprey	Prefer habitat where the temperature rarely exceeds 25*C in the summer.		
Kokanee	Prefer 10-15*C		
Largemouth bass	Growth can occur from 10-35C, prefer 27C. Juveniles prefer 30-32C.	Can live in salinities up to 16 ppt, but in CA they avoid salinities >5 ppt.	
Longfin smelt	Temperature range in summer 16-18*C	Can be found in salinities from 0 ppt to almost pure sea water, although prefer 15-30 ppt. once past early juvenile stages.	Spawning takes place in fresh water at night in temps 7-14.5C (SF Bay) and has been observed at lower temps else where. Eggs hatch in 40 days at 7C.
Longjaw mudsucker	Prefer 9-23*C	Salinity range 82.5-12 ppt. Can only survive freshwater for 2-3 days.	
Mosquitofish	Persist 10-35C, optimal growth 25-30C (Moyle 2002). Temp at 20, 25, and 30*C with ad lib feed= growth rate increased with temp. Growth rates cycling 20-30*C were faster than at 25*C (Vondracek et al. 1988). Activity increased with temp and was usually highest at intermediate feeding levels. Temp of 10,15, 20, 25, 30, 35 were used. Max growth occurred at 30C and declined slightly at 35C. On reduced food, max growth occurred at 25C (Wurtsbaugh and Cech 1983).	Salinity tolerance 0-58 ppt. persist mainly in salinities under 25 ppt. (Moyle 2002)	Temp increase from 20-30C age at reproduction decreased from 191 to 56 days, brood size and mass of offspring increased. Fish at cooler temps started reproduction at a smaller size (Vondracek et al. 1988).
Pacific lamprey	Prefer temps below 20*C. Response to temperature was measured as the number of individuals surviving to the next growth stage and/or exhibiting abnormalities. Survival was greatest at 18C then 14, 10, and 22C. Greatest number of abnormalities in the larval stage was at 22C followed by 18,	Phase 5 metamorphs unable to withstand salinities>13.4%. P6 survived direct transfer to sea water (30% S) (Richards and Beamish 1981)	Spawning takes place earlier in the Santa Clara R. than in more northern rivers (Jan-May vs. April-July). Earlier timing of both upstream migration and spawning is likely an adaption to the timing of precipitation in S. CA. --> stream flow a necessity of lamprey spawning (Chase 2001). Temp observations for nests 12-18 C (Moyle 2002). Spawning at 2-3 m and at 50cm --undirectional

Table 10-1: Physiological variables of selected fish species in the San Francisco Estuary.

Species	Prefered/Optimal Temperature	Salinity tolerance	Spawning Preferences
	10, and 14C (Meeuwig et al. 2005).		flow may not always be a requirement for spawning (Russell et al. 1987).
Prickly sculpin	Both cold and warm temperatures (28-30°C summer temps).		Spawning occurs Feb-June with stream temps of 8-13C.
Pumpkinseed	Prefer 24-32C.	Can tolerate up to 17 ppt	
Rainbow trout	0°C in winter to 26-27°C in summer. Optimal temp for growth 15-18C.		
Rainwater killifish	10-25°C	Salinity tolerance 0-80 ppt.	Spawning observed at 17-25C and salinities of 0-18 ppt.
Red shiner	Prefer 25-30C	In lab can tolerate salinities up to 10 ppt. Can live with seasonal salinities of 5-12 ppt. and can quickly adjust to changing salinities. Can tolerate up to 20 ppt.	Spawning takes place throughout the summer between 21-24°C (Wang 1986, Moyle 2002)
Redear sunfish	Warm water species.		
Redeye bass	Exist in clear and warm stream 26-28C summer temps.		Spawn in late spring when temps reach 17-21C.
Riffle sculpin	Prefer temperatures not exceeding 25-26C		Eggs hatch in 11 days at 15C and 24 days at 10C.
River lamprey			Spawn in gravelly riffles, ammocoetes live in silty backwaters and eddies.
Sacramento pikeminnow	Common temperature range 18-28C. Max preferred temp. ~26C Optimum temp. 22-28C (Moyle 2002). Growth rates increased with temperature. 3 temp treatments; cool (17-18C), medium (24-26C), warm (27.5-30C) were used (Cech et al. 1990).	Observed at salinities as high as 8 ppt, but are rarely found above 5 ppt.	Spawning thought to occur most often April-July at 12-24C in shallow areas w/ heavy plant growth. Spawning has been observed in 90cm of water over dense vegetation as well as over rocks <18cm deep (Moyle 2002).
Sacramento blackfish		Commonly found in salinities of 7 ppt., but have been found at 9 ppt. (Moyle 2002)	Spawning occurs March- Aug in temps of 18-29°C (Moyle 2002). Spawning from June-Aug. when water temps reached 20°C (Vigg and Kucera 1981).
Sacramento perch	Range 18-28°C	Can survive and reproduce in salinities 0-18 ppt.	

Table10-1: Physiological variables of selected fish species in the San Francisco Estuary.

Species	Prefered/Optimal Temperature	Salinity tolerance	Spawning Preferences
Sacramento splittail	Typical temperature range is 5-24°C Preferred temp appears to be 20-25°C, but found in streams with temps not exceeding 15-16C and as high as 29-30C.	Salinity tolerance increases with size- adults can withstand up to 29 ppt for a short time. Regularly found in 10-18 ppt, but seem to prefer the lower levels (Moyle 2002). Splittail salinity range 0-10% (Sommer et al. 1997).	Spawning appears to be associated with temps 14-19C at depths 0.5-2m within floodplains. Young fish are most abundant in shallow water <2m (Moyle 2002).
Sacramento sucker		Adults have been found in salinities above 13 ppt.	Spawning occurs over gravel riffles, Feb-June at temps of 12-18C.
Shimofuri goby		Have been found in salinities as high as 19 ppt. Embryos can develop between 13-34C and 0-7 ppt.	
Shiner perch	Occur at 7-26C uncommon where temps are over 24-25C.	Found at salinities of 0-34 ppt.	
Smallmouth bass	Mostly occur where summer temps range 20-27°C, optimum growth 25-27°C.	Some salinity tolerance.	Spawning occurs spring/summer when temp reach 13-16°C. Spawning most likely induced by rising water temps and/or high flow events. At 18-19C eggs hatch in ~6 days.
Speckled dace	Can live in a wide temperature range 0-29C		
Spotted bass	Prefer habitat with summer temps of 24-31°C .	Low salinity tolerance, have been found in waters up to 10 ppt. Juveniles tolerant of high salinities (over 67 ppt), In SF Estuary they are found in salinities 0-34 ppt.	Spawn in late spring when temps reach 15-18°C continues till June when temps reach 22-23°C.
Staghorn sculpin			
Starry flounder	Usually found at temps 10-20°C.	Salinities of 0-15 ppt.	
Steelhead	Growth rate highest at 19C than either 11 or 15C.		
Striped bass		Can withstand abrupt changes in temp in conjunction with changes in salinity. Often move between fresh and marine waters.	
Threadfin shad	Best growth and survival occur at temps not below 7-9C in winter and not above 22-24C in summer.	Live mainly in freshwater and are much less abundant as salinity increases, although they can grow and survive in sea water, which appears to inhibit reproduction.	Spawning occurs April-Aug. when water temps > 20C, although spawning has been observed at 14-18C.

Table10-1: Physiological variables of selected fish species in the San Francisco Estuary.

Species	Prefered/Optimal Temperature	Salinity tolerance	Spawning Preferences
Threespine stickleback	Require cool water for long term survival <23-24°C. Food-deprived fish preferred cooler temperatures (mean = 15.9°C, final = 15.8°C) than fed fish (mean = 20.1°C, final = 19.0°C (Magee et al. 1999). Thermal preference= 9-12°C in lab setting (Lachance et al. 1987)	Can complete lifecycle in fresh or marine water, broad salinity tolerance. Prefers: 7-14 ppt in lab setting (Audet et al. 1985)	Spawning takes place April-July
Tidewater goby	Can live and breed at temperatures of 8-25°C	Can live and breed at salinities of 2-27 ppt. and can live at salinities of 0-41ppt.	Annual lifecycle completely within the lagoon-- Spawning takes place April to May in 18-22 C water, salinity 5-10 ppm (Swift 1989)
Topsmelt	Occur at temps 5-29°C	Occur at salinities 0-34 ppt. Live in salinities 0-19 ppt. and have been found at salinities as high as 30 ppt.	Spawning occurs March- Oct. at 10-27°C and up to 72 ppt. - optimal spawning: 13-27°C, around 30 ppt.
Tule perch	Prefer temps below 22C and rarely found above 25C.		
Wakasagi	optimal: 14-21°C for growth and reproduction.	Salinity tolerance 0-29 ppt.	
Warmouth	Optimal summer temps: 22-28°C.	Avoid salinities > 1-4 ppt. but can survive up to 17 ppt.	Spawning takes place late spring-early summer when temps reach ~ 21°C.
White catfish	Perfer temps > 21°C --	Can survive salinities up to 11-14.5 ppt.	Spawning usually takes place in June-July when temps > 21°C.
White crappie	Optimal temps: 27-29°C	Have been collected at salinities as high as 10 ppt.	Spawning begins April-May with temps 17-20°C.
white sturgeon		There is a gradual increase in the upper salinity tolerance with weight; 5-10ppt for 0.4-0.9g fish, 10-15ppt for 0.7-1.8g, 15ppt for 4.9-50.0g. Young adults are able to tolerate higher salinities (35ppt) than juveniles (McEnroe and Cech 1985).	Optimal spawning temp 14-16C (Kohlhorst 1976). Females require exposure to cold (ca. 10C) for oocyte development and ovulation to proceed normally (Webb et al. 1999, Linares-Casenave et al. 2002)
Yellowfin goby	Have been found in temps 15-32°C	Have been found in salinities 16-40 ppt.	Require salinities of at least 5 ppt for breeding.

Table10-1: Physiological variables of selected fish species in the San Francisco Estuary.

Species	Velocity Preferences	Migration Preferences	Citation
American shad		American shad migration in the Connecticut River began at 19C, peaked at 14-19 C and ended at 10-8C.	Moyle 2002, (O'Leary and Kynard, 1986), Moss 1970, Marcy et al., 1972, Chittenden 1972
Bigscale logperch			Moyle, 2002
Black bullhead			Moyle 2002, [Smale and Rabeni 1995], (Black 1953)
Black crappie			Moyle 2002 , [Houston 1982, (Baker and Heidinger 1996), Becker 1983]
Blue catfish			Moyle, 2002
Bluegill			Moyle, 2002 Houston 1982, Peterson et al. 1987, Carveth et al. 2004
Brook trout			Moyle, 2002
Brown bullhead			Moyle, 2002, Becker 1983
Brown trout			Moyle, 2002, Armour 1994
California roach	Observed in slow velocity waters (<40 cm/sec) as well as fast current.		Moyle, 2002, Cech et al., 1990
Chameleon goby			Eschmeyer et al., 1983
Channel catfish			Moyle, 2002, Allen and Strawn 1968, Becker 1983, Clemens and Sneed 1957
Chinook salmon			Marine and Cech 2004, Myrick and Cech 2002, 2004
Common carp			Moyle, 2002

Table10-1: Physiological variables of selected fish species in the San Francisco Estuary.

Species	Velocity Preferences	Migration Preferences	Citation
Delta smelt	62% of fish captured were in water less than 4 m deep, the rest were caught in deeper water (Moyle and Herbold). Prefer areas of low velocity-- max swimming velocities of around 28 cm/sec (Moyle 2002). 58% of Ucrit test group able to sustain at a mean of 27.6+/-5.1 cm/s. Ucrit not effected by acclimation temp or fish size (3.2-6.8cm SL). The rest of the fish failed to swim at velocities above 10-15 cm/s (Swanson 1998). Able to swim 43.3 cm/s v. 28.2 cm/s (acclimated to 17°C and freshwater (0 ppt) (Swanson 2000)). Night conditions decreased delta smelt swimming velocities (Young 2004).		Moyle et al. 1992, Moyle 2002, Swanson et al., 1998, Young et al., 2004
fathead minnow	swimming velocity rates under lab conditions- (Ward 2003)		Moyle, 2002, Castleberry and Cech, Carveth et al., 2004
Golden shiner			Moyle, 2002
Goldfish			Moyle, 2002
Green sturgeon			Allen et al. 2006, Mayfield and Cech, 2004, Van Eenennaam et al., 2005, Fry 1973, Moyle 1995, 2002, Cech et al., 2000
Green sunfish			Moyle, 2002, McCarraher 1972, Peterson 1988, Becker 1983, Carveth et al. 2004
Hardhead	Prefer clear, deep pools (>80cm) and runs w/ rocky substrate and slow velocity (20-40cm/sec). Also observed in pools or runs 40-140cm deep, velocity 0-30 cm/sec (Moyle).		Moyle, 2002, Grant and Maslin, 1999, Myrick and Cech, 2000, Cech et al., 1990, Knight 1985
Hitch	Found in slow moving, quiet water.		Moyle, 2002
Inland silverside			Moyle, 2002, Hubbs et al. 1971, Kramer et al. 1987
Kern brook lamprey	Adults prefer riffles, ammocoetes are usually in shallow pools and where flows are light		Moyle, 2002
Kokanee			Moyle, 2002
Largemouth bass			Moyle, 2002, Carveth et al., 2004
Longfin smelt			Moyle, 2002
Longjaw mudsucker			Moyle, 2002

Table 10-1: Physiological variables of selected fish species in the San Francisco Estuary.

Species	Velocity Preferences	Migration Preferences	Citation
Mosquitofish			Moyle 2002, Vondracek et al., 1988, Wurtssbaugh and Cech, 1985, Carveth et al., 2004
Pacific lamprey	Flow observations for nests: swift flow 11-84cm/sec, depth observations for nests 30-150cm (Moyle). Larvae associated with low velocity, fine particulate burrowing substratum and pools significant only at small spatial scales(1-10m). Water depth, open riparian canopy positively associated with larval abundance at large scales (1-10km) (Torgersen&Close).	Increase in discharge (flow rate) initiated downstream migration of young adults (Beamish&Levings)	Beamish and Levings 1991, Chase 2001, Meeuwig et al., 2005, Moyle 2002, Richards and Beamish 1981, Russel et al. 1987, Torgersen and Close 2004, van de Wetering and Ewing 1999
Prickly sculpin	89% (n=981) of sculpin used habitat with water velocity < 5 cm/sec, 37% were found in depths > 7m (White&Harvey)		Moyle 2002, White and Harvey 1999
Pumpkinseed			Moyle, 2002 Houston 1982, Becker 1983, Peterson 1988, Keast 1968
Rainbow trout			Moyle, 2002, Hokanson et al. 1977, Bjornn and Reiser 1991, Kubicek and Price 1976, Strange et al., 1993
Rainwater killifish			Moyle, 2002, Wang 1986
Red shiner	Large numbers found in velocities of 10-50 cm/sec, in water less than 30 cm, over silt near cover.		Moyle, 2002, Carlander 1969, Peters 1989, Carveth et al. 2004
Redear sunfish			Moyle, 2002, Jenkins and Burkhead 1994, Peterson 1988, Wang, 1986
Redeye bass			Moyle, 2002, Lambert 1990
Riffle sculpin	Cold headwater, riffle streams. Observed mean water velocity, 42-44 cm/sec, mean depth 38-39 cm. Shelter velocity 8-9 cm/sec.		Moyle, 2002, Cech et al., 1990
River lamprey			Moyle, 2002
Sacramento pikeminnow	Fish greater than 12 cm SL found in water deeper than 1 m w/ mean velocity <40cm/sec. Smaller fish migrate towards slower, shallower water.		Moyle 2002, Cech et al., 1990
Sacramento blackfish			Cech et al. 1982, Moyle, 2002
Sacramento perch			Moyle 2002, Vigg and Kucera, 1981
Sacramento splittail			Moyle 2002, Young and Cech, 1996
Sacramento sucker	Juveniles (<50 mm LS) forage in shallow (20-60cm deep), slow <10 cm/sec water along stream margins. Adults usually found in deep pools and runs <40 cm/sec during the day.		Moyle, 2002, Cech et al., 1990, Knight 1985.

Table 10-1: Physiological variables of selected fish species in the San Francisco Estuary.

Species	Velocity Preferences	Migration Preferences	Citation
Shimofuri goby			Moyle, 2002, Matern 1999, 2001
Shiner perch			Moyle, 2002, Baxter et al., 1999, Emmett et al., 1991
Smallmouth bass			Moyle 2002, Edwards et al. 1983, Armour 1993, Coble 1975, Lambert and Handley 1984
Speckled dace	Prefer shallow (<60 cm), rocky riffles and runs. Speckled dace were found in higher densities in years with the highest spring flows (Propst and Gido 2004)		Moyle, 2002, Carveth et al., 2004
Spotted bass			Moyle, 2002, Houston 1982, Peterson 1988, Aasen and Henry 1981
Staghorn sculpin			Moyle, 2002, Morris 1960, Baxter et al., 1999
Starry flounder			Moyle, 2002, Baxter et al., 1999
Steelhead			Myrick and Cech, 2005
Striped bass			Moyle, 2002
Threadfin shad			Lewis 1977, Moyle 2002
Threespine stickleback			Moyle, 2002, Snyder and Dingle 1989, Magee et al. 1999, Lachance and Magan, 1987, Cowen, 1981, Audet et al., 1985
Tidewater goby			Moyle, 2002, Swift et al., 1989
Topsmelt			Moyle, 2002, Baxter et al. 1999, Emmett et al. 1991, Middaugh and Shenker 1988
Tule perch	Use pools and runs 0.5-1 m deep and forage where water runs 1-14 cm/sec.		Moyle, 2002, Cech et al., 1990
Wakasagi			Moyle, 2002, Swanson et al., 2000
Warmouth			Moyle, 2002, Jenkins and Burkhead 1994, Becker 1983, Larimore 1957
White catfish			Moyle 2002, Ganssle 1966, Kendall and Schwartz 1968, E. Miller 1966

Table10-1: Physiological variables of selected fish species in the San Francisco Estuary.

Species	Velocity Preferences	Migration Preferences	Citation
White crappie			Moyle, 2002, Becker 1983
white sturgeon		Adults migrate of the Sac R. for SF bay during late fall and stay at low temps (7-12C) before spawning (Cech and Doroshov 2004).	Cech and Doroshov, 2004, McEnroe and Cech, 1985
Yellowfin goby			Moyle, 2002, Williams et al. 1998, Wang 1986

Table 10-2: Habitat suitability index parameters							
species/taxa	scientific name	family	Parameter	GAM Deviance explained(%)	Salinity	Estuarine Use	Months Used for Analysis
California Department of Fish and Wildlife- Bay Study, midwater trawl survey							
American shad	<i>Alosa sapidissima</i>	Clupeidae	Salinity	30.8	Mesohaline	anadromous	Jul-Dec
American shad	<i>Alosa sapidissima</i>	Clupeidae	Surface Temperature	4.54	Mesohaline	anadromous	Jul-Dec
American shad	<i>Alosa sapidissima</i>	Clupeidae	Secchi	7.21	Mesohaline	anadromous	Jul-Dec
American shad age0	<i>Alosa sapidissima</i>	Clupeidae	Salinity	32.2	Mesohaline	anadromous	Jul-Dec
American shad age0	<i>Alosa sapidissima</i>	Clupeidae	Surface Temperature	4.58	Mesohaline	anadromous	Jul-Dec
American shad age0	<i>Alosa sapidissima</i>	Clupeidae	Secchi	7.14	Mesohaline	anadromous	Jul-Dec
delta smelt	<i>Hypomesus transpacificus</i>	Osmeridae	Salinity	14.9	Oligohaline	resident	Jan-Dec
delta smelt	<i>Hypomesus transpacificus</i>	Osmeridae	Surface Temperature	3.91	Oligohaline	resident	Jan-Dec
delta smelt	<i>Hypomesus transpacificus</i>	Osmeridae	Secchi	7.93	Oligohaline	resident	Jan-Dec
delta smelt age0	<i>Hypomesus transpacificus</i>	Osmeridae	Salinity	29.5	Oligohaline	resident	Jun-Dec
delta smelt age0	<i>Hypomesus transpacificus</i>	Osmeridae	Surface Temperature	4.63	Oligohaline	resident	Jun-Dec
delta smelt age0	<i>Hypomesus transpacificus</i>	Osmeridae	Secchi	8.02	Oligohaline	resident	Jun-Dec
jacksmelt	<i>Atherinopsis californiensis</i>	Atherinopsidae	Salinity	7.46	Polyhaline	Obligate nursery	Mar-Nov
jacksmelt	<i>Atherinopsis californiensis</i>	Atherinopsidae	Surface Temperature	4.67	Polyhaline	Obligate nursery	Mar-Nov
jacksmelt	<i>Atherinopsis californiensis</i>	Atherinopsidae	Secchi	3.53	Polyhaline	Obligate nursery	Mar-Nov
jacksmelt age0	<i>Atherinopsis californiensis</i>	Atherinopsidae	Salinity	11.6	Polyhaline	Obligate nursery	Jun-Dec
jacksmelt age0	<i>Atherinopsis californiensis</i>	Atherinopsidae	Surface Temperature	3.27	Polyhaline	Obligate nursery	Jun-Dec
jacksmelt age0	<i>Atherinopsis californiensis</i>	Atherinopsidae	Secchi	9.46	Polyhaline	Obligate nursery	Jun-Dec

Table 10-2: Habitat suitability index parameters

species/taxa	scientific name	family	Parameter	GAM Deviance explained(%)	Salinity	Estuarine Use	Months Used for Analysis
longfin smelt	<i>Spirinchus thaleichthys</i>	Osmeridae	Salinity	8.88	Polyhaline	anadromous	Jan-Dec
longfin smelt	<i>Spirinchus thaleichthys</i>	Osmeridae	Surface Temperature	6.01	Polyhaline	anadromous	Jan-Dec
longfin smelt	<i>Spirinchus thaleichthys</i>	Osmeridae	Secchi	11	Polyhaline	anadromous	Jan-Dec
longfin smelt age0	<i>Spirinchus thaleichthys</i>	Osmeridae	Salinity	9.87	Polyhaline	anadromous	May-Dec
longfin smelt age0	<i>Spirinchus thaleichthys</i>	Osmeridae	Surface Temperature	2.28	Polyhaline	anadromous	May-Dec
longfin smelt age0	<i>Spirinchus thaleichthys</i>	Osmeridae	Secchi	8.98	Polyhaline	anadromous	May-Dec
northern anchovy	<i>Engraulis mordax</i>	Engraulidae	Salinity	30.8	Polyhaline	opportunistic	Mar-Oct
northern anchovy	<i>Engraulis mordax</i>	Engraulidae	Surface Temperature	6.32	Polyhaline	opportunistic	Mar-Oct
northern anchovy	<i>Engraulis mordax</i>	Engraulidae	Secchi	2.6	Polyhaline	opportunistic	Mar-Oct
northern anchovy age0	<i>Engraulis mordax</i>	Engraulidae	Salinity	30	Polyhaline	opportunistic	Mar-Nov
northern anchovy age0	<i>Engraulis mordax</i>	Engraulidae	Surface Temperature	5.9	Polyhaline	opportunistic	Mar-Nov
northern anchovy age0	<i>Engraulis mordax</i>	Engraulidae	Secchi	2.51	Polyhaline	opportunistic	Mar-Nov
Pacific herring	<i>Clupea pallasii</i>	Clupeidae	Salinity	5.32	Polyhaline	Obligate nursery	Feb, April-Oct
Pacific herring	<i>Clupea pallasii</i>	Clupeidae	Surface Temperature	15.4	Polyhaline	Obligate nursery	Feb, April-Oct
Pacific herring	<i>Clupea pallasii</i>	Clupeidae	Secchi	0.893	Polyhaline	Obligate nursery	Feb, April-Oct
Pacific herring age0	<i>Clupea pallasii</i>	Clupeidae	Salinity	5.14	Polyhaline	Obligate nursery	April-Oct
Pacific herring age0	<i>Clupea pallasii</i>	Clupeidae	Surface Temperature	15.7	Polyhaline	Obligate nursery	April-Oct
Pacific herring age0	<i>Clupea pallasii</i>	Clupeidae	Secchi	0.8	Polyhaline	Obligate nursery	April-Oct
plainfin midshipman	<i>Porichthys notatus</i>	Batrachoididae	Salinity	1.79	Polyhaline	Obligate	April-Oct, Dec

Table 10-2: Habitat suitability index parameters							
species/taxa	scientific name	family	Parameter	GAM Deviance explained(%)	Salinity	Estuarine Use	Months Used for Analysis
						nursery	
plainfin midshipman	Porichthys notatus	Batrachoididae	Surface Temperature	0.744	Polyhaline	Obligate nursery	April-Oct, Dec
plainfin midshipman	Porichthys notatus	Batrachoididae	Secchi	4.37	Polyhaline	Obligate nursery	April-Oct, Dec
shiner perch	Cymatogaster aggregata	Embiotocidae	Salinity	5.63	Polyhaline	Obligate nursery	Feb-Oct
shiner perch	Cymatogaster aggregata	Embiotocidae	Surface Temperature	3.68	Polyhaline	Obligate nursery	Feb-Oct
shiner perch	Cymatogaster aggregata	Embiotocidae	Secchi	0.729	Polyhaline	Obligate nursery	Feb-Oct
shiner perch age0	Cymatogaster aggregata	Embiotocidae	Salinity	7.26	Polyhaline	Obligate nursery	Jun-Dec
shiner perch age0	Cymatogaster aggregata	Embiotocidae	Surface Temperature	4.09	Polyhaline	Obligate nursery	Jun-Dec
shiner perch age0	Cymatogaster aggregata	Embiotocidae	Secchi	0.261	Polyhaline	Obligate nursery	Jun-Dec
striped bass	Morone saxatilis	Moronidae	Salinity	21.9	Mesohaline	anadromous	Jan-Dec
striped bass	Morone saxatilis	Moronidae	Surface Temperature	2.44	Mesohaline	anadromous	Jan-Dec
striped bass	Morone saxatilis	Moronidae	Secchi	19.2	Mesohaline	anadromous	Jan-Dec
striped bass age0	Morone saxatilis	Moronidae	Salinity	24.4	Mesohaline	anadromous	Jan-April, Jun-Dec
striped bass age0	Morone saxatilis	Moronidae	Surface Temperature	4.64	Mesohaline	anadromous	Jan-April, Jun-Dec
striped bass age0	Morone saxatilis	Moronidae	Secchi	14.2	Mesohaline	anadromous	Jan-April, Jun-Dec
threadfin shad	Dorosoma petenense	Clupeidae	Salinity	24.3	Mesohaline	opportunist	Jul-Dec
threadfin shad	Dorosoma petenense	Clupeidae	Surface Temperature	10.2	Mesohaline	opportunist	Jul-Dec
threadfin shad	Dorosoma petenense	Clupeidae	Secchi	4.44	Mesohaline	opportunist	Jul-Dec
topsmelt	Atherinops affinis	Atherinopsidae	Salinity	8.45	Polyhaline	resident	Jan-April, July-Dec
topsmelt	Atherinops affinis	Atherinopsidae	Surface Temperature	0.457	Polyhaline	resident	Jan-April, July-Dec

Table 10-2: Habitat suitability index parameters							
species/taxa	scientific name	family	Parameter	GAM Deviance explained(%)	Salinity	Estuarine Use	Months Used for Analysis
topsmelt	Atherinops affinis	Atherinopsidae	Secchi	5.96	Polyhaline	resident	Jan-April, July-Dec
topsmelt age0	Atherinops affinis	Atherinopsidae	Salinity	9.32	Polyhaline	resident	Jan-April, Aug-Dec
topsmelt age0	Atherinops affinis	Atherinopsidae	Surface Temperature	0.527	Polyhaline	resident	Jan-April, Aug-Dec
topsmelt age0	Atherinops affinis	Atherinopsidae	Secchi	6.46	Polyhaline	resident	Jan-April, Aug-Dec
white croaker	Genyonemus lineatus	Sciaenidae	Salinity	1.57	Polyhaline	non-obligate nursery	Feb-Sept
white croaker	Genyonemus lineatus	Sciaenidae	Surface Temperature	1.56	Polyhaline	non-obligate nursery	Feb-Sept
white croaker	Genyonemus lineatus	Sciaenidae	Secchi	2.18	Polyhaline	non-obligate nursery	Feb-Sept
white croaker age0	Genyonemus lineatus	Sciaenidae	Salinity	3.3	Polyhaline	non-obligate nursery	May-Oct
white croaker age0	Genyonemus lineatus	Sciaenidae	Surface Temperature	1.99	Polyhaline	non-obligate nursery	May-Oct
white croaker age0	Genyonemus lineatus	Sciaenidae	Secchi	1.31	Polyhaline	non-obligate nursery	May-Oct
California Department of Fish and Wildlife- Bay Study, otter trawl survey							
bay goby	Lepidogobius lepidus	Gobiidae	depth	3.69	Polyhaline	resident	Jan-Dec
bay goby	Lepidogobius lepidus	Gobiidae	Bottom Salinity	11.3	Polyhaline	resident	Jan-Dec
bay goby	Lepidogobius lepidus	Gobiidae	SurfaceSalinity	12.3	Polyhaline	resident	Jan-Dec
bay goby	Lepidogobius lepidus	Gobiidae	Bottom Temperature	9.14	Polyhaline	resident	Jan-Dec
bay goby	Lepidogobius lepidus	Gobiidae	Surface Temperature	8.33	Polyhaline	resident	Jan-Dec
bay goby	Lepidogobius lepidus	Gobiidae	Secchi	3.41	Polyhaline	resident	Jan-Dec
bay goby age0	Lepidogobius lepidus	Gobiidae	depth	2.25	Polyhaline	resident	Jan-Jul, Nov-Dec
bay goby age0	Lepidogobius lepidus	Gobiidae	SurfaceSalinity	6.5	Polyhaline	resident	Jan-Jul, Nov-Dec
bay goby age0	Lepidogobius lepidus	Gobiidae	Bottom Salinity	5.28	Polyhaline	resident	Jan-Jul, Nov-Dec

Table 10-2: Habitat suitability index parameters

species/taxa	scientific name	family	Parameter	GAM Deviance explained(%)	Salinity	Estuarine Use	Months Used for Analysis
bay goby age0	Lepidogobius lepidus	Gobiidae	Surface Temperature	7.42	Polyhaline	resident	Jan-Jul, Nov-Dec
bay goby age0	Lepidogobius lepidus	Gobiidae	Bottom Temperature	7.83	Polyhaline	resident	Jan-Jul, Nov-Dec
bay goby age0	Lepidogobius lepidus	Gobiidae	Secchi	0.586	Polyhaline	resident	Jan-Jul, Nov-Dec
California halibut	Paralichthys californicus	Paralichthyidae	depth	1.96	Polyhaline	non-obligate nursery	Jan-Dec
California halibut	Paralichthys californicus	Paralichthyidae	SurfaceSalinity	4.54	Polyhaline	non-obligate nursery	Jan-Dec
California halibut	Paralichthys californicus	Paralichthyidae	Bottom Salinity	5.24	Polyhaline	non-obligate nursery	Jan-Dec
California halibut	Paralichthys californicus	Paralichthyidae	Surface Temperature	2.89	Polyhaline	non-obligate nursery	Jan-Dec
California halibut	Paralichthys californicus	Paralichthyidae	Bottom Temperature	3.16	Polyhaline	non-obligate nursery	Jan-Dec
California halibut	Paralichthys californicus	Paralichthyidae	Secchi	3.98	Polyhaline	non-obligate nursery	Jan-Dec
California tonguefish	Symphurus atricaudus	Cynoglossidae	depth	1.63	Polyhaline	non-obligate nursery	Feb-Oct
California tonguefish	Symphurus atricaudus	Cynoglossidae	SurfaceSalinity	2.31	Polyhaline	non-obligate nursery	Feb-Oct
California tonguefish	Symphurus atricaudus	Cynoglossidae	Bottom Salinity	3.34	Polyhaline	non-obligate nursery	Feb-Oct
California tonguefish	Symphurus atricaudus	Cynoglossidae	Surface Temperature	1.71	Polyhaline	non-obligate nursery	Feb-Oct
California tonguefish	Symphurus atricaudus	Cynoglossidae	Bottom Temperature	1.83	Polyhaline	non-obligate nursery	Feb-Oct
California tonguefish	Symphurus atricaudus	Cynoglossidae	Secchi	0.455	Polyhaline	non-obligate nursery	Feb-Oct
California tonguefish age0	Symphurus atricaudus	Cynoglossidae	depth	1.43	Polyhaline	non-obligate nursery	April-Oct
California tonguefish age0	Symphurus atricaudus	Cynoglossidae	SurfaceSalinity	1.38	Polyhaline	non-obligate nursery	April-Oct
California tonguefish age0	Symphurus atricaudus	Cynoglossidae	Bottom Salinity	2.18	Polyhaline	non-obligate nursery	April-Oct

Table 10-2: Habitat suitability index parameters							
species/taxa	scientific name	family	Parameter	GAM Deviance explained(%)	Salinity	Estuarine Use	Months Used for Analysis
California tonguefish age0	Symphurus atricaudus	Cynoglossidae	Surface Temperature	1.64	Polyhaline	non-obligate nursery	April-Oct
California tonguefish age0	Symphurus atricaudus	Cynoglossidae	Bottom Temperature	1.71	Polyhaline	non-obligate nursery	April-Oct
California tonguefish age0	Symphurus atricaudus	Cynoglossidae	Secchi	0.373	Polyhaline	non-obligate nursery	April-Oct
chameleon goby	Tridentiger trigonocephalus	Gobiidae	depth	2.59	Polyhaline	resident	Jan-Dec
chameleon goby	Tridentiger trigonocephalus	Gobiidae	SurfaceSalinity	7.68	Polyhaline	resident	Jan-Dec
chameleon goby	Tridentiger trigonocephalus	Gobiidae	Bottom Salinity	5.43	Polyhaline	resident	Jan-Dec
chameleon goby	Tridentiger trigonocephalus	Gobiidae	Surface Temperature	1.25	Polyhaline	resident	Jan-Dec
chameleon goby	Tridentiger trigonocephalus	Gobiidae	Bottom Temperature	1.15	Polyhaline	resident	Jan-Dec
chameleon goby	Tridentiger trigonocephalus	Gobiidae	Secchi	0.888	Polyhaline	resident	Jan-Dec
cheekspot goby	Ilypnus gilberti	Gobiidae	depth	5.43	Polyhaline	resident	Jan-Dec
cheekspot goby	Ilypnus gilberti	Gobiidae	SurfaceSalinity	10	Polyhaline	resident	Jan-Dec
cheekspot goby	Ilypnus gilberti	Gobiidae	Bottom Salinity	6.94	Polyhaline	resident	Jan-Dec
cheekspot goby	Ilypnus gilberti	Gobiidae	Surface Temperature	0.755	Polyhaline	resident	Jan-Dec
cheekspot goby	Ilypnus gilberti	Gobiidae	Bottom Temperature	0.894	Polyhaline	resident	Jan-Dec
cheekspot goby	Ilypnus gilberti	Gobiidae	Secchi	1.12	Polyhaline	resident	Jan-Dec
English sole	Parophrys vetulus	Pleuronectidae	depth	3.58	Polyhaline	non-obligate nursery	Feb-Oct
English sole	Parophrys vetulus	Pleuronectidae	SurfaceSalinity	12.7	Polyhaline	non-obligate nursery	Feb-Oct
English sole	Parophrys vetulus	Pleuronectidae	Bottom Salinity	12.2	Polyhaline	non-obligate nursery	Feb-Oct
English sole	Parophrys vetulus	Pleuronectidae	Surface Temperature	15.7	Polyhaline	non-obligate nursery	Feb-Oct

Table 10-2: Habitat suitability index parameters

species/taxa	scientific name	family	Parameter	GAM Deviance explained(%)	Salinity	Estuarine Use	Months Used for Analysis
English sole	Parophrys vetulus	Pleuronectidae	Bottom Temperature	15.7	Polyhaline	non-obligate nursery	Feb-Oct
English sole	Parophrys vetulus	Pleuronectidae	Secchi	3.5	Polyhaline	non-obligate nursery	Feb-Oct
English sole age0	Parophrys vetulus	Pleuronectidae	depth	3.7	Polyhaline	non-obligate nursery	Feb-Oct
English sole age0	Parophrys vetulus	Pleuronectidae	SurfaceSalinity	12.1	Polyhaline	non-obligate nursery	Feb-Oct
English sole age0	Parophrys vetulus	Pleuronectidae	Bottom Salinity	11.3	Polyhaline	non-obligate nursery	Feb-Oct
English sole age0	Parophrys vetulus	Pleuronectidae	Surface Temperature	15.6	Polyhaline	non-obligate nursery	Feb-Oct
English sole age0	Parophrys vetulus	Pleuronectidae	Bottom Temperature	15.4	Polyhaline	non-obligate nursery	Feb-Oct
English sole age0	Parophrys vetulus	Pleuronectidae	Secchi	2.74	Polyhaline	non-obligate nursery	Feb-Oct
longfin smelt	Spirinchus thaleichthys	Osmeridae	depth	1.04	Polyhaline	anadromous	Jan-Mar, May-Dec
longfin smelt	Spirinchus thaleichthys	Osmeridae	SurfaceSalinity	4.47	Polyhaline	anadromous	Jan-Mar, May-Dec
longfin smelt	Spirinchus thaleichthys	Osmeridae	Bottom Salinity	4.74	Polyhaline	anadromous	Jan-Mar, May-Dec
longfin smelt	Spirinchus thaleichthys	Osmeridae	Surface Temperature	2.86	Polyhaline	anadromous	Jan-Mar, May-Dec
longfin smelt	Spirinchus thaleichthys	Osmeridae	Bottom Temperature	2.66	Polyhaline	anadromous	Jan-Mar, May-Dec
longfin smelt	Spirinchus thaleichthys	Osmeridae	Secchi	0.586	Polyhaline	anadromous	Jan-Mar, May-Dec
longfin smelt age0	Spirinchus thaleichthys	Osmeridae	depth	1.04	Polyhaline	anadromous	May-Dec
longfin smelt age0	Spirinchus thaleichthys	Osmeridae	SurfaceSalinity	6.11	Polyhaline	anadromous	May-Dec
longfin smelt age0	Spirinchus thaleichthys	Osmeridae	Bottom Salinity	6.22	Polyhaline	anadromous	May-Dec
longfin smelt age0	Spirinchus thaleichthys	Osmeridae	Surface Temperature	4.73	Polyhaline	anadromous	May-Dec

Table 10-2: Habitat suitability index parameters

species/taxa	scientific name	family	Parameter	GAM Deviance explained(%)	Salinity	Estuarine Use	Months Used for Analysis
longfin smelt age0	<i>Spirinchus thaleichthys</i>	Osmeridae	Bottom Temperature	5.03	Polyhaline	anadromous	May-Dec
longfin smelt age0	<i>Spirinchus thaleichthys</i>	Osmeridae	Secchi	0.996	Polyhaline	anadromous	May-Dec
Pacific herring	<i>Clupea pallasii</i>	Clupeidae	depth	1.42	Polyhaline	Obligate nursery	Jan-Jun, Aug
Pacific herring	<i>Clupea pallasii</i>	Clupeidae	SurfaceSalinity	2.92	Polyhaline	Obligate nursery	Jan-Jun, Aug
Pacific herring	<i>Clupea pallasii</i>	Clupeidae	Bottom Salinity	2.86	Polyhaline	Obligate nursery	Jan-Jun, Aug
Pacific herring	<i>Clupea pallasii</i>	Clupeidae	Surface Temperature	3.46	Polyhaline	Obligate nursery	Jan-Jun, Aug
Pacific herring	<i>Clupea pallasii</i>	Clupeidae	Bottom Temperature	3.16	Polyhaline	Obligate nursery	Jan-Jun, Aug
Pacific herring	<i>Clupea pallasii</i>	Clupeidae	Secchi	1.5	Polyhaline	Obligate nursery	Jan-Jun, Aug
Pacific staghorn sculpin	<i>Leptocottus armatus</i>	Cottidae	depth	1.52	Polyhaline	resident	Mar-Oct
Pacific staghorn sculpin	<i>Leptocottus armatus</i>	Cottidae	SurfaceSalinity	9.42	Polyhaline	resident	Mar-Oct
Pacific staghorn sculpin	<i>Leptocottus armatus</i>	Cottidae	Bottom Salinity	10.5	Polyhaline	resident	Mar-Oct
Pacific staghorn sculpin	<i>Leptocottus armatus</i>	Cottidae	Surface Temperature	5.63	Polyhaline	resident	Mar-Oct
Pacific staghorn sculpin	<i>Leptocottus armatus</i>	Cottidae	Bottom Temperature	6.71	Polyhaline	resident	Mar-Oct
Pacific staghorn sculpin	<i>Leptocottus armatus</i>	Cottidae	Secchi	2.08	Polyhaline	resident	Mar-Oct
Pacific staghorn sculpin age0	<i>Leptocottus armatus</i>	Cottidae	depth	0.459	Polyhaline	resident	April-Oct
Pacific staghorn sculpin age0	<i>Leptocottus armatus</i>	Cottidae	SurfaceSalinity	8.26	Polyhaline	resident	April-Oct
Pacific staghorn sculpin age0	<i>Leptocottus armatus</i>	Cottidae	Bottom Salinity	9.51	Polyhaline	resident	April-Oct
Pacific staghorn sculpin age0	<i>Leptocottus armatus</i>	Cottidae	Surface Temperature	5.03	Polyhaline	resident	April-Oct

Table 10-2: Habitat suitability index parameters							
species/taxa	scientific name	family	Parameter	GAM Deviance explained(%)	Salinity	Estuarine Use	Months Used for Analysis
Pacific staghorn sculpin age0	Leptocottus armatus	Cottidae	Bottom Temperature	5.63	Polyhaline	resident	April-Oct
Pacific staghorn sculpin age0	Leptocottus armatus	Cottidae	Secchi	3	Polyhaline	resident	April-Oct
Pacific tomcod	Microgadus proximus	Gadidae	depth	13	Polyhaline	opportunist	Jan-Dec
Pacific tomcod	Microgadus proximus	Gadidae	SurfaceSalinity	3.63	Polyhaline	opportunist	Jan-Dec
Pacific tomcod	Microgadus proximus	Gadidae	Bottom Salinity	4.92	Polyhaline	opportunist	Jan-Dec
Pacific tomcod	Microgadus proximus	Gadidae	Surface Temperature	7.85	Polyhaline	opportunist	Jan-Dec
Pacific tomcod	Microgadus proximus	Gadidae	Bottom Temperature	9.53	Polyhaline	opportunist	Jan-Dec
Pacific tomcod	Microgadus proximus	Gadidae	Secchi	8.34	Polyhaline	opportunist	Jan-Dec
plainfin midshipman	Porichthys notatus	Batrachoididae	depth	8.4	Polyhaline	Obligate nursery	May-Dec
plainfin midshipman	Porichthys notatus	Batrachoididae	SurfaceSalinity	15	Polyhaline	Obligate nursery	May-Dec
plainfin midshipman	Porichthys notatus	Batrachoididae	Bottom Salinity	14.5	Polyhaline	Obligate nursery	May-Dec
plainfin midshipman	Porichthys notatus	Batrachoididae	Surface Temperature	4.34	Polyhaline	Obligate nursery	May-Dec
plainfin midshipman	Porichthys notatus	Batrachoididae	Bottom Temperature	5.2	Polyhaline	Obligate nursery	May-Dec
plainfin midshipman	Porichthys notatus	Batrachoididae	Secchi	2.69	Polyhaline	Obligate nursery	May-Dec
plainfin midshipman age0	Porichthys notatus	Batrachoididae	depth	7.23	Polyhaline	Obligate nursery	Jul-Dec
plainfin midshipman age0	Porichthys notatus	Batrachoididae	SurfaceSalinity	13.6	Polyhaline	Obligate nursery	Jul-Dec
plainfin midshipman age0	Porichthys notatus	Batrachoididae	Bottom Salinity	12.4	Polyhaline	Obligate nursery	Jul-Dec
plainfin midshipman age0	Porichthys notatus	Batrachoididae	Surface Temperature	2.3	Polyhaline	Obligate nursery	Jul-Dec
plainfin midshipman age0	Porichthys notatus	Batrachoididae	Bottom Temperature	2.77	Polyhaline	Obligate nursery	Jul-Dec

Table 10-2: Habitat suitability index parameters							
species/taxa	scientific name	family	Parameter	GAM Deviance explained(%)	Salinity	Estuarine Use	Months Used for Analysis
plainfin midshipman age0	Porichthys notatus	Batrachoididae	Secchi	2.4	Polyhaline	Obligate nursery	Jul-Dec
shimofuri goby	Tridentiger bifasciatus	Gobiidae	depth	5.55	Oligohaline	resident	Jan-Jun, Aug-Dec
shimofuri goby	Tridentiger bifasciatus	Gobiidae	SurfaceSalinity	22	Oligohaline	resident	Jan-Jun, Aug-Dec
shimofuri goby	Tridentiger bifasciatus	Gobiidae	Bottom Salinity	21.4	Oligohaline	resident	Jan-Jun, Aug-Dec
shimofuri goby	Tridentiger bifasciatus	Gobiidae	Surface Temperature	1.52	Oligohaline	resident	Jan-Jun, Aug-Dec
shimofuri goby	Tridentiger bifasciatus	Gobiidae	Bottom Temperature	1.43	Oligohaline	resident	Jan-Jun, Aug-Dec
shimofuri goby	Tridentiger bifasciatus	Gobiidae	Secchi	2.97	Oligohaline	resident	Jan-Jun, Aug-Dec
shiner perch	Cymatogaster aggregata	Embiotocidae	depth	2.68	Polyhaline	Obligate nursery	Jan-Dec
shiner perch	Cymatogaster aggregata	Embiotocidae	SurfaceSalinity	15	Polyhaline	Obligate nursery	Jan-Dec
shiner perch	Cymatogaster aggregata	Embiotocidae	Bottom Salinity	12.5	Polyhaline	Obligate nursery	Jan-Dec
shiner perch	Cymatogaster aggregata	Embiotocidae	Surface Temperature	3.41	Polyhaline	Obligate nursery	Jan-Dec
shiner perch	Cymatogaster aggregata	Embiotocidae	Bottom Temperature	3.33	Polyhaline	Obligate nursery	Jan-Dec
shiner perch	Cymatogaster aggregata	Embiotocidae	Secchi	3.74	Polyhaline	Obligate nursery	Jan-Dec
shiner perch age0	Cymatogaster aggregata	Embiotocidae	depth	3.24	Polyhaline	Obligate nursery	May-Dec
shiner perch age0	Cymatogaster aggregata	Embiotocidae	SurfaceSalinity	15.6	Polyhaline	Obligate nursery	May-Dec
shiner perch age0	Cymatogaster aggregata	Embiotocidae	Bottom Salinity	13.5	Polyhaline	Obligate nursery	May-Dec
shiner perch age0	Cymatogaster aggregata	Embiotocidae	Surface Temperature	2.34	Polyhaline	Obligate nursery	May-Dec
shiner perch age0	Cymatogaster aggregata	Embiotocidae	Bottom Temperature	1.88	Polyhaline	Obligate nursery	May-Dec
shiner perch age0	Cymatogaster aggregata	Embiotocidae	Secchi	5.21	Polyhaline	Obligate nursery	May-Dec

Table 10-2: Habitat suitability index parameters							
species/taxa	scientific name	family	Parameter	GAM Deviance explained(%)	Salinity	Estuarine Use	Months Used for Analysis
shokihaze goby	Tridentiger barbatus	Gobiidae	depth	9.56	Polyhaline	resident?	Jan-Dec
shokihaze goby	Tridentiger barbatus	Gobiidae	SurfaceSalinity	10.8	Polyhaline	resident?	Jan-Dec
shokihaze goby	Tridentiger barbatus	Gobiidae	Bottom Salinity	11.2	Polyhaline	resident?	Jan-Dec
shokihaze goby	Tridentiger barbatus	Gobiidae	Surface Temperature	0.636	Polyhaline	resident?	Jan-Dec
shokihaze goby	Tridentiger barbatus	Gobiidae	Bottom Temperature	0.716	Polyhaline	resident?	Jan-Dec
shokihaze goby	Tridentiger barbatus	Gobiidae	Secchi	3.52	Polyhaline	resident?	Jan-Dec
speckled sanddab	Citharichthys stigmaeus	Pleuronectidae	depth	5.15	Polyhaline	non-obligate nursery	Jan-Dec
speckled sanddab	Citharichthys stigmaeus	Pleuronectidae	SurfaceSalinity	13.8	Polyhaline	non-obligate nursery	Jan-Dec
speckled sanddab	Citharichthys stigmaeus	Pleuronectidae	Bottom Salinity	13.4	Polyhaline	non-obligate nursery	Jan-Dec
speckled sanddab	Citharichthys stigmaeus	Pleuronectidae	Surface Temperature	9.43	Polyhaline	non-obligate nursery	Jan-Dec
speckled sanddab	Citharichthys stigmaeus	Pleuronectidae	Bottom Temperature	9.73	Polyhaline	non-obligate nursery	Jan-Dec
speckled sanddab	Citharichthys stigmaeus	Pleuronectidae	Secchi	5.78	Polyhaline	non-obligate nursery	Jan-Dec
speckled sanddab age0	Citharichthys stigmaeus	Pleuronectidae	depth	3.29	Polyhaline	non-obligate nursery	Jan-Dec
speckled sanddab age0	Citharichthys stigmaeus	Pleuronectidae	SurfaceSalinity	11.2	Polyhaline	non-obligate nursery	Jan-Dec
speckled sanddab age0	Citharichthys stigmaeus	Pleuronectidae	Bottom Salinity	10.8	Polyhaline	non-obligate nursery	Jan-Dec
speckled sanddab age0	Citharichthys stigmaeus	Pleuronectidae	Surface Temperature	8.5	Polyhaline	non-obligate nursery	Jan-Dec
speckled sanddab age0	Citharichthys stigmaeus	Pleuronectidae	Bottom Temperature	8.72	Polyhaline	non-obligate nursery	Jan-Dec
speckled sanddab age0	Citharichthys stigmaeus	Pleuronectidae	Secchi	4.04	Polyhaline	non-obligate nursery	Jan-Dec
starry flounder	Platichthys stellatus	Pleuronectidae	depth	7.43	Mesohaline	Obligate nursery	Jan-Dec

Table 10-2: Habitat suitability index parameters

species/taxa	scientific name	family	Parameter	GAM Deviance explained(%)	Salinity	Estuarine Use	Months Used for Analysis
starry flounder	Platichthys stellatus	Pleuronectidae	SurfaceSalinity	5.83	Mesohaline	Obligate nursery	Jan-Dec
starry flounder	Platichthys stellatus	Pleuronectidae	Bottom Salinity	6.92	Mesohaline	Obligate nursery	Jan-Dec
starry flounder	Platichthys stellatus	Pleuronectidae	Surface Temperature	2.17	Mesohaline	Obligate nursery	Jan-Dec
starry flounder	Platichthys stellatus	Pleuronectidae	Bottom Temperature	2.47	Mesohaline	Obligate nursery	Jan-Dec
starry flounder	Platichthys stellatus	Pleuronectidae	Secchi	2.61	Mesohaline	Obligate nursery	Jan-Dec
starry flounder age0	Platichthys stellatus	Pleuronectidae	depth	4.56	Mesohaline	Obligate nursery	May-Dec
starry flounder age0	Platichthys stellatus	Pleuronectidae	SurfaceSalinity	14	Mesohaline	Obligate nursery	May-Dec
starry flounder age0	Platichthys stellatus	Pleuronectidae	Bottom Salinity	14	Mesohaline	Obligate nursery	May-Dec
starry flounder age0	Platichthys stellatus	Pleuronectidae	Surface Temperature	6.2	Mesohaline	Obligate nursery	May-Dec
starry flounder age0	Platichthys stellatus	Pleuronectidae	Bottom Temperature	7.02	Mesohaline	Obligate nursery	May-Dec
starry flounder age0	Platichthys stellatus	Pleuronectidae	Secchi	6.73	Mesohaline	Obligate nursery	May-Dec
striped bass	Morone saxatilis	Moronidae	depth	7.39	Mesohaline	anadromous	Jan-Dec
striped bass	Morone saxatilis	Moronidae	SurfaceSalinity	27.7	Mesohaline	anadromous	Jan-Dec
striped bass	Morone saxatilis	Moronidae	Bottom Salinity	29.1	Mesohaline	anadromous	Jan-Dec
striped bass	Morone saxatilis	Moronidae	Surface Temperature	6.03	Mesohaline	anadromous	Jan-Dec
striped bass	Morone saxatilis	Moronidae	Bottom Temperature	6.5	Mesohaline	anadromous	Jan-Dec
striped bass	Morone saxatilis	Moronidae	Secchi	3.95	Mesohaline	anadromous	Jan-Dec
striped bass age0	Morone saxatilis	Moronidae	depth	6.54	Mesohaline	anadromous	Jan-April, Jun-Dec
striped bass age0	Morone saxatilis	Moronidae	SurfaceSalinity	20.4	Mesohaline	anadromous	Jan-April, Jun-Dec
striped bass age0	Morone saxatilis	Moronidae	Bottom Salinity	20.5	Mesohaline	anadromous	Jan-April, Jun-Dec

Table 10-2: Habitat suitability index parameters

species/taxa	scientific name	family	Parameter	GAM Deviance explained(%)	Salinity	Estuarine Use	Months Used for Analysis
striped bass age0	Morone saxatilis	Moronidae	Surface Temperature	7.66	Mesohaline	anadromous	Jan-April, Jun-Dec
striped bass age0	Morone saxatilis	Moronidae	Bottom Temperature	8.01	Mesohaline	anadromous	Jan-April, Jun-Dec
striped bass age0	Morone saxatilis	Moronidae	Secchi	3.03	Mesohaline	anadromous	Jan-April, Jun-Dec
white croaker	Genyonemus lineatus	Sciaenidae	depth	7.25	Polyhaline	non-obligate nursery	Feb-Oct
white croaker	Genyonemus lineatus	Sciaenidae	SurfaceSalinity	9.05	Polyhaline	non-obligate nursery	Feb-Oct
white croaker	Genyonemus lineatus	Sciaenidae	Bottom Salinity	11.2	Polyhaline	non-obligate nursery	Feb-Oct
white croaker	Genyonemus lineatus	Sciaenidae	Surface Temperature	5.35	Polyhaline	non-obligate nursery	Feb-Oct
white croaker	Genyonemus lineatus	Sciaenidae	Bottom Temperature	5.89	Polyhaline	non-obligate nursery	Feb-Oct
white croaker	Genyonemus lineatus	Sciaenidae	Secchi	2.67	Polyhaline	non-obligate nursery	Feb-Oct
white croaker age0	Genyonemus lineatus	Sciaenidae	depth	5.79	Polyhaline	non-obligate nursery	April-Oct
white croaker age0	Genyonemus lineatus	Sciaenidae	SurfaceSalinity	5.01	Polyhaline	non-obligate nursery	April-Oct
white croaker age0	Genyonemus lineatus	Sciaenidae	Bottom Salinity	5.32	Polyhaline	non-obligate nursery	April-Oct
white croaker age0	Genyonemus lineatus	Sciaenidae	Surface Temperature	6.79	Polyhaline	non-obligate nursery	April-Oct
white croaker age0	Genyonemus lineatus	Sciaenidae	Bottom Temperature	8.04	Polyhaline	non-obligate nursery	April-Oct
white croaker age0	Genyonemus lineatus	Sciaenidae	Secchi	1.1	Polyhaline	non-obligate nursery	April-Oct
yellowfin goby	Acanthogobius flavimanus	Gobiidae	depth	2.63	Mesohaline	resident	Jan-Mar, May-Dec
yellowfin goby	Acanthogobius flavimanus	Gobiidae	SurfaceSalinity	5.64	Mesohaline	resident	Jan-Mar, May-Dec
yellowfin goby	Acanthogobius flavimanus	Gobiidae	Bottom Salinity	6.39	Mesohaline	resident	Jan-Mar, May-Dec

Table 10-2: Habitat suitability index parameters							
species/taxa	scientific name	family	Parameter	GAM Deviance explained(%)	Salinity	Estuarine Use	Months Used for Analysis
yellowfin goby	Acanthogobius flavimanus	Gobiidae	Surface Temperature	2.77	Mesohaline	resident	Jan-Mar, May-Dec
yellowfin goby	Acanthogobius flavimanus	Gobiidae	Bottom Temperature	2.81	Mesohaline	resident	Jan-Mar, May-Dec
yellowfin goby	Acanthogobius flavimanus	Gobiidae	Secchi	8.72	Mesohaline	resident	Jan-Mar, May-Dec
yellowfin goby age0	Acanthogobius flavimanus	Gobiidae	depth	3.22	Mesohaline	resident	May-Dec
yellowfin goby age0	Acanthogobius flavimanus	Gobiidae	SurfaceSalinity	7.77	Mesohaline	resident	May-Dec
yellowfin goby age0	Acanthogobius flavimanus	Gobiidae	Bottom Salinity	8.48	Mesohaline	resident	May-Dec
yellowfin goby age0	Acanthogobius flavimanus	Gobiidae	Surface Temperature	3.26	Mesohaline	resident	May-Dec
yellowfin goby age0	Acanthogobius flavimanus	Gobiidae	Bottom Temperature	3.47	Mesohaline	resident	May-Dec
yellowfin goby age0	Acanthogobius flavimanus	Gobiidae	Secchi	8.72	Mesohaline	resident	May-Dec
California Department of Fish and Wildlife- fall midwater trawl survey							
American shad	Alosa sapidissima	Clupeidae	Salinity	3.9	Mesohaline	anadromous	Sep-Dec
American shad	Alosa sapidissima	Clupeidae	Surface Temperature	0.804	Mesohaline	anadromous	Sep-Dec
American shad	Alosa sapidissima	Clupeidae	Secchi	7.69	Mesohaline	anadromous	Sep-Dec
Crangon spp	Crangon spp	Crangonidae	Salinity	13.2	Mesohaline*	non-obligate nursery	Sep-Dec
Crangon spp	Crangon spp	Crangonidae	Surface Temperature	0.577	Mesohaline*	non-obligate nursery	Sep-Dec
Crangon spp	Crangon spp	Crangonidae	Secchi	20	Mesohaline*	non-obligate nursery	Sep-Dec
delta smelt	Hypomesus transpacificus	Osmeridae	Salinity	14.2	Oligohaline	resident	Sep-Dec
delta smelt	Hypomesus transpacificus	Osmeridae	Surface Temperature	0.848	Oligohaline	resident	Sep-Dec
delta smelt	Hypomesus	Osmeridae	Secchi	16.9	Oligohaline	resident	Sep-Dec

<i>Table 10-2: Habitat suitability index parameters</i>							
species/taxa	scientific name	family	Parameter	GAM Deviance explained(%)	Salinity	Estuarine Use	Months Used for Analysis
	transpacificus						
delta smelt age0	Hypomesus transpacificus	Osmeridae	Salinity	13.3	Oligohaline	resident	Sep-Dec
delta smelt age0	Hypomesus transpacificus	Osmeridae	Surface Temperature	0.506	Oligohaline	resident	Sep-Dec
delta smelt age0	Hypomesus transpacificus	Osmeridae	Secchi	7.84	Oligohaline	resident	Sep-Dec
delta smelt age1plus	Hypomesus transpacificus	Osmeridae	Salinity	3.26	Oligohaline	resident	Sep-Dec
delta smelt age1plus	Hypomesus transpacificus	Osmeridae	Surface Temperature	4.21	Oligohaline	resident	Sep-Dec
delta smelt age1plus	Hypomesus transpacificus	Osmeridae	Secchi	7.17	Oligohaline	resident	Sep-Dec
longfin smelt	Spirinchus thaleichthys	Osmeridae	Salinity	11.1	Polyhaline	anadromous	Sep-Dec
longfin smelt	Spirinchus thaleichthys	Osmeridae	Surface Temperature	3.48	Polyhaline	anadromous	Sep-Dec
longfin smelt	Spirinchus thaleichthys	Osmeridae	Secchi	18.9	Polyhaline	anadromous	Sep-Dec
longfin smelt age0	Spirinchus thaleichthys	Osmeridae	Salinity	9.56	Polyhaline	anadromous	Sep-Dec
longfin smelt age0	Spirinchus thaleichthys	Osmeridae	Surface Temperature	1.05	Polyhaline	anadromous	Sep-Dec
longfin smelt age0	Spirinchus thaleichthys	Osmeridae	Secchi	5.3	Polyhaline	anadromous	Sep-Dec
longfin smelt age1	Spirinchus thaleichthys	Osmeridae	Salinity	6.15	Polyhaline	anadromous	Sep-Dec
longfin smelt age1	Spirinchus thaleichthys	Osmeridae	Surface Temperature	8.12	Polyhaline	anadromous	Sep-Dec
longfin smelt age1	Spirinchus thaleichthys	Osmeridae	Secchi	4.43	Polyhaline	anadromous	Sep-Dec
northern anchovy	Engraulis mordax	Engraulidae	Salinity	26.3	Polyhaline	opportunist	Sep-Dec
northern anchovy	Engraulis mordax	Engraulidae	Surface Temperature	6.6	Polyhaline	opportunist	Sep-Dec
northern anchovy	Engraulis mordax	Engraulidae	Secchi	1.41	Polyhaline	opportunist	Sep-Dec

Table 10-2: Habitat suitability index parameters							
species/taxa	scientific name	family	Parameter	GAM Deviance explained(%)	Salinity	Estuarine Use	Months Used for Analysis
Pacific herring	Clupea pallasii	Clupeidae	Salinity	10.6	Polyhaline	Obligate nursery	Sep-Dec
Pacific herring	Clupea pallasii	Clupeidae	Surface Temperature	3.09	Polyhaline	Obligate nursery	Sep-Dec
Pacific herring	Clupea pallasii	Clupeidae	Secchi	1.1	Polyhaline	Obligate nursery	Sep-Dec
Palaemon spp.	Palaemon spp.	Palaemonidae	Salinity	8.56	Polyhaline		Sep-Dec
Palaemon spp.	Palaemon spp.	Palaemonidae	Surface Temperature	0.753	Polyhaline		Sep-Dec
Palaemon spp.	Palaemon spp.	Palaemonidae	Secchi	16	Polyhaline		Sep-Dec
striped bass age0	Morone saxatilis	Moronidae	Salinity	9.49	Mesohaline	anadromous	Sep-Dec
striped bass age0	Morone saxatilis	Moronidae	Surface Temperature	0.42	Mesohaline	anadromous	Sep-Dec
striped bass age0	Morone saxatilis	Moronidae	Secchi	17.4	Mesohaline	anadromous	Sep-Dec
striped bass age1	Morone saxatilis	Moronidae	Salinity	5.2	Mesohaline	anadromous	Sep-Dec
striped bass age1	Morone saxatilis	Moronidae	Surface Temperature	0.554	Mesohaline	anadromous	Sep-Dec
striped bass age1	Morone saxatilis	Moronidae	Secchi	12.7	Mesohaline	anadromous	Sep-Dec
striped bass age2plus	Morone saxatilis	Moronidae	Salinity	3.6	Mesohaline	anadromous	Sep-Dec
striped bass age2plus	Morone saxatilis	Moronidae	Surface Temperature	0.832	Mesohaline	anadromous	Sep-Dec
striped bass age2plus	Morone saxatilis	Moronidae	Secchi	7.85	Mesohaline	anadromous	Sep-Dec
threadfin shad	Dorosoma petenense	Clupeidae	Salinity	10.4	Mesohaline	opportunist	Sep-Dec
threadfin shad	Dorosoma petenense	Clupeidae	Surface Temperature	4.91	Mesohaline	opportunist	Sep-Dec
threadfin shad	Dorosoma petenense	Clupeidae	Secchi	2.56	Mesohaline	opportunist	Sep-Dec
California Department of Fish and Wildlife - summer townet survey							
American shad	Alosa sapidissima	Clupeidae	Salinity	7.21	Mesohaline	anadromous	Jun-Aug
American shad	Alosa sapidissima	Clupeidae	Surface Temperature	6.94	Mesohaline	anadromous	Jun-Aug

Table 10-2: Habitat suitability index parameters

species/taxa	scientific name	family	Parameter	GAM Deviance explained(%)	Salinity	Estuarine Use	Months Used for Analysis
American shad	<i>Alosa sapidissima</i>	Clupeidae	Secchi	0.968	Mesohaline	anadromous	Jun-Aug
delta smelt	<i>Hypomesus transpacificus</i>	Osmeridae	Salinity	6.49	Oligohaline	resident	Jun-Aug
delta smelt	<i>Hypomesus transpacificus</i>	Osmeridae	Surface Temperature	4.42	Oligohaline	resident	Jun-Aug
delta smelt	<i>Hypomesus transpacificus</i>	Osmeridae	Secchi	12.7	Oligohaline	resident	Jun-Aug
delta smelt age0	<i>Hypomesus transpacificus</i>	Osmeridae	Salinity	5.54	Oligohaline	resident	Jun-Aug
delta smelt age0	<i>Hypomesus transpacificus</i>	Osmeridae	Surface Temperature	4.54	Oligohaline	resident	Jun-Aug
delta smelt age0	<i>Hypomesus transpacificus</i>	Osmeridae	Secchi	10.5	Oligohaline	resident	Jun-Aug
longfin smelt	<i>Spirinchus thaleichthys</i>	Osmeridae	Salinity	17.4	Polyhaline	anadromous	Jun-Aug
longfin smelt	<i>Spirinchus thaleichthys</i>	Osmeridae	Surface Temperature	12.4	Polyhaline	anadromous	Jun-Aug
longfin smelt	<i>Spirinchus thaleichthys</i>	Osmeridae	Secchi	6.48	Polyhaline	anadromous	Jun-Aug
Mississippi silverside	<i>Menidia beryllina</i>	Atherinopsidae	Salinity	3.74	Polyhaline		Jun-Aug
Mississippi silverside	<i>Menidia beryllina</i>	Atherinopsidae	Surface Temperature	7.2	Polyhaline		Jun-Aug
Mississippi silverside	<i>Menidia beryllina</i>	Atherinopsidae	Secchi	0.776	Polyhaline		Jun-Aug
northern anchovy	<i>Engraulis mordax</i>	Engraulidae	Salinity	40.5	Polyhaline	opportunist	Jun-Aug
northern anchovy	<i>Engraulis mordax</i>	Engraulidae	Surface Temperature	9.08	Polyhaline	opportunist	Jun-Aug
northern anchovy	<i>Engraulis mordax</i>	Engraulidae	Secchi	0.925	Polyhaline	opportunist	Jun-Aug
splittail	<i>Pogonichthys macrolepidotus</i>	Cyprinidae	Salinity	1.06	Oligohaline	resident	Jun-Aug
splittail	<i>Pogonichthys macrolepidotus</i>	Cyprinidae	Surface Temperature	0.67	Oligohaline	resident	Jun-Aug
splittail	<i>Pogonichthys macrolepidotus</i>	Cyprinidae	Secchi	7.53	Oligohaline	resident	Jun-Aug
striped bass age0	<i>Morone saxatilis</i>	Moronidae	Salinity	9.05	Mesohaline	anadromous	Jun-Aug

Table 10-2: Habitat suitability index parameters

species/taxa	scientific name	family	Parameter	GAM Deviance explained(%)	Salinity	Estuarine Use	Months Used for Analysis
striped bass age0	Morone saxatilis	Moronidae	Surface Temperature	1.51	Mesohaline	anadromous	Jun-Aug
striped bass age0	Morone saxatilis	Moronidae	Secchi	7.6	Mesohaline	anadromous	Jun-Aug
threadfin shad	Dorosoma petenense	Clupeidae	Salinity	11.7	Mesohaline	opportunist	Jun-Aug
threadfin shad	Dorosoma petenense	Clupeidae	Surface Temperature	16.6	Mesohaline	opportunist	Jun-Aug
threadfin shad	Dorosoma petenense	Clupeidae	Secchi	1.87	Mesohaline	opportunist	Jun-Aug
Tridentiger spp.	Tridentiger spp.	Gobiidae	Salinity	6.02	Polyhaline		Jun-Aug
Tridentiger spp.	Tridentiger spp.	Gobiidae	Surface Temperature	2.23	Polyhaline		Jun-Aug
Tridentiger spp.	Tridentiger spp.	Gobiidae	Secchi	0.079	Polyhaline		Jun-Aug
yellowfin goby	Acanthogobius flavimanus	Gobiidae	Salinity	4.69	Mesohaline	resident	Jun-Aug
yellowfin goby	Acanthogobius flavimanus	Gobiidae	Surface Temperature	2.99	Mesohaline	resident	Jun-Aug
yellowfin goby	Acanthogobius flavimanus	Gobiidae	Secchi	10.8	Mesohaline	resident	Jun-Aug

2. OTHER DELIVERABLES

a. Manuscripts

Published

(This list of published manuscripts includes both CASCaDE I and CASCaDE II products, because the two project phases were highly interdependent. Of the 69 publications listed, 42 were published during the CASCaDE II term.)

1. Florsheim, J.L., and Dettinger, M.D. 2007. Climate and floods still govern California levee breaks. *Geophys. Res. Lett.* **34**(22).
<http://onlinelibrary.wiley.com/doi/10.1029/2007GL031702/pdf>
2. Cayan, D., Luers, A., Franco, G., Hanemann, M., Croes, B., and Vine, E. 2008a. Overview of the California climate change scenarios project. *Clim. Change* **87**(0): 1-6. http://meteora.ucsd.edu/cap/pdf/Cayan_overview_jan2008.pdf
3. Cayan, D., Maurer, E., Dettinger, M., Tyree, M., and Hayhoe, K. 2008b. Climate change scenarios for the California region. *Clim. Change* **87**(0): 21-42.
http://meteora.ucsd.edu/cap/pdf/Cayan_calif_scen_jan2008.pdf
4. Cayan, D., Bromirski, P., Hayhoe, K., Tyree, M., Dettinger, M., and Flick, R. 2008c. Climate change projections of sea level extremes along the California coast. *Clim. Change* **87**(0): 57-73.
http://meteora.ucsd.edu/cap/pdf/Cayan_sealevel_jan2008.pdf
5. Flint, A.L., Flint, L.E., and Dettinger, M.D. 2008. Modeling Soil Moisture Processes and Recharge under a Melting Snowpack. *Vadose Zone Journal* **7**(1): 350-357.
<http://tenaya.ucsd.edu/~dettinge/flint08.pdf>
6. Ganju, N.K., Knowles, N., and Schoellhamer, D.H. 2008. Temporal downscaling of decadal sediment load estimates to a daily interval for use in hindcast simulations. *Journal of Hydrology* **349**(3-4): 512-523.
http://ca.water.usgs.gov/user_projects/sfbay/publications_group/Ganju_et_al_sed_load_ad.pdf
7. Healey, M., Dettinger, M.D., and Norgaard, R. 2008. The State of Bay-Delta Science 2008. Summary for Policymakers and the Public. Calfed Science Program, Sacramento, CA.
http://www.science.calwater.ca.gov/pdf/publications/sbds/sbds_final_update_122408.pdf

8. Ganju, N.K., and Schoellhamer, D.H. 2009. Calibration of an estuarine sediment transport model to sediment fluxes as an intermediate step for simulation of geomorphic evolution. *Cont. Shelf Res.* **29**: 148-158.
<http://ca.water.usgs.gov/projects/baydelta/publications/Ganju%20and%20Schoellhamer%202009.pdf>
9. Hidalgo, H.G., Dettinger, M., and Cayan, D. 2008. Downscaling with constructed analogues: Daily precipitation and temperature fields over the United States CEC-500-2007-123. California Energy Commission, PIER Energy-Related Environmental Research. <http://www.energy.ca.gov/2007publications/CEC-500-2007-123/CEC-500-2007-123.PDF>
10. Peterson, D.H., Stewart, I., and Murphy, F. 2008. Principle Hydrologic Responses to Climatic and Geologic Variability in the Sierra Nevada, California. *San Francisco Estuary and Watershed Science*, Vol. 6, Issue 1 (February), Article 3. Available from http://water.usgs.gov/nrp/proj.bib/Publications/2008/peterson_stewart_etal_2008.pdf
11. Brown, L.R., and Bauer, M., 2009. Effects of hydrologic infrastructure on flow regimes of California's Central Valley rivers: Implications for Fish Populations. *River Res. Appl.*, Volume 26, Issue 6, pages 751–765. DOI: 10.1002/rra.1293
<http://citeseerx.ist.psu.edu/viewdoc/download?doi=10.1.1.364.7763&rep=rep1&type=pdf>
12. Lucas, L.V., Brown, L.R., and Thompson, J.K. 2009. Why are diverse relationships observed between phytoplankton biomass and transport time? *Limnol. Oceanogr.* **54**(1): 381-390. http://www.aslo.org/lo/toc/vol_54/issue_1/0381.pdf
13. Ganju, N.K., Schoellhamer, D.H., and Jaffe, B.E., 2009, Hindcasting of decadal-timescale estuarine bathymetric change with a tidal-timescale model, *Journal of Geophysical Research-Earth Surface*, 114, F04019, doi:10.1029/2008JF001191.
<http://ca.water.usgs.gov/projects/baydelta/publications/Ganju%20et%20al%202009.pdf>
14. Ganju, N.K., and Schoellhamer, D.H., 2010, Decadal-timescale estuarine geomorphic change under future scenarios of climate and sediment supply. *Estuaries and Coasts*, 33, 15-29.
<http://ca.water.usgs.gov/projects/baydelta/publications/Ganju%20and%20Schoellhamer%202010.pdf>
15. Knowles, N. 2008. Potential inundation due to rising sea levels in the San Francisco Bay region. CEC-500-2009-023-F. California Climate Change Center.
<http://www.energy.ca.gov/2009publications/CEC-500-2009-023/CEC-500-2009-023-F.PDF>

16. Van der Wegen, M., Jaffe, B.E., Dastgheib, A., and Roelvink, D., 2010, Bed composition generation for process-based morphodynamic modeling: case study San Pablo Bay, California, *Ocean Dynamics* doi:10.1007/s10236-010-0314-2 <http://www.springerlink.com/content/r77332h251h1125j/>
17. van der Wegen, M., B. E. Jaffe, and J. A. Roelvink (2011), Process-based, morphodynamic hindcast of decadal deposition patterns in San Pablo Bay, California, 1856–1887, *J. Geophys. Res.*, 116, F02008, doi:10.1029/2009JF001614. <http://onlinelibrary.wiley.com/doi/10.1029/2009JF001614/pdf>
18. Stewart AR, Luoma SN, Elrick KA, Carter JL, van der Wegen M (2013) Influence of estuarine processes on spatiotemporal variation in bioavailable selenium. *Mar Ecol Prog Ser* 492:41-56. http://www.int-res.com/articles/meps_oa/m492p041.pdf
19. Wagner, R.W., Stacey, M., Brown, L.R., and Dettinger, M.D., 2011, Statistical models of temperature in the Sacramento-San Joaquin Delta under climate-change scenarios and ecological implications: *Estuaries and Coasts* 34(3): 544-556. doi:10.1007/s12237-010-9369-z. http://water.usgs.gov/nrp/proj.bib/Publications/2011/wagner_stacey_etal_preprint2011.pdf
20. Luoma, S.N. 2009. Ingredients in sustainably managing water in semi-arid environments. *Environmental Science and Policy* 12(6): 737-740. **(Please see attached PDF)**
21. Cloern, J.E., Knowles, N., Brown, L.R., Cayan, D., Dettinger, M.D., Morgan, T.L., Schoellhamer, D.H., Stacey, M., van der Wegen, M., Wagner, R.W., and Jassby, A.D., 2011, Projected evolution of California's San Francisco Bay-Delta river system in a century of climate change: *PLoS One*, 26 p., <http://dx.plos.org/10.1371/journal.pone.0024465>.
22. Ganju, N.K., Jaffe, B.E., and Schoellhamer, D.H., 2011, Discontinuous hindcast simulations of estuarine bathymetric change: a case study from Suisun Bay, California, *Estuarine, Coastal and Shelf Science*, v. 93, p. 142-150. doi:10.1016/j.ecss.2011.04.004 <http://ca.water.usgs.gov/projects/baydelta/publications/Ganju%20et%20al%202011%20ECSS.pdf>
23. Dettinger, M.D., 2011, Climate change, atmospheric rivers and floods in California—A multimodel analysis of storm frequency and magnitude changes: *Journal of American Water Resources Association*, 47, 514-523. http://tenaya.ucsd.edu/~dettinge/md_jawra2011.pdf

24. Dettinger, M.D., Ralph, F.M., Das, T., Neiman, P.J., and Cayan, D., 2011, Atmospheric rivers, floods, and the water resources of California: *Water*, 3, 455-478, <http://www.mdpi.com/2073-4441/3/2/445/>.
25. Das, T., M.D. Dettinger, D.R. Cayan and H.G. Hidalgo, 2011: Potential increase in floods in California's Sierra Nevada under future climate projections. *Climatic Change*, 24 pp, doi:10.1007/s10584-011-0298-z. http://tenaya.ucsd.edu/~dettinge/das_climchg_floods.pdf
26. F. M. Ralph, T. Coleman, P. J. Neiman, R. J. Zamora, M. D. Dettinger. (2013) Observed Impacts of Duration and Seasonality of Atmospheric-River Landfalls on Soil Moisture and Runoff in Coastal Northern California. *Journal of Hydrometeorology* 14:2, 443-459 http://tenaya.ucsd.edu/~dettinge/czd_jhm2013.pdf
27. Brown, L.R., W.A. Bennett, R.W. Wagner, T. Morgan-King, N. Knowles, F. Feyrer, D. Schoellhamer, M. Stacey, M. Dettinger, 2013. Implications for Future Survival of Delta Smelt from Four Climate Change Scenarios for the Sacramento-San Joaquin Delta, California. *Estuaries and Coasts* 36:4, 754-774. 10.1007/s12237-013-9585-4 [URL: <http://ca.water.usgs.gov/pubs/BrownEtAl2013.pdf>
28. Lucas, L. V., and J. K. Thompson. 2012. Changing restoration rules: Exotic bivalves interact with residence time and depth to control phytoplankton productivity. *Ecosphere* 3(12):117. <http://www.esajournals.org/doi/pdf/10.1890/ES12-00251.1>
29. Dettinger MD, 2012. Projections and downscaling of 21st Century temperatures, precipitation, radiative fluxes and winds over the southwestern US, with a focus on the Lake Tahoe basin: *Climatic Change*, 116, 17-33. http://tenaya.ucsd.edu/~dettinge/Tahoe_dscaling.pdf
30. Schoellhamer, D., Wright, S.A., and Drexler, J.Z., 2013. Adjustment of the San Francisco estuary and watershed to reducing sediment supply in the 20th century. *Marine Geology* 345:63-71. <http://ca.water.usgs.gov/pubs/2013/SchoellhamerEtAl2013.pdf>
31. van der Wegen, M., Jaffe B, Roelvink JA, 2013. Does centennial morphodynamic evolution lead to higher channel efficiency in San Pablo Bay, California? *Marine Geology* 345:254-265. <http://www.sciencedirect.com/science/article/pii/S0025322713001412#> **(Please see attached PDF)**
32. van der Wegen, M., and Jaffe, B.E. 2013. Towards a probabilistic assessment of process-based, morphodynamic models. *Coastal Engineering*, Vol. 75, pp 52-63, doi: 10.1016/j.coastaleng.2013.01.009.

<http://www.sciencedirect.com/science/article/pii/S0378383913000227> (Please see attached PDF)

33. Van der Wegen, M. and B.E. Jaffe (2014), Processes governing decadal-scale depositional narrowing of the major tidal channel in San Pablo Bay, California, USA, JGR-ESP, DOI: 10.1002/2013JF002824 (Please see attached PDF)
34. Florsheim, J., and Dettinger, M., 2015, Promoting atmospheric-river and snowmelt fueled biogeomorphic processes by restoring river-floodplain connectivity in California's Central Valley: in Hudson, P., and Middelkoop, H. (eds.), Geomorphic approaches to integrated floodplain management of lowland fluvial systems in North America and Europe, Springer, 23 p.
35. Dettinger MD and Ingram BL, 2013. The Coming Megafloods. Scientific American 308, 64 – 71. http://tenaya.ucsd.edu/~dettinge/Dettinger_Ingram_sciam13.pdf
36. Franco, G., D. Cayan, S. C. Moser, M. H. Hanemann, and M. A. Jones (2011). Second California Assessment: Integrated Climate Change Impacts Assessment of Natural and Managed Systems - An Introduction. Climatic Change 109(Suppl. 1), DOI: 10.1007/s10584-011-0318-z. <http://www.susannemoser.com/documents/Francoetal.2011.SecondCAAssessmentIntro.pdf>
37. Das, T., D.W. Pierce, D.R. Cayan, J.A. Vano and D.P. Lettenmaier, 2011: The importance of warm season warming to western U.S. streamflow changes. Geophysical Research Letters, 38, L23403, doi:10.1029/2011GL049660. <http://onlinelibrary.wiley.com/doi/10.1029/2011GL049660/pdf>
38. Brooks, B.A., G. Bawden, D. Manjunath, C. Werner, N. Knowles, J. Foster, J. Dudas and D.R. Cayan, 2012: Contemporaneous Subsidence and Levee Overtopping Potential, Sacramento-San Joaquin Delta, California. San Francisco Estuary and Watershed Science, 10(1), 18pp. <https://escholarship.org/uc/item/15q1b9tm>
39. Hanson, R.T., L.E. Flint, A.L. Flint, M.D. Dettinger, C.C Faunt, D. Cayan and W. Schmid, 2012: A method for physically based model analysis of conjunctive use in response to potential climate changes. Water Resources Research, 48, W00L08, 23pp, doi:10.1029/2011WR010774 <http://onlinelibrary.wiley.com/doi/10.1029/2011WR010774/pdf>
40. Pierce, D.W., T. Das, D.R. Cayan, E.P. Maurer, N.L. Miller, Y. Bao, M. Kanamitsu, K. Yoshimura, M.A. Snyder, L.C. Sloan, G. Franco and M. Tyree, 2013: Probabilistic estimates of future changes in California temperature and precipitation using

statistical and dynamical downscaling. *Climate Dynamics*, 40, 839-856.
doi:10.1007/s00382-012-1337-9.

http://tenaya.ucsd.edu/~cayan/New_Pubs/D30_Pierce_etal_2012_CD.pdf

41. Pierce, D.W., and D.R. Cayan, 2013: The uneven response of different snow measures to human-induced climate warming. *Journal of Climate*, 26, 4148-4167.
doi:10.1175/JCLI-D-12-00534.1 <http://journals.ametsoc.org/doi/pdf/10.1175/JCLI-D-12-00534.1> **(Please see attached PDF)**
42. Swanson, K.M., Drexler, J.Z., Schoellhamer, D.H., Thorne, K., Casazza, M., Overton, C., Callaway, J., and Takekawa, J.Y., 2014, The Wetland Accretion Rate Model of Ecosystem Resilience (WARMER) and its application to questions of habitat sustainability in the San Francisco Estuary: *Estuaries and Coasts*, v. 37, no. 2, p. 476-492. <http://ca.water.usgs.gov/pubs/2013/SwansonEtAl2013.pdf>
43. Swanson, K.M., Drexler, J.Z., Fuller, C.M., and Schoellhamer, D.H., 2015. Modeling tidal freshwater marsh sustainability in the Sacramento-San Joaquin Delta under a broad suite of potential future scenarios *San Francisco Estuary and Watershed Science*, 13:1. <https://escholarship.org/uc/item/9h8197nt>
44. Hestir, E.L., Schoellhamer, D.H., Morgan, T.L., and Ustin, S.L., 2013. A step decrease in sediment concentration in a highly modified tidal river delta following the 1983 El Niño floods: *Marine Geology* 345:304-313.
<http://ca.water.usgs.gov/pubs/2013/HestirEtAl2013.pdf>
45. Pierce, D.W., D.R. Cayan, T. Das, E.P. Maurer, N.L. Miller, Y. Bao, M. Kanamitsu, K. Yoshimura, M.A. Snyder, L.C. Sloan, G. Franco and M. Tyree, 2013: The key role of heavy precipitation events in climate model disagreements of future annual precipitation changes in California. *Journal of Climate* August 2013, Vol. 26, No. 16 : pp. 5879-5896 <http://journals.ametsoc.org/doi/pdf/10.1175/JCLI-D-12-00766.1>
(Please see attached PDF)
46. Polade, S.D., A. Gershunov, D.R. Cayan, M.D. Dettinger and D.W. Pierce, 2013: Natural climate variability and teleconnections to precipitation over the Pacific-North American region in CMIP3 and CMIP5 models. *Geophysical Research Letters*, 40, 1-6. 10.1002/grl.50491 <http://onlinelibrary.wiley.com/doi/10.1002/grl.50491/pdf>
(Please see attached PDF)
47. DeFlorio, M.J., D.W. Pierce, D.R. Cayan and A.J. Miller, 2012: Western U.S. Extreme Precipitation Events and Their Relation to ENSO and PDO in CCSM4. *Journal of Climate* 26, 4231–4243. <http://journals.ametsoc.org/doi/pdf/10.1175/JCLI-D-12-00257.1> **(Please see attached PDF)**

48. Kimmerer, W.J., and J.K. Thompson, 2014. Phytoplankton growth balanced by clam and zooplankton grazing and net transport into the low-salinity zone of the San Francisco Estuary. *Estuaries and Coasts*, Volume 37, Issue 5, pp 1202-1218, DOI 10.1007/s12237-013-9753-6 <http://link.springer.com/article/10.1007/s12237-013-9753-6>
49. Thompson, J.K. and F. Parchaso. 2012. Conceptual Model for *Potamocorbula amurensis*. DRERIP Conceptual Model. Sacramento (CA). Ecosystem Restoration Program. http://www.dfg.ca.gov/erp/current_models.asp
50. Maurer, E.P., Brekke, L., Pruitt, T., Thrasher, B., Long, J., Duffy, P., Dettinger, M., Cayan, D., and Arnold, J., 2014, An enhanced archive facilitating climate impact analysis: *Bull. American Meteorological Soc.*, 95, 1011-1019, DOI:10.1175/BAMS-D-13-00126.1. <http://journals.ametsoc.org/doi/pdf/10.1175/BAMS-D-13-00126.1>
51. Polade, S.D., Pierce, D.W., Cayan, D.R., Gershunov, A., and Dettinger, M.D., 2014, The key role of dry days in changing regional climate and precipitation regimes: *Nature Scientific Reports*, 4:4364, 8 p., doi:10.1038/srep04364. <http://www.nature.com/srep/2014/140313/srep04364/pdf/srep04364.pdf>
52. Dettinger, M.D., and Cayan, D.R., 2014, Drought and the California Delta—A matter of extremes: *San Francisco Estuary & Watershed Science*, 12(2), 7 p, <http://escholarship.org/uc/item/88f1j5ht>.
53. Stahle, D.W., Griffin, R.D., Therrell, M.D., Edmondson, J.R., Cleaveland, M.K., Stahle, L.N., Burnette, D.J., Abatzoglou, J.T., Redmond, K.T., Meko, D.M., Dettinger, M.D., and Cayan, D.R., 2013, The ancient blue oak woodlands of California—Longevity and hydroclimatic history: *Earth Interactions*, 17, 1-23 p., doi:10.1175/2013EI000518.1. <http://journals.ametsoc.org/doi/pdf/10.1175/2013EI000518.1>
54. Das, T., Maurer, E.P., Pierce, D.W., Dettinger, M.D., and Cayan, D.R., 2013, Increases flood magnitudes in California under warming climates: *J. Hydrology*, 501, 101-110, doi:10.1016/j.jhydrol.2013.07.042. http://woodland.ucsd.edu/?page_id=184
55. Dettinger, M., 2015, Sturm und Drang—California's Remarkable Storm-Drought Connection: *HydroLink*, 20-12. Preview at: <http://riversandsky.tumblr.com/post/106063024617/sturm-und-drang-californias-remarkable>
56. Stern, M.A., 2014. Characterizing flow and sediment trends in the Sacramento River Basin, CA using Hydrologic Simulation Program – FORTRAN (HSPF). Master's

Thesis. California State University, Sacramento.

<http://hdl.handle.net/10211.3/125018>

57. Stern, M.A., Flint, L.E., Flint, A.L., Wright, S.A., and Minear, J.T., 2014. Characterizing flow and sediment trends in the Sacramento River Basin, CA, using the Hydrologic Simulation Program – FORTRAN, Abstract 17793 presented at 2014 Fall Meeting, AGU, San Francisco, Calif., 15-19 Dec. **(Please see attached PDF)**
58. Achete, F.M., van der Wegen, M, Jaffe, B.E., Roelvink, J. A., 2015. A 2D Process-Based Model for Suspended Sediment Dynamics: a first Step towards Ecological Modeling", HESS, hess-2014-550 **(Please see attached PDF)**
59. Van der Wegen, M., L. Lucas, N. Knowles, D. Senn, M. Stacey, S. Monismith, B. Jaffe, P. Barnard, O. Fringer, H. Los , 2014, Building a Public Community around the D3D-FM San Francisco Bay-Delta Model: 8th Biennial Bay-Delta Science Conference, Sacramento, California, October 2014. (Poster, Presented by van der Wegen). <http://www.d3d-baydelta.org>
60. Borsa, A.A., Agnew, D.C., and Cayan, D.R. 2014. Ongoing drought-induced uplift in the western United States. *Science* 345(6204): 1587-1590. **(Please see attached PDF)**
61. Ralph, F.M., Dettinger, M., and others. 2014. A vision for future observations for Western U.S. Extreme Precipitation and Flooding. *J. Contemporary Water Research & Education* 153: 16-32. **(Please see attached PDF)**
62. Dettinger M.D. and M.L. Anderson, 2015. Storage in California's reservoirs and snowpack in this time of drought. *San Francisco Estuary and Watershed Science*, 13(2). <http://escholarship.org/uc/item/8m26d692>
63. Cayan, D., M. Tyree, K.E. Kunkel, C. Castro, A. Gershunov, J. Barsugli, A.J. Ray, J. Overpeck, M. Anderson, J. Russell, B. Rajagopalan, I. Rangwala and P. Duffy, 2013: Future Climate: Projected Average. Chapter 6 in *Assessment of Climate Change in the Southwest United States: A Report Prepared for the National Climate Assessment*, G. Garfin, A. Jardine, R. Merideth, M. Black, and S. LeRoy (eds), Southwest Climate Alliance report, Washington, DC, *Island Press*, pp 101-125. <http://swccar.org/sites/all/themes/files/SW-NCA-color-FINALweb.pdf>
64. Dettinger, M.D., 2013: Atmospheric rivers as drought busters on the US west coast. *Journal of Hydrometeorology*, **14**, 1721-1732. doi:10.1175/JHM-D-13-02.1 <http://journals.ametsoc.org/doi/abs/10.1175/JHM-D-13-02.1>
65. Georgakakos, A., P. Fleming, M. Dettinger, C. Peters-Lidard, Terese (T.C.) Richmond, K. Reckhow, K. White, and D. Yates, 2014: Chapter 3: Water

Resources. *Climate Change Impacts in the United States: The Third National Climate Assessment*, J.M. Melillo, Terese (T.C.) Richmond, and G. W. Yohe, Eds., U.S. Global Change Research Program, 69-112.

doi:10.7930/J0G44N6T.

http://nca2014.globalchange.gov/system/files_force/downloads/low/NCA3_Full_Report_03_Water_Resources_LowRes.pdf?download=1

66. Gershunov, A., B. Rajagopalan, J. Overpeck, K. Guirguis, D. Cayan, M. Hughes, M. Dettinger, C. Castro, R.E. Schwartz, M. Anderson, A. J. Ray, J. Barsugli, T. Cavazos and M. Alexander, 2013: Future Climate: Projected Extremes. Chapter 7 in *Assessment of Climate Change in the Southwest United States: A Report Prepared for the National Climate Assessment*, G. Garfin, A. Jardine, R. Merideth, M. Black, and S. LeRoy (eds), Southwest Climate Alliance report, Washington, DC, *Island Press*, pp 126-147. <http://swccar.org/sites/all/themes/files/SW-NCA-color-FINALweb.pdf>
67. Hoerling, M.P., M. Dettinger, K. Wolter, J. Lukas, J. Eischeid, R. Nemani, B. Liebmann and K.E. Kunkel, 2013: Present Weather and Climate: Evolving Conditions. Chapter 5 in *Assessment of Climate Change in the Southwest United States: A Report Prepared for the National Climate Assessment*, G. Garfin, A. Jardine, R. Merideth, M. Black and S. LeRoy (eds), Southwest Climate Alliance report, Washington, DC, *Island Press*, pp 74-100. <http://swccar.org/sites/all/themes/files/SW-NCA-color-FINALweb.pdf>
68. Pierce, D.W., D.R. Cayan and B.L. Thrasher, 2014: Statistical Downscaling Using Localized Constructed Analogs (LOCA). *Journal of Hydrometeorology*, **15**, 2558-2585. <http://journals.ametsoc.org/doi/abs/10.1175/JHM-D-14-0082.1>
69. Schwartz, R.E., A. Gershunov, S.F. Iacobellis and D.R. Cayan, 2014: North American west coast summer low cloudiness: Broad-scale variability associated with sea surface temperature. *Geophysical Research Letters*, **41**, 8 pages, online article, DOI:10.1002/2014GL059825. <http://onlinelibrary.wiley.com/doi/10.1002/2014GL059825/full>

In preparation/review

1. Brown, L.R., L.M. Komoroske, R.W. Wagner, T. Morgan-King, J.T. May, R.E. Connon, and N.A. Fangue. *Submitted*. Climate change on management-relevant scales: Coupling water temperature models with physiological tolerances. *Ecological Applications*.

2. Achete, F. M., van der Wegen, M., Roelvink, D., and Jaffe. *Submitted*. Suspended Sediment Dynamics in a tidal channel network under Peak River Flow, Ocean Dynamics.
3. Achete, F.M. *In prep*. Multiple scales of suspended sediment dynamics in a complex geometry estuary. PhD Thesis, UNESCO-IHE.
4. Dettinger, M.D. *In review*, On the relations between large storms and droughts in California: Water Resources Research, 29 p.
5. Stern, M.A., Flint, L.E., Flint, A.L., Wright, S.A., and Minear, J.T. *In prep*. Characterizing historical flow and sediment trends in the Sacramento River Basin, CA using the Hydrologic Simulation Program – FORTRAN.
6. Stern, M.A., Flint, L.E., Flint, A.L., Wright, S.A., and Minear, J.T. *In prep*. Projections of future sediment supply to the San Francisco Bay-Delta, Ca using Localized Constructed Analogs (LOCA) downscaled Global Climate Model scenarios.
7. Kleckner AE, Kakouros E, Stewart AR. *In prep*. A practical method for the determination of selenium in biological samples using Isotope Dilution-Hydride Generation-Inductively Coupled Plasma-Mass Spectrometry. Ready to submit by September 30, 2015.
8. Martyr, R., Lucas, L., Knowles, N., van der Wegen, M., Kernkamp, H., van Dam, A., van der Pijl, S., Helly, J. *In prep*. Application of a novel 3D finite volume numerical model for hydrodynamic and water-quality transport in the San Francisco Bay-Delta System.
9. H. R. Moftakhari , D. A. Jay , S. A. Talke , and D. H. Schoellhamer. *In revision* Estimation of historic flows and sediment loads to San Francisco Bay. Journal of Hydrology.
10. Morgan-King, T.L., and Schoellhamer, D.H., *In prep*. Trend in sediment supply from the Sacramento River and implications for future supply.
11. Van der Wegen, M., Jaffe, B.E., Roelvink, D. *Submitted*. Predicting centuries of morphodynamics in San Pablo Bay, California: Hindcast and forecast including sea level rise. Submitted for Proceedings of the Coastal Sediments 2015 Conference, San Diego, CA.
12. Knowles N, Cronkite-Ratcliff C. *In prep*. Translation of GCM and regional ocean and atmospheric model outputs into boundary conditions for a hydrodynamic model of the San Francisco Bay-Delta estuary. U.S. Geological Survey Open File Report.

b. Presentations

(CASCaDE-related and Bay-Delta Science Conference [bold])

Achete, F., van der Wegen, M., Schoellhamer, D., and Jaffe, B.E., 2012 Assessing Suspended Sediment Dynamics in the San Francisco Bay-Delta System: Coupling Landsat Satellite Imagery, in situ Data and a Numerical Model, Physics of Estuaries and Coastal Seas, New York

Achete, F., van der Wegen, M., and Jaffe, B.E., 2012 Tracking sediments through the Bay-Delta system over a water year with a 2D process based model (D-Flow FM).

Achete, F., van der Wegen, M. and Jaffe, B.E., 2012 Assessment of long-term impacts due to SSC changes in San Francisco Bay-Delta, American Geophysical Union fall meeting, San Francisco

Achete, F., van der Wegen, M., Jaffe, B.E., and Roelvink, D., 2013 Sediment Transport in a Complex Estuarine Channel Network, Coastal and Estuarine Research Federation annual meeting, San Diego

Achete, F., van der Wegen, M., Jaffe, B.E., and Roelvink, D., and Morgan T., 2012 2D Process-Based Model for Assessment of Suspended Sediment Budget, **Bay-Delta Science Conference**, Sacramento

Achete, F., van der Wegen, M., Jaffe, B.E., and Roelvink, D., 2014 Modeling suspended sediment dynamics in San Francisco Bay Delta system, Physics of Estuaries and Coastal Seas, Porto de Galinhas, Brazil

Achete, F., van der Wegen, M., Jaffe, B.E., and Roelvink, D., 2015 2D Process-based model for assessment of suspended sediment budget, Coastal and Estuarine Research Federation annual meeting, Portland

Achete, F., van der Wegen, M., Jaffe, B.E., and Roelvink, D., 2015 Modeling estuarine sediment budget impacts: anthropogenic or natural?, International Conference on Cohesive Sediment Transport Processes, Leuven, Belgium

Brown, L.R., L.M. Komoroske, T. Morgan-King, R.W. Wagner, N.A. Fangué, J.T. May, R.E. Connon. Climate change projections on management-relevant scales: Coupling local-scale models of water temperatures to maturation of Delta Smelt. IEP 2015 Annual Workshop, Folsom, CA, March 18-20, 2015. (Poster)

Brown, L.R., L.M. Komoroske, R.W. Wagner, T. Morgan-King, J.T. May, R.E. Connon, and N.A. Fangué. Climate change projections on management-relevant scales: Coupling local-scale models of water temperatures to maturation of Delta Smelt. To be presented at: 145th Annual Meeting American Fisheries Society, Portland, OR, August 16-20, 2015.

Brown, L.R., L.M. Komoroske, T. Morgan-King, R.W. Wagner, N.A. Fangué, J.T. May, R.E. Connon. Climate change projections on management-relevant scales: Coupling local-scale models of water temperatures to maturation of Delta Smelt. 49th Annual Cal-Neva Conference, California-Nevada Chapter American Fisheries Society, Santa Cruz, CA, April 8-10, 2015.

Brown, L.R., R.W. Wagner, L.M. Komoroske, T. Morgan-King, N.A. Fangué, J.T. May. Implications of Water Temperatures from Climate Change Projections for Delta Smelt in the Sacramento-San Joaquin Delta, California. 8th Biennial **Bay-Delta Science Conference**, Sacramento, CA, October 28-30, 2014.

Brown, L.R. R.W. Wagner, L. Komoroske, T. Morgan-King, N.A. Fangué, and J.T. May. 2014. Implications of water temperatures from climate change projections for Delta Smelt in the Sacramento-San Joaquin Delta, California. 48th Annual Cal-Neva Conference, California-Nevada Chapter American Fisheries Society, Sacramento, CA, March 27-29, 2014.

Brown, L.R. 2014. So, what does climate change mean for fishes? A Practical Workshop: The Science Behind Delta Climate Change Impacts. The Delta Conservancy and Water Education Foundation, West Sacramento, CA, 13 February 2014. (Invited)

Cayan, D.R. "Water loss from western drought recorded by GPS network" Presentation to DOI Deputy Secr Anne Castle (with Joe Holomuski, Mark Sogge, Eric Reichard)

Cayan, D.R. 2015 "California Climate Change" Presentation to US Representative Scott Peters, Scripps Institution of Oceanography, La Jolla CA 10 Feb 2015

Cayan, D.R. 2015 "Climate change adaptation and mitigation strategies", Discussion with California Governor Jerry Brown and United Nations Climate Framework Exec Secretary Christiana Figueres, County Museum of Los Angeles, 15 June 2015.

Cayan, D.R. 2014. "How Can Climate Science Best Influence Public Policy in an Era of Drought?" Climate Science Drought Communication Panel (Sam Luoma Chair) **Bay-Delta Science Conference**, Sacramento, CA, Oct 28 2014

Cayan, D.R. 2014. "Climate change and California's mountain snow pack--how much will we lose?" **Bay-Delta Science Conference**, Sacramento, CA 30 Oct 2014

- Cayan, D.R. 2014. "Downscaling extremes--Abilities of regional downscaling in studying ecological drought through the lens of statistical downscaling" Ecological Society of America Meeting Sacramento, CA, 11 August /2014
- Cayan, D.R. 2014. "Winter 2014-15 El Niño or No Niño?" San Diego County Water Authority Board of Directors, 28 Aug, 2014
- Cayan, D.R. 2014. "Climate Variability and Change and Southern California Water" San Gabriel Valley Water Forum, Pomona, CA, October 2, 2014
- Cayan, D.R. 2014. "Climate Change, California Lahontan area" Lahontan Regional Water Board Workshop, 13 Nov 2014
- Cayan, D.R. 2015. "Planning for climate change on top of already high climate variability" Climate Informed Monitoring Workshop, Camp Pendleton Marine Base, Oceanside, CA, 18 Nov 2015
- Cayan, D.R. 2014. "Climate Variability and Change and Southern California Water National Hydropower Association Los Angeles, CA (USC), 11 Dec, 2014
- Cayan, D.R. 2015. "Multiple Model Climate Scenarios California" Workshop 4th Climate Change Assessment, California Energy Commission 27 February 2015
- Cayan, D.R. 2015. "This drought is different" Urban Water Institute Annual Meeting Palm Springs, CA, 5 March 2015
- Cayan, D.R. 2015. "Earth's Crustal Response to Drought registered by GPS sensors" National Ground Water Summit, San Antonio TX, 18 March 2015
- Cayan, D.R. 2015. "Climate Variability and California Drought" Chapman Drought Conference, Beckman Center, Irvine California, 20 April, 2015
- Cayan, D.R. 2015. "Recent changes in Coastal Cloud" (co-authored, Sam Iacobellis presented) Pacific Anomalies Workshop, Scripps Institution of Oceanography 5 May, 2015 (*Cayan helped organize, Cayan and Gershunov attended*)
- Cayan, D.R. 2015. "Global Sea Level Rise effects on the California Coast" Aquarium of the Pacific, Long Beach California, Evening Talk, June 1, 2015
- Cayan, D.R. 2015. "California Drought a geological and a climate perspective" Yosemite Forum, Yosemite Park, CA, June 9. 2015
- Crauder, J., Parchaso, F., Thompson, J., Gehrts, K., Fuller, H. Spatial and temporal recruitment patterns of the freshwater bivalve, *Corbicula fluminea*, in Suisun Bay and

the Sacramento-San Joaquin Delta (Poster). Biennial **Bay- Delta Science Conference**, Sacramento, CA, October 15-18, 2012

Dettinger, M.D., Ralph, M., White, A., Anderson, M., Florsheim, J., Cayan, D., and Hinojosa, A., 2014, Severe storms and the Delta—Historical impacts and a new monitoring network: **Bay-Delta Science Conference**, Sacramento, November 2014.

Dettinger, M.D., Das, T., and Cayan, D.R., 2011, Climate change and future California floods: Pacific Climate (PACLIM) Workshop, March 2011, Pacific Grove, CA.

Dettinger, M.D., Das, T., and Cayan, D.R., 2011, Climate change and future California floods: Western States Water Council, March 2011, San Diego, CA.

Dettinger, M.D., 2011, Climate change, future California floods and an observation network for both: National Hydrologic Warning Council Meeting, May 2011, San Diego, CA.

Dettinger, M.D., 2011, Estimating climate-change impact probabilities: ASCE Environment and Water Resources Institute Annual Meeting, May 2011, Palm Springs, CA.

Dettinger, M.D., 2011, Atmospheric rivers, floods, and the water and living resources of California: Seminar, USGS Western Region, June 2011, Menlo Park, CA.

Dettinger, M.D., 2011, Assessing Hydrometeorological Extremes for Resource and Hazards Management under Climate Change: American Geophysical Union Fall Meeting, San Francisco, December 2011.

Dettinger, M.D., 2012, Water-relevant climate change projections for the Mediterranean regions: Mediterranean Cities Conference, Los Angeles, June 2012.

Dettinger, M.D., 2012, Water-related climate change projections for California's urban supplies: Urban Water Institute, San Diego, August 2012.

Dettinger, M.D., 2012, Storms, floods and atmospheric rivers in a changing West: Webinar, Water Information Coordination Program Advisory Committee on Water Information, September 2012.

Dettinger, M.D., 2013, ARkStorm as a Context for California Flood Planning: Water Education Foundation, Sacramento, CA, March 2013.

Dettinger, M.D., 2013, Latest (CMIP5) climate-change projections for the Sierra Nevada: Mountain Counties Water Resources Association, March 2013, Auburn, CA.

Dettinger, M.D., 2013, Quasi-decadal precipitation variations in Northern California—How seriously should we take them?: California Department of Water Resources Winter 2014 Outlook Meeting, La Jolla, November 2013.

Dettinger, M.D., 2014, Storms, floods & climate change in the Southwest: Southwest Climate Science Center webinar, January 2014.

Dettinger, M.D., 2014, Atmospheric rivers as drought makers and breakers: California Drought Summit, Sacramento, May 2014.

Dettinger, M.D., and Ralph, M., 2014, New opportunities for monitoring severe storms, floods and impacts in the mountainous Western United States: Global Mountain Observations Fair and Workshop, Reno, July 2014.

Dettinger, M.D., 2014, Drought in California—It's all about the biggest storms: AGU Fall Meeting, San Francisco, December 2014.

Dettinger, M.D., and Ralph, F.M., 2014, Landfalling atmospheric rivers in California—Historical and future impacts: AGU Fall Meeting, San Francisco, December 2014.

Dettinger, M.D., 2015, Climate variability and change, and California water: North Lahontan Water Board, South Lake Tahoe, Jan 2015.

Dettinger, M.D., 2015, California water supplies in a changing climate: California Municipal Utilities Association Conference, Carlsbad, April 2015.

Dettinger, M.D., 2015, Panel: New Approaches for responding to climate change in the San Francisco Bay-Delta: UC Davis, May 2015.

Drexler, J.Z. 2014. Using Process-Level Science on Peat Formation to Inform Wetland Restoration. 8th Biennial **Bay-Delta Science Conference**, Sacramento, CA, October 2014.

Drexler, J.Z. Marsh sustainability in the Sacramento-San Joaquin Delta, CA. The Science Behind Delta Climate Change Impacts: A Practical Workshop by the Delta Conservancy Water Education Foundation, West Sacramento, CA, February 2014.

Drexler, J.Z. Wetlands as sentinels and mitigators of climate change. Department of Interior, U.S. Fish & Wildlife Service, National Conservation Training Center's Conservation Science Webinar Series, September 2013.

Jaffe, B., Foxgrover, A., and Finlayson, D., Fregoso, T., Takekawa, J., and Marvin-DiPasquale, M., 2012, Will salt pond restoration in South San Francisco Bay cause erosion of mudflats and sloughs? (abs.) 7th Biennial **Bay-Delta Science Conference**, Sacramento, California, October 2012.

Jaffe, B., van der Wegen, M., Foxgrover, A., and Roelvink, D., 2014, Estuarine tidal flat evolution at decadal and seasonal time scales (abs.) 8th Biennial **Bay-Delta Science Conference**, Sacramento, California, October 2014.

Jones, C. and Jaffe, B.E., 2012, Influence of history and environment on sediment dynamics of intertidal flats, (abs.) 7th Biennial **Bay-Delta Science Conference**, Sacramento, California, October 2012.

Kimmerer, WJ., T.R. Ignoffo, A.M. Slaughter, and E.S. Gross. 2014. Effects of variable freshwater flow on fish and foodwebs of the San Francisco Estuary. **Bay-Delta Science Conference**, Sacramento, October 2014.

Kimmerer, W. 2012. The food environment of delta smelt in fall: a synthesis of recent findings. **Bay-Delta Science Conference**, Sacramento, October 2012.

Kleckner, AE, AR Stewart, J Thompson, and F Parchaso. 2014. Effect of drought conditions on the distribution and bioaccumulation of selenium in two invasive bivalve clam species in North San Francisco Bay. **Bay-Delta Science Conference**, Sacramento, October 2014.

Knowles, N., and Lucas, L.V., 2012, CASCaDE: Computational Assessments of Scenarios of Change for the Delta Ecosystem. Presentation at USGS Chesapeake Bay Workshop, Reston, VA (2012) (co-presented)

Knowles, N., and Lucas, L.V., 2012, CASCaDE: Computational Assessments of Scenarios of Change for the Delta Ecosystem. Seminar at USGS Headquarters, Reston, VA (2012) (co-presented)

Knowles, N., and Lucas, L.V., 2013, CASCaDE: Computational Assessments of Scenarios of Change for the Delta Ecosystem. USGS Water Resources Seminar, Menlo Park, CA (co-presented)

Knowles, N., and Lucas, L.V., 2014, CASCaDE: Computational Assessments of Scenarios of Change for the Delta Ecosystem: Delta Conservancy & Water Education Foundation Workshop on “The Science behind Delta Climate Change Impacts”, West Sacramento, California, February, 2014. (Presented by Knowles, Invited)

Knowles, N. and Lucas, L.V. 2014. CASCaDE: Computational Assessments of Scenarios of Change for the Delta Ecosystem. Briefings provided at USGS Drought Press Roundtable. Menlo Park, CA.

Knowles, N. 2011. CASCaDE I and II. Pacific Southwest Area Executive meeting, Sacramento, California, April 7, 2011.

Knowles, N. 2012. CASCaDE II: Computational Assessments of Scenarios of Change in the (Bay-)Delta Ecosystem. U.S. Geological Survey NRP Branch Chiefs Meeting, National Wetlands Research Center, Lafayette, Louisiana (by WebEx from Menlo Park), February 1, 2012.

Knowles, N. 2012. Cascading Effects of Climate Change in the Sacramento-San Joaquin Delta and its Watershed. U.S. Geological Survey Bay-Delta Executive Board Meeting, Sacramento, California, September 4, 2012.

Knowles, N. 2013. CASCaDE: Computational Assessments of Scenarios of Change for the Delta Ecosystem. Delta Stewardship Council Independent Science Board Meeting, Sacramento, California, February 14, 2013.

Knowles, N. and Cronkite-Ratcliff, C. 2014. Projecting Boundary Conditions for a Hydrodynamic Model of the Bay-Delta Under Scenarios of Climate Change. 8th Biennial **Bay-Delta Science Conference**, Sacramento, California, October 28-30, 2014. Poster.

Knowles, N. 2014. CASCaDE: Computational Assessments of Scenarios of Change for the Delta Ecosystem. Workshop On Proposed Research Portfolio For California's 4th Climate Change Assessment: Seeking Collaboration With External Efforts, Governor's Council Room, California State Capitol Building, Sacramento, California, December 1, 2014.

Lucas, L.V., 2011, Timescales for understanding and linking biology and physics together – Application to plankton dynamics: International Workshop/School on Tracer and Timescale Methods for Understanding Complex Geophysical and Environmental Processes, Louvain-la-Neuve, Belgium, August 2011. (Invited lecture)

Lucas, L.V., 2012. From super-simple to complex 3D: Building meaningful models of coupled physics and biology in tidal aquatic systems. University of Notre Dame, Dept. of Civil and Environmental Engineering & Earth Sciences, Challenges & Innovation in Civil & Environmental Engineering Seminar Series. South Bend, IN (Invited)

Lucas, L.V., 2014. Hydrodynamics IS an ecosystem process: Integrating fluid mechanics and biology for understanding and managing our aquatic ecosystems. Stanford University, Dept. of Civil and Environmental Engineering, Environmental Fluid Mechanics and Hydrology Seminar Series. Stanford, CA (Invited)

Lucas, L.V., 2014. Invited presentation. Stanford University, Environmental and Water Studies Program 50th Anniversary Celebration. Stanford, CA

Lucas, L.V. 2014. Presented briefing on CASCaDE research and educational "Tule Talks" aboard Delta boat tour for USGS VIP's. (Invited)

Lucas, L.V. and A.R. Stewart. 2015. Presented briefing on CASCaDE research and educational “Tule Talks” aboard Delta boat tour for DOI VIP’s. (Invited)

Lucas, L.V., 2013, CASCaDE: Computational Assessments of Scenarios of Change for the Delta Ecosystem. Briefing for USGS Bay-Delta Executive Board. Menlo Park, CA. (Invited)

Lucas, L.V., 2011. Let’s make more phytoplankton!!! Presentation on CASCaDE research for Asst. Secy. of Interior Anne Castle aboard R/V Turning Tide in San Francisco Bay

Lucas, L.V., Thompson, J.K., and Cloern, J.E., 2012, Are shallower, slower habitats necessarily “greener”? How clams upend conceptual models guiding ecosystem management in the Delta: 7th Biennial **Bay-Delta Science Conference**, Sacramento, California, October 2012.

Lucas, L.V., and Thompson, J.K., 2013, General, idealized models for integrating effects of bivalve grazing with physical habitat attributes to better understand phytoplankton dynamics and inform ecosystem management: 22nd Biennial International Conference of the Coastal and Estuarine Research Federation, San Diego, California, November 2013. (Invited)

Lucas, L.V., 2014, Modeling climate change effects on Delta phytoplankton in CASCaDE II: Delta Conservancy & Water Education Foundation Workshop on “The Science behind Delta Climate Change Impacts”, West Sacramento, California, February, 2014. (Invited)

Lucas, L.V. , J.E. Cloern, J.K. Thompson, J.R. Koseff, M.T. Stacey, S.G. Monismith, 2014, What caused the diatom decline in Suisun Bay after 1986?: 8th Biennial **Bay-Delta Science Conference**, Sacramento, California, October 2014. (Invited)

Martyr, R.M., J. Helly, L. Lucas, N. Knowles, M. van der Wegen, F. Achete, A. van Dam, S. van der Pijl, H. Kernkamp, B. Jaffe, T. Fregoso, 2014, Calibration of a 3D hydrodynamic model to assess water quality indicators in the Bay-Delta: 8th Biennial **Bay-Delta Science Conference**, Sacramento, California, October 2014. (Poster)

Martyr, R., Helly, J., Lucas, L., Knowles, N., van der Wegen, M., and van Dam, A., 2013, An application of a hydrodynamic model in the San Francisco-Bay Delta: Insights into the impact of rapid sea level rise on regional hydrodynamic and salinity fields: 22nd Biennial International Conference of the Coastal and Estuarine Research Federation, San Diego, California, November 2013.

- Parchaso, F., Crauder, J., Thompson, J., Gehrts, K., Fuller, H. Spatial and temporal recruitment patterns of the estuarine bivalve *Potamocorbula amurensis* in San Francisco Bay and Delta (Poster). Biennial **Bay-Delta Science Conference**, Sacramento, CA, October 15-18, 2012
- Martyr, Van der Wegen, Helly, Knowles, Lucas, 2013 An application of a hydrodynamic-sediment transport model in the San Francisco-Bay Delta: insights into the impact of rapid sea level rise on regional hydrodynamic and salinity fields, Coastal and Estuarine Research Federation annual meeting, San Diego
- Stern, M.A., Flint, L.E., Minear, J.T., Wright, S.A., and Flint, A.L. 2012. Development of a coupled sediment transport and hydrologic (HSPF) model of the Sacramento River basin, CA, to estimate future sediment supply to the Bay-Delta system. Presented at the **Bay-Delta Science Conference**, October 17, 2012.
- Stern, M.A., Flint, L.E., Flint, A.L., Wright, S.A., and Minear, J.T., 2014. Characterizing flow and sediment trends in the Sacramento River Basin, CA, using the Hydrologic Simulation Program – FORTRAN, Abstract 17793 presented at 2014 Fall Meeting, AGU, San Francisco, Calif., 15-19 Dec.
- Stewart, AR, A Kleckner, F Feyrer, RC Johnson. 2014. Connecting Fish Tissue Selenium Concentrations To Sources and Exposure In A Dynamic Estuary: The Case Of Sacramento Splittail. **Bay-Delta Science Conference**, Sacramento, October 2014
- Stewart, AR 2014. Long-term monitoring as part of a multidisciplinary approach to ecosystem research. USGS Water Quality Conference in Shepherdstown, West Virginia, Oct 2014.
- Stewart, AR 2014. Understanding selenium exposure of the San Francisco Bay food web: 1995 through 2012. Regional Monitoring Program Selenium Strategy Team Meeting, April 2014.
- Stewart, AR 2014. *How do drought conditions Change Selenium exposure of the San Francisco Bay food web?* Speed-dating with the media on the drought, Menlo Park, March 2104.
- Swanson, K.M., Drexler, J.Z., and Schoellhamer, D.H. 2013. Future sustainability of tidal freshwater marshes in the Sacramento-San Joaquin Delta, CA under multiple scenarios of sea-level rise. Interagency Ecosystem Program Workshop, Folsom, CA, April 2013.
- Thompson, J.K. 2011. Understanding *Corbula amurensis*' and *Corbicula fluminea*'s distribution as part of the fall experiments. Interagency Estuarine Ecology Team Workshop, Sacramento, CA, August 17, 2011 (Invited)

Thompson, J.K. 2011. Briefing and field trip for Anne Castle (Assistant Secretary of Interior for Water and Science) and Lori Caramanian (Deputy Assistant Secretary for Water and Science) on the Ecological and Infrastructure Issues in SF Bay and Delta. SF Bay and Delta on the RV Turning Tide, October 18, 2011

Thompson, J.K. 2012. Presentation of early results from Fall Low Salinity Habitat experiment. Fall Low Salinity Habitat Meeting, Sacramento, CA, January 26, 2012

Thompson, J.K. 2012. Presentation/led discussion group. Technical Workshop on Estuarine Habitat in the Bay Delta Estuary: Managing the Low Salinity Zone to Improve Estuarine Habitat and Protect Fish Populations, Sacramento, CA, March 27, 2012 (Invited)

Thompson, J.K. 2012. Presentation on fall flow experiments and bivalves. Annual Interagency Ecology Program Meeting, Folsom, CA, April 18-20, 2012 (Invited)

Thompson, J.K. 2012. Presentation on FLaSH Study. Meeting on Fall Low Salinity Habitat (FLaSH) Study Synthesis – Year One of the Delta Fall Outflow, Sacramento, CA, July 31-August 1, 2012 (Invited)

Thompson, J.K. 2012. Opposing seasonal biomass cycles influence the grazing effects of *Corbicula* and *Potamocorbula*. Biennial **Bay- Delta Science Conference**, Sacramento, CA, October 15-18, 2012 (Invited)

Thompson, J.K. 2014. Ecological Impacts: Benthos. A Practical Workshop: The science behind Delta climate change impacts, Sacramento, CA, Feb 13, 2014

Thompson, J.K. 2014. Population persistence of the invasive suspension-feeding bivalve *Potamocorbula amurensis* and *Corbicula fluminea* in San Francisco estuary: what can we learn about future spread and impacts? (Poster) Annual Interagency Ecology Program Meeting, Folsom, CA, February 26-28 2014

Thompson, J.K. 2014. Benthos (animals that live on/in the bottom). Briefing for Congressional staffers on Bay-Delta status, science and policy. USGS R/V Polaris, August 21, 2014

Thompson, J.K. 2014. Biomass and Grazing Rates of Two Exotic Bivalves, *Corbicula fluminea* and *Potamocorbula amurensis*, Show Surprising Variability Over 20–30 Year Sampling Period: What Does it Mean for Future Food Webs? Biennial **Bay- Delta Science Conference**, Sacramento, CA, October 28-30, 2014

van der Wegen, Jaffe, 2013 Morphoprobabilistics - a way to assess uncertainty levels in process-based deterministic models, NCK Den Haag, Netherlands

van der Wegen, Jaffe, Roelvink, 2013 Why did the channel narrow over the past 150 years in San Pablo Bay, California? Morphodynamic modeling effort of decadal channel evolution, RCEM, Santander, Spain

van der Wegen, M., L. Lucas, N. Knowles, P. Barnard, B. Jaffe, D. Senn, M. Stacey, O. Fringer, S. Monismith, E. Elias, H. Los, D. Roelvink, 2014 Building a public community around the D3D-FM San Francisco Bay-Delta model. **Bay-Delta Science Conference**, Sacramento

van der Wegen, M., Jaffe, B.E., and Roelvink, D., 2012 Morphodynamic modeling hindcast decadal channel evolution in San Pablo Bay, California: why does the channel narrow?, Physics of Estuaries and Coastal Seas, New York

van der Wegen, M., 2013 (invited) Skillscore in morphodynamic predictions over centuries, ICOASsT (EU project), Liverpool

van der Wegen, M., L. Lucas, N. Knowles, D. Senn, M. Stacey, S. Monismith, B. Jaffe, P. Barnard, O. Fringer, H. Los , 2014, Building a Public Community around the D3D-FM San Francisco Bay-Delta Model: 8th Biennial **Bay-Delta Science Conference**, Sacramento, California, October 2014. (Poster)

c. Delta Science Program/Delta Stewardship Council Service

Achete, F., van der Wegen, M., Roelvink, D., and B. Jaffe. Bay-Delta Sediment Modeling in CASCaDE II. Delta Science Program Workshop on Integrated Environmental Modeling for Estuarine System Management, Davis, CA May 21, 2015. (Interactive model demonstration/animation, presented by L. Lucas)

Brown, L. Currently working on the State of Bay Delta Science Report. This includes co-lead of the Food Web Chapter, and co-author on the Delta Smelt Chapter and Climate Change Chapter.

Brown, L. Member of Panel for Lower Food Web Dynamics in California's Bay-Delta EcoSystem. The Delta Science Program and U.C. Davis Center for Aquatic Biology and Aquaculture, Davis, CA, February 18, 2014.

Brown, L.R. 2013. Ecological context for the Delta: A lot can happen in 150 years... State of the Science Workshop on Fish Predation on Central Valley Salmonids in the Bay-Delta Watershed. California Department of Fish and Wildlife, Delta Science Program, and National Marine Fisheries Service, Davis, CA, July 22-23, 2013. (Oral Presentation and on-line Powerpoint Presentation)

Brown, L.R. 2013. Tidal wetlands, restoration, and fish in the San Francisco Estuary: what have we learned in the past 10 years? Tidal Marshes and Native Fishes in the Delta: Will Restoration Make a Difference, The Delta Science Program, U.C. Davis Center for Aquatic Biology and Aquaculture, and California-Nevada Chapter of the American Fisheries Society, Davis, CA, June 10, 2013. (Oral Presentation and on-line Powerpoint Presentation).

Cayan, D.R. 2014. Climate Change and the Delta. Oral presentation to the Delta Stewardship Council. Sacramento CA. 20 Nov 2014

Cayan, D.R. 2014. Expected climate changes on top of already high climate variation. Oral presentation, Delta Challenges Workshop, Delta Stewardship Council. Sacramento CA. 17 Mar 2015

Dettinger, M.D., Editorial board, 2015 State of Bay-Delta Science Report; and lead author for Chapter 3 (Climate Change and the Delta)

Dettinger, M.D., 2011, Atmospheric rivers, floods, and the water and living resources of California: Seminar, Delta Stewardship Council, June 2011, Sacramento, CA.

Dettinger, M.D., 2013, Atmospheric rivers, floods, and the water and living resources of California: Bay-Delta Stewardship Council Independent Science Board, February 2013, Sacramento, CA.

Drexler, J.Z. Opportunities for applying new science to restoring wetlands and storing carbon in the SF Estuary. Delta Stewardship Council, California Resources Agency, Carbon Seminar Series, April 2014.

Kimmerer, W.J. 2015. Effects of variable freshwater flow on fish and foodwebs of the San Francisco Estuary. Association of California Water Agencies Spring Conference, May 2015, Sacramento. (Invited by R. Fiorini, DSC Chair)

Kimmerer, W.J. 2014. Causes, consequences, and potential remedies to low foodweb productivity in brackish waters of the San Francisco Estuary. Center for Aquatic Biology and Aquaculture workshop on foodwebs, March 2014, Davis, CA. (Invited presentation)

Kimmerer, W. 2013. Where does pelagic fish food in the Delta currently come from? Center for Aquatic Biology and Aquaculture workshop on tidal marsh restoration, June 2013, Davis, CA. (Invited presentation)

Knowles, N. and L. V. Lucas. The CASCaDE Journey: Computational Assessments of Scenarios of Change for the Delta Ecosystem. Delta Science Program Workshop on Integrated Environmental Modeling for Estuarine System Management, Davis, CA May 21, 2015. (Invited Oral Presentation)

Lucas, L.V., and Thompson, J.K., 2013, Are shallower, slower habitats necessarily “greener”? How clams upend conceptual models guiding ecosystem management in the Delta: Meeting of the Delta Independent Science Board, Sacramento, California, February 2013. (Invited)

Lucas, L.V., 2014, Hydrodynamic influences on phytoplankton in the San Francisco Bay-Delta: Delta Science Program and UC Davis Workshop on “Lower Food Web Dynamics in California’s Bay-Delta Ecosystem”, Davis, California, February, 2014. (Invited)

Lucas, L.V., 2014. Synthesis Team Member, Delta Science Program and UC Davis Workshop on “Lower Food Web Dynamics in California’s Bay-Delta Ecosystem”, Davis, California, Feb 2014 (Invited)

Lucas, L.V., and Thompson, J.K., 2014, Residence time is a double-edged sword (and other ways clams can upend engrained conceptual models of phytoplankton dynamics): Delta Science Program Workshop on “Delta Outflows and Related Stressors”, Sacramento, California, February 2014. (Invited)

Schoellhamer, D. and S. Wright, 2013. Habitat restoration and suspended sediment. Presentation to the Delta Independent Science Board, Sacramento, CA. February 2013.

Schoellhamer, D. Reviewed draft white paper on Delta sedimentation by Emily Mortazavi, a California Sea Grant State Fellow with the Delta Science Program, 2013.

Schoellhamer, D., J. Burau, and B. Bergamaschi. 2013. Flow, Sediment, and Water Quality Monitoring in the Delta: A Case for a High-Frequency, Flux-Based Monitoring Program. Seminar for Delta Science Program, Sacramento, CA, November 2013.

Schoellhamer, D. Lead author for the State of Bay-Delta Science report chapter on flow dynamics and transport of water-quality constituents in the Delta, 2015.

Schoellhamer, D. Associate Editor for *San Francisco Estuary and Watershed Science*.

Thompson, J.K. 2013. Biomass and Grazing of *Corbicula* and *Potamocorbula* today and in the future. Briefing for Independent Science Board (Bay Delta Science), Sacramento, CA, Feb 14, 2013 (Invited)

Thompson, J.K. 2014. Benthic Impacts – Clam Grazing. Delta Science Program and UC Davis CABA workshop on “Lower Food Web Dynamics in California’s Bay-Delta Ecosystem: Current Understanding and Future Interactions in a Changing Landscape”, Davis, CA, Feb 18, 2014

d. Other CASCaDE-Related Service and Outreach

- 1) *San Francisco Estuary Institute/San Francisco Bay Nutrient Management Strategy*: planning to use CASCaDE models as foundation of nutrient modeling effort (Lucas, Martyr, van der Wegen)
- 2) *National Weather Service*: interested in developing an operational model of the Delta based on the CASCaDE Delft3D-FM hydrodynamic model (Knowles, Lucas, van der Wegen)
- 3) *California Energy Commission*: invited CASCaDE to join the 4th California Climate Assessment. So far, we have provided information and participated in conference calls and meetings (Cayan, Knowles, Lucas)
- 4) *Portland State University*: interested in applying CASCaDE hydrodynamic model for research (van der Wegen). Currently using 2-D version.
- 5) *San Francisco Estuary Institute and others*: discussions of Bay-Delta community model (Knowles, Jaffe, Lucas, van der Wegen, with multiple team discussions to work out details of model sharing)
- 6) *Delta Independent Science Board*: science briefings (Cayan, Dettinger, Knowles, Lucas, Schoellhamer, Thompson)
- 7) *Delta Science Program*: joint CASCaDE presentation at workshop on “Integrated Environmental Modeling for Estuarine System Management” (Knowles, Lucas and demo by Achete)
- 8) *USGS Drought Press Roundtable*: press interviews (Dettinger, Knowles, Lucas, Stewart, Thompson, Wright)
- 9) *USGS Water Resources Seminar Series, Menlo Park*: joint CASCaDE seminar (Knowles, Lucas)
- 10) *USGS Chesapeake Bay Workshop, Reston, VA*: joint CASCaDE presentation (Knowles, Lucas)
- 11) *USGS Headquarters, Reston, VA*: joint CASCaDE seminar (Knowles, Lucas)
- 12) *Prof. John Tracy, U. of Idaho*: discussed possible future collaboration (Knowles, Lucas, Stewart, Thompson)
- 13) *Mike Chotkowski, Chair USGS Bay-Delta Executive Board*: CASCaDE status briefing (Knowles, Lucas, Stewart)

- 14) *Mike Chotkowski, Chair USGS Bay-Delta Executive Board*: In-depth CASCaDE status meeting (all USGS CASCaDE team members, Martyr)
- 15) *DOI VIP's*: briefing and Delta boat tour (Lucas, Stewart)
- 16) *USGS VIP's*: briefing and Delta boat tour (Lucas)
- 17) *USGS Bay-Delta Executive Board*: CASCaDE presentation (Lucas)
- 18) *Ariel Rubissow-Okamoto, Editor, Estuary News*: Provided information on CASCaDE project for article (Knowles)
- 19) Provided information on CASCaDE project to Laura Walker at the Delta Science Program for an article in *Science News* (Nov 2011) (Lucas)
- 20) *Asst. Secretary of Interior Anne Castle*: briefings and San Francisco Bay boat tour (Knowles, Lucas, Thompson)
- 21) *NOAA-led interdisciplinary SESAME project*: invited guest at kick-off meeting (Lucas)
- 22) *Andy Gunther, Executive Coordinator for Bay Area Ecosystems Climate Change Consortium*: invited CASCaDE to become "Affiliated Project" of the Bay Area Ecosystems Climate Change Consortium (Knowles)
- 23) *Delta Conservancy*: Participated in Board meeting (Jan 18, 2011) (Knowles)
- 24) *Deltares Views Magazine*: Provided information on CASCaDE for article (van der Wegen, Lucas)
- 25) *USGS Director Marcia McNutt*: provided CASCaDE material for plenary talk at Bay-Delta Science Conference (Knowles, Lucas)
- 26) *Patrick Barnard and colleagues, USGS-Coastal and Marine Geology*: maintain regular communication with to coordinate and share information between CASCaDE and OCOF (<http://data.prbo.org/apps/ocof>) SLR/Bay modeling project (Knowles, van der Wegen, Stewart, Martyr, Lucas)
- 27) *Ben Sleeter and Chris Souldard, USGS Geography*: met to share CASCaDE results for use in their studies of land-use and land-cover change at local to regional scales (Knowles)
- 28) *Matthew Anderson, National Coordinator of USGS Priority Ecosystems Science*: detailed CASCaDE briefings for coordinator of major USGS funding source for CASCaDE (entire CASCaDE team)

- 29) *Prof. Mark Stacey, UC Berkeley*: discussed potential research synergies with CASCaDE and other USGS projects (Lucas, van der Wegen, Knowles)
- 30) *Delta Conservancy and Water Education Foundation*: CASCaDE presentations and panel discussion at workshop on “The Science behind Delta Climate Change Impacts” (Brown, Drexler, Knowles, Lucas, Thompson)
- 31) *Claudia Faunt and Randy Hanson, USGS Groundwater Hydrologists*: Discussion of potential collaboration (Knowles, van der Wegen)
- 32) *Prof. Olivier Ragueneau, Director, LEMAR, French Institute for Exploration of the Sea, Brest, France*: Discussed the San Francisco Bay-Delta as a possible site for studying science-policy linkages (Lucas)
- 33) *UC-US DOE: Water-Energy Nexus Workshop* (Cayan)
- 34) *PPIC: Report/Blogs on Climate and California Water Supply, Pacific Anomalies and El Nino 2015* (<http://www.ppic.org/main/publication.asp?i=1131>, http://www.ppic.org/main/blog_detail.asp?i=1781, http://www.ppic.org/main/blog_detail.asp?i=1810) (Cayan)
- 35) *Second California Climate Scenarios Assessment, Springer 2013 (originally Climatic Change Supplement 20011)*: Editor (Cayan)
- 36) *Southwest Climate Change Assessment, 2013*: Steering team member and lead author (Cayan)
- 37) *National Research Council: West Coast Sea Level Rise Report, 2012*. Report Committee member (Cayan)
- 38) *California Department of Water Resources: Climate Change Advisory Team (CCTAG)*. Helping to construct climate change scenarios. Provided climate input to California Water Plan. Report to be published 2015/2016. Committee Member (Cayan)
- 39) *US National Climate Change Assessment: Sea Level Rise Report*, Contributor. NOAA Tech Memo OAR CPO-1. 37 pp. (Cayan)
- 40) *Baylands Ecosystem Habitat Goals Update*: Science Review Panel (Cayan)
- 41) *California Ocean Protection Council: Science Advisory Team* (Cayan)
- 42) *California 4th Climate Change Assessment*: Provided supporting and organizing information (Cayan)
- 43) *California AB 32 Scoping Document*: Expert reviewer (Cayan)

- 44) *California Climate Extremes Workshop*: Designed (with help from SIO and agency colleagues), garnered funding, invited speakers, was the host of the workshop, which brought together a set of experts to describe extreme events in the present and future climate in California. La Jolla, CA (Cayan)
- 45) *Sacramento Bee*: Wrote OP/Ed on California Climate Change, with assistance from R. Monroe. (Cayan)
- 46) *US Congressman Henry Waxman*: Chief writer and editor of SIO's Responses to Questions on the Impact of Climate Change in California submitted by Congressman Waxman's staff. (Cayan)
- 47) *University of Southern California Ocean Climate Workshop*: Presented and participated. (Cayan)
- 48) *Long Beach Aquarium Public Lecture Series*: Presented lecture and discussion of Climate Change and Sea Level Rise (Cayan)
- 49) *CNAP and California Department of Water Resources*: Hydrological Extremes in California Workshop. Hosted workshop and presented talk on coastal extremes. (Cayan)
- 50) *California Department of Water Resources (DWR)*: Co-hosted Winter Outlook Workshop with Jeanine Jones, DWR. (Cayan)
- 51) *Southwest Climate Science Center Webinar*: Presented climate change projections for the Southwest U.S. (Cayan)
- 52) *California Department of Food and Agriculture*: Climate Change Workshop presentation on drought and climate change projections. (Cayan)
- 53) *100G and Beyond CalIT2 Workshop*: Presentation on climate observational and model data and regional projections. (Cayan)
- 54) *Climate Change/America's Infrastructure*: Workshop presentation on projected climate change impacts, Southwest U.S. (Cayan)
- 55) *California Governor's Office of Planning and Research*: California local government Climate Action Planning. Presented an overview of climate change and downscaling climate projections, California. (Cayan)
- 56) *Delta Independent Science Board*: Presentation on climate variability and change impacts on the Bay/Delta. (Cayan)

- 57) *California Energy Commission*: Integrated Energy Policy Report. Provided climate-energy briefing (Cayan)
- 58) *National Research Council*: West Coast Sea Level Rise – gaps, needs, new science opportunities. Participant and presenter. (Cayan)
- 59) *U.S. Representative Duncan Hunter*: Contributed to a discussion about climate change. (Cayan)
- 60) *State Climatologists Western Observations Subcommittee*: WERA 1012 Meeting. Host/participant. (Cayan)
- 61) *Advanced Energy Initiative Our Energy Future*: UCSD. Public Lecture (Cayan)
- 62) *UC Santa Cruz*: Climate Through the Looking Glass Climate Change Symposium. Presenter/panelist. (Cayan)
- 63) *Sierra Nevada and Sacramento/San Joaquin Delta Conservancy*: Presented to the two Conservancy Boards on projected climate change from Sierra to Delta. (Cayan)
- 64) *USGS*: Presented Seminar, Menlo Park, CA (Cayan)
- 65) *USGS*: Public Lecture, Menlo Park, CA (Cayan)
- 66) *California Drought Summit*: Climate and the ongoing California Drought, organized by UC Davis. Presenter/panelist. Capitol Building, Sacramento, CA (Cayan)
- 67) *California Drought Forum--Climate and the ongoing California Drought*: Presenter/participant. Sacramento, CA (Cayan)
- 68) *NASA AMES NEX*: Keynote lecture on climate change vulnerability assessment for California <https://nex.nasa.gov/nex/static/htdocs/site/extra/opennex/>. (Cayan)
- 69) *California Governors Office and Legislature Climate Seminar*: Participated in climate change panel and discussion with California Energy Commission and Resources Agency. Governor's Conference Room, Sacramento, CA (Cayan)
- 70) *CALFIRE Wildfire Management Symposium*: Participated and presented talk, Climate Change and Wildfire in California, Sacramento, CA (Cayan)
- 71) *CNAP (California Nevada Climate Applications Program)*: Web page <http://meteora.ucsd.edu/cnap/> contains an ongoing series of information for California and Nevada decision makers. Senior architect. (Cayan)

72) *California Coastal Conservancy and Ocean Protection Council: Workshop on “Understanding Climate Change Effects on San Francisco Bay: What can modeling offer?” Participant. (Thompson)*

73) *California Coastal Conservancy, CA Bay Conservation Development Commission: Baylands Habitat Goals Update – Adjusting for climate change. Multiple Workshops. Participant. (Thompson)*

74) *CA Coastal Conservancy, Stanford University, University of CA Berkeley: Workshop on “Science Priorities for Understanding Climate Change Impacts on the Ecosystems of San Francisco Bay and the Gulf of the Farallones”. Participant. (Thompson)*